2017

Improving Vaccine Design For Viral Diseases Using Modified Antigens And Vectors

Michael John Hogan
University of Pennsylvania, mihogan@mail.med.upenn.edu

Improving Vaccine Design For Viral Diseases Using Modified Antigens And Vectors

Abstract
Two of the principal challenges facing vaccine design today are how to generate protective antibody responses against viruses that have evolved sophisticated strategies to evade the humoral immune system and how to more rapidly and effectively produce vaccines to address emerging epidemics. In this regard, we explored multiple strategies to improve vaccine design for HIV-1 and Zika virus. In one approach, we derived CD4-independent variants of HIV-1 envelope (Env) with the hypothesis that such Envs would expose conserved epitopes that may be targets of protective, non-neutralizing antibodies. We characterized the biological and structural properties of two CD4-independent Env clones and found that they exhibited significantly greater exposure of a relatively conserved, linear epitope in the second variable loop (V2) that had previously been associated with decreased risk of infection in a clinical HIV-1 vaccine trial. This epitope was significantly more immunogenic in mice and nonhuman primates and, intriguingly, was associated with more rapid development of antibody-dependent cell-mediated cytotoxicity. In another approach, we designed mutations in the cytoplasmic tail of HIV-1 Env that were predicted to increase its cell surface expression and thus its immunogenicity in a vaccinia prime-protein boost vaccine protocol. We found that the highest level of surface expression was mediated by Envs with truncated cytoplasmic tails, and this was associated with higher levels of binding and neutralizing antibodies after vaccinia primes and protein boosts, respectively. These two studies revealed that modifications to HIV-1 Env immunogens are able to influence both the quality and magnitude of desirable antibody responses. Finally, we used a newly developed vaccine platform based on nucleoside-modified mRNA to design a vaccine against Zika virus. This vaccine, encoding the surface prM and E proteins, was potently immunogenic and elicited high and sustained titers of neutralizing antibodies in mice and nonhuman primates following a single intradermal immunization. We observed rapid and durable protection from Zika virus infection in mice and a high level of protection in monkeys challenged five weeks after vaccination. This vaccine thus represents a promising candidate for clinical use in controlling the spread of Zika virus.

Degree Type
Dissertation

Degree Name
Doctor of Philosophy (PhD)

Graduate Group
Cell & Molecular Biology

First Advisor
Drew Weissman

Second Advisor
James A. Hoxie

Keywords
Antibody, Envelope, HIV, mRNA, Vaccine, Zika

Subject Categories
Virology

IMPROVING VACCINE DESIGN FOR VIRAL DISEASES USING MODIFIED ANTIGENS AND VECTORS

Michael J. Hogan

A DISSERTATION

in

Cell and Molecular Biology

Presented to the Faculties of the University of Pennsylvania

in

Partial Fulfillment of the Requirements of the

Degree of Doctor of Philosophy

2017

_____	_____
James A. Hoxie, M.D.	Drew Weissman, M.D., Ph.D.
Professor of Medicine	Professor of Medicine
Co-Supervisor of Dissertation	Co-Supervisor of Dissertation

_____
Daniel S. Kessler, Ph.D.
Associate Professor of Cell and Developmental Biology
Graduate Group Chairperson

Dissertation Committee:

Paul F. Bates, Ph.D., Professor of Microbiology
Beatrice H. Hahn, M.D., Professor of Medicine
Scott E. Hensley, Ph.D., Associate Professor of Microbiology
David B. Weiner, Ph.D., Emeritus Professor of Pathology and Laboratory Medicine

DEDICATION

This dissertation is dedicated to my mother, Mary Ellen Hogan, and my step-father, Robert H. Friel, Esq. Mom and Bob are the epitome of selfless people. Without their support over the years, both emotional and material, I would not have been able to realize the educational path I have chosen, nor would I now be guided by such a clear moral compass. With this dedication, I hope to express my sincere gratefulness for their sacrifice and their example.

ACKNOWLEDGMENTS

None of the projects in this dissertation would have been possible—truly—without the contributions of many wonderful collaborators, so I owe thanks to many people. First, I have benefitted from a very productive co-mentorship under Jim Hoxie and Drew Weissman. I did not necessarily know what I was getting into when I signed up for this, but what I received was an excellent and well-rounded scientific training from two outstanding but, stylistically, very different scientists. Jim has taught me how to be careful and methodical as an investigator and as a presenter. His questions have helped me think more clearly about controls and experimental plans before picking up the pipette. Drew has inspired me to be adventurous as a scientist, to take risks and strike while the iron is hot, but has also shown me how to keep priorities in perspective. What both Jim and Drew have in common is that they have each given me complete flexibility and independence over my projects and have supported me in whatever I chose to do, and I am grateful for that.

I am extremely thankful that I have had the opportunity to work with Norbert Pardi as a close collaborator, particularly on the Zika work. Norbi and I match each other well in our zeal for our work, and have made a great scientific team. I am confident that I could not have taken up the project of producing a vaccine for Zika virus with anyone less dependable and dedicated to his work. Outside the lab, I am also grateful for Norbi's sharing his love of wine.

I also worked extremely closely with Angela Conde-Motter for much of the earlier half of my graduate career, and many of the mouse experiments in this dissertation are as much her work as they are mine. The CD4 independence and cytoplasmic tail work would not have been started without her critical contributions.

Our labs have been fortunate to find ourselves in the midst of excellent collaborators from other institutions. I am very grateful to Barton Haynes for recognizing early on the potential of the mRNA vaccine platform and providing us access to monkeys for evaluation of the Zika vaccine. Since then, he continues to generously contribute critical reagents and data. I also benefitted from our labs' membership in a Gates Foundation vaccine discovery consortium. As part of this group, we worked closely with the labs of Shiu-Lok Hu, Kelly Lee, and Shan Lu to advance our vaccines in mice and monkeys. This would not have been possible without the invaluable contributions of Lifei Yang, Brad Cleveland, Wenjin Guo, Tad Davenport, Yu Liang, Shixia Wang, Dong Han, Patricia Firpo, and Deb Diamond, as well as the core facilities of David Montefiori, Georgia Tomaras, Guido Ferrari, and others.

All the other members of the Hoxie and Weissman labs have contributed significantly to my success in graduate school. I would like to especially thank Josephine Romano, Beth Haggarty, and Andrea Jordan for taking such good care of me, and Adrienne Swanstrom, Samra Elser, Kitu Kumar, Son Nguyen, and George Leslie for their support, both scientific and otherwise. I cannot imagine entering into a more loving lab family than these wonderful people.

I would like to thank my previous mentor, Carthene Bazemore-Walker, for starting me on my research career, my brilliant classmates, Bob Doms for continued guidance, and my support through the NIH T32 training grant in HIV Pathogenesis. Special thanks to my loving grandparents, who taught me enduring life lessons, my father Michael and devoted stepmom Kim, my kind and talented siblings including my older sister and excellent role model, Dr. Katherine Hogan, my Aunt Barbara and many other dear family and friends who have been so generous to my immediate family in recent years, and my partner Joe for his love and support.

ABSTRACT

IMPROVING VACCINE DESIGN FOR VIRAL DISEASES USING MODIFIED ANTIGENS AND VECTORS

Michael J. Hogan

Drew Weissman, M.D., Ph.D. and James A. Hoxie, M.D.

Two of the principal challenges facing vaccine design today are how to generate protective antibody responses against viruses that have evolved sophisticated strategies to evade the humoral immune system and how to more rapidly and effectively produce vaccines to address emerging epidemics. In this regard, we explored multiple strategies to improve vaccine design for HIV-1 and Zika virus. In one approach, we derived CD4-independent variants of HIV-1 envelope (Env) with the hypothesis that such Envs would expose conserved epitopes that may be targets of protective, non-neutralizing antibodies. We characterized the biological and structural properties of two CD4-independent Env clones and found that they exhibited significantly greater exposure of a relatively conserved, linear epitope in the second variable loop (V2) that had previously been associated with decreased risk of infection in a clinical HIV-1 vaccine trial. This epitope was significantly more immunogenic in mice and nonhuman primates and, intriguingly, was associated with more rapid development of antibody-dependent cell-mediated cytotoxicity. In another approach, we designed mutations in the cytoplasmic tail of HIV-1 Env that were predicted to increase its cell surface expression and thus its immunogenicity in a vaccinia prime-protein boost vaccine protocol. We found that the highest level of

surface expression was mediated by Envs with truncated cytoplasmic tails, and this was associated with higher levels of binding and neutralizing antibodies after vaccinia primes and protein boosts, respectively. These two studies revealed that modifications to HIV-1 Env immunogens are able to influence both the quality and magnitude of desirable antibody responses. Finally, we used a newly developed vaccine platform based on nucleoside-modified mRNA to design a vaccine against Zika virus. This vaccine, encoding the surface prM and E proteins, was potently immunogenic and elicited high and sustained titers of neutralizing antibodies in mice and nonhuman primates following a single intradermal immunization. We observed rapid and durable protection from Zika virus infection in mice and a high level of protection in monkeys challenged five weeks after vaccination. This vaccine thus represents a promising candidate for clinical use in controlling the spread of Zika virus.

TABLE OF CONTENTS

LIST OF TABLES

CHAPTER 1:

CHAPTER 4:

LIST OF ILLUSTRATIONS

CHAPTER 1:

CHAPTER 2:

CHAPTER 1

GENERAL INTRODUCTION

1.1. Successes and Failures of Modern Vaccines

Vaccines are perhaps the most effective type of medical intervention ever introduced. Vaccines save over two million lives every year and have greatly reduced the incidence and severity of many infectious diseases [1–3]. Through mass vaccination campaigns, smallpox and rinderpest (the bovine ancestor of measles virus) have been completely eradicated from the Earth; and others, such as poliovirus, are nearly eliminated [4,5]. Beyond its life-saving capacity, vaccination has also been credited with substantial economic benefits and the potential to lessen health disparities between socioeconomic groups [6].

While it is difficult to overstate the success of vaccines, current approaches have two major limitations. First, conventional vaccine designs have been largely ineffective against a class of pathogens that have evolved to successfully evade the adaptive immune response. And second, current approaches are inadequate to address rapidly emerging epidemics on an appropriate timescale. The following is a discussion of the sources of these problems and ways they can be addressed by new vaccine approaches. The scope of this overview is limited to viruses; bacteria and eukaryotic parasites present further hurdles to effective vaccine design and are reviewed in [7]. Sections 1.2–1.9 summarize the pitfalls and progress in vaccine design for the most challenging viral targets, while Sections 1.10–1.14 describe the landscape of vaccine development for new viral outbreaks.

1.2. Challenging Viral Vaccine Targets

Many viruses for which effective vaccines have been developed have a natural history of acute infection that resolves with either complete clearance by the adaptive immune system or death caused by an overwhelming infection or immunopathology. In the case of successful clearance, the host typically enjoys life-long protection against re-infection. Viruses susceptible to host immune control are usually also sensitive to vaccine-mediated immunity [8]. Such self-limiting infections that can be prevented using current vaccines include the measles, mumps, and rubella viruses, variola virus (smallpox), the flaviviruses, and others [9].

In contrast, viruses that establish chronic or repeated infections are by definition capable of evading the adaptive immune response, and these pathogens constitute a class of largely challenging vaccine targets [10]. Common immune evasion strategies include immune cell dysregulation, latency, antigenic variation, mutational escape, conformational masking of sensitive epitopes, and shielding of surface glycoproteins from neutralizing antibody (NAb) responses. These strategies are used in various combinations and degrees by the human immunodeficiency virus (HIV) (discussed in detail starting in Section 1.5), hepatitis C virus (HCV), respiratory syncytial virus (RSV), and several members of the herpes family to establish chronic or repeated infections in humans [11–16]. Most vaccine-related protection against viral infections correlates with NAb activity [8]. However, viral surface proteins are often rendered poor targets for the antibody response by extensive glycosylation, due to homology to self antigen and the occlusion of peptide epitopes [17]. Highly diverse surface antigens among circulating strains present another key obstacle to generating protective NAbs, since a vaccine must induce responses against all antigenic variants or against the most conserved epitopes. For viruses presenting

such challenges, the traditional vaccine approaches, including inactivated virus, live attenuated virus, and subunit vaccines, have in many cases failed to protect.

Still, there can be exceptions to this rule. Human papillomaviruses, for example, avoid triggering a robust antibody response in humans and can sometimes establish chronic infections [18]. However, they are susceptible to antibody-mediated neutralization, which is induced at high titers by current virus-like particle (VLP)-based vaccines [19,20].

1.3. Shifting to More Rational Vaccine Design

What advances in vaccinology are needed to generate protection against challenging pathogens for which even natural immunity is insufficient? Many investigators observe that such progress is already underway, as recent advances in molecular biology, structural biology, and basic immunology contribute to a transition from empirical to "rational" vaccine designs [9,21–25]. Here, the empirical approach refers to traditional methods of vaccine production, including the isolation, growth, and attenuation or inactivation of viruses. This approach requires no detailed understanding of viral biology or host immunology; nevertheless, it has produced effective vaccines for many viruses, particularly those causing acute infections [9]. Rational vaccine design here refers to methods guided by knowledge of viral biology and structure that mainly became possible following the advent of PCR, DNA sequencing, and recombinant technology in the late 20th century. With these techniques and others, we have expanded our repertoire of vaccine formats, with notable examples including DNA plasmid and messenger RNA (mRNA) vectors, and gained a finer understanding of viral immune evasion strategies, immune cell populations, and antibody development. Importantly, we can now directly visualize

antibody-mediated neutralization of viral glycoproteins with atomic-level resolution, paving the way for structure-guided vaccine design [26,27].

1.4. Structure-Guided Vaccine Design

Structure-guided vaccine design seeks to translate information about the structure of an antigen into a strategy to elicit protective antibodies. The utility of this strategy, and its potential applicability to an HIV vaccine, was recently highlighted when it was used to solve a long-standing problem in vaccine design for RSV. This member of the *paramyxoviridae* family causes an acute febrile respiratory illness in humans, with the first instance of infection typically occurring within the first year of life [28]. RSV is the primary cause of lower respiratory infections in children under 1 year of age globally, resulting in over 200,000 deaths in 2010 [29,30]. RSV is unusual among acute viruses in that the natural immune response does not confer complete protection against reinfection [28]. Instead, primary infection generates low titers of NAbs that can limit subsequent infections to the upper airway, where disease is mitigated compared to the lower airway [28], and several infections are required to boost neutralizing titers to fully protective levels [31]. The mechanism of this incomplete immunity remained unresolved for decades.

In the 1960s, an RSV vaccine was produced by the conventional approach of growing the virus in a monkey cell line and inactivating it with formalin [32]. Children were vaccinated, but NAb responses were low and did not protect from infection. Worse, those who were immunized with formalin-inactivated virus experienced a higher incidence of severe lower respiratory disease [32]. Vaccine-enhanced disease was later reproduced in cotton rat and mouse models, in which Th2-biased $CD4^+$ T cells were required for the effect [33,34]. Live attenuated and purified fusion

(F) protein RSV vaccines were similarly flawed, and the latter was tentatively associated with mild disease enhancement in rats [34–36]. Due to safety concerns and low efficacy, an RSV vaccine remained an elusive goal for many years.

Finally, in the 2010s, a series of structural insights changed the prospects for an RSV vaccine. McLellan and colleagues obtained a crystal structure of a soluble F protein trimer and discovered that the protein had adopted an elongated postfusion conformation [37,38]. The significance of this structural rearrangement for the antibody response was not clear until they obtained a crystal of the prefusion conformation, generated in part by stabilizing the structure with a monoclonal antibody (mAb), D25, which neutralized RSV with high potency compared to previously isolated mAbs. D25 binding to RSV-infected cells was competed by other potently neutralizing mAbs, and all mAbs of this specificity lacked binding to postfusion F protein. The prefusion crystal structure showed that this highly neutralization-sensitive quaternary epitope was formed solely on the prefusion structure. The authors proposed a structure-based model that explained all of the above phenomena: RSV F protein existed in a metastable prefusion conformation that is highly neutralization-sensitive but easily triggered to adopt the weakly neutralization-sensitive postfusion conformation. In support of this, virion-associated F protein was shown to quickly degrade towards the postfusion state when incubated at 37 °C, and solubilization of F protein or formalin-inactivation of RSV particles caused trimers to trigger [39]. Previous RSV immunogens, including wild-type and attenuated viruses, likely displayed a large proportion of postfusion F and biased the antibody response toward weak neutralization epitopes. Based on this model, an effective RSV vaccine would have to display F protein trimers stabilized in the prefusion conformation.

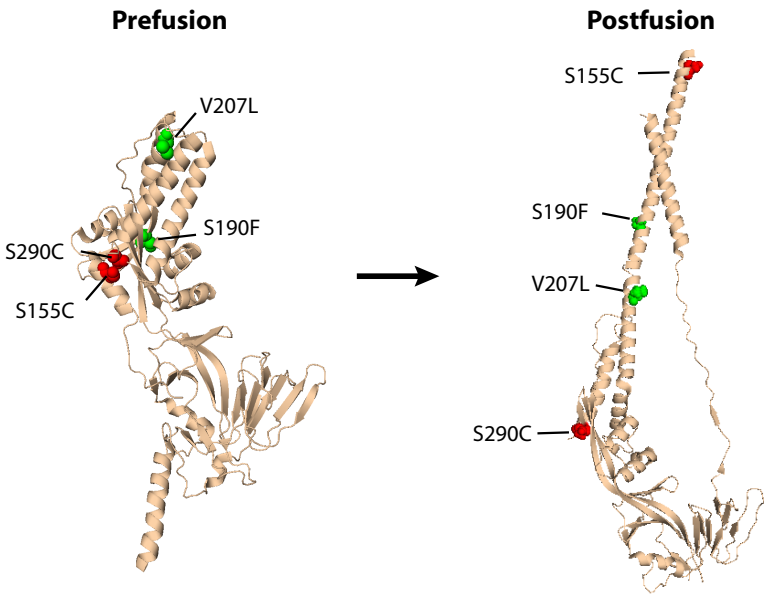

Fig. 1.1. Structure-guided design of RSV prefusion F protein immunogen. Shown are monomers from the crystal structures of the prefusion (left) and postfusion (right) RSV F protein trimers. Red spheres indicate Ser155 and Ser290, both mutated to Cys in the prefusion-stabilized mutant DS-Cav1. These residues are separated by 4.4 Å in the prefusion structure and 124.2 Å apart in the postfusion state, which is prevented in part by the formation of a disulfide bridge. Green spheres indicate the hydrophobic cavity-filling mutations, S190F and V207L. Images were adapted in Pymol from the crystal structures PDB 4JHW and 3RRR [37,40].

In one of the first notable successes of structure-guided vaccine design, McLellan and colleagues rationally engineered a stabilized prefusion F protein immunogen. Their approach relied on the crystal structures of the F protein in its prefusion and postfusion conformations, and they identified mutations predicted to stabilize the prefusion state [41]. Mutants were screened for their physical and antigenic properties, including the binding of site Ø mAbs under harsh physico-chemical conditions. One mutant with favorable properties, termed DS-Cav1, was stabilized by two bulky hydrophobic residues that filled hydrophobic cavities in the prefusion structure and two cysteines predicted to constrain the trimer in its prefusion state via a disulfide bridge (depicted in Fig. 1.1). DS-Cav1 was crystallized

without D25 and indeed formed a compact prefusion structure. Mice and rhesus macaques that were immunized with DS-Cav1 trimers or other more stabilized iterations [42] developed up to 100-fold higher NAb titers than those that received postfusion F trimers. Cotton rats immunized with the prefusion F trimer showed a high level of protection from RSV challenge, with no detectable viral replication in the lung and no evidence of vaccine-enhanced disease [43]. The prefusion RSV F protein vaccine is currently being tested in a human clinical trial [44].

The success of the prefusion RSV vaccine in animal models has strengthened the case for a structure-guided vaccine approach for other challenging targets such as HIV. This proof of concept suggests that viral strategies of antibody evasion might be overcome by identifying the epitopes that are most susceptible to protective antibody responses and using structural information to enhance their exposure or stability. Structure-guided vaccine approaches are now being employed in the HIV vaccine field. Recent progress towards the generation of potent HIV-specific NAbs was made when Sanders, Moore, and colleagues reported a method to generate stabilized, soluble HIV-1 Env trimers, termed SOSIPs, using a method similar to the prefusion RSV F vaccine [45,46] (discussed in Section 1.8). Alternative Env immunogens that are designed to elicit non-neutralizing antibodies, such as CD4-independent Envs (Chapter 2), may also be amenable to a structure-guided approach to increase the immunogenicity of epitopes of interest.

1.5. The Human Immunodeficiency Virus

HIV is the etiologic agent of the acquired immune deficiency syndrome (AIDS). An estimated 37 million people are infected with HIV globally, including 1.2 million in the United States [47,48]. HIV is a retrovirus of the lentivirus genus (*lente*-,

Latin for "*slow*"), and as such establishes a chronic, life-long infection in its host. HIV type 1 (HIV-1) group M ("major") is the predominant taxon of HIV infecting humans. Group M is further classified into the clades or subtypes A-D, F-H, J, K and several circulating recombinant forms (CRFs) (reviewed in [49,50]).

Like all primate lentiviruses, HIV-1 primarily infects $CD4^+$ T helper cells using CD4 as a primary receptor and a seven-transmembrane spanning chemokine receptor as a co-receptor to trigger membrane fusion with its envelope (Env) glycoprotein (reviewed in [51]). Transmitted-founder variants and other primary isolates of HIV-1 most commonly use CCR5 as a co-receptor; CXCR4 tends to be used in cases of more advanced disease, though it is unclear whether its usage is a cause or effect of disease progression [52–55]. After fusion, the virion contents are delivered into the cytosol, where capsid uncoating and reverse transcription occur [56,57]. The viral genome is shuttled into the nucleus and is integrated into the host chromosome by the viral integrase [58]. Viral transcripts are produced from the long terminal repeat (LTR) promoter, which is enhanced by the binding of the transcriptional activator Tat [59]. Viral protein production begins from multiply spliced RNA transcripts encoding for Tat, Rev, and the accessory protein Nef. The nuclear export factor Rev then allows for translation of singly spliced and unspliced transcripts, producing the other accessory proteins (Vif, Vpr, and Vpu), Env, and finally Gag and Gag-Pol from full-length genomic RNA [60]. Gag is a polyprotein that encodes multiple structural proteins required for the viral life cycle, including matrix, capsid, nucleocapsid, p6, and other peptides; Pol encodes the viral enzymes reverse transcriptase, integrase, and protease. Gag directs the budding of viral particles at the plasma membrane [61], and Env is incorporated into these virions in a process that is coordinated by the cytoplasmic tail and the matrix protein but remains poorly understood [62–65].

Once virions bud from the cell surface, protease cleaves Gag and Gag-Pol into functional subunits, and the virus is able to mediate a new round of infection.

HIV-1 infection results in an acute state of high viral replication, which partially contracts at the onset of the adaptive immune response, particularly cytotoxic T lymphocytes (CTLs) [66–68]. At this stage, viremia reaches a dynamic equilibrium called the set point, which is maintained throughout the clinically latent chronic phase of infection [69]. During this time, viral replication is ongoing and $CD4^+$ T cells turn over rapidly [70,71] due to direct cytopathic effects, immune clearance, and bystander effects such as pyroptosis [72]. Infected individuals experience high levels of systemic inflammation and immune cell activation, which, along with $CD4^+$ T cell count and plasma viral load, are predictors of disease progression [73]. In the absence of combination antiretroviral therapy (ART), infection can result in gradual fibrosis and degradation of the secondary lymphoid tissue architecture [74], a decline in peripheral $CD4^+$ T cells, and the emergence of opportunistic infections and malignancies, the defining features of AIDS [75,76].

ART has had remarkable success as a life-saving treatment for people infected with HIV-1 and as a highly effective pre-exposure prophylactic (PrEP) against HIV-1 infection [77–79]. However, there remain substantial barriers to the accessibility and affordability of life-long ART treatment, especially in developing countries [80]. Even in the presence of effective ART, a population of latently infected cells with transcriptionally quiescent but replication-competent virus persists indefinitely [81]. The latent reservoir is considered the principal barrier to developing a cure for HIV-1 infection, and the establishment and clearance of this reservoir are topics of intense research (reviewed in [82,83]). Additionally, chronic immune activation is not always eliminated by ART and may, in some individuals, lead to

non-AIDS morbidity and mortality [84,85]. A vaccine that offers durable protection from HIV-1 infection would therefore be of significant benefit to global public health.

1.6. Immune Evasion by HIV-1

HIV-1 is well adapted to evade control by the human immune system. This fact presents significant challenges for the host immune response to HIV-1 and for the design of effective therapies and prophylactics. HIV-1 is able to dysregulate or evade the innate, humoral, and cell-mediated arms of the immune system. The innate immune pathways undermined by HIV-1 include the type I interferon response [86], host restriction factor activities [87], and early cytokine signals that regulate innate and adaptive immune control as well as pathogenesis [88–90].

The cellular immune response is critical to maintain HIV-1 viremia at the set point but is also dampened by multiple mechanisms. The role of $CD8^+$ T cells in limiting viral replication is evident both during the partial resolution of acute viremia [66] and throughout the chronic phase of infection. In chronically SIV-infected macaques, antibody-mediated depletion of $CD8^+$ T cells results in a rapid increase in viral load, which returns to the set point once $CD8^+$ T cells repopulate [91]. Several alleles of MHC class I are associated with enhanced viral control in humans [92,93], further supporting a role for $CD8^+$ T cells in controlling viremia. Alleles B27 and especially B57 are enriched alleles among elite controllers, a small subset (<1%) of HIV-infected individuals who suppress viral replication beyond the limit of detection of commercial assays in the absence of ART [94–96]. These individuals have been shown to mount $CD8^+$ T cells expressing a higher level of perforin and other combinations of effector molecules compared with non-controllers [97,98]. Although cell-mediated immunity is beneficial in limiting HIV-1 disease progression, it is

undermined by the virus in multiple ways. First, the viral replication and error rates are high, and many viral proteins are able to tolerate substantial antigenic variation. As a result, escape mutants readily emerge to evade cytotoxic T cell responses [99,100]. HIV-1 further evades surveillance by $CD8^+$ T cells by down-regulating surface expression of the MHC class I proteins HLA-A and HLA-B via the Nef accessory protein [101–103] and HLA-C via the Vpu protein [104]. By infecting and eliminating $CD4^+$ T cells, HIV-1 reduces their ability to provide helper functions to $CD8^+$ T cells and B cells. In fact, HIV-1 has been shown to preferentially infect HIV-specific $CD4^+$ T cells and T follicular helper cells, two cell types that might contribute to immune control [105–107]. HIV-1 infection additionally results in a number of functional defects in uninfected $CD4^+$ and $CD8^+$ T cells, including anergy, exhaustion, and sensitivity to apoptosis [108–112].

The ability of HIV-1 to evade the humoral immune response is exceptional and is likely the most important immune evasion strategy with regard to vaccine protection from HIV-1 infection. Env is the only surface protein of HIV-1 and is thus the sole target of protective antibodies. Env is synthesized as a trimeric gp160 precursor with a single membrane-spanning domain. The precursor is cleaved in the Golgi by furin-like proteases [113] into gp120 (surface) and gp41 (transmembrane) subunits, which remain associated in a metastable configuration until receptor interaction. The mature Env trimer is heavily glycosylated in the endoplasmic reticulum (median of 93 N-linked glycosylation sites per trimer) and develops a mix of complex glycans and densely packed, immature high-mannose glycans, accounting for over 50% of the mass of gp120 [114,115]. This extensive and constantly evolving array of glycans, termed the “glycan shield” [116], constitutes a major obstacle to mounting protective antibody responses to against Env.

Carbohydrates naturally decorate self proteins, and responses to them are largely deleted from the B cell repertoire by self-tolerance mechanisms [117]. On the native HIV-1 Env trimer, there are minimal protein surfaces accessible to antibody binding without simultaneous interaction with carbohydrates [17]. HIV-1 also employs more direct forms of host mimicry in order to evade antibody binding: the membrane-proximal external region (MPER) of gp41 contains homology to two human proteins, kynureninase (KYNU) and splicing factor 3b subunit 3 (SF3B3), at epitopes recognized by the broadly neutralizing mAbs 2F5 and 4E10, respectively [118]. The host must therefore break self-tolerance to some degree in order to make NAbs against this sensitive epitope and others that include glycan moieties.

Beyond glycosylation, the Env trimer is folded such that one of its most conserved and neutralization-sensitive surfaces, the CD4 receptor binding site (CD4bs), is recessed in a cavity surrounded by glycans [17]. Structural studies of Env interacting with CD4bs-specific antibodies have demonstrated that this geometry [119,120] places constraints on the angle of approach of NAbs that may hamper their production. Additional conserved epitopes, such as the co-receptor binding site and the C1 constant region, are not exposed to solvent at the surface of the native protein or are only induced upon CD4 binding, i.e. CD4-induced epitopes [121,122]. In some cases, CD4-induced epitopes can be exposed on the surface of infected cells, particularly when CD4 is present, where they are sensitive to antibody binding and Fc-mediated effector functions [123,124].

HIV-1 further limits antibody responses to Env by maintaining a low level of Env expression on the surface of infected cells and on viral particles [125–127]. This is regulated in large part by the various endocytosis motifs and other intracellular trafficking signals present in the exceptionally long cytoplasmic tail of HIV-1 Env

(discussed in Chapters 3 and 5 and reviewed in [64,128]). HIV-1 viral particles incorporate a remarkably low number of Env trimers, only 7-14 per virion [125,126], thus reducing the probability of multivalent, high-avidity binding by Env-specific antibodies. This limits the efficiency of B cell receptor (BCR) cross-linking and may lead to poor activation of low-affinity naïve B cells [129]. Env expression is also maintained at low levels on the surface of infected cells and other Env-expressing cells, as in genetic and viral vector vaccines. As a result of low cell surface expression, Env-expressing cells are partially protected from antibody-dependent cell-mediated cytotoxicity (ADCC) and other Fc-mediated effector functions that can limit viral replication [130]. During ADCC, antigen expressed on the surface of infected cells is bound by IgG antibodies, which engage Fcγ receptor-bearing cells, particularly natural killer (NK) cells, activating them to release cytotoxic granules containing perforin and granzymes, similarly to CTLs [131,132].

The glycan shield that covers the Env ectodomain and the underlying protein surface are subject to extensive and ongoing antigenic variation. The Env nucleotide sequence divergence is approximately 15-20% and 25-35% for strains within and between subtypes, respectively [133]. Devising a vaccine strategy that elicits antibodies capable of binding to all or most of these strains is a major challenge. Infected individuals are capable of generating NAbs that exert selective pressure on HIV-1; however, these responses are invariably associated with the emergence of escape mutants, and they are often limited in breadth [116,134–136]. Diverse HIV or SIV strains can have drastically different sensitivities to antibody-mediated neutralization [137]. Most primary and transmitted-founder viruses are relatively neutralization-resistant and are designated “Tier-2” viruses [137]. In contrast, lab-adapted viral isolates tend to be highly neutralization-sensitive and are considered

"Tier-1." For an antibody or serum to confer significant protection in a vaccine, it is believed it must be able to neutralize genetically diverse Tier-2 strains. HIV-1 infection results in a spectrum of NAb breadth, which is directly correlated with viral load and $CD4^+$ T cell depletion [136,138]. After 2 to 4 years of untreated infection, about 20% of HIV-1 infected individuals generate NAb responses with some breadth. A smaller fraction of these individuals (~2%) develop broadly neutralizing antibodies that have exceptional breadth and potency against diverse HIV-1 isolates [138].

Broadly neutralizing antibodies (bNAbs) are a major goal of prophylactic HIV vaccines. In recent years, dozens of potent and broad NAbs have been isolated from HIV-1-infected individuals (reviewed in [139]). In numerous passive transfer experiments in nonhuman primates, bNAbs have conferred sterilizing immunity against chimeric HIV-1/SIV (SHIV) viruses bearing HIV-1 Env, demonstrating their likely efficacy in an HIV-1 vaccine [140–146]. However, bNAbs typically exhibit one or more highly unusual properties that make them a difficult vaccine goal: (i) Many contain a high degree of somatic hypermutation, i.e. genetic divergence from the germline-encoded immunoglobulin gene segments. The average nucleotide mutation frequency in the heavy chain of available HIV-1 bNAbs is over 20%, or even 30% for some CD4bs-specific bNAbs, while this figure is often 10% or less in antibodies induced by licensed vaccines and experimental HIV-1 vaccines [147–149]. (ii) Many have a long heavy chain complementarity-determining region 3 (HCDR3) of >30 amino acids, compared to an average of ~15 amino acids [147,149]. In the case of bNAbs PG9 and PG16, which bind to glycan-dependent epitopes involving variable loops 1 and 2 (V1V2), the long HCDR3 forms a loop that protrudes out and contacts a small conserved area of protein surface in between two glycans [150,151]. (iii) Many are autoreactive and polyreactive with various self antigens [152]. This is true

for some MPER-specific bNAbs that interact in part with the cellular membrane and also for those that interact with glycans. This property suggests that some degree of tolerance bypass may be required for certain bNAb lineages. For all the above reasons, the generation of bNAbs represents a formidable challenge for HIV-1 vaccines using conventional designs. As discussed in the following sections, however, there may be more feasible alternative viable paths to HIV-1 vaccine protection that are currently being pursued alongside the bNAb strategy.

1.7. History of HIV-1 Vaccine Trials

Numerous experimental HIV-1 vaccines have been tested in humans within the last few decades, mostly in small Phase I and II trials to establish safety and immunogenicity (reviewed in [153]). To date, six large efficacy trials have been completed, and one is ongoing (see details in Table 1.1). The traditional approaches of live attenuated or inactivated virus vaccines have unacceptable safety risks for HIV-1 due to the possible emergence of a pathogenic virus, so HIV-1 vaccines have made use of newer technologies such as recombinant protein, nucleic acid vectors, and non-HIV viral vectors. However, due to the poor performance of experimental HIV-1 vaccines in animal models and humans, including a complete inability to elicit bNAbs, HIV-1 vaccine trials have necessarily been guided by an empirical approach, often with little proof-of-concept data to support them. Though this has been criticized as futile or counterproductive, at least one such trial has provided some in the field with renewed hope that an effective vaccine for HIV-1 might be possible.

HIV-1 vaccine efficacy trials have so far evaluated three vaccine formats: protein subunit, adenovirus vector with or without DNA priming, and poxvirus prime with protein subunit boost. The first two trials, Vax004 and Vax003, aimed to induce

protective antibodies using purified recombinant gp120 protein in alum adjuvant. Despite the absence of supporting preliminary data, two formulations of gp120 based on different clades (AIDSVAX B/B' or B/E) were evaluated in thousands of volunteers. Both trials elicited low, transient levels of NAbs with no Tier-2 activity and had no efficacy in preventing HIV-1 infection or reducing the viral set point [154,155].

Study	Phase	Immunizations	Start	End	Institutions	Volun-teers	Population	Vaccine efficacy	Refs.
Vax004	3	AIDSVAX B/B': 600 µg gp120 with 600 µg alum i.m. at mo. 0, 1, 6, 12, 18, 24, 30	1998	2003	VaxGen	5,417	MSM, other high risk (N. America & Netherlands)	None	[154]
Vax003	3	AIDSVAX B/E: 600 µg gp120 with 600 µg alum i.m. at mo. 0, 1, 6, 12, 18, 24, 36	1999	2003	VaxGen	2,546	Injection drug users (Thailand)	None	[155]
STEP/ HVTN 502	2b	Ad5 (*gag*, *pol*, *nef*), $1.5x10^{10}$ vp ea., at wk 0, 4, 26	2004	2007	Merck, HVTN	3,000	MSM, other high risk (Americas, Australia)	-28.6% (*P*=0.03)	[161,164]
Phambili/ HVTN 503	2b	Ad5 (*gag*, *pol*, *nef*), $3x10^{10}$ vp ea., at wk 0, 4, 26	2007	2010	Merck, HVTN	801	Sexually active adults (South Africa)	-77.8% (*P*=0.01)	[162,164]
HVTN 505	2b	DNA (*gag*, *pol, nef, envs*), 4 mg i.d. at wk 0, 4, 8; Ad5 (*gag-pol*, *envs*), 10^{10} vp i.m. at wk 24	2009	2013	VRC, HVTN	2,530	MSM, Ad5-neg., circumcized (U.S.)	None	[178]
RV144	3	ALVAC (gag/pro/env) i.m. at wk 0, 4, 12; ALVAC +AIDSVAX B/E' i.m. at wk 12, 24	2003	2009	Thai Ministry of Public Health, U.S. Army	16,402	Adults age 18-30 (Thailand)	31.2% (*P*=0.04)	[187]
HVTN 702	2b/3	ALVAC *(gag/pro/env)* i.m. at mo. 0, 1; ALVAC+gp120/MF59 at mo. 3, 6, & 12	2016	2021	U.S. Army, HVTN	~5,400	Sexually active adults (South Africa)	n/a	[214]

Table 1.1. Completed and ongoing clinical efficacy trials of HIV-1 vaccines. Abbreviations: ALVAC = recombinant canarypox vector; HVTN = HIV Vaccine Trials Network; VRC = Vaccine Research Center at NIH; Ad5 = adenovirus serotype 5 vector; MSM = men who have sex with men; vp = viral particles.

After the disappointing conclusion of these antibody-based trials, interest intensified in eliciting T cell-based immunity that might control ongoing viral replication, if not prevent infection altogether. A promising report by Shiver and colleagues in 2002 showed that a replication-incompetent adenovirus serotype 5 (Ad5) vector expressing SIVmac239 Gag elicited strong $CD8^+$ T cell responses in rhesus macaques [156]. When the macaques were challenged with a high intravenous dose of pathogenic SHIV 89.6P, they became infected but showed reductions in viremia and AIDS-related disease. However, follow-up studies soon

showed that much of the protective effect could be attributed to the MHC class I allele *Mamu-A*01* in vaccinated macaques [157–159]. Additionally, when Ad5-vaccinated animals were challenged with wild-type SIVmac239 instead of SHIV 89.P, they had little protection from viremia or disease progression [160], calling into question whether this vaccine approach would be successful in humans.

Nonetheless, Ad5-based vaccine regimens have advanced to efficacy testing, beginning with the Merck STEP [161] and Phambili [162] clinical trials. Both trials immunized participants with Ad5 vectors encoding Gag, Pol, and Nef. While the vaccine elicited antigen-specific $CD8^+$ T cells in the majority of individuals [163], no efficacy was observed in either study, either in preventing infection or reducing the viral set point. The STEP study was terminated three years into its operation when pre-specified conditions of futility were met. The Phambili study, just started, was also halted. Unexpectedly, the Merck Ad5 vaccine in both trials caused an increased risk of HIV-1 infection relative to placebo (combined hazard ratio of 1.4 as of 2014) [164]. The possible risk factors (e.g. Ad5 seropositivity, male circumcision status) and mechanisms of this increased rate of infection have been the topic of extensive research, although these questions still remain controversial [161,164–176].

In 2009, the HVTN 505 efficacy trial was launched to test DNA plasmid primes followed by an Ad5 vector boost [177,178]. Both components encoded Gag, Pol, and Nef from clade B and Envs from clades A, B, and C. This regimen was developed to elicit broad T and B cell-based immunity and had showed a modest protective effect against heterologous SIV challenge in rhesus macaques [179]. In humans, the DNA/Ad5 vaccine induced moderate $CD4^+$ and $CD8^+$ T cell responses and low NAb responses. It did not generate any protection against acquisition of HIV-1 or subsequent viremia, and the trial was halted in 2013 due to futility.

Collectively, the results of the three Ad5-based trials were disappointing for the prospects of eliciting protection against HIV-1 through conventional T cell responses. They additionally raised important questions about the usefulness of the SIV and SHIV challenge models for predicting vaccine efficacy in humans [180,181]. It is not clear which aspects of the macaque model failed to reflect HIV-1 acquisition in humans, but relevant factors may include the titer and route of viral inoculum, the pathogenicity and neutralization resistance of the challenge virus(es), the genetic diversity within the challenge stock, host genetic factors, and species-specific responses to vaccine vectors. Despite the drawbacks of Ad5, research has continued into alternative, rare, or non-human serotypes of adenovirus that would elicit T cell responses with greater breadth or functionality and that would not raise concerns about pre-existing immunity and enhanced HIV-1 infection [182–186].

In contrast to these disappointing vaccine trials, one Phase III vaccine trial did exhibit some degree of efficacy: the RV144 “Thai” trial, sponsored by the U.S. Army and conducted by the Thailand Ministry of Public Health from 2003 to 2006 [187]. The RV144 regimen consisted of four injections of replication-incompetent canarypox vector (ALVAC) expressing Gag, Env, and protease antigens and two injections of the AIDSVAX B/E gp120 in alum. This regimen combined two vaccine components that, individually, had shown little promise to confer protective immunity [154,155,188–190]. With RV144, it was speculated that the combination of two weakly immunogenic vaccines might generate a more protective immune response than either component alone. The decision to press ahead with the RV144 trial despite the lack of supporting data was heavily criticized [191]. Nonetheless, the trial proceeded as planned, and over 16,000 volunteers received vaccine or placebo. Surprisingly, the results of the trial revealed 31.2% vaccine efficacy (95% CI: 1.1-

52.1%; *P* = 0.04) in preventing HIV-1 infection relative to placebo after 42 months of follow-up (Fig. 1.2). In a post-hoc analysis, vaccine efficacy appeared to be higher after 12 months of follow up, at 60.5% (95% CI: 22-80%), suggesting that there may have been substantial early protection that waned rapidly after one year. This result has reinvigorated the HIV vaccine field and has significantly influenced the course of vaccine discovery research, including the work presented here.

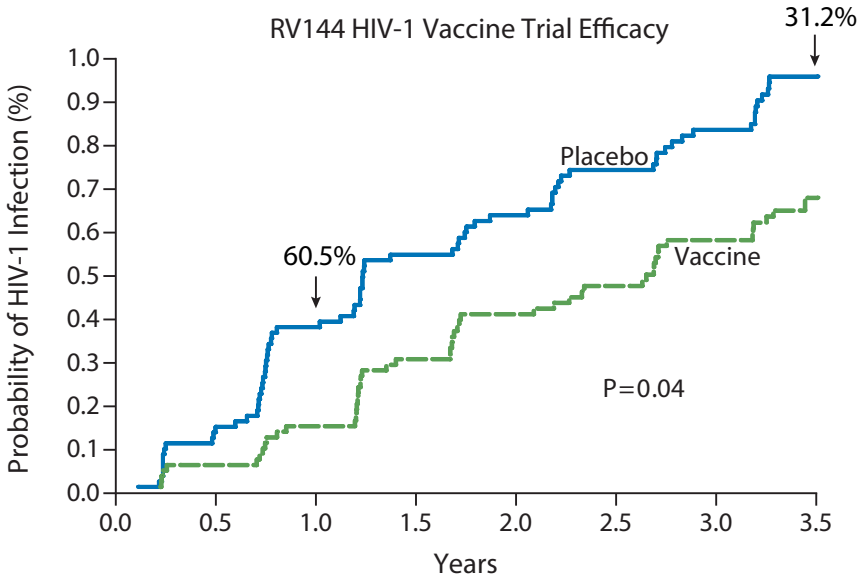

Fig. 1.2. Probability of infection in the RV144 HIV vaccine trial in Thailand. Shown is the proportion of volunteers in placebo and vaccine groups diagnosed with HIV-1 infection over time, with vaccine efficacies indicated with arrows. Analysis is limited to the modified intention-to-treat group, who were not HIV-1-infected at the time of enrollment. The figure is reproduced with permission from Rerks-Ngarm et al., *NEJM* 2009 [187], copyright Massachusetts Medical Society.

An extensive analysis of the immune correlates of protection was conducted on samples from RV144 vaccinees [192]. In the absence of natural protective immunity to HIV-1 infection, such analyses contribute critical insights into which immune cell functions and antibody activities are protective in humans, and basic research can be directed to understand how to better elicit such activities. Interestingly, the level of NAbs in RV144 was lower than in the Vax003 trial using

gp120 only [193]. RV144 vaccinee plasma had no Tier-2 activity and only low and transient Tier-1 activity. Despite this, the vast majority of vaccinees made binding antibody responses against Env, and the strongest correlate of protection was IgG directed to V1V2, a domain at the apex of the Env trimer (odds ratio = 0.57 per S.D., P = 0.02) [192]. This binding activity was measured against a scaffold protein containing the V1V2 sequence genetically fused to a murine leukemia virus (MLV) gp70 protein. The other significant correlate was Env-specific plasma IgA, which directly correlated with infection (odds ratio = 1.54 per S.D., P = 0.03). An interaction analysis found that, within vaccinees with low Env-specific plasma IgA, multiple additional variables inversely correlated with infection, including Env-specific IgG avidity, NAbs, ADCC, and the Env-specific $CD4^+$ T cell response.

The RV144 immune correlates study suggested that non-neutralizing antibodies might contribute to protection from HIV-1 infection in humans. This was an unexpected result: while Fc-dependent functions have been shown to augment the protective effect of passively transferred NAbs in nonhuman primates [145], they have not yet demonstrated protection in the absence of neutralizing activity [194,195]. This led to the hypothesis that the partial protection in RV144 was due to ADCC or other Fc-mediated effector functions, such as infectious virion capture, antibody-dependent cell-mediated phagocytosis or viral inhibition, or complement deposition. The ADCC theory was supported by a number of studies that followed. Bonsignori and colleagues found that up to 90% of RV144 vaccinees generated ADCC activity against cells coated with gp120 [196]. ADCC-mediating mAbs were isolated from RV144 vaccinees and bound predominantly to the epitope of A32, a C1-specific mAb that also mediates potent ADCC [196,197]. The A32 epitope and adjacent regions have been extensively characterized as sensitive targets of ADCC-

mediating antibodies [198,199] and are typically exposed upon engagement with CD4 and/or on the surface of infected cells [123,124,200]. RV144 vaccinee plasma also contained IgA antibodies that bound to the A32 epitope and blocked ADCC mediated by purified IgG from vaccinees [201], offering a potential mechanism for the direct correlation of plasma IgA with infection risk. Another portion (~13%) of mAbs isolated from RV144 vaccinees bound to a relatively conserved linear peptide epitope in the V2 loop (residues 163-183 in HXB2 numbering). Two such mAbs, CH58 and CH59, recognized the V2 peptide folded into different secondary structures, but both were dependent on amino acids K169, H173, F176, and Y177 [202]. Both bound to Env on the surface of infected cells but did not have broad or potent neutralizing activity. Importantly, these mAbs were shown to mediate potent ADCC and synergized with C1-directed antibodies in this activity [202,203]. The linear V2 peptide was shown to be a commonly targeted epitope in RV144 vaccinee plasma [202,204,205]. Finally, a genetic “sieve” analysis of viruses that established infection in RV144 participants demonstrated that there was significant selection against V2 residue K169 in vaccinees relative to placebo recipients [206,207]. This suggested a protective role of V2-specific antibodies by an orthogonal approach, although *bona fide* protection by passive transfer has yet to be established.

Recent data offer some clues as to why RV144 appeared to generate partial protection, while its two individual components had failed. After RV144, it was discovered that one of the AIDSVAX gp120s, from strain A244, exhibited increased antigenicity for antibodies binding to C1, V2, and V1V2 epitopes fortuitously as a result of an N-terminal deletion of 11 amino acids, which had facilitated purification of monomeric protein [208]. Another study comparing the antibody responses in RV144 and Vax003 demonstrated that the ALVAC prime was crucial to suppress the

generation of IgG4 subclass antibodies, which have poor Fc-mediated ADCC activity and may block the more effective subclasses, IgG1 and IgG3 [209].

If the model of vaccine efficacy in RV144 is true and reproducible, it would suggest that an effective antibody-based vaccine for HIV-1 is feasible. Among a panel of C1 and V2-specific mAbs from RV144, the average somatic mutation frequency of the heavy chain was very low, at about 2.4% [196,202]. This has two important implications: (i) that non-neutralizing, antiviral antibodies that bind to C1 and V2 do not require extensive somatic hypermutation and are therefore an achievable goal given the limitations of current vaccine technology, and (ii) that there is likely much room for improvement of the RV144 vaccine regimen through increasing affinity maturation and somatic hypermutation.

Multiple clinical trials have been launched to validate the findings of RV144 and expand its approach to other geographic areas where different clades of HIV-1 circulate [210–214]. The RV305 and RV306 trials, started in 2012-2013, aim to characterize the immune response to additional booster immunizations other variations of the RV144 vaccine regimen [212,213]. In RV305, 176 people who participated in RV144 received two additional boosts with ALVAC canarypox and/or AIDSVAX gp120 6 to 8 years after the end of the initial trial. This intervention raised the titer of Tier-1 NAbs, increased the frequency of mutations in the variable heavy chain gene segment in gp120-specific mAbs from 3.1% to 6.9%, and significantly increased the proportion of gp120-specific mAbs with HCDR3 loops longer than 22 amino acids [215]. Further investigation is needed to determine whether these antibodies are more protective. Several more trials are planned to optimize other aspects of the RV144 regimen, including the poxvirus vector, adjuvant, dosing schedule, and antigen sequence [216]. Notably, clade C versions of the ALVAC

vector and gp120 protein have been constructed for use in South Africa, and the alum adjuvant has been replaced with MF59. The initial evaluation of this vaccine in HTVN 100 showed excellent immunogenicity compared with RV144, including frequent V1V2-specific antibody responses [217]. However, caution has been urged by a recent study in an SIV/macaque model of the RV144 regimen showing that, while MF59 was more effective than alum in generating Env-specific IgG and multiple Fc-dependent activities, only alum was associated with protection from SIV infection [218]. Nonetheless, the MF59-adjuvanted vaccine is advancing into a large efficacy trial, HVTN 702, in Southern Africa, with results anticipated in 2021 [214].

1.8. The Future of Vaccine Design for HIV-1

In the wake of the multiple failed HIV-1 vaccine trials and the partially successful RV144, the HIV-1 vaccine field now appears to be taking three broad approaches. The first involves incrementally building on the success of RV144. Much of the optimization of the RV144 regimen is being conducted empirically in human clinical trials, as outlined in Section 1.7. Other insights can be gained by studying modifications to poxvirus prime-protein boost regimens in animal models, as in Chapters 2 and 3 of this dissertation. More targeted vaccine approaches attempt to elicit specific non-neutralizing antibody specificities or functions that were associated with protection in RV144, in particular binding to the V1V2 domain and V2 peptide epitope. For example, scaffolded V1V2 immunogens were recently shown in guinea pigs to efficiently elicit V1V2-specific IgG that mediated antibody-dependent cell-mediated phagocytosis [219]. The work presented in Chapter 2 regarding the immunogenicity of the V2 peptide in CD4-independent Envs is also directly relevant to this research interest.

The second heavily pursued approach to an HIV-1 vaccine is based on the generation of bNAbs using a variety of rational design strategies (reviewed in [220]). One idea is to mimic the events that naturally lead to the development of bNAbs in HIV-1-infected individuals. Researchers are characterizing the co-evolution between virus and antibodies in these individuals [221–223] in order to generate a series of Env immunogens that could guide the development of bNAb specificities in a vaccine context [224,225]. Other bNAb-focused strategies include the engineering of Env immunogens to specifically activate the germline precursors of bNAbs, which frequently do not recognize wild-type Env trimers and thus are not expanded by conventional immunogens [226–232]. A related strategy aims to generate bNAbs that can accommodate glycans by first priming with Envs lacking glycosylation sites, and later boosting with the natively glycosylated Env [17]. Other approaches have attempted to generate bNAbs by perturbing the normal B cell processes of survival, activation, and tolerance checkpoints, with the rationale that bNAb lineages may be disfavored by normal tolerance mechanisms [233–235].

Most notably among the bNAb strategies, stabilized soluble Env trimers have been constructed in much the same way as done for the RSV prefusion trimer vaccine. Real-time analysis of Env conformational dynamics suggests neutralization resistance is related to the proportion of time the trimer spends in a closed versus open conformation [236]. A model has emerged in which neutralization of Tier-2 Envs occurs only when an antibody binds specifically to the compact, ground-state trimer with high affinity [237]. In this context, promising immunogens have been devised by engineering soluble HIV-1 Env trimers that are stabilized in their closed ground-state conformation. The first iteration of the stabilized soluble trimer is the SOSIP, named for the mutations I559P (IP), promoting trimerization, and A501C and

T605C, creating a disulfide bridge (SOS) between gp120 and gp41 [238] (depicted in Fig. 1.3). The SOSIP was also engineered to have a more efficient cleavage site in between gp120 and gp41 [239] and a premature stop codon before the MPER region, at position 664, to prevent aggregation [240]. A stable and compact SOSIP was first engineered from clade A Env BG505 and was shown to react specifically to HIV-1-specific NAbs but not non-NAbs [45]. This reagent permitted a series of breakthroughs in structure-guided vaccine design for HIV-1, including the first crystal structure of a trimeric HIV-1 Env [241–243]. Immunization of rabbits and macaques with SOSIPs generated strain-specific Tier-2 NAbs [46], an impressive accomplishment, but alternative strategies are needed to generate broader neutralizing activity.

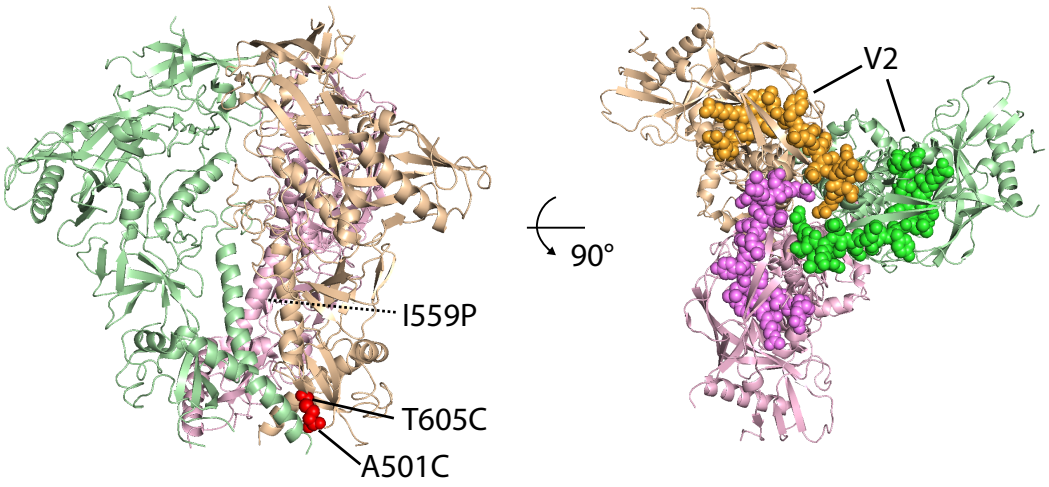

Fig. 1.3. Structure of the stabilized Env trimer of BG505 SOSIP.644. At left, red spheres indicate the mutations A501C and T605C that form a stabilizing disulfide bridge, while only the general area of I559P is shown, as that residue was not ordered in the crystal structure. At right, the V2 peptide epitope (HXB2 a.a. 163-183) is shown as spheres. Images were adapted in Pymol from PDB 4TVP (Pancera et al., *Nature* 2014) [243].

It has been proposed that the Tier-2 NAb response generated against stable Env trimers are primarily directed at “glycan holes,” or patches of exposed peptide surface in between glycans [244]. Unfortunately, the glycan holes vary considerably

strain to strain; consequently, such Tier-2 NAbs are not broadly neutralizing. A range of ongoing research efforts seek to improve the breadth of this response, including: (i) further increasing the stability of soluble trimers [245], (ii) generating stabilized trimers from multiple Env strains to be used in combination [246–248], (iii) deleting glycans to prime epitope-specific responses [17,249], (iv) increasing the multivalency of trimer presentation [250], and (v) investigating ways to enhance somatic hypermutation (discussed further below).

A third approach in HIV-1 vaccine design is to forego the generation of Env-specific antibodies and elicit protection through cell-mediated immunity. Although conventional T cell-based vaccines have failed in clinical trials, Hansen, Picker, and colleagues have described a highly unusual type of $CD8^+$ T cell response elicited by a rhesus cytomegalovirus vector that completely eliminates SIV infection after acute viremia in 50% of challenged macaques [251,252]. The CD8 response is of an effector phenotype, is extremely broad in terms of SIV proteomic coverage, and includes unusual MHC class II- and MHC class I E-restricted responses [253–255]. Plans are underway to test the applicability of this approach in humans [256].

These alternative immunogen concepts and structure-guided vaccine designs have generated optimism for an effective HIV-1 vaccine. However, there remain important questions about the optimal way to display or deliver the immunogens in order to generate desirable antibody responses. These topics are a focus of Chapters 2–4 of this dissertation. One of the most fundamental of these questions is how to promote higher levels of antibody somatic hypermutation and affinity maturation. These processes are viewed as key to generating HIV-1 bNAbs, given their unusually high rate of somatic mutation and the likely requirement to develop high affinity for poorly immunogenic surfaces that include glycan moieties [257]. In

order to increase somatic hypermutation and affinity maturation, it will be necessary for future vaccines to potently activate the immune cells that execute and regulate this process: germinal center B cells and T follicular helper cells.

1.9. The Germinal Center Reaction and T Follicular Helper Cells

The germinal center (GC) reaction occurs within the B cell follicles of secondary lymphoid tissue, when B cells proliferate and mutate in response to antigenic stimulation (reviewed in [258]). They are composed of a “dark zone” of rapidly proliferating B cells or centroblasts and a “light zone” of non-proliferating B cells or centrocytes. In the dark zone, centroblasts express activation-induced cytidine deaminase (AID), an enzyme required for class-switch recombination and somatic hypermutation. Class-switching refers to the B cell transition from secretion of the IgM antibody isotype to IgG, IgA, or IgE. Somatic hypermutation describes the accumulation of non-germline-encoded mutations within the variable immunoglobulin gene segments, which can result in increased or decreased affinity for antigen. When GC B cells cycle from dark zone to light zone, they bind and internalize antigen presented on follicular dendritic cells. Through a process of natural selection, only the highest-affinity B cells are able to capture a limiting amount of antigen. Captured antigen is proteolytically processed into peptide epitopes, which are presented on MHC class II to cognate $CD4^+$ T helper cells in the follicle, termed T follicular helper (Tfh) cells (reviewed in [259,260]). Tfh cells provide survival and proliferation signals to GC B cells in the form of the peptide-MHC/T cell receptor interaction, CD40/CD40L interaction, and secretion of IL-21 and other cytokines. B cells that do not receive these signals due to low-affinity BCRs are eliminated by apoptosis. Those that are activated may undergo repeated cycling through the dark

and light zones, iteratively increasing the antibody affinity to nanomolar levels and driving differentiation of GC B cells into memory B cells and long-lived, antibody-secreting plasma cells that reside in the bone marrow [261,262].

Tfh cells, first described in 2000, are a $CD4^+$ T cell subset that localizes to the B cell follicle [263,264]. Tfh cells highly express CXCR5, which allows for homing to CXCL13 expressed in the follicles and serves as a distinguishing marker of Tfh cells along with high levels of PD-1 and the transcriptional regulator Bcl6. Tfh cells are the critical drivers of the GC processes of somatic hypermutation, affinity maturation, and long-lived plasma cell generation. However, the factors that contribute to Tfh differentiation are poorly understood. A few studies have begun to elucidate the factors that positively and negatively regulate Tfh cell development. Notably, Locci and colleagues took an unbiased approach and tested a panel of over 2,000 secreted proteins for factors that inhibited or promoted differentiation of $CD4^+$ T cells *in vitro* into Tfh-like cells expressing CXCR5 and PD-1 [265]. They identified activin A as the most potent promoter of Tfh marker expression, although the mechanism is unknown. In contrast, multiple type I interferons (IFNs) were among the most potent inhibitors, a finding in accordance with other studies [266,267].

Extensive hypermutation is a cardinal feature of HIV-1-specific bNAbs; therefore, HIV-1 represents an obvious target for efforts to specifically promote Tfh and GC B cell responses [149]. Indeed, the Tfh-dependent generation of high-affinity and long-lived antibody responses is relevant for protection against most viruses. For acute viruses that do not constitute difficult vaccine targets, strategies that enhance Tfh and GC B cell responses would likely serve to improve vaccine efficacy, decrease the required doses and the need for booster immunizations, and strengthen our ability to respond to rapidly emerging epidemics.

1.10. Vaccine Design for Emerging Acute Viruses

While the greatest challenges in vaccinology arguably derive from chronically infecting viruses like HIV-1 and HCV, there are also substantial hurdles to effective vaccine design for acute viral illnesses, especially those causing emerging epidemics. Current technology and regulation do not allow for rapid, large-scale deployment of new vaccines against rapidly emerging viruses. The 2014-2016 outbreak of Ebola virus in West Africa offers an informative example. The first cases of Ebola were identified in March of 2014 [268]. Over the next 2 years, an estimated 28,600 people became infected with Ebola and 11,300 died [269]. While the public health response to Ebola was rapid, vaccine development lagged far behind. During the final months of the epidemic, an experimental vaccine made with recombinant vesicular stomatitis virus expressing the surface glycoprotein of Ebola virus Zaire (rVSV-ZEBOV), first described in 2005 [270], was evaluated for safety, immunogenicity, and efficacy in humans. This trial concluded that the rVSV-ZEBOV vaccine had extremely high efficacy (100%, 95% C.I. 75-100%) [271], and stockpiles were ordered to combat future epidemics [272]; however, by this time in late 2015, the epidemic had already been contained. Thus, the slow pace of manufacturing and safety testing renders modern vaccine development impractical for rapidly emerging diseases. It is also worth noting that rVSV-ZEBOV vaccination was associated with moderate adverse reactions, such as fever and arthritis, suggesting that a safer vaccine would be more suitable for mass preventive vaccination efforts. The ideal vaccine platform to respond to similar outbreaks would have the following characteristics: (i) versatility for use with diverse pathogens, (ii) a consistent record of safety and potent immunogenicity, preferably after a single immunization, and (iii) amenability to rapid and large-scale manufacturing. The need for a more rapid

response to emerging viral infections was made apparent again during the recent explosive reemergence of Zika virus.

1.11. The Origins and Reemergence of Zika Virus

Zika virus (ZIKV) is an enveloped, single-stranded, positive-sense RNA virus of the family *flaviviridae*. It is closely related to the dengue viruses (DENV), with ~56% amino acid identity to each of the four DENV serotypes on the amino acid level [273]. The first isolation of ZIKV occurred in 1947, when Dick and colleagues installed sentinel rhesus macaques in cages in the canopy of the Zika Forest, Uganda [274]. Their objective was to monitor mosquito-borne infections and to collect new isolates of yellow fever virus, another flavivirus that was prevalent in the monkey population of the Zika Forest. Serum was collected from a sentinel monkey with an elevated body temperature and was injected intracerebrally into mice. A filterable, transmissible agent was isolated from the infected brain that caused weakness, paralysis, and death in mice and a mildly symptomatic infection in rhesus macaques [275]. The agent was not neutralized by convalescent sera from other known viral infections and was therefore deemed a new virus and named for the forest in which it was first isolated. Serological surveys of monkeys and humans in the 1950s–1980s suggest that ZIKV or a close relative was endemic to much of sub-Saharan Africa and South and Southeast Asia, without any known association with significant disease symptoms (reviewed in [276]). The primary vector of ZIKV infection in humans is considered to be the *Aedes aegypti* or yellow fever mosquito, although sexual transmission has also been documented [277,278].

In the 2000s, ZIKV reemerged in a series of outbreaks in naïve populations in the Pacific islands. Epidemics occurred first on Yap Island of Micronesia in 2007,

then in French Polynesia, New Caledonia, Cook Islands, and Easter Island in 2013 and 2014 (reviewed in [276]). In 2015, the virus arrived in Brazil and initiated a major epidemic involving South America, Central America, and limited parts of the United States. By early 2017, an estimated half million to 1.5 million people in the western hemisphere were infected with ZIKV. Previous to this, ZIKV infection in humans was associated with asymptomatic, mild, or moderate illness, with common symptoms of fever, maculopapular rash, and conjunctivitis. More recently, it has become apparent that ZIKV infection can rarely (~2 in 10,000 infections) have severe neurological outcomes, such as Guillain-Barré syndrome [279], an autoimmune-mediated and potentially lethal paralytic disorder. Most alarmingly, the recent spread of ZIKV has been associated with a range of birth defects including microcephaly in infants born to women who were infected with ZIKV during pregnancy. Microcephaly is defined by head circumference below the third percentile for infants of the same height and weight, and it is characterized by a profound loss of cerebral cortex and other brain structures [280,281]. As a result, infants born with microcephaly suffer a range of profound neurological and cognitive impairments, including poor motor control, difficulty swallowing, developmental delays, hearing or vision loss, and seizures. The causal link between ZIKV and microcephaly was first suggested by a temporal association; then, ZIKV RNA was detected in the placenta and brain of microcephalic fetuses or neonates [282,283], and susceptible animal models recapitulated fetal ZIKV symptoms of central nervous system infection, intrauterine growth restriction, and abortion [284–287]. A longitudinal study of Brazilian pregnant women who presented to the clinic with a rash showed that 30% of the ZIKV RNA(+) women gave birth to children with congenital defects, and earlier infection during pregnancy was associated with more severe birth defects [288]. Between 2015 and

2016, an estimated 5,000 cases of microcephaly occurred throughout Latin America. While Brazil experienced about 40% of the outbreak's ZIKV infections, it suffered 80% of microcephaly cases [289]. The biological, social, and economic factors that contributed to this disparity are as yet unknown.

Given the severity and rapidity of the 2015-2016 ZIKV epidemic, the World Health Organization (WHO) declared it a global public health emergency from February until November of 2016. The epidemic was addressed with mosquito-control measures and educational outreach, but a vaccine would have been the most effective way to prevent ZIKV infection and microcephaly, especially in some Brazilian communities where mosquito control is minimal and legal and religious norms discourage contraception and abortion. WHO and UNICEF issued a vaccine target product profile in July of 2016 specifying that the ideal vaccine for ZIKV would be a non-replicating vector that stimulates durable protective immunity with a single injection, with minimal adverse reactions [290].

1.12. Vaccine Approaches for Zika Virus

Like other flaviviruses, ZIKV infection of humans results in the development of potent NAb titers and likely protective immunity [291]. Therefore, there is a great optimism for the feasibility of an effective vaccine. ZIKV virions are encapsulated in a shell of 180 copies of the envelope (E) protein paired with the membrane (M) protein, the proteolytically processed form of the pre-membrane precursor (prM) [292,293]. These proteins are arranged on the viral membrane in a herringbone pattern with icosahedral symmetry. The E protein covers most of the virion surface and is the major target of NAbs to ZIKV. E protein features only a single glycosylation site and is therefore a relatively simple target for neutralization. Most, if

not all, vaccine designs for ZIKV have aimed to elicit NAbs against the E protein (reviewed in [294]). The experimental ZIKV vaccine approaches published to date are listed in Table 1.2 and summarized below.

Vaccine type(s)	Immunizations	Animals	Peak NAb titers	Protection from ZIKV challenge	Year	Reference
DNA, PIV	50 µg DNA (M-E) i.m. (x 1 or 2); 1 µg PIV with alum i.m. or s.c.	Mice	MN ~1,000 (DNA x 2)	Undectable viremia (DNA or PIV)	2016	Larocca, Abbink, et al. [295]
DNA, PIV, RhAd52	5 µg PIV with alum i.m. x 2; 5 mg DNA (M-E) i.m. x 2; RhAd52 10^{11} vp i.m. x 1	Rhesus macaques	MN 5,000 (PIV), ~200 (DNA and RhAd52)	Undectable viremia (DNA, PIV, RhAd52)	2016	Abbink, Larocca, et al. [297]
DNA	1 or 4 mg prM-E DNA x 1 or 2 with needle-free injector	Mice, Rhesus macaques	RVP ~8,000, MN ~1,300, & FRNT ~1,600	Undetectable viremia in 94% of macaques (2 doses DNA)	2016	Dowd, Ko, et al. [298]
E protein subunit, Ad5	E ectodomain+foldon: Ad5 10^{11} vp s.c. wk 0, i.n. wk 2; purified protein, 20 µg i.d. in CMC-MNA wk 0, 2 i.d.	Mice	PRNT ~1,000 for Ad5	No disease in passively immunized 7 day old pups	2016	Kim et al. [300]
DNA + EP	prM-E DNA 25 µg i.m. x 3 in mice or 2 mg i.d. x 2 in macaques, with CELLECTRA electroporation	Mice, Rhesus macaques	PRNT ~500 in macaques	100% and 80% survival in active and passive immunization of IFN-deficient mice	2016	Muthumani et al. [299]
mRNA-LNP (m1Ψ, purified) *	prM-E m1Ψ-modified, HPLC-purified mRNA-LNPs, 1x 30 µg i.d. in mice or 50-600 µg in macaques	Mice, Rhesus macaques	RVP 10^4-10^5, PRNT/FRNT 400-1000	Undetectable viremia in mice; 99-100% reduced viremia in macaques	2017	Pardi, Hogan, et al. [307]
mRNA-LNP (m1Ψ)	prM-E m1Ψ-modified mRNA-LNP, 10 µg i.m. x 1 or 2	Mice	RVP 10^4-10^5	100% survival in IFN-deficient mouse models (2 doses), reduced ADE	2017	Richner, Himansu et al. [306]
Live attenuated	Live ZIKV with 10 nt deletion in 3' UTR, 10^4 IFU s.c. x 1	Mice	mMN 10^3-10^4	Undetectable viremia inIFN-deficient mice	2017	Shan et al. [301]

Table 1.2. Preclinical ZIKV vaccine publications to date. Abbreviations: PIV = purified inactivated virus; RhAd52 = rhesus adenovirus serotype 52 vector; m1Ψ = 1-methylpseudouridine (modified nucleoside); (pr)M-E = (pre)membrane-envelope protein; vp = viral particles; EP = electroporation; (m)MN = (modified) micro-neutralization assay; RVP = reporter viral particle neutralization assay; PRNT/FRNT = plaque/focus reduction neutralization test; LNP = lipid nanoparticle; IFU = infectious focus units; CMC-MNA = carboxymethyl cellulose microneedle array; ADE = antibody-dependent enhancement. Asterisk indicates the report described in this dissertation.

One of the earliest experimental vaccines described for ZIKV was made using a DNA plasmid approach. In August 2016, Larocca, Barouch, and colleagues described a DNA vaccine encoding the M and E proteins from a Brazilian strain of

ZIKV [295]. Two intramuscular (i.m.) injections of the plasmid into BALB/c mice generated high NAb titers and complete protection from challenges with homologous and heterologous ZIKV strains. Whereas genetic variation is a major obstacle for HIV-1 vaccines, ZIKV strains in the Americas and Asia are ~99% identical on the amino acid level [296], and all global ZIKV isolates form a single serotype [291]. Larocca et al. also described a vaccine made with purified inactivated virus (PIV) in alum adjuvant that elicited low but protective NAb titers in mice. A subsequent report by the same group showed that rhesus macaques immunized twice with either DNA or PIV, or a single time with a rhesus adenovirus serotype 52 (RhAd52) vector expressing prM and E, developed high NAb titers and were protected from ZIKV challenge [297]. This study also established that antibodies alone were capable of protecting macaques from ZIKV, and that protection was achieved by a NAb titer >100 (reciprocal dilution EC_{50}) as measured by a microneutralization assay.

These were followed by other studies using similar vaccine designs. Dowd et al. developed two DNA plasmid vaccines encoding prM and E and showed that two i.m. injections of 1 to 4 mg of plasmid generated protective immune responses in rhesus macaques [298]. In this study, a NAb titer of 1,000, as measured by a reporter viral particle (RVP) neutralization assay, was associated with about a 70% reduction in ZIKV viremia in macaques. The RVP assay is highly sensitive to NAb activity, and ID_{50} values determined by the RVP assay tend to be roughly 1 log higher than those of the plaque reduction neutralization test (PRNT) and other assay formats based on infection of a cell monolayer [291].

Muthumani and colleagues described an additional DNA plasmid vaccine encoding prM-E, which they delivered to mice and rhesus macaques with *in vivo* electroporation to enhance delivery [299]. This study used a more stringent, highly

pathogenic mouse model of infection, type I IFN α/β receptor knockout (IFNAR-/-) mice, to show that two i.m. injections of 25 μg of the plasmid elicited an immune response that could protect against ZIKV-mediated brain pathology and death. Likewise, two intradermal injections of 2 mg of plasmid elicited a robust NAb response in rhesus macaques. When IFNAR-/- mice were passively immunized by infusion of macaque serum, they were 80% protected from a lethal ZIKV challenge.

These vaccine approaches and others [300,301] are promising for their ability to elicit protective NAb responses to ZIKV, and, in fact, many of them are already proceeding into clinical trials (reviewed in [294]). However, with the exception of the RhAd52 vector, which has no documented efficacy in humans, the strategies discussed above were not reported to elicit protective NAb titers after one immunization in primates. Additionally, several of the published ZIKV vaccine candidates are subject to limitations in the scalability of manufacturing. One promising vaccine platform that does not appear subject to these limitations is messenger RNA (mRNA). mRNA-based vaccines are synthesized enzymatically by *in vitro* transcription in a process that has the potential to be rapidly and massively scaled up [302,303]. Recent advances in the design and delivery of mRNA vaccines has led to the development of potent, single-dose vaccines for use against ZIKV and other pathogens [302,304–307].

1.13. Nucleoside-Modified Messenger RNA Vaccines

While mRNA was investigated as a therapeutic vector as early as the 1990s, its widespread use has been restricted by a number of technical challenges, including sensitivity to degradation by RNases, low translatability, and inefficient *in vivo* delivery. However, recent technological and conceptual advances have solved

these major problems facing mRNA therapeutics. Carrier molecules have been devised that shield RNA from degradation and allow uptake into the cytosol *in vivo* [308]. One highly effective carrier is lipid nanoparticles (LNPs) that comprise an ionizable cationic lipid, cholesterol, polyethylene glycol, and a phospholipid [306,307,309]. *In vivo* delivery of mRNA complexed to LNPs results in high and prolonged protein expression when delivered by a variety of routes [309]. A number of design features in the mRNA can improve its stability and translatability to various degrees, including enzymatic addition of a 5' cap, efficient 5' and 3' untranslated regions (UTR) sequences, and codon optimization [310]. A major impediment to translation stems from the strong induction of type I interferons (IFN) by *in vitro* transcribed mRNA preparations, which contain aberrant double stranded RNA (dsRNA) species [311]. Type I IFN signaling leads to an increase in the dsRNA sensors PKR and OAS, which, when activated, result in the inhibition of translation elongation or the degradation of cellular mRNA and ribosomal RNA [312–315]. Two critical types of modifications have been described by our laboratory that remove detrimental innate immune signaling and dramatically increase the translation of mRNA in cultured dendritic cells (DCs) and *in vivo*. First, the enzymatic incorporation of naturally occurring, modified nucleosides during *in vitro* transcription abrogates the recognition of mRNA by toll-like receptors (TLR) 7 and 8 and other sensors. TLR7 and TLR8 bind to single-stranded RNA (ssRNA) in the endosome by distinct mechanisms that are each dependent in part on the presence of uridine [316,317]. Replacement of uridine with its isomer pseudouridine or the related 1-methyl-pseudouridine blocks recognition by TLR7 and TLR8, prevents type I IFN production, and increases translation of mRNA [318–320]. The second modification is the purification of *in vitro* transcribed mRNA to remove dsRNA contaminants, which serve as

ligands for the endosomal sensor TLR3 and various cytosolic RNA sensors including MDA5, RIG-I, OAS, and PKR (reviewed in [321]). This can be achieved by reverse-phase liquid chromatography (specifically, fast protein liquid chromatography, or FPLC), and the resulting purity can be verified using a mAb that binds specifically to dsRNA [311,322]. As a result of these two combined mRNA modifications, type I IFN production can be prevented *in vitro* and *in vivo* and the level of protein translation can be increased by a remarkable 4 to 5 logs in DCs [311] (see Fig. 1.4).

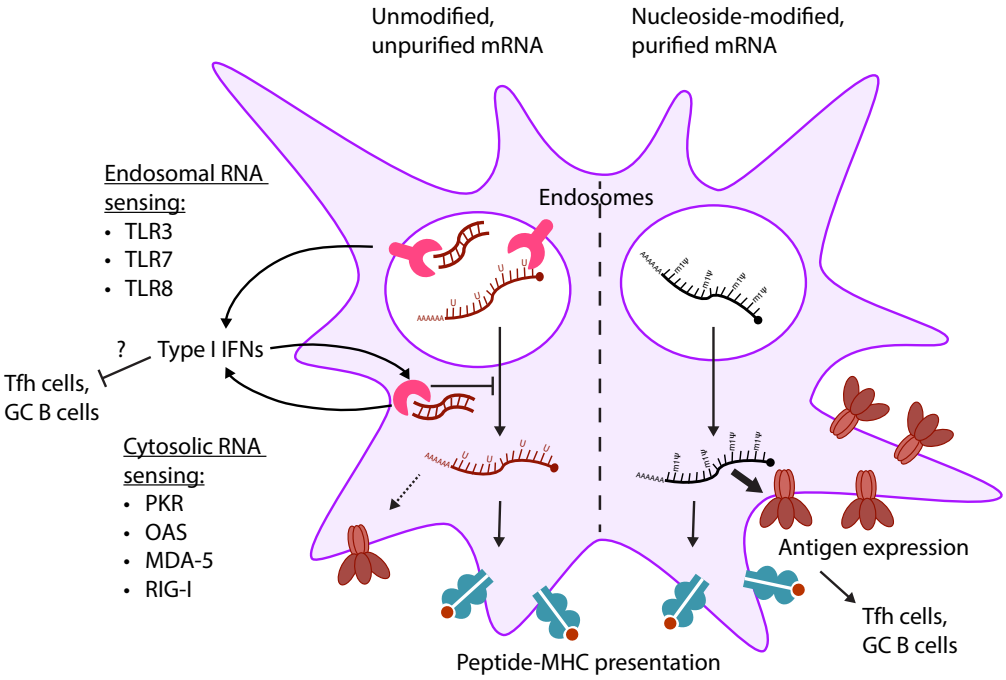

Fig. 1.4. Schematic of innate immune sensing of *in vitro* transcribed mRNA. In this model DC, a variety of sensors (pink) in the endosomes and cytoplasm detect dsRNA and unmodified exogenous ssRNA, resulting in the production of type I IFNs. IFN-stimulated genes inhibit translation of the antigen (red trimers) and may also inhibit the differentiation of Tfh cells and germinal center B cell responses.

Nucleoside-modified, purified mRNA complexed with LNPs (mRNA-LNPs) can be used to encode a protein immunogen and generate potent immune responses by vaccination. Preliminary data from our laboratory show that a single

intradermal injection of mice with influenza hemagglutinin-encoding mRNA, prepared as described above, results in strong polyfunctional $CD4^+$ T cell responses and exceptionally high hemagglutination inhibition (HAI) titers (Chapter 4, Fig. 4.3). The HAI titers generated by this vaccine greatly exceeded those typically induced by a conventional inactivated influenza vaccine or even pathogenic influenza infection in mice ([323,324] and E. Willis, personal communication). We investigated the mechanism of this potent NAb response and discovered that the mRNA vaccine stimulated a high level of total and antigen-specific Tfh cells and GC B cells. Current experiments aim to investigate the Tfh response induced by mRNA-LNP vaccines in nonhuman primates, with promising results (discussed in Chapter 4). Overall, these preliminary studies indicate that the nucleoside-modified, purified mRNA-LNP vaccine platform offers a number of advantages over traditional vaccine approaches, including the capacity for rapid development, versatility, and potent immunogenicity characterized by robust Tfh and GC B cell responses.

1.14. Goals of this Thesis

This dissertation seeks to address multiple outstanding questions in modern vaccine development, particularly for the challenging chronic infection caused by HIV-1 and the acute illness and birth defects resulting from ZIKV.

In Chapter 2, I present a body of work detailing the biological, structural, and immunogenic properties of CD4-independent HIV-1 Env immunogens. CD4-independent Envs tend to display an opened trimer conformation (detailed in Section 2.1) and thus present conserved epitopes in an altered fashion compared to CD4-dependent, wild-type Envs. This strategy represents a conceptual departure from SOSIPs and other attempts to generate bNAbs against closed-conformation trimers.

Instead, this approach offers the potential to generate broadly cross-reactive, non-neutralizing antibodies that may potentially be protective based on the immune correlates analysis of RV144.

In Chapter 3, I investigate the importance of HIV-1 Env multivalency on the cell surface in the context of a prime-boost vaccine regimen. Many HIV-1 vaccine designs that encode Env on a viral or genetic vector use a mutant with a deleted cytoplasmic tail [325–327]. This approach has been shown to increase HIV-1 Env surface expression, albeit modestly. Few head-to-head comparisons between truncated and WT Env have been conducted, particularly in prime-boost regimens [328,329]. Attempts to further increase the cell surface display of Env are hampered by our poor understanding of Env intracellular trafficking signals. Here, I evaluate the impact of novel cytoplasmic tail mutations on the surface expression and immunogenicity of HIV-1 Env in a clinically relevant prime-boost vaccine protocol.

In Chapter 4 and in a recent publication [307], I report the implementation of the nucleoside-modified, purified mRNA-LNP vaccine platform to make an effective vaccine against ZIKV. I describe the design of the mRNA encoding prM and E from a 2013 ZIKV strain, show translation of the mRNA *in vitro*, and characterize the immune response and protection from infection in mice and rhesus macaques. The ability of this platform to potently activate Tfh cells is also investigated.

Finally, the implications of this work and a number of promising future directions are discussed in Chapter 5.

CHAPTER 2

CD4-INDEPENDENT HIV-1 ENVELOPES INDUCE A V2-SPECIFIC ANTIVIRAL ANTIBODY RESPONSE IN VACCINIA PRIME-PROTEIN BOOST VACCINATION

Adapted from the following manuscript:

Michael J. Hogan*, Lifei Yang*, Angela Conde-Motter, Patricia Firpo, Andrea P.O. Jordan, Beth S. Haggarty, Josephine Romano, Thaddeus M. Davenport, Yu Liang, Brad Cleveland, Wenjin Guo, Nicole L. Yates, Xiaoying Shen, Greg Finak, Dora Dong, Bronwyn M. Gunn, Dong Han, Shixia Wang, Houping Ni, Norbert Pardi, Galit Alter, Shan Lu, Celia C. LaBranche, David C. Montefiori, Guido Ferrari, Georgia D. Tomaras, Kelly K. Lee, Drew Weissman, James A. Hoxie, and Shiu-Lok Hu

(Manuscript in preparation)

*These authors contributed equally to this work.

2.1. ABSTRACT

Neutralizing antibodies against the HIV-1 envelope (Env) glycoprotein have demonstrated the potential to protect from HIV-1 infection in animal models; however, these antibodies have proven extraordinarily difficult to elicit in vaccination. An alternative and perhaps more viable path towards vaccine protection from HIV-1 is through non-neutralizing antibodies that mediate antiviral activities through Fc-dependent interactions with effector cells. A protective role for these antibodies was recently suggested by the partially effective RV144 vaccine trial, in which decreased risk of infection correlated with non-neutralizing antibodies against Env variable loops 1 and 2 (V1V2) and antibody-dependent cell-mediated cytotoxicity (ADCC). However, the structural basis of eliciting such antibody specificities and functions is poorly understood. In this context, we investigated the immunologic impact of adapting HIV-1 Envs to mediate CD4-independent infection, a phenotype previously associated with striking structural perturbations. We demonstrate that two CD4-independent Env clones derived from HIV-1 89.6 exhibit a number of antigenic changes, including increased exposure of a linear epitope in V2 that was a target of ADCC-mediating antibodies in RV144 vaccinees. Importantly, the immunogenicity of this epitope was markedly enhanced on CD4-independent Envs when mice and nonhuman primates were immunized using a vaccinia prime-protein boost protocol. Moreover, the ability of the vaccinia primes to generate ADCC-mediating antibodies was enhanced for one of the CD4-independent Envs. Therefore, CD4-independent Envs may represent a favorable class of immunogens to elicit potentially protective non-neutralizing antibody activities.

2.2. INTRODUCTION

The HIV-1 pandemic remains a major global health concern, as more than 2 million people become infected with the virus each year and require life-long antiretroviral treatment [330]. Therefore, an effective vaccine is urgently needed. A principal goal of HIV-1 vaccine research is the generation of protective antibodies (Abs) against the HIV-1 envelope (Env) glycoprotein [25]. Passive Ab transfer experiments in nonhuman primate models have demonstrated the protective ability of Env-specific Abs, with contributions from both neutralizing activity and non-neutralizing Fc-mediated effector functions [140–146].

Neutralizing and non-neutralizing Abs differ considerably in their modes of recognition of HIV-1 Env. Fusion-competent Env exists as a trimer of gp160 protomers that are each cleaved into surface gp120 and transmembrane gp41 subunits. In recent years, there has been substantial progress in understanding the structure of this trimer and its recognition by neutralizing antibodies (NAbs). Real-time analysis of Env conformation by single-molecule fluorescence resonance energy transfer (smFRET) has revealed that the pre-fusion trimer samples multiple open and closed conformations in a dynamic equilibrium [236]. The closed state is the principal target of broadly neutralizing antibodies (bNAbs) that have been isolated from HIV-1-infected individuals [236,331], yet typically the Ab response against this structure is profoundly impeded by conformational masking, extensive glycosylation, and other mechanisms [118,119,129,244,332,333]. Structural resolution of the closed state has been revealed by X-ray crystallography [241,243,245] and cryo-electron microscopy [242,334] structures of a stabilized soluble Env trimer called SOSIP [45,335], which reveal a compact trimer stabilized at

its apex by packing of the V1V2 region atop the intraprotomeric V3 loop and by interprotomeric contacts between V1V2 and V3. SOSIPs and other stabilized trimers [245,247] have made it possible to test whether Abs raised solely against the closed trimer neutralize primary, neutralization-resistant (Tier-2) strains of HIV-1. Promisingly, immunization with SOSIP protein elicited Tier-2 NAbs against autologous virus in rabbits and monkeys [46,336]; however, this activity was restricted in breadth, and it may have been limited by a number of factors, including incomplete stability of the trimer under physiologic conditions [337], immunodominance of neo-epitopes at the trimer base [338], or insufficient germinal center B cell activation [339].

While the closed trimer conformation serves as the target of Tier-2 NAbs, Env adopts other conformations during infection that may be susceptible to other protective Ab responses. When Env binds to its primary receptor, CD4, the trimer undergoes a dramatic structural rearrangement and opening: gp120 subunits rotate 45° away from the central 3-fold axis of symmetry and 15° around a perpendicular axis [340–343]; the V1V2 loops are reoriented away from the trimer apex to lateral positions; and the V3 loop becomes exposed and primed to interact with the co-receptor, CCR5 or CXCR4 [344,345]. This CD4-induced, open conformation is bound by Abs that do not have potent Tier-2 neutralizing activity, but which can Fc-mediated effector functions, including Ab-dependent cell-mediated cytotoxicity (ADCC), phagocytosis (ADCP), viral inhibition (ADCVI), and infectious virion capture [123,124,198,200,346,347].

No HIV-1 vaccine trial to date has elicited significant levels of Tier-2 NAb or a high level of protection from HIV-1 infection in humans. A modest protective effect of 31.2% was achieved in the RV144 vaccine trial at one year of follow-up [187], but

protection did not correlate significantly with NAb activity. Instead, non-neutralizing IgG against V1V2 correlated with decreased risk of infection, and Env-specific plasma IgA correlated with increased risk [192]. The impact of V1V2-specific Abs was corroborated by an analysis of breakthrough viruses showing selection against specific amino acid signatures in the V2 region [206]. A post-hoc analysis revealed that ADCC was one of several Ab activities that were associated with decreased risk of infection in the presence of low Env-specific plasma IgA [192]. In follow-up studies, ADCC-mediating monoclonal antibodies (mAbs) were isolated from RV144 vaccinees that bound predominantly to the C1 region [196] or a linear V2 peptide [202] of Env, and Env-specific plasma IgA from vaccinees was found to block C1-directed ADCC [348]. This set of studies has raised significant interest in the potential of non-neutralizing IgG to offer an alternative or more feasible path to HIV-1 vaccine protection than bNAbs [349,350]. Despite this promise, little is known about how to specifically generate Abs with the desired epitope specificities (V2 and C1) or Fc-mediated effector functions. Therefore, characterization of Ab responses elicited by novel Env immunogen concepts and vaccination strategies is needed.

CD4-independent Envs, which mediate infection using a co-receptor in the absence of CD4, represent a rare class of Envs with distinct biological and structural characteristics compared to CD4-dependent Envs (reviewed in [351]). CD4 tropism is a highly conserved feature of all primate lentiviruses [352,353]; however, CD4-independent variants of HIV-1, HIV-2, and simian immunodeficiency viruses (SIV) have occasionally been described *in vivo* [354–367], especially in central nervous system infection or in severely $CD4^+$ T cell-depleted hosts, and they can be readily derived *in vitro* [368–373]. CD4-independent Envs tend to be highly sensitive to Ab-mediated neutralization, suggesting why they are selected against *in vivo*

[122,359,373–377]. These Envs characteristically exhibit an open trimer conformation that resembles the CD4-induced state, with laterally displaced V1V2 loops and exposed co-receptor binding site [343,378]. Accordingly, CD4 independence is often associated with a loss of quaternary epitopes in V1V2 at the trimer apex and greater exposure of highly conserved epitopes [122,375,379]. Depicted in Fig. 2.0 is a model of Env trimer opening, as determined by cryo-electron tomography with fitted densities from available gp120 crystal structures.

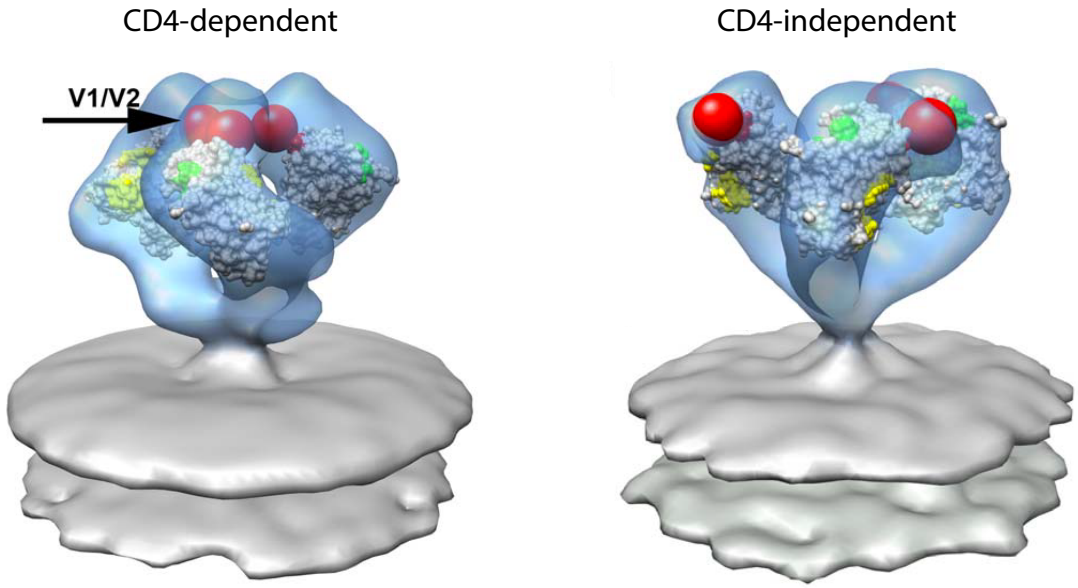

Figure 2.0. Characteristic trimer opening and rotation of V1V2 domain in a CD4-independent SIV. Shown are cryo-electron tomography structures (blue) of viral membrane-associated Env trimers from CD4-dependent SIVmac239 (left) and CD4-independent SIV CP-MAC (right). Crystal structures of the HIV-1 gp120 (PDB: 1GC1 [380]) were fitted into the tomography structures. Red spheres indicate the V1V2 domain, which is rotated from the apex (left) to lateral positions (right). Green residues show the base of the V3 loop, and yellow residues show the CD4 binding site. The figure was adapted with permission from White et al, *Plos Path*. 2010 [343].

CD4-independent Envs represent an intriguing concept for alternative immunogen design, as their structure is highly perturbed yet functionally intact;

however, little is known about how these structural changes affect the quality of the Ab response in vaccination. A few reports have examined the immunogenicity of HIV-1 Envs that mediated a single round of infection in the absence of CD4 [367,372,381–383]. Two of these studies evaluated Envs with a deleted N-linked glycosylation site at residue N197, located immediately C-terminal to V2. This glycan participates in interprotomeric contacts with V3 and partially shields the CD4 binding site (CD4bs) [241,249]. Loss of N197 has been shown to contribute to CD4-independent infectivity [372,382] and sensitivity to neutralization by mAbs directed against the CD4bs, CD4-induced epitopes, and V3 [384–386]. Interestingly, immunization of pig-tailed macaques with HIV-1 89.6 N197Q Env resulted in significantly higher levels of NAb compared to WT Env in a vaccinia prime-gp120 boost regimen [382], and immunization of guinea pigs with soluble HIV-1 ADA Env-gp140 trimers containing a similar N197S mutation induced greater levels of Tier-1 NAb, C1-specific IgG, and ADCC [383]. However, a limitation of these studies is that the examined Envs were not shown to be fully CD4-independent in a spreading infection, and thus the immunologic outcomes of CD4 independence have not yet been rigorously investigated.

The goal of the present study was to determine how CD4 independence impacts the humoral immune response to HIV-1 Env through structural perturbations and altered epitope exposure. We therefore characterized the structure and immunogenicity of two fully CD4-independent Env clones derived from the dual-tropic clade B HIV-1 89.6 Env. These Envs were evaluated as immunogens in mice and pig-tailed macaques: in both species, CD4-independent Envs elicited a higher level of IgG to conserved epitopes in the V2 region, which was better exposed as a result of CD4 independence. Strikingly, immunization with one CD4-independent

clone was associated with more rapid generation of ADCC activity in macaques. CD4-independent Envs thus represent an alternative immunogen strategy that might be used to elicit potentially protective non-neutralizing Ab responses to HIV-1.

2.3. RESULTS

Derivation of CD4-independent HIV-1 Envs

It was previously shown that HIV-1 89.6 N197Q (N7) Env mediated a single round of CD4-independent infectivity and elicited a higher and broader NAb response in a vaccinia prime-gp120 boost immunization of pig-tailed macaques [382]. To allow a more comprehensive investigation of the impact of CD4 independence in this Env, 89.6 WT and N7 Envs were adapted to be fully CD4-independent in a spreading infection. Viruses expressing these Envs were adapted to replicate in a CD4-negative T cell line (Fig. 2.1A), and Env clones were screened for CD4-independent fusion. Clones A2 and D4T, derived respectively from WT and N7 Envs, mediated cell-cell fusion using CCR5 and to a lesser extent CXCR4 in the absence of CD4 (Fig. 2.1B). A2 and D4T were cloned into replication-competent viruses, and both were found to mediate a robust spreading infection in CD4-negative cells compared to WT and N7 (Fig. 2.1C).

A variety of distinct mutational pathways have been shown to confer CD4 independence to HIV-1 Envs during *in vitro* adaptation. The CD4-independent Envs A2 and D4T acquired mutations throughout gp120 and gp41 (Fig. 2.1D): A2 acquired 21 amino acid changes relative to WT, and D4T acquired 16 changes relative to N7 but retained the initial N197Q substitution. Several mutations occurred at sites predicted to participate in intrasubunit or intersubunit interactions based on a crystal structure of the HIV-1 Env trimer (Fig. 2.1E) [243]. Both Envs acquired a premature stop codon in the cytoplasmic tail and two identical mutations in gp41 (N656D and D758N); all other mutations were distinct. Interestingly, A2 acquired G367R and

D368N mutations that are predicted to ablate CD4 receptor binding [353,380], whereas D4T did not acquire any mutations at residues that directly contact CD4.

CD4-independent Envs show altered exposure of V2, CD4-induced, and CD4 binding site epitopes

CD4-independent Envs are characterized by several structural features that may influence the Ab response, including an opened trimer conformation, exposure of CD4-induced epitopes, and loss of quaternary V1V2 epitopes [122,343,375]. The structural and antigenic changes in A2 and D4T were therefore characterized by multiple approaches. First, the WT, N7, A2, and D4T Envs were expressed on the surface of HEK 293T cells by recombinant vaccinia virus (rVV) and were assessed for reactivity to mAbs and CD4-based ligands by flow cytometry. Data are expressed as relative changes in mean fluorescence intensity (MFI) (Figs. 2.2A and B) or as representative histograms (Fig. 2.2C).

Striking differences were noted in the binding of mAbs specific for linear and conformational epitopes in the V2 loop. To test exposure of a linear peptide epitope in V2, also known as the V2p epitope, spanning amino acids 163-183 (HXB2 numbering), we used mAbs Ab8505 and Ab8488, which were isolated from vaccinees in the RV305 trial and bind to the V2 peptide (David Easterhoff, Barton Haynes, personal communication). Other V2 peptide-specific mAbs isolated from RV144 vaccinees, CH58 and CH59, are capable of potent ADCC activity [202] but do not bind to 89.6 gp120 (data not shown). Ab8505 bound to A2 and D4T gp120 protein at levels 2 and 10 fold higher than to parental gp120s, as quantified by EC_{50} values in ELISA (Fig. 2D). Ab8488 also reacted to a low level with D4T but not with any other gp120 (data not shown). As a control, 2G12 did not bind more strongly to

A2 or D4T than parental Envs. The notion that the V2 peptide is more exposed on the CD4-independent Envs, including monomeric gp120, was further supported by a hydrogen-deuterium exchange (HDX) assay, which directly probed the exposure of gp120 peptides to solvent. HDX analysis revealed that the V2 peptide was moderately more exposed on D4T and slightly more exposed on A2 relative to WT or N7 in the context of soluble gp120 proteins (Fig. 2.2E). In contrast, D4T exhibited the highest amount of order (reduced solvent exposure) in its core structure of all gp120s (Kelly Lee, personal communication).

Compared to linear V2 peptide, we observed a distinct pattern of binding by antibodies specific for conformational epitopes in V2 [387–389]. The conformation-dependent mAbs 697-30D and 2158 bound 2-fold better to A2 than WT, while they respectively bound >10-fold and 2-fold lower to D4T than N7. This suggests that the exposure of linear and conformational epitopes in V2 may be dissociable processes.

The antigenicity of quaternary epitopes in V1V2 could not be assessed using available mAbs, since PG16, PGT145, and CH01 did not bind to WT 89.6 Env or any of the variants. Interestingly, PG9, which recognizes both quaternary and, to a lesser extent, non-quaternary epitopes in V1V2 [151,390], bound to surface-expressed D4T but did not bind to WT, N7, or A2 (Fig. 2.2C). This interaction was confirmed by immunoprecipitation (Supp. Fig. S2.1), which also showed that PG9 recognized the full-length trimeric Env but not the gp120 monomer.

MAbs that recognize CD4-induced epitopes have been divided into clusters A, B, and C (shown in Fig. 2.2B) based on their specificity and ADCC potency, which tends to be higher in clusters A and B compared to C [198]. Binding of cell-associated A2 and D4T Envs by all three clusters of CD4-induced mAbs was increased approximately 2-fold compared to WT and N7 (Fig. 2.2B). A2 and D4T

also gained reactivity to the CD4-induced mAb C11, which did not bind to WT or N7 (data not shown). Binding kinetics to gp120 were measured using biolayer interferometry, and A2 and D4T exhibited modest increases in on-rate (~2-fold or less) of CD4-induced mAbs 17b, A32, 48d, and N5-i5 (Fig. 2.2F). Env antigenicity was also assessed by neutralization sensitivity, which reflects binding to functional Env trimers [391,392]. 17b neutralized WT relatively weakly but was several fold more potent against N7, A2, and D4T (Fig. 2.2G). When viruses were pre-incubated with a sub-neutralizing concentration of soluble CD4 (sCD4), they did not gain additional neutralization sensitivity to 17b. Together, these results suggest that multiple distinct CD4-induced epitopes are moderately more accessible on A2 and D4T compared to their parent Envs, in agreement with previous studies of CD4-independent Envs [374,376].

Pronounced antigenic changes in A2 and D4T also occurred in the CD4 binding site (CD4bs). As predicted based on the D368N mutation, A2 exhibited a disrupted CD4bs, with >10-fold reductions in cell-associated binding of mAbs b12 and VRC03 compared to WT (Fig. 2.2A). Despite this, cell-associated A2 retained binding to VRC01 and a bivalent CD4-IgG fusion protein. As a gp120 monomer, A2 showed 300-fold lower affinity for CD4-IgG, mostly attributable to an increased off-rate, but only a 4-fold decrease in affinity for VRC01 (Fig. 2.2F). A2 also exhibited greatly increased neutralization resistance (1-2 log) to b12, sCD4, and CD4-IgG, but did not vary significantly in VRC01 neutralization (Fig. 2G). In contrast, cell-associated D4T showed >3-fold increased binding to VRC01 (Fig. 2.2A), and D4T gp120 had several fold higher affinity for VRC01 and CD4-IgG (Fig. 2.2F). D4T was highly sensitive to neutralization by CD4bs ligands, similar to N7 (Fig. 2.2G), as previously reported [382]. Overall, these data indicate that the CD4bs epitope on A2

is disrupted, while not completely ablated, and that the same epitope on D4T is highly accessible to antibody binding and neutralization.

Antibody recognition of V3 on surface-expressed A2 and D4T was largely unchanged from the parent Envs (Fig. 2.2A), and no differences in solvent exposure of a V3 peptide were detected by HDX (Fig. 2.2E). However, A2 became several fold more sensitive to neutralization by V3 crown-specific mAb 447-52D, and D4T became >10-fold more resistant to V3- and high mannose glycan-specific mAbs 447-52D, PGT121, PGT126, and 2G12. This was unexpected, since all of these mAbs bound well to cell-associated D4T (Figs. 2.2A and C). No changes in cell-associated Env binding or neutralization sensitivity were observed for epitopes in gp41 or the gp120-gp41 interface, including mAbs 2F5, 4E10, 35O22, and PGT151 (Fig. 2.2A). Finally, all Env variants exhibited sensitivity to neutralization by pooled patient plasma, but no increase was observed for A2 and D4T; unexpectedly, they were slightly more resistant than their parent Envs (Fig. 2.2G).

CD4-independent Envs elicit a high-titer IgG response in mice

The immunogenicity of CD4-independent Envs A2 and D4T was evaluated using recombinant vaccinia virus (rVV) immunization with or without gp120 protein boosts, as detailed in Fig. 2.3A and in the Methods. Mice were primed twice with rVV vectors encoding WT, N7, A2, or D4T gp160 and, if applicable, boosted twice with autologous gp120 protein with alum adjuvant. A control group received rVV expressing SIV Gag-Pol as the prime and WT gp120 as the boost. Immunizations were performed in both C57BL/6 mice and human CD4 transgenic (huCD4) mice, which lack murine CD4 and express human CD4 under normal developmental regulation [393]. Since HIV-1 Env binds to human but not murine CD4 and may thus

affect epitope accessibility or signaling to $CD4^+$ T cells [109–112,394,395], the huCD4 mouse model was included to complement wild-type mice in evaluating CD4-independent Env immunogens. The huCD4 mouse strain was previously shown to permit MHC class II-restricted $CD4^+$ T cell activation and $CD4^+$ T cell-dependent B cell responses [396].

The humoral immune response was monitored over time by gp120-specific IgG ELISA. Both CD4-independent Envs induced a significantly higher IgG response than either parent Env at every time point post-vaccination. After two primes in huCD4 mice, the IgG response was 36-fold and 16-fold greater for A2 and D4T, respectively, compared to their parent Envs (Fig. 2.3B). After two subsequent boosts in the same mouse strain, the responses to A2 and D4T were each ~5-fold higher than those induced by WT or N7. There was a similar effect in C57BL/6 mice primed with A2 and D4T (Supp. Fig. S2.2A). A majority of the enhancement in gp120-specific IgG in huCD4 were attributable to the IgG1 subclass, while in C57BL/6 mice the contributions of the subclasses were more balanced (Fig. 2.3C and Supp. Fig. S2.2B). IgG3, IgM, and serum IgA were negligible at the examined time points (data not shown). To control for the effective dose of the rVV vectors, the IgG against total VV antigen was measured in huCD4 mice, and no significant differences were observed between groups (Supp. Fig. S2.2B). All immunogens elicited low Tier-1 NAb titers, yet the response mounted to A2 was several fold greater than the response to WT, and D4T trended slightly higher than N7 as well (Fig. 2.3D).

T cell responses were measured in the spleens collected after the second prime (Supp. Fig. S2.3A) or second boost (Supp. Fig S2.3B). At both time points, all rVV vectors stimulated equivalent T cell responses to VV peptides. As expected based on previous reports, the VV-specific $CD4^+$ responses were low and VV-

specific $CD8^+$ responses were extremely high [397,398]. Env-specific T cell responses showed a high degree of variability, and there was no significant difference in the frequency of IFN-γ or TNF-secreting cells between A2 or D4T and either of the parent Envs. These data support the model that differences in the humoral response induced by A2 and D4T are determined at the level of B cell recognition rather than the T helper cell response.

V3-specific IgG response to CD4-independent Env immunogens in mice

We hypothesized that the epitope specificities of the Ab response would be altered as a result of CD4 independence and associated structural changes. CD4-bound Envs and a CD4-independent Env have been shown to expose the V3 loop by displacing V1V2 from its position apical to V3 and by rotating the base of V3 towards the target cell membrane [340]. To determine whether V3 became more immunogenic on A2 and D4T in mice, the IgG response was measured against a linear V3 peptide at all available time points and against a V3 scaffold protein at terminal bleed time points (Supp. Fig. S2.3). Surprisingly, by both measures, D4T elicited a low V3-specific response that was equal to that of WT and N7. A2 induced a slightly increased response to linear V3 starting after the second prime, but this was highly variable and largely overlapped with WT. The response to V3 scaffold was equivalent for all Envs, and both measures of V3 response were similar between huCD4 and C57BL/6 mice.

CD4-independent Envs elicit broadly cross-reactive IgG to V1V2-scaffold and linear V2 peptide in mice

The antibody responses to A2 and D4T in mice were further characterized with respect to epitopes in V1V2, a domain that is dramatically reoriented and antigenically altered in CD4-bound and CD4-independent Envs [343,378]. V1V2 reactivity was measured by ELISA using a protein scaffold of V1V2 from clade B HIV-1 92US715 fused to murine leukemia virus (MLV) gp70, following the approach of the RV144 correlates analysis [192]. V1V2 scaffolds display linear and conformational, but not quaternary, antigenic determinants [219]. A2 and D4T induced dramatically higher IgG to V1V2 scaffold compared to WT and N7 at post-prime and available post-boost time points (Figs. 2.4A and B). Although large differences were observed in both strains of mice, the pattern of response differed markedly depending on the mouse strain. In huCD4 mice, 30% and 50% of animals immunized with A2 and D4T, respectively, made moderate V1V2-specific responses after the first rVV prime (Fig. 2.4A). With further priming and boosting, the proportion of responders grew to ~80%. A bimodal distribution of V1V2-specific responses was apparent for both A2 and D4T, and the average V1V2-specific IgG response to these Envs reached a level roughly 2 logs higher than WT and N7, which elicited little to no detectable IgG to the V1V2 scaffold.

In C57BL/6 mice, the V1V2 response was comparatively higher, more rapid, and, most strikingly, unimodal (Fig. 2.4B). The V1V2 response rate in C57BL/6 mice immunized with A2 or D4T was 80-90% after a single prime and 90-100% after two primes. After prime 2, the V1V2-specific IgG responses to these Envs was estimated to be 2 to 3 logs higher than WT and N7, which generated no detectable response. Interestingly, mice immunized with N7 did generate V1V2-specific IgG, but only after gp120 boosting and only in the C57BL/6 strain. This effect was not observed with the WT immunogen.

The V1V2-specific antibodies induced by CD4-independent Envs were more finely mapped by conducting a multiplex binding assay, which measured IgG against a panel of V1V2 scaffolds and linear V2 peptides from diverse strains of HIV-1 (Figs. 2.4C-F). V2 peptide-specific IgG agreed closely with V1V2 scaffold-specific IgG: the responses generated by A2 and D4T were consistently multiple orders of magnitude greater than the responses to WT and N7, which generally did not exceed background, with the exception of the post-boost 2 time point in C57BL/6 mice immunized with N7. Notably, the responses measured by the multiplex assay were characterized by the same bimodal and unimodal distributions noted above in huCD4 and C57BL/6 mice, respectively, for the A2 and D4T immunogens (Figs. 2.4C and D). IgG responses to a consensus clade B V2 peptide and the 92US715 V1V2 scaffold were plotted against each other and were strongly positively correlated (R^2 = 0.84, p<0.0001) (Fig. 2.4E). Most importantly, the Abs generated by A2 and D4T against V1V2 scaffolds and linear V2 peptides had extraordinarily breadth, as they bound to epitopes from a wide variety of isolates across clades B, C, AE, and BC (Fig. 2.4F). The level of IgG to the consensus clade B V2 peptide was as a strong predictor of both the magnitude and the breadth of the response to V1V2 scaffolds and other V2 peptides. Therefore, we hypothesize that the V1V2 scaffold-specific IgG generated by A2 and D4T immunizations is predominantly composed of antibodies that bind to the linear V2 peptide epitope.

Immunogenicity of CD4-independent Envs pig-tailed macaques

In order to evaluate the immunogenicity of CD4-independent Envs in nonhuman primates, we used an immunization scheme similar to the one used in mice, and which corresponded to a previous study that had shown a relatively high

and broad NAb response against the 89.6 N7 Env [382]. In this protocol, pig-tailed macaques were given a series of two rVV primes, which co-delivered HIV-1 Env and SIV Gag-Pol immunogens, and three boosts, each consisting of separate injections of gp120 protein in alum and SIV Gag-expressing plasmid (Fig. 2.5A). Macaques were bled at multiple time points and the binding antibody response against diverse gp120 and gp140 antigens was monitored by a multiplex immunoassay. According to a magnitude-breadth statistical analysis, we observed a trend toward greater gp120- and gp140-specific IgG breadth in the D4T group compared to N7 at the post-prime 2 and post-boost 1 time points (Fig. 2.5B and C), although this was not statistically significant (linear mixed-effects model). This trend was not observed after boosts 2 and 3, when the magnitude-breadth curves of D4T and N7 overlapped (Supp. Fig. S2.5). In contrast, the gp120 and gp140 responses to A2 and WT were of similar magnitude and breadth after prime 2 and boost 1 time points, but at later time points A2 showed a significantly lower response than WT. These trends were also apparent in the responses to individual antigens, including 89.6 WT gp120 (Fig. 2.5D) and a consensus group M gp120 (Fig. 2.5E).

The NAb response was measured in macaque immune sera against a panel of HIV-1 strains, and, as in mice, the response tended to be low and limited to Tier-1 strains. D4T and N7 NAb titers were not significantly different, but the response to A2 was significantly lower than WT at the post-boost 3 time point for the neutralization-sensitive strains MN.3 and SF162.LS (Fig. 2.5F). Autologous responses to Tier-2 89.6 WT were low, and other responses to more neutralization-resistant viruses were generally negligible (data not shown).

The $CD4^+$ and $CD8^+$ T cell responses against Env and Gag were measured in PMBC and axillary lymph nodes before the first immunization, after prime 2, and

after each boost. The frequency of antigen-specific $CD4^+$ cells producing intracellular cytokines (IFN-γ, IL-2, IL-5, and IL-21) was generally low and was not significantly different between groups (Kathy Foulds, Rick Koup, personal communication). $CD8^+$ T cell responses were generally negligible and did not differ between groups. Overall, slightly higher responses were observed after the first boost compared to after the second prime.

CD4-independent Env clone D4T elicits a higher V1V2 scaffold- and V2 peptide-specific IgG response in pig-tailed macaques

The multiplex immunoassay also measured IgG against a panel of V1V2-scaffold and linear V2 peptide reagents (Fig. 2.6). To both sets of reagents, the response elicited by D4T was of a greater magnitude and breadth compared to its parent, N7, or to WT and A2. The enhanced response to D4T was observed after both rVV primes and was maintained after one or multiple protein boosts. In contrast, the response to A2 was generally comparable to WT at all time points. These trends were apparent both when examining the responses to individual V2 peptides (Figs. 2.6A and B) and V1V2 scaffolds (Fig. 2.6C), and when considering the average V1V2-specific response (Fig. 2.6D) or magnitude-breadth scores for V1V2 binding (Supp. Fig. S2.5).

The V3-specific response was also measured using the same multiplex assay. No differences between groups were observed in the binding response to a clade B V3 scaffold (Supp. Fig. S2.6A). Notably, A2 elicited a significantly lower IgG response to linear V3 peptides from clade A and C, while D4T, N7, and WT all generated higher and similar responses (Supp. Figs. S2.6B and C).

CD4-independent Env clone D4T generates antibody-dependent cell-mediated cytotoxicity (ADCC) antibody activity after vaccinia priming

The ability of antibodies in CD4-independent Env immunization to mediate a non-neutralizing, antiviral activity was assessed by measuring the Fc-dependent function, ADCC. We used an assay involving primary human PBMCs as effector cells and 89.6 WT gp120-coated CEM.NKR-CCR5 cells as targets. ADCC activity was quantified based on the ability of macaque sera to stimulate transfer of active granzyme B from effector to target cells. Interestingly, D4T was the only Env that generated ADCC after the two rVV primes, and this was significantly elevated over all other groups. This was true when ADCC was expressed either as the peak granzyme B-positive frequency (Fig. 2.7A) or as an endpoint dilution titer (Fig. 2.7B). When one or two boosts were administered, all groups of macaques exhibited ADCC activity, and the response to D4T was not significantly increased over N7. At post-boost time points, the A2 group showed a significantly lower ADCC response.

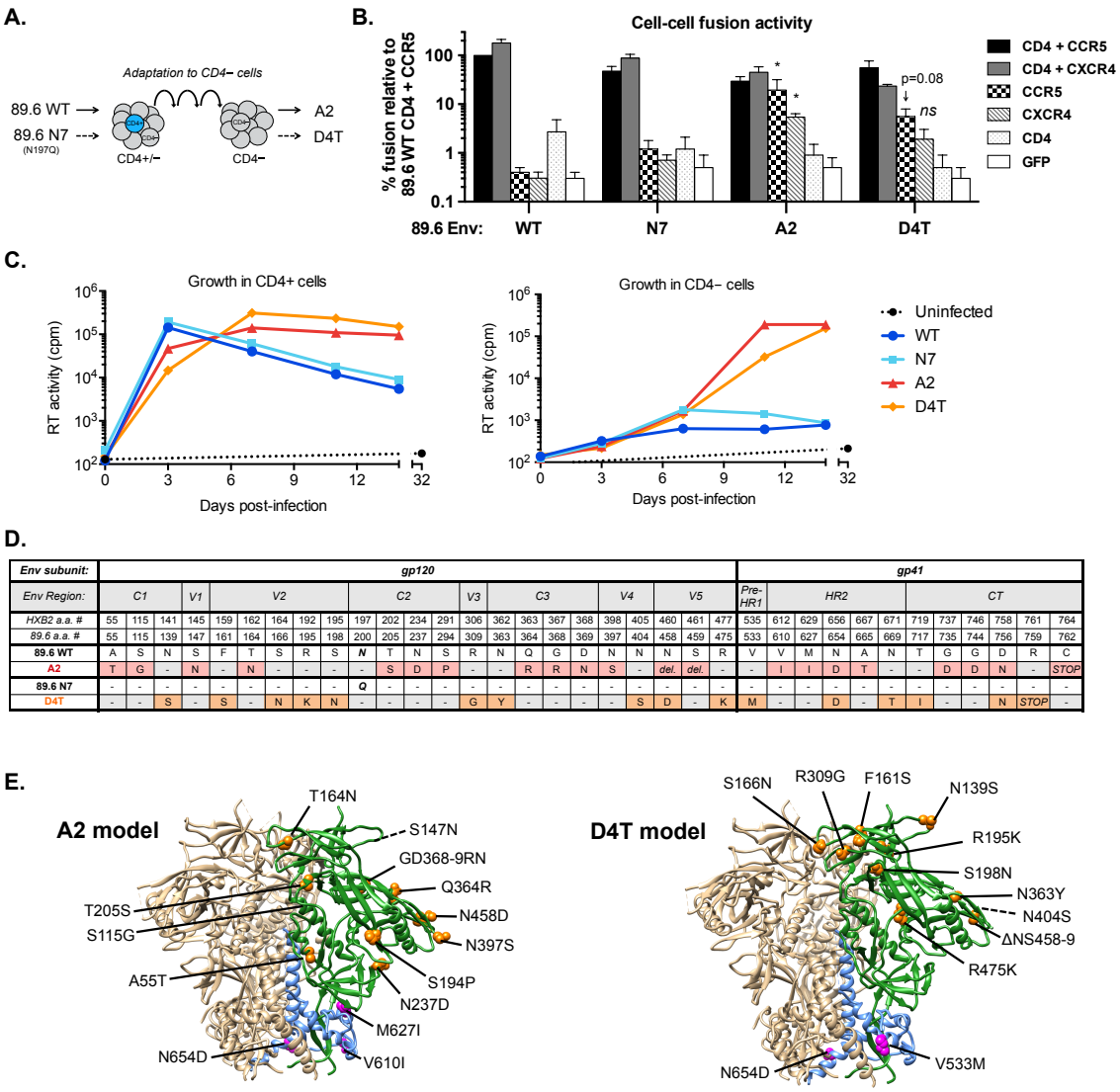

Env subunit:	gp120																						gp41												
Env Region:	C1			V1	V2					C2				V3	C3				V4		V5			Pre-HR1	HR2					CT						
HXB2 a.a. #	55	115	141	145	159	162	164	192	195	197	202	234	291	306	362	363	367	368	398	405	460	461	477	535	612	629	656	667	671	719	737	746	758	761	764
89.6 a.a. #	55	115	139	147	161	164	166	195	198	200	205	237	294	309	363	364	368	369	397	404	458	459	475	533	610	627	654	665	669	717	735	744	756	759	762
89.6 WT	A	S	N	S	F	T	S	R	S	N	T	N	S	R	N	Q	G	D	N	N	N	S	R	V	V	M	N	A	N	T	G	G	D	R	C
A2	T	G	-	N	-	N	-	-	-	-	S	D	P	-	-	R	R	N	S	-	del.	del.	-	-	I	I	D	T	-	-	D	D	N	-	STOP
89.6 N7	-	-	-	-	-	-	-	-	-	Q	-	-	-	-	-	-	-	-	-	-	-	-	-	-	-	-	-	-	-	-	-	-	-	-	-
D4T	-	-	S	-	S	-	N	K	N	-	-	-	-	G	Y	-	-	-	-	S	D	-	K	M	-	-	D	-	T	I	-	-	N	STOP	-

Figure 2.1. Derivation of CD4-independent Env variants from HIV-1 89.6. (A) Env clones A2 and D4T were derived from 89.6 WT and N7 Envs, respectively, by adaptation to replicate in a CD4-negative, SupT1-based cell line as SHIVs. (B) The cell-cell fusion activity of each Env was tested with the indicated receptors or GFP control in quail QT6 cells (n=3). A2 and D4T were compared to their respective parent Envs by one-way ANOVA with Sidak correction on log-transformed data. Asterisk: $p<0.05$. ns: $p>0.05$. (C) Viral growth was quantified in SupT1 cells expressing (left) or lacking (right) CD4. A representative experiment is shown (n=3). (D) Table of mutations acquired during adaptation of A2 and D4T. (E) The locations of mutated residues, where possible, were indicated on the HIV-1 BG505 SOSIP.644 crystal structure (PDB 4TVP) from [243]. Error bars represent the s.e.m.

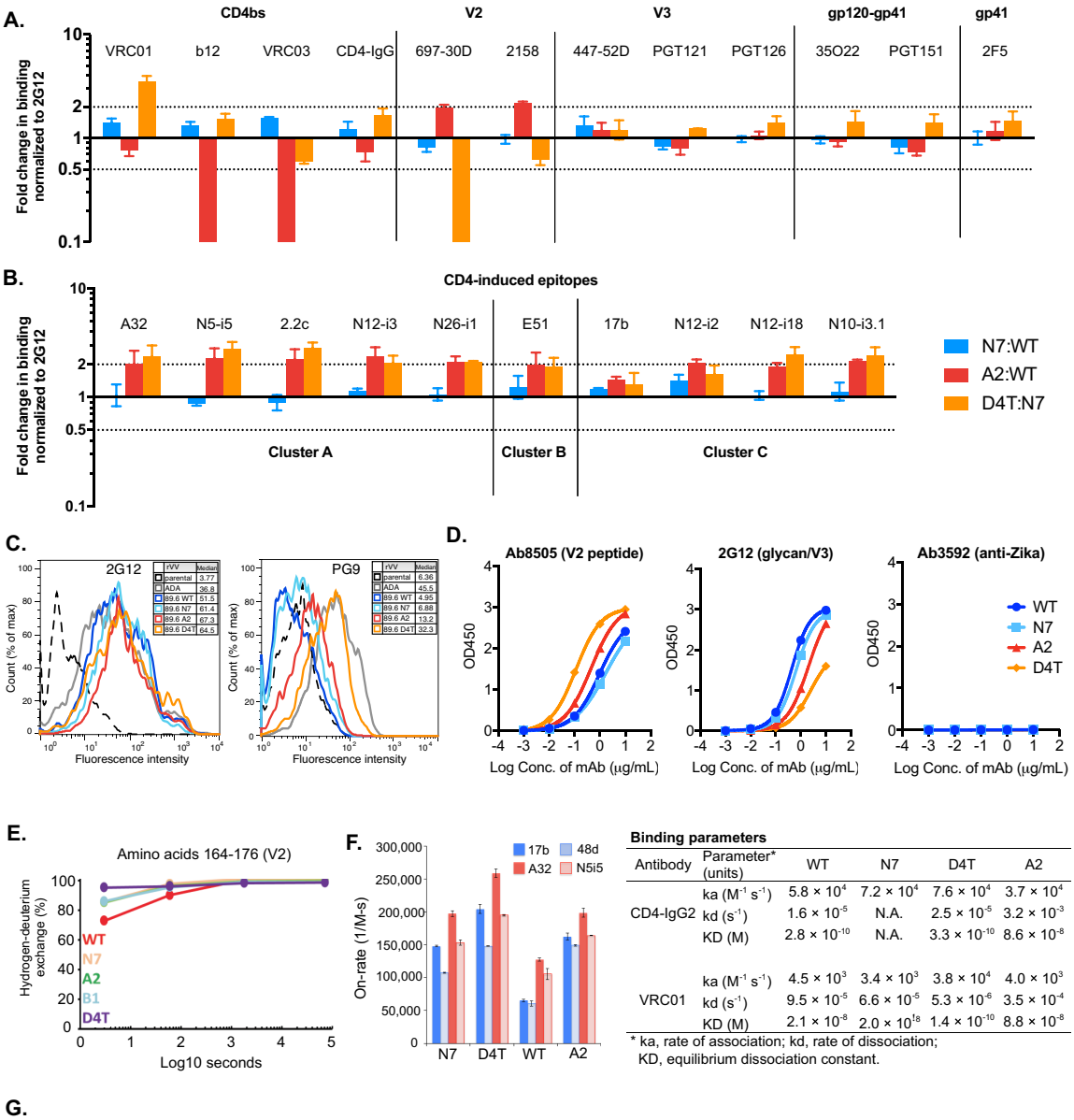

Binding parameters

Antibody	Parameter* (units)	WT	N7	D4T	A2
CD4-IgG2	ka (M^{-1} s^{-1})	5.8×10^{4}	7.2×10^{4}	7.6×10^{4}	3.7×10^{4}
	kd (s^{-1})	1.6×10^{-5}	N.A.	2.5×10^{-5}	3.2×10^{-3}
	KD (M)	2.8×10^{-10}	N.A.	3.3×10^{-10}	8.6×10^{-8}
VRC01	ka (M^{-1} s^{-1})	4.5×10^{3}	3.4×10^{3}	3.8×10^{4}	4.0×10^{3}
	kd (s^{-1})	9.5×10^{-5}	6.6×10^{-5}	5.3×10^{-6}	3.5×10^{-4}
	KD (M)	2.1×10^{-8}	2.0×10^{18}	1.4×10^{-10}	8.8×10^{-8}

* ka, rate of association; kd, rate of dissociation; KD, equilibrium dissociation constant.

G.

Virus	Neutralization IC_{50} (ug/ml)														
	CD4 binding site				V3 glycan				CD4i		V1/V2 glycan		gp41 MPER		pooled patient plasma
	b12	VRC01	CD4-IgG	sCD4	447-52D	PGT121	PGT126	2G12	17b	17b + sCD4	PG9	PG16	2F5	4E10	
WT	0.039	1.44	0.024	0.34	0.056	0.019	0.0075	0.095	1.85	1.53	>20	>20	0.12	0.19	5,701
N7	0.0083	0.13	0.017	0.066	0.014	0.024	0.0079	0.09	0.27	0.42	>20	>20	0.17	0.35	19,501
A2	>20	2.78	0.34	>20	0.0066	0.021	0.017	0.31	0.28	0.27	>20	>20	0.052	0.15	1,473
D4T	0.0077	0.11	0.0098	0.049	0.34	>20	>20	>20	0.39	1.13	>20	>20	0.086	0.41	10,817

Figure 2.2. Structural characterization of CD4-independent HIV-1 89.6 Env variants. (A-C) Antigenicity of antibody epitopes was probed by flow cytometry and expressed as (A,B) the fold changes in MFI after normalizing to the 2G12 MFI in each experiment (n≥3) or as (C) histograms with median fluorescence intensity indicated. (D) ELISA binding of the indicated mAbs to each gp120. A Zika virus-specific mAb served as a negative control. (E) Percent hydrogen-deuterium exchange over time for amino acids 164-176 of V2, as measured by mass spectrometry. Note: B1 is an Env clone not included in this study. (F) Binding

parameters for indicated mAbs to monomeric gp120 proteins, measured by biolayer interferometry (n=3). (G) Neutralization sensitivity of SHIVs expressing indicated Envs to a panel of mAbs and CD4bs reagents, expressed as IC_{50} in μg/mL or ID_{50} as a reciprocal dilution. Error bars: s.e.m.

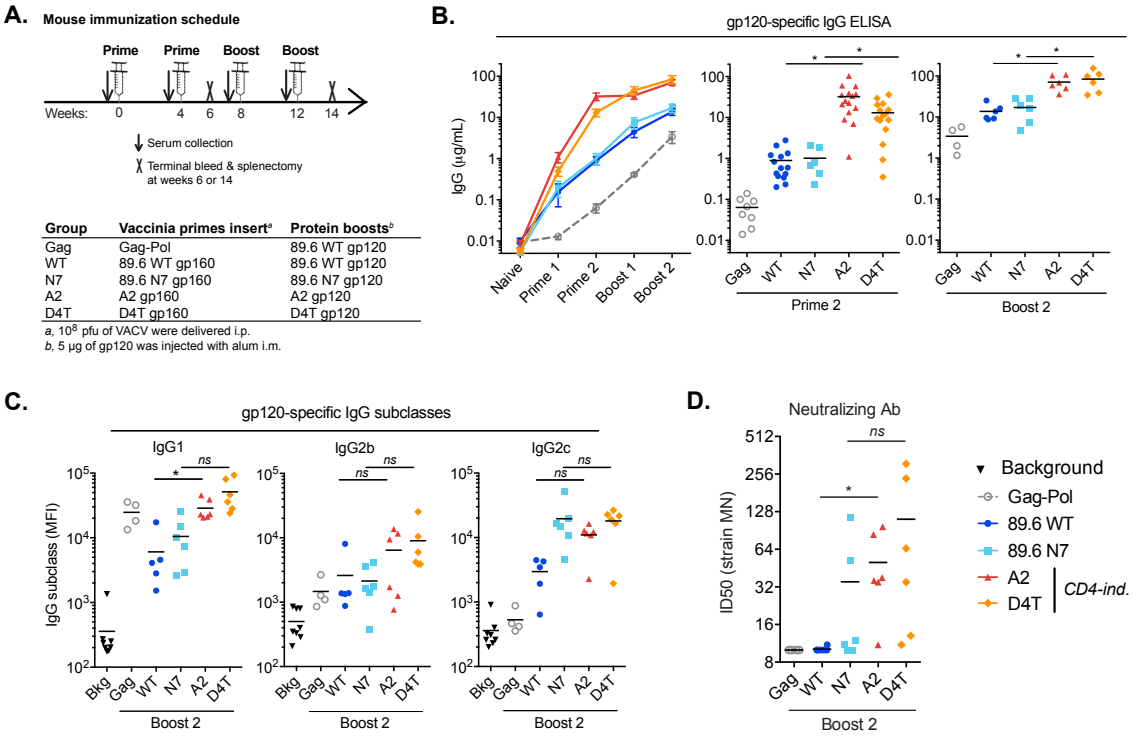

Figure 2.3. Immunogenicity of CD4-independent Envs in vaccinia prime-gp120 boost vaccination of mice. (A) Schematic of prime-only and prime-boost immunization regimens, for which data were pooled as applicable. (B-D) Antibody data are shown here for huCD4 mice, and corresponding data for C57BL/6 mice are shown in Supp. Fig. S2.2. (B) Binding of serum IgG to 89.6 WT gp120 by ELISA after each immunization. (C) Subclass-specific IgG, measured by multiplex immunoassay using 1:100 post-boost 2 serum. (D) Neutralizing antibodies against the Tier-1 virus MN.3, measured in TZM-bl cells, and quantified as the reciprocal dilution resulting in 50% inhibition of infection (ID50). Data points represent individual mice, horizontal bars represent the mean and error bars show s.e.m. Statistical comparisons were made between WT vs. A2 and N7 vs. D4T using the Kruskal-Wallis test with Dunn's correction. Asterisk: $p<0.05$; ns: $p>0.05$.

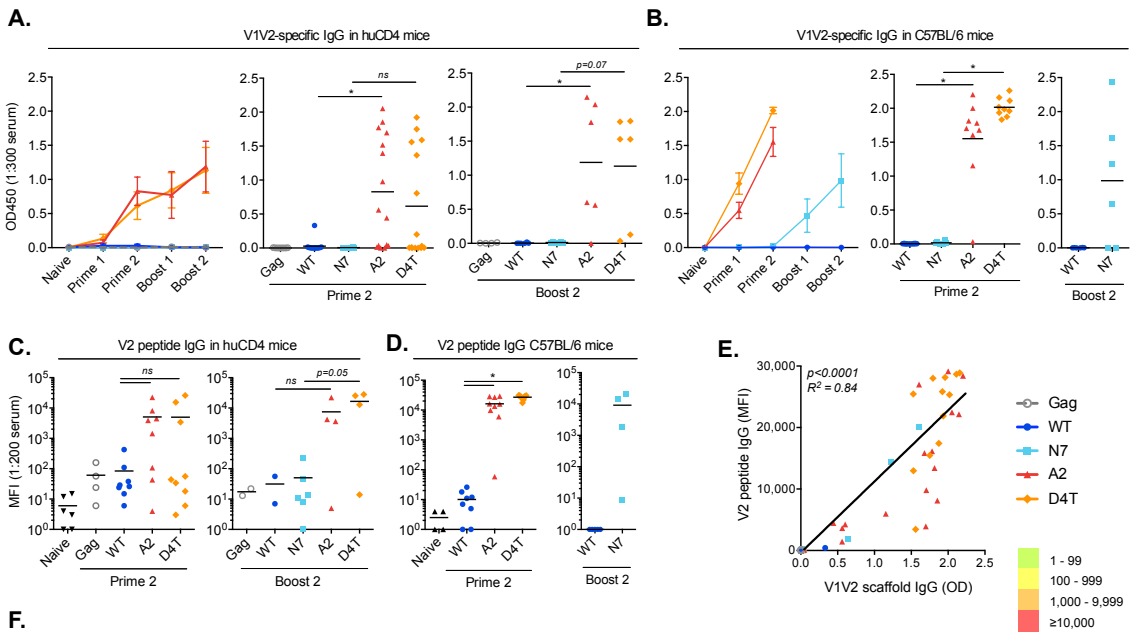

F.

MFI of IgG binding to V1V2 epitopes

	V2 peptide (a.a. 163-183)			V1V2-gp70 scaffold												
	Clade B		Clade C	Clade B			Clade C							Clade AE		Clade BC
Group (n)	WITO4160.33	Consensus Clade B	Consensus Clade C	B.CaseA	RHPA4259.7	TT31P.2F10.2792	7060101641	TV1.21	CAP210.2.00.E8	96ZM651.02	Ce1086_B2	BF1266_431a	CM244.ec1	C2101.c01	BJOX002000.03.2
Naïve (14)	5	3	9	1	1	1	9	1	1	2	4	1	2	1	3
huCD4 mice / Prime 2															
Gag (4)	35	61	87	1	1	46	26	569	1	1	1	1	1	1	1
WT (8)	74	84	136	706	1	85	1	923	1	1	9	1	1	14	1
A2 (8)	314	5,075	711	10,240	233	3,141	867	11,289	7,075	2,561	1,920	11,635	3,407	1,013	1,635
D4T (9)	371	4,990	1,565	7,281	1	3,969	2,607	7,382	5,406	3,972	3,166	8,085	3,829	2,210	2,877
huCD4 mice / Boost 2															
Gag (2)	13	18	69	1	1	12	1	1	1	1	1	1	1	1	1
WT (2)	17	31	109	1	1	9	1	1	1	1	1	1	1	1	1
N7 (6)	36	50	126	3	1	26	1	1	1	1	1	1	1	1	9
A2 (4)	316	7,514	956	15,156	1	6,364	1	16,106	10,200	2,323	2,714	13,963	5,117	52	1,402
D4T (4)	1,035	16,616	5,920	19,463	329	15,872	7,832	22,890	18,375	9,537	12,961	21,866	13,205	8,330	8,373
C57BL6 mice / Prime 2															
WT (8)	61	10	121	1	1	30	1	1	1	1	1	1	1	1	1
A2 (9)	794	16,201	2,017	20,061	2,822	9,595	3,420	20,191	15,711	4,720	6,281	26,727	8,742	3,382	3,733
D4T (9)	1,445	26,997	4,219	25,119	3,495	18,131	8,041	24,217	23,235	12,884	12,819	31,422	16,987	8,215	9,126
C57BL6 mice / Boost 2															
WT (5)	34	1	56	1	1	25	1	1	1	1	1	1	1	1	1
N7 (4)	346	9,124	1,249	13,109	31	5,938	3,519	13,244	10,376	5,141	5,326	17,746	7,041	4,101	3,513

Figure 2.4. Enhanced antibody responses against V1V2 domain and linear V2 peptide generated by CD4-independent Env immunization of mice. (A,B) Binding IgG against scaffolded V1V2, from clade B HIV-1 92US715, fused to MLV gp70 in (A) huCD4 mice and (B) C57BL/6 mice by ELISA. (C,D) Binding IgG to a linear V2 peptide, amino acids 163-183, with a consensus clade B sequence, measured by a multiplex immunoassay, in (C) huCD4 and (D) C57BL/6 mice. (E) Correlation of V1V2 scaffold- and V2 peptide-specific IgG shown in panels A-D. (F) Average binding IgG to multiple V2 peptide and V1V2 scaffold antigens, from the indicated HIV-1 strains, measured by multiplex immunoassay using 1:200 serum. Responses are color-coded by magnitude of MFI. A2 and D4T were compared with WT and N7, respectively, by Kruskal-Wallis test with Dunn's correction. Asterisk: $p<0.05$. ns: $p>0.05$. Horizontal bars: mean. Error bars: s.e.m.

A.

Macaque group	N=	Primes: VV SIV gag-pol & VV HIV Env		SIV Gag-Pol DNA and HIV Env gp120 protein boosts:		
		1st (week 0)	2nd (week 8)	1st (wk 24)	2nd (wk 40)	3rd (wk 56)
WT	6	WT Env	WT Env	WT gp120	WT gp120	WT gp120
N7	6	N7 Env	N7 Env	N7 gp120	N7 gp120	N7 gp120
A2	6	A2 Env	A2 Env	A2 gp120	A2 gp120	A2 gp120
D4T	6	D4T Env	D4T Env	D4T gp120	D4T gp120	D4T gp120

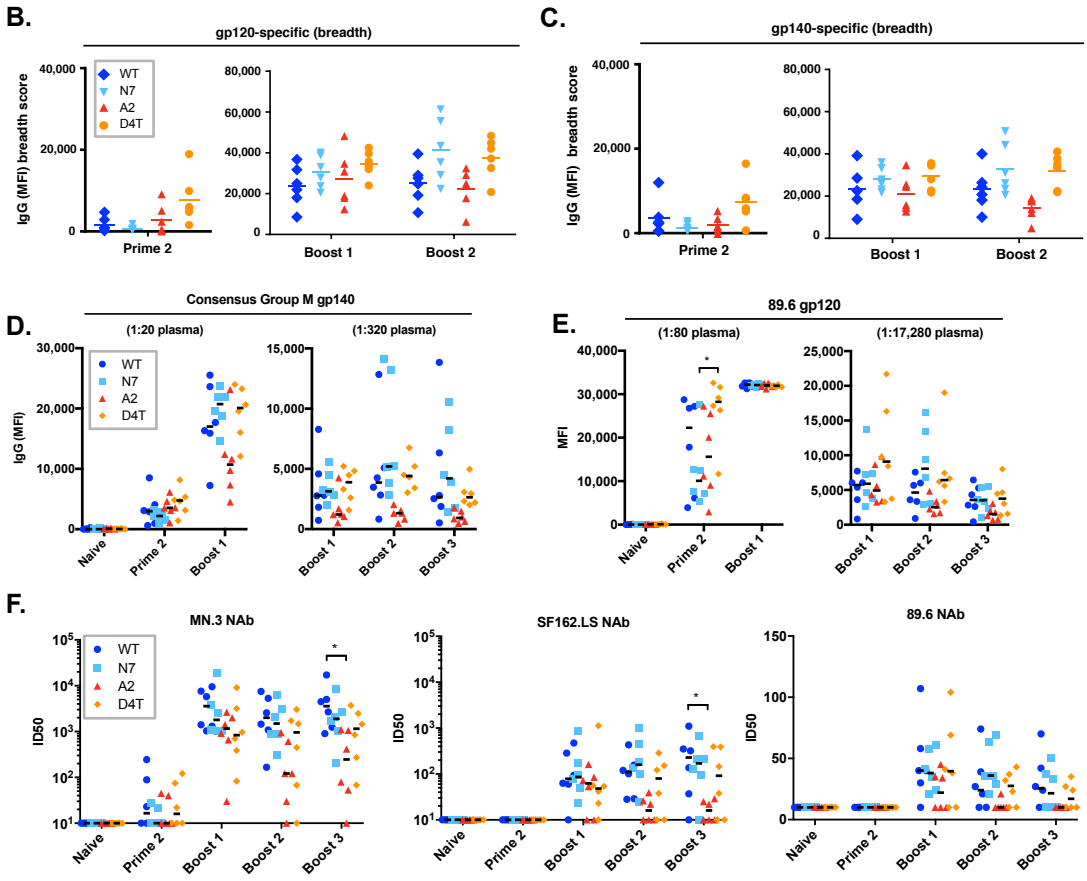

Figure 2.5. Immunogenicity of CD4-independent Envs in vaccinia prime-gp120 boost vaccination of pig-tailed macaques. (A) Schematic of pig-tailed macaque immunization timeline. (B-E) IgG responses measured by a multiplex immunoassay using the indicated plasma dilutions. The linear range in B and C extends from 100 to 23,000. Shown are magnitude-breadth scores against (B) a panel of 17 gp120 reagents and (C) 12 gp140 reagents representing diverse HIV-1 strains, and binding to (C) 89.6 WT gp120 or (D) a consensus group M gp140 protein. (F) Neutralizing antibody (NAb) titers (ID50) against Tier-1 strains (MN.3, SF162.LS) and the autologous Tier-2 strain 89.6. Horizontal bars represent the median in panels B, C, and F and the mean in D and E. A2 and D4T responses were compared to WT and N7, respectively, by one-way (prime) or two-way (boosts) ANOVA with Sidak correction. Asterisk: $p<0.05$.

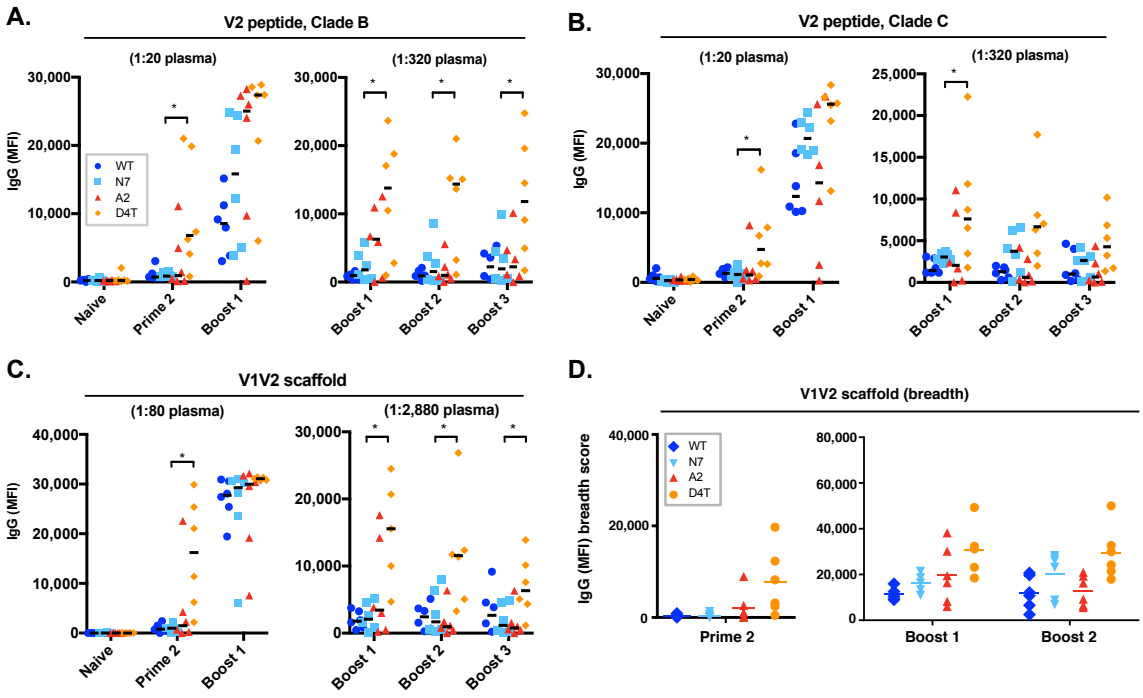

Figure 2.6. Enhanced antibody responses against V1V2 domain and linear V2 peptide by CD4-independent Env D4T immunization of pig-tailed macaques. A multiplex immunoassay was used to quantify binding IgG responses against (A) a consensus clade B V2 peptide, (B) a consensus clade C V2 peptide, (C) the clade B CaseA V1V2 scaffold, and (D) a panel of 16 V1V2 scaffolds representing diverse clades of HIV-1, yielding a composite breadth score. In A-C, the linear range extends from an MFI of 100 to 23,000. Horizontal bars: mean in A-C, median in D. A2 and D4T responses were compared to WT and N7, respectively, by one-way (prime) or two-way (boosts) ANOVA with Sidak correction. Asterisk: $p<0.05$.

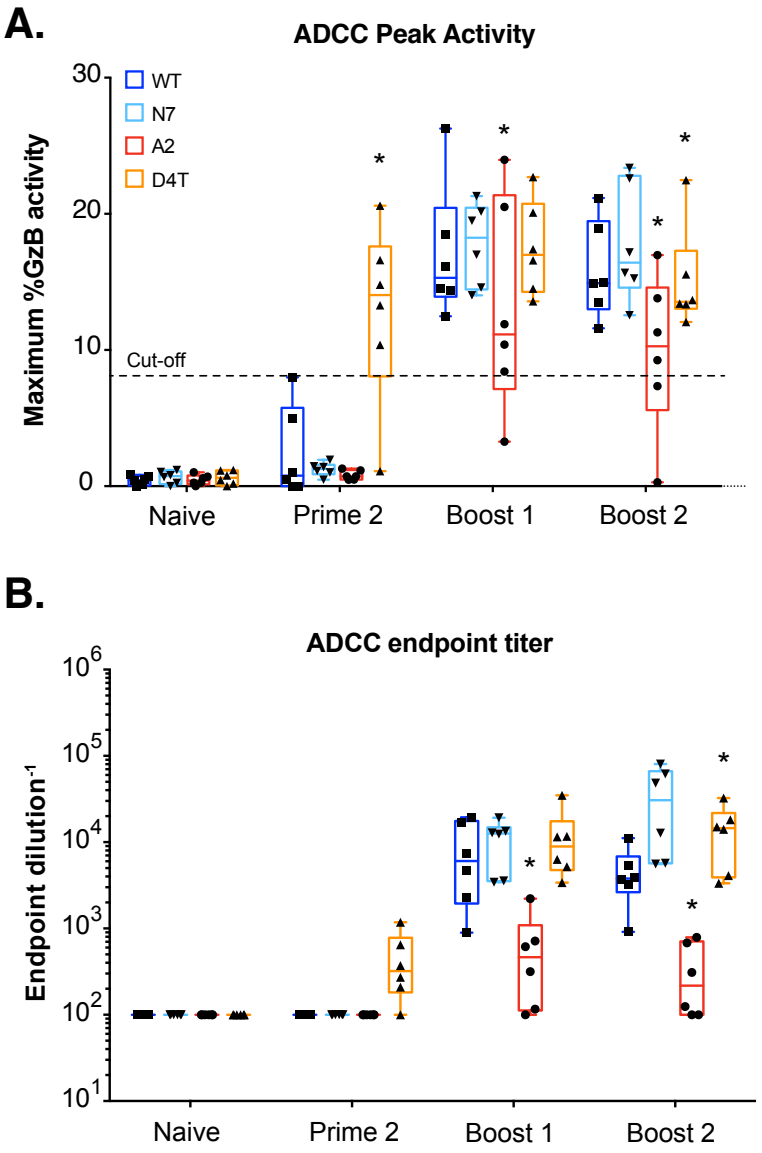

Figure 2.7. Enhanced antibody-dependent cell-mediated cytotoxicity (ADCC) response generated by vaccinia prime with CD4-independent Env D4T. ADCC was measured using HIV-seronegative human PBMCs as effector cells and CEM.NKR-CCR5 cells coated with 89.6 WT gp120 as target cells. Monkey plasma were tested at serial dilutions starting at 1:100, and the frequency of target cells positive for granzyme B (GzB) activity was measured by flow cytometry using a fluorogenic substrate for GzB. Data are expressed as (A) the highest percentage of GzB^+ target cells among the dilution series (peak activity) and as (B) the highest reciprocal plasma dilution yielding a positive signal of ≥8% GzB^+ (endpoint titer). Responses to A2 and D4T were compared to WT and N7, respectively, by Fisher's Exact Test for response rates (Prime 2 only) and peak activity and endpoint titers (Boosts 1 and 2). Significant differences relative to the parent Env ($p<0.05$) are shown by asterisks (response rate statistical analysis show in graph A).

2.4. DISCUSSION

Here we have described the structural and immunologic outcomes of biologically selecting for CD4 independence in two variants of HIV-1 89.6 Env, termed A2 and D4T. Although there were unique features in each adapted variant, both showed increased exposure of CD4-induced epitopes and a linear segment of V2—two antibody specificities that were linked with ADCC activity, and, in the latter case, reduced risk of infection in the RV144 human vaccine trial. Importantly, V2 peptide exposure was greatest on D4T gp120, and this Env generated a significantly increased V2 peptide-specific IgG response in both mice and pig-tailed macaques. We thus observed a clear association between the biological phenotype, structural alterations, and immunogenicity *in vivo*.

This characterization of CD4-independent Envs has prompted a variety of questions and future directions, several of which are already underway. First, it will be critical to determine whether the linear V2 epitope is better exposed in the context of trimeric CD4-independent Envs, in addition to the monomeric gp120 analysis conducted here. Since priming with rVV expressing D4T Env generated significantly greater V2 peptide-specific IgG in macaques, and both A2 and D4T generated an increase in this specificity in mice, it is probable that the trimeric forms of these Envs, in particular D4T, will exhibit greater reactivity to Ab8505 and other V2 peptide-specific mAbs. It will be interesting to determine whether this epitope is most exposed on D4T trimers, in agreement with its greater immunogenicity in macaques. Another question under active investigation is what antibody specificity or specificities are responsible for the more effective ADCC response to D4T during vaccinia priming in macaques. This will be addressed by testing which mAbs,

including those specific for C1 and V2 peptide, block the ADCC activity in macaque immune serum. In addition, it will be useful to determine if CD4-independent Envs elicit high levels of other non-neutralizing, Fc-mediated effector functions besides ADCC, such as antibody-dependent cell-mediated phagocytosis (ADCP) and infectious virion capture. As in this study, ADCP analysis will be focused on macaque serum, as mouse serum has shown issues of high background and low reproducibility in Fc-dependent functional assays.

One important area of uncertainty regards the nature of the structural differences between A2 and D4T and the basis of their differing immunogenicity. In mice, D4T induced modestly higher responses than A2 to scaffolded V1V2 and linear V2 peptide from multiple isolates (Fig. 2.4F). In macaques, D4T elicited a significantly higher and broader V1V2 response than all other Envs (Fig. 2.5 and Supp. Fig. S2.5). The consistently high immunogenicity of V2 in D4T could be explained by the fact that a linear V2-specific mAb bound 4-15 fold better to D4T gp120 than to any other gp120. In agreement with this finding, a portion of the V2 peptide was found to be most exposed to solvent on D4T (Fig. 2.2E). Interestingly, D4T was the only Env recognized by the V1V2-specific bNAb PG9 (Fig. 2.2C); it is unclear whether this reflects a unique conformation or orientation of V1V2 in D4T compared to the other Envs. Overall, these data demonstrate that the linear V2 peptide, and perhaps other parts of the V1V2 domain, may be better exposed or more stably presented on D4T than the other Envs, including A2, leading to greater antibody recognition and immunogenicity. The determinants of the V3 response, including differences between species, are less well understood. A2 generated a slightly higher V3 peptide-specific response in mice, but a significantly lower response in macaques. The basis of this difference is unclear, as A2 was highly

sensitive to neutralization by V3-specific mAbs, whereas D4T was highly resistant to these mAbs. Further structural characterization of the A2 and D4T trimers may offer potential explanations for this pattern of response.

Despite the abundant antigenic data gathered on A2 and D4T, little is known about the extent of openness of these Envs in their trimeric form. This is an important consideration, since the Env trimer has been shown capable of adopting conformations with multiple degrees of openness [236,245], and it is possible that these conformations exhibit distinct immunogenic properties. Conventionally, open vs. closed Env trimers can be distinguished based on the binding of mAbs to quaternary V1V2 epitopes, which are intact in the closed conformation only. Unfortunately, this approach was not feasible for 89.6 Env and its derivatives, which lack an N-linked glycosylation site at position 160. This glycan is important for the binding of most quaternary V1V2-specific bNAbs, including PG9, PG16, PGT141-145, CH01-04, PGDM1400-1412, and others [151,399–402]. Alternatively, the overall structure of A2 and D4T trimers could be elucidated using cryo-electron microscopy [343], and the differences in sampling of open and closed trimer conformations could be monitored in real time using smFRET [236]. As indirect evidence of openness, A2 and D4T trimers exhibit increased reactivity to mAbs at multiple CD4-induced epitopes with distinct antigenic footprints (Fig. 2.2B), indicating the exposure of a wide surface area encompassing the co-receptor binding site and the gp41-interactive face of gp120 [198]. However, the increase in exposure of these epitopes was modest (~2-fold). Further analysis of A2 and D4T revealed that neither Env became globally neutralization-sensitive, as has been reported for some other CD4-independent Envs [122,373,375]. On the contrary, both Envs became slightly more resistant to pooled patient plasma. This might be explained by a previous

observation by Kolchinsky and colleagues that some CD4-independent Envs only showed high neutralization sensitivity on target cells that lacked CD4, but not on those that expressed CD4, as in our assay [374]. Another unexpected result was that D4T and N7 were equally sensitive to 17b, while A2 was moderately (7-fold) more sensitive than WT. Previously derived CD4-independent HIV-1 Envs have demonstrated various levels of increased sensitivity to 17b, ranging from 7 to >3000-fold [122,375]. It is also interesting that these CD4-independent Envs did not exhibit increased antigenicity of the V3 loop, and D4T in particular did not show any indications of having an exposed V3 loop, in contrast to the prevailing view of a CD4-independent trimer [374,375]. These data suggest that D4T might not be stabilized in a completely opened conformation; the exposure of V2 and apparent occlusion of V3 suggest that the dynamic equilibrium of D4T could instead favor a partially opened state or a prefusion intermediate bound to one CD4 molecule, as proposed by Kwon and colleagues [245]. If true, there may be significant heterogeneity among CD4-independent Envs in trimer conformation, antigenicity, and possibly immunogenicity.

It is not yet known whether the pattern of antibody response described in this study, in particular the high V2-specific IgG, is representative of all CD4-independent Envs, or whether it is an unusual phenotype for A2 and D4T. In a recent report, a soluble gp140 protein from the CD4-independent Env ADA N197S exhibited several of the same structural properties as A2 and D4T [374,383] and elicited a significantly higher ADCC response in guinea pigs, suggesting that there may be commonalities across diverse CD4-independent Envs. Conversely, it is apparent from the current investigation that even A2 and D4T do not elicit identical responses, at least in pig-tailed macaques, supporting the notion that structurally divergent CD4-independent Envs likely induce different antibody specificities and functions. Future studies will be

able to clarify whether there are any generalizable features of the humoral immune response elicited by CD4-independent Envs.

An interesting feature of the antibody response to A2 and D4T was the distribution of V1V2-specific IgG responses in huCD4 mice compared to C57BL/6 mice and macaques. The mechanism of the bimodal, or partially inhibited, V1V2 response in huCD4 mice is not yet known. It does not appear to be attributable to an inhibitory effect of CD4 binding, since A2 and D4T elicited similar distributions of V1V2 responses in mice despite drastically different affinities for CD4. This explanation would also not be consistent with the observation that pig-tailed macaque CD4 interacts relatively poorly with HIV-1 Env [403,404]. Another possibility is that the B cell response in huCD4 mice is impaired as a result of the transgenic nature of CD4 expression, although it is unclear how such a defect would result in a bimodal response to only one epitope specificity. It is also possible that huCD4 and C57BL/6 mice have genetic differences besides CD4, since the transgenic strain was derived from C57BL/6/SJL mice back-crossed with C57BL/6.

Our work suggests several future directions to further define the utility and efficacy of CD4-independent Env immunogens. First, it should be determined whether CD4-independent Env vaccination can prevent or delay infection in a clinically relevant challenge model, such as repeated low-dose mucosal inoculation of macaques with a chimeric HIV-1/SIV (SHIV) encoding a transmitter-founder HIV-1 Env with affinity for macaque CD4 [405]. A limitation of the current study is that such a challenge was not possible. If any level protection were observed in a challenge, then the correlates of protection would provide useful insights into the protective mechanisms of non-neutralizing antibodies. Such information could guide the design of future immunogens, including alternative CD4-independent Envs.

Although the vaccinia prime-gp120 boost regimen described here was able to generate a favorable antibody response with CD4-independent Envs, both prime and boost might be improved using newly developed vaccine approaches. For example, nucleoside-modified mRNA is emerging as an extremely potent and versatile vaccine platform that generates high levels of NAb against HIV-1 Env and other pathogens ([305–307] and unpublished observations). Compared to vaccinia, an mRNA vaccine encoding a CD4-independent Env may elicit a more potent antibody response to the same epitopes, leading to higher levels of ADCC or other activities. In addition, a CD4-independent Env prime may be boosted with an immunogen specifically designed to elicit NAbs, such as a SOSIP trimer [46]. In this way, non-neutralizing V1V2-specific antibodies might theoretically be matured to develop into Tier-2 NAbs with specificity similar to PG9.

HIV-1 has developed a host of strategies to evade the humoral immune response, in particular NAbs, and is therefore an exceptionally challenging vaccine target. The present study suggests that CD4-independent Env immunogens may represent a viable path to eliciting non-neutralizing antibodies with broad reactivity, antiviral activity, and epitope specificities that have previously been associated with clinical vaccine protection from HIV-1 infection.

2.5. METHODS

Ethics statement

The investigators faithfully adhered to the “Guide for the Care and Use of Laboratory Animals” by the Committee on Care of Laboratory Animal Resources Commission on Life Sciences, National Research Council. Mouse studies were conducted at University of Pennsylvania facilities that are accredited by the American Association for Accreditation of Laboratory Animal Care (AAALAC) under protocols approved by the University of Pennsylvania Institutional Animal Care and Use Committee (IACUC). Pig-tailed macaques (*Macaca nemestrina*) were housed at the Washington National Primate Research Center (WaNPRC). WaNPRC is accredited by the Association for the Assessment and Accreditation of Laboratory Animal Care (AAALAC) International and registered as a USDA Class R research facility. WaNPRC is certified by the NIH Office of Laboratory Animal Welfare (OLAW A3464-01). All animal-related experiments were performed under protocol 2370–23, approved by the University of Washington IACUC. This study was carried out in strict accordance with the recommendations in the Guide for the Care and Use of Laboratory Animals of the NIH (The Guide). All animals were housed by the WaNPRC and included in standard monitoring procedures, including at least twice-daily observation by animal technicians for basic husbandry parameters (e.g., food intake, activity, stool consistency, overall appearance) as well as daily observation by a veterinary technician and/or veterinarian. All efforts were made to minimize animal pain and suffering, in accordance with the recommendations. Analgesics, anesthetics, and/or tranquilizers were used to limit the discomfort, distress, or pain associated with experimental procedures.

Mice

C57BL/6 mice were purchased from NCI. HuCD4 mice, which lack murine CD4 and express human CD4 (human $CD4^{-/-}$, murine $CD4^{-/-}$) [393], were derived from doubly heterozygous mice (human $CD4^{+/-}$, murine $CD4^{+/-}$) obtained from MMRRC (strain 000222-UNC). All mice were housed in a BSL2 containment facility. Female mice were used for immunizations and were approximately 6 weeks of age at the first injection.

Pig-tailed macaques

The 24 naïve male pig-tailed macaques used on this study were bred in captivity and originated from the WaNPRC breeding colony (WaNPRC at SNBL USA-SRC, Alice TX). Immunizations started when macaque ages were 1.7-3.5 years and weights were 2.5 kg-5.7 kg. Animals were fed daily of a commercial monkey chow, which was supplemented with fresh fruits and vegetables, given access to water, and fasted prior to sedation. Environmental enrichment included grouping in compound, large activity, or run-through connected cages, perches, toys, food treats, and foraging activities. No genotyping was done.

Cells

The SupT1/CCR5 cell line ($CD4^+$ $CCR5^+$ $CXCR4^+$) was generated from human $CD4^+$ T lymphoblastoid SupT1 cells by expressing human CCR5 via lentiviral transduction. The BC7/CCR5 ($CD4^-$ $CCR5^+$ $CXCR4^+$) cell line was similarly generated by lentivirally expressing human CCR5 in BC7 cells, a spontaneous CD4-negative clone of SupT1 cells [368]. Both cell lines were grown in RPMI 1640 supplemented with 10% FBS, 2 mM L-glutamine, and penicillin-streptomycin

(Invitrogen). Human embryonic kidney (HEK) 293T cells were obtained from ATCC and were grown in DMEM with 10% FBS, 2 mM L-glutamine, and penicillin-streptomycin (complete DMEM). The Japanese quail fibrosarcoma QT6 cells, BSC40 cells, and TZM-bl cells (a $CD4^+$ $CCR5^+$ $CXCR4^+$ modified HeLa cell line) (NIH AIDS Reagent Program) were grown in DMEM with 10% FBS.

Derivation of CD4-independent HIV-1 Envs

CD4-independent Envs were cloned into a SHIV/89.6 proviral plasmid encoding the either 89.6 WT Env or 89.6 N197Q (N7) Env in an SIVmac239 background. Plasmids containing the 5' and 3' halves of the viral genome (hemigenomes) were linearized, ligated, and electroporated into SupT1/CCR5 cells to start viral growth. Viral stocks were prepared by propagating virus in SupT1/CCR5 or BC7/CCR5 cells. Equal amounts of virus (50 ng p27) were added to a 1:9 mixed culture of $CD4^+$ SupT1/CCR5 cells and $CD4^-$ BC7/CCR5 cells. Cell-free virus was serially passaged on mixed cultures and infection was monitored by a Gag-specific immunofluorescence assay (IFA). When >50% of cells were Gag^+ by IFA (after 54 passages), virus was propagated in a pure culture of BC7/CCR5 cells for 8-9 more passages and Env sequences were amplified from genomic cellular DNA and cloned into the expression vectors pCR2.1 (Thermo) and pCIneo (Promega), into an unmutated SHIV/89.6 3' hemigenome plasmid, and into a vaccinia shuttle vector.

Cell-cell fusion assay

Env fusogenicity was measured quantitatively by a cell-cell fusion assay as previously described [406]. Briefly, QT6 effector cells were transfected with Env expression vectors and transduced with rVV encoding T7 polymerase, and QT6

target cells were transfected with a T7-driven luciferase reporter plasmid plus various combinations of the human receptors CD4, CCR5, and CXCR4, or GFP as a control. Target cells were incubated overnight at 37°C and effector cells were incubated overnight at 32°C in the presence of rifampicin. The cells were then mixed and incubated at 37°C, and luciferase activity was read 8 hr later.

Viral growth curves

Replication-competent SHIV/89.6 viral stocks were produced in SupT1/CCR5 (WT and N7) or BC7/CCR5 cells (A2 and D4T), and viral titers were quantified by p27-Gag ELISA (Advanced Bioscience Laboratories). Equal amounts of virus (50 ng of p27-Gag) were used to inoculate 1 million SupT1/CCR5 or BC7/CCR5 cells by spinoculation [407]. After 24 hr, cells were washed once and supplied with fresh growth medium. Medium was added as needed to maintain cell densities under ~2 million/mL. Viral replication was monitored over time by measuring reverse transcriptase activity in the supernatant by a standard [3H]thymidine incorporation assay.

Recombinant vaccinia viruses

Recombinant vaccinia virus (rVV) vectors expressing HIV-1 Envs or SIV Gag-Pol under a synthetic early-late promoter were made by homologous recombination between a shuttle vector and the thymidine kinase (TK) gene of v-NY, a replication-competent vaccinia virus that was plaque purified from the New York City Board of Health strain. Recombinant viruses were grown under negative selection in TK− 143B cells with 25 μg/mL 5-bromodeoxyuridine for two rounds of plaque purification, followed by a third round in BSC40 cells without selection pressure. Plaques were

screened for transgene by PCR using a primer set specific for TK and the transgene. Recombinant viruses were expanded in BSC40 cells and sequence verified by PCR.

Purified viral stocks were prepared as follows: rVV-infected BSC40 cell pellets were homogenized in 10 mM Tris buffer (pH=9) with a Dounce homogenizer on ice; the material was centrifuged for 5 min at 1360 RPM at 4°C, and supernatant was collected. Cold Tris buffer was added and the material was re-centrifuged. Supernatants from both spins were pooled and sonicated in a 550 Sonic Dismembrator at an amplitude setting of 8 for three 1-min intervals. The material was layered onto 36% sucrose in Tris buffer and ultra-centrifuged at 15,800 rpm in an SW28 rotor for 80 min at 4°C. The supernatant was discarded and the virus pellet was resuspended in cold 1 mM Tris (pH=9.0) and sonicated as above before being stored at -80°C. Crude viral stocks were prepared similarly as above, but without ultra-centrifugation over sucrose.

Antigenicity assay of surface-expressed Envs

Env antigenicity was assessed by measuring the binding of mAbs and ligands to surface-expressed Env on HEK 293T cells. 293T cells were infected with crude stocks of rVV vectors expressing 89.6 WT, N7, A2, and D4T Envs at a multiplicity of infection (MOI) of 3. Virus was absorbed onto cells at 37°C for 1 hr in 0.5 mL PBS with 10 mM $MgCl_2$ and 0.01% BSA, and then replaced with 2 mL of DMEM with 10% FBS. After 16 hr of incubation, cells were harvested and stained without permeabilization using the following reagents: 2G12, VRC01, VRC03, b12, CD4-IgG, 697-30D, 2158, 447-52D, PGT121, PGT126, PG9, PG16, 35O22, PGT151, 2F5 (NIH AIDS Reagent Program), A32, N5-i5, 2.2c, N12-i3, N26-i1, E51, 17b, N12-i2, N12-i18, N10-i3.1 (kindly provided by Dr. George Lewis). Antibody binding was

detected using 1:100 goat anti-human IgG Alexa Fluor 647 conjugate (Invitrogen, A-21445). VV A33 protein was simultaneously stained using 1:300 rabbit anti-A33 serum (kindly provided by Dr. Stuart Isaacs) and 7.5 μg/mL goat anti-rabbit IgG FITC conjugate (BD Biosciences 552420). Each stain was performed for 30 min on ice. Samples were fixed with paraformaldehyde after staining and fluorescence was measured using a FACSCalibur flow cytometer. Ten thousand events were collected and live, $A33^+$ cells were gated to determine the mean fluorescence intensity (MFI). Analysis was performed using FlowJo software (Tree Star). MFI values were normalized to the corresponding 2G12 signal to account for differences in surface expression, and these values are expressed as fold changes relative to parental Envs.

Immunoprecipitation and Western blot

Cell lysates of BSC40 cells producing HIV-1 Env gp160- or gp120-expressing rVV were subjected to immunoprecipitation analysis. Briefly, 50 μL of protein G Dynabeads (Invitrogen) were added to an Eppendorf tube, washed twice with PBS, and resuspended in 500 μL of PBS. 1 μg of antibody (PG9, PG16, b12) was added to the tubes. The mixture was rotated for 10 min at room temperature and then washed three times with PBST (0.02% Tween-20). 100 μL of cell lysates were added to the tubes containing the antibody and protein G Dynabeads. The mixture was rotated for 30 min at room temperature, and then washed three times with PBST. The protein G-antibody-antigen complex was then resuspended in 50 μL of SDS-PAGE loading buffer. The protein complexes were resolved on 4-12% Bis-Tris NuPAGE Protein Gel (Invitrogen) and followed by western blot [408], using an

alkaline phosphatase (AP)-conjugated anti-human IgG antibody (Sigma) according to the manufacturer's instructions.

Neutralization assays

HIV-1-neutralizing activity in the serum of immunized animals and neutralization sensitivity of SHIVs expressing 89.6 WT, N7, A2, and D4T Envs was measured in a luciferase reporter assay using TZM-bl cells, similarly to previously described [409]. Antibodies (listed in Fig. 2.2) were obtained from the NIH AIDS Reagent Program, and pooled patient plasma was obtained commercially from NABI. Briefly, 150-200 $TCID_{50}$ of virus was incubated with serial three-fold dilutions of antibody or serum/plasma in duplicate in a volume of 50 µL for 1.5 h at 37°C before addition to 10,000 TZM-bl cells in 100 uL of growth medium containing DEAE-dextran. Virus control wells received only virus and cells, and background control wells received only cells. After 48 h of incubation, luciferase activity was quantified as relative light units (RLU) using BrightGlo substrate solution (Promega). Neutralization activity was expressed as the concentration of antibody or ligand (expressed as IC_{50}) or reciprocal serum dilution (expressed as ID_{50}) that resulted in 50% reduction in RLU.

Preparation of gp120 protein

89.6 WT, N7, A2, and D4T gp120 proteins were purified from the supernatant of BSC40 cells infected with rVV as described previously [410]. Briefly, BSC40 cells were infected with rVV at an MOI of 3 and supernatant was harvested at 48 h post infection. Monomeric gp120 was purified by a three-step process using lectin affinity (Galanthus nivalis lectin-coupled agarose), ion exchange (DEAE-dextran), and size

exclusion chromatography (HighLoad 26/600 Superdex 200). The monomeric nature of the gp120 was verified by native PAGE, and purity was determined by SDS-PAGE with Coomassie stain.

Preparation of gp70-V1V2 scaffold protein

The V1V2 region of HIV-1 clade B strain 92US715 [411] was PCR-amplified from its *env* clone using paired primers (forward primer 5'-TCAACTGGTACCGTGAAGCTGACCCCCCTGTG-3' and reverse primer 5'-TCAACTGGATCCCTATTAGGCCTGGGTGATCACGCTGG-3'). The V1V2 DNA fragment was cloned into a mammalian expression vector pJW4303 with the MLV gp70 backbone [412] using KpnI and BamHI cloning sites. V1V2 was fused at the C-terminus of the gp70 protein, with a 6xHis tag at the N-terminus of the fusion protein. The constructed was sequenced-verified and used to transfect HEK 293T cells. Supernatant was harvested at 72 hours and V1V2 scaffold was purified by nickel column affinity chromatography. The scaffold protein was verified by Western-blot analysis using rabbit anti-V1V2 polyclonal antibody.

Hydrogen-deuterium exchange with mass spectrometry (HDX)

Samples for HDX were prepared essentially as described previously [413] by adding 8 µL of gp120 at 1.25 mg/mL with 0.5 µg/mL Pro-Pro-Pro-Ile peptide as an internal standard [414] to 93 µL of D_2O (Cambridge Isotopes) supplemented with 11 mM sodium phosphate, 160 mM sodium chloride, and 0.02% sodium azide at pH 7.4. Exchange reactions were carried out in this 88% deuterium buffer at 22^{o}C for 3 sec, 1 min, 30 min, and 20 hours prior to the addition of 90 µL cold quench solution consisting of 0.2% formic acid, and 200 mM Tris carboxy-ethane-phosphate (TCEP),

titrated with 10 M NaOH to a pH of 2.5. Quenched samples were digested with 10 µL of 2 mg/mL pepsin for 5 min on ice prior to flash freezing in liquid nitrogen and storage at -80^{o}C. Samples were prepared in triplicate, in parallel with controls: undeuterated (H_2O-based buffer), "zero exchange" (pre-mixed deuterium and quench solutions), and fully deuterated (gp120 proteins were denatured in 2 M guanidine HCl with 40 mM dithiothreitol (DTT) at 60^{o}C for 30 min prior to the addition of deuterated buffer and incubation at 37^{o}C for 4 hours prior to the addition of quench solution). Peptides and glycopeptides generated by pepsin digestion were identified by manually sequencing tandem mass spectrometry data collected on natively glycosylated and PNGaseF-treated gp120 peptides using a Waters Acquity UPLC system integrated with a Synapt HDMS Q-TOF mass spectrometer. The deuterium uptake of sequenced peptides, identified by exact mass and elution time, was measured in duplicate for each gp120 construct on the same LC-MS system as previously described [413]. Data were analyzed using HX-Express 2 [415,416].

Kinetic analysis by biolayer interferometry

A FortéBio Octet Red instrument (Menlo Park, CA) was used to study kinetics of 89.6 WT, N7, A2, and D4T gp120s binding to CD4-IgG2, VRC01, b12, NIH45-46, 17b, A32, 48d, and N5i5. The kinetic assays were performed at 25°C. Antibodies (10 µg/ml) in Octet running buffer (10 mM HEPES, 150 mM NaCl, 3 mM EDTA, and 0.05% Tween-20, pH 7.4, with 0.01% BSA and 0.02% azide) were loaded on the surface of pre-hydrated Anti-Human IgG Fc Capture (AHC) biosensors for 7 min, followed by a 3 min washing step in running buffer to reach a stable baseline. The analysis of gp120 association was conducted by dipping the antibody-AHC biosensors into gp120 samples serially diluted in running buffer. For most antibody-

gp120 interactions, gp120 concentration ranged from 1 μM to 15.6 nM in a two-fold dilution series, but the gp120 concentrations were adjusted within a relevant range in accordance with the observed binding affinities for each antibody. Dissociation was monitored by returning biosensors to running buffer. The interval times for association and dissociation were optimized for each antibody in order to achieve sufficient curvature for fitting. Biosensors were regenerated after dissociation by incubation in 10 mM glycine pH 1.5 for 30 sec. Data analysis and curve fitting were processed using Octet software version 7.0. Prior to data processing, the averaged reference measurements were subtracted. Experimental data were fitted with a 1:1 binding model. The ensemble dissociation constants ($K_D = k_a/k_d$) were calculated by the obtained association rate (k_a) and dissociation rate (k_d) rate constants. Each experiment was repeated at least twice with similar results.

Mouse immunizations

Mouse immunizations were conducted in two separate experiments. The first was a prime-boost experiment that included injections at weeks 0 and 4 of 10^8 plaque-forming units (PFU) of rVV expressing SIV Gag-Pol (n=4) or 89.6 WT, N7, A2, or D4T Envs (n=6/group). Purified rVV vectors were injected i.p. in a volume of 100 μL in sterile Dulbecco's phosphate-buffered saline without magnesium or calcium (DPBS). All five rVV vectors were administered to female huCD4 mice, and WT and N7 vectors were also administered to female C57BL/6 mice. All groups of mice received protein boosts at weeks 8 and 12 consisting of 5 μg of purified gp120 in 1% alum (Alhydrogel, Invivogen) in DPBS. Protein boosts were administered by injection of 25 μL into each quadricep. Env-primed mice were boosted with the same gp120 sequences used in the rVV prime, and Gag-Pol-primed mice were boosted

with WT 89.6 gp120. In a second prime-only experiment, huCD4 mice were similarly primed at weeks 0 and 4 with 10^8 PFU of rVV expressing SIV Gag-Pol (n=5) or WT, A2, or D4T Envs (n=8-9/group), and C57BL/6 mice were primed with WT, A2, and D4T Envs (n=8-9/group), and no boosts were administered. In both experiments, serum was collected prior to each injection and at the time of euthanasia and splenectomy, which were conducted 10 days following the second prime or 14 days following the second boost. Data from the two experiments were graphically combined for mice of the same strain and injection history.

Pig-tailed macaque immunizations

Pig-tailed macaques (*Macaca nemestrina*) were immunized in a vaccinia prime-protein boost regimen (n=6/group). Each prime consisted of a mixture of 10^8 rVV expressing SIV Gag-Pol and 10^8 rVV expressing full-length HIV-1 Env (WT, N7, A2, or D4T) administered at 0 and 8 weeks via skin scarification. Each boost consisted of (i) 100 µg of autologous gp120 in 1% alum (Alhydrogel, Invivogen) in 0.4 mL, delivered intramuscularly, split between left and right arms, and, separately, (ii) 5 mg of DNA encoding SIVmac239 Gag on the pV1R plasmid [417] (prepared by Aldevron) in 2.2 mL, delivered intramuscularly, split between two arms. Boosts were administered at weeks 26, 42 and 58. Blood samples were collected at weeks 0, 2, 4, 8, 10, 12, 16, 20, 26, 28, 30, 34, 38, 42, 44, 46, 51, 58, 60, 62.

ELISAs for antigen-specific IgG

HIV-1 gp120-specific IgG in mouse serum was quantified by ELISA using a gp120-specific murine mAb, 3B3, as a standard. Immulon 4HBX 96-well plates were coated with 100 uL of 1 µg/mL 89.6 WT gp120 in PBS overnight at 4°C. Plates were

washed once with wash buffer (0.05% Tween-20 in PBS) and blocked with blocking buffer (2% BSA in PBS) for 1 hr, followed by three washes. Dilutions of sera and standard were made in blocking buffer and incubated on the plates for 1.5 hr. Samples were removed and plates were washed four times. Goat anti-mouse IgG HRP conjugate (Sigma-Aldrich A8924) at 1:10,000 in blocking buffer was incubated for 1 hr. After four washes, TMB substrate mixture (KPL) was added for 20 min. 2 N sulfuric acid (50 µL/well) was used to stop the reaction, and the optical density (OD) was read at 450 nm on a Dynex MRX Revelation microplate reader.

VV-, V3-, and V1V2-specific IgG ELISAs were performed similarly to gp120-specific IgG ELISA, with the following modifications. For VV, the coating antigen was Western Reserve VV lysed in RIPA buffer, diluted 1:200 in PBS (kindly provided by Dr. Stuart Isaacs). For V3, the coating antigen was synthetic 89.6 Env V3 peptide (GenScript) at 5 µg/mL in PBS. For V1V2, the coating antigen was a scaffold protein containing HIV-1/92US715 V1V2 fused to MLV gp70 at 1 µg/mL in PBS.

Murine IgG subclass assay

Mouse sera was diluted 1:100 in PBS, and relative titers of antigen-specific antibody titers of total IgG, IgG1, IgG2a, IgG2b, IgG2c, IgG3, IgM, and IgA were determined by multiplexed bead assay, as described in [418]. Specifically, antigens (89.6 gp120, SF162 gp120, CaseA2 gp70 V1/V2, V3, gp70, influenza HA, and Ebola GP) were coupled to microspheres (Luminex) using EDC/Sulfo NHS carbodiimide crosslinking chemistry. Diluted sera were incubated with antigen-coupled beads (2500 total beads/well) overnight at 4C with shaking. Beads were washed three times with PBS containing 0.05% Tween 20, and incubated with the following PE-conjugated secondary antibodies for 2 hours at room temperature: anti-mouse IgG,

anti-mouse IgG1, anti-mouse IgG2a, anti-mouse IgG2b, anti-mouse IgG2c, anti-mouse IgG3, anti-mouse IgM, and anti-mouse IgA (Southern Biotech). Beads were washed three times with PBS containing 0.05% Tween 20, and resuspended in BioPlex Sheath Fluid (Bio-Rad) prior to acquisition on BioPlex 3D Suspension array system (Bio-Rad). A minimum of 50 beads/region for all bead regions was collected, and the data are reported as mean fluorescent intensity (MFI).

Murine splenocyte stimulation and intracellular cytokine staining

To quantify Env- and VV-specific T cell responses in mice, splenocytes (2 x 10^6) were incubated with four separate SHIV/89.6P Env peptide pools (NIH AIDS Reagent Program) or one immunodominant VV peptide pool (NR-4058, BEI Resources) at 37°C and 5% CO_2. All peptides were used at 1 mg/mL, and DMSO was used as a control for background. After 1 hr, GolgiPlug (brefeldin A), GolgiStop (monensin), and anti-CD107a-FITC (BD Biosciences) were added and cells were incubated for an additional 5 hrs. Cells were washed in PBS and resuspended in live/dead Aqua Blue stain (Invitrogen) for 10 min at room temperature. A mixture of anti-CD44-PE/Cy5, anti-CD27-PE (BD Biosciences), anti-CD8-Pacific Blue, and anti-CXCR5-Brilliant Violet 605 (BioLegend) antibodies was added and incubated for 30 min at room temperature. Cells were washed in FACS buffer (PBS, 1% FBS), resuspended in FIX & PERM (BD Biosciences), and incubated for 20 min at room temperature. Cells were washed with Perm/Wash (BD Biosciences), then resuspended in a mixture of anti-TNFα-PE/Cy7, anti-IFNγ-Alexa Fluor 700, anti-IL2-APC, and anti-CD3-APC/Cy7 antibodies (BD Biosciences) and incubated at room temperature for 1 hr. Cells were washed, resuspended in 1% paraformaldehyde in PBS, and analyzed for fluorescence using an LSRII (BD Biosciences). Analysis was

performed using FlowJo software (Tree Star). Events were gated on live (Aqua Blue$^-$) cells. CD4$^+$ cells were identified as CD3$^+$/CD8$^-$ cells. Background-subtracted percentages of cytokine-positive cells for each Env peptide pool were added together to yield the Env-specific CD4$^+$ or CD8$^+$ T cell response.

Binding antibody multiplex binding assay (BAMA)

HIV-1 specific IgG antibodies to gp120/gp140 proteins, Env peptides and V1/V2 scaffolds were measured by an HIV-1 binding antibody multiplex assay as previously described [192,419], and the detecting antibody was an anti-macaque IgG or goat anti-mouse IgG, Human ads-PE (Southern Biotech), as applicable. All assays were run under GCLP compliant conditions, including tracking of positive controls by Levy-Jennings charts using 21CFR Part 11 compliant software. Positive controls included a HIVIG and CH58 mAb IgG titration. Negative controls included in every assay were blank (uncoupled) and MulVgp70_His6 (empty gp70 scaffold) coupled beads, a blank well on each assay plate, as well as HIV-1 negative sera. To control for antigen performance, we used the preset criteria that the positive control titer (HIVIG) included on each assay (and for assays with V1V2 antigens, CH58 mAb [209]), had to be within 3 standard deviations of the mean for each antigen (tracked with a Levy-Jennings plot with preset acceptance of titer and calculated with a four-parameter logistic equation, SigmaPlot, Systat Software). Antibody measurements were acquired on a Bio-Plex instrument (Bio-Rad, Hercules, CA) using 21CFR Part 11 compliant software and the readout is in MFI. Area under MFI-plasma dilution curve (AUC) was calculated using the Trapezoidal Curve Fit method [420]. Positivity of plasma binding response was determined with the following positivity criteria: 1) MFI > antigen-specific cutoff (which is 95th percentile MFI of all

baseline plasma samples, and 100 minimum); 2) MFI > 3-fold MFI of the matched baseline sample.

Antibody-dependent cell-mediated cytotoxicity (ADCC)

The ADCC assay was conducted using the GranToxiLux method as previously described [421]. Briefly, primary human PBMCs from HIV-seronegative donors served as effector cells and CEM.NKR-CCR5 cells served as targets. Target cells were coated with 89.6 WT gp120 and mixed 1:30 (target:effector) with PBMCs in the presence of six 4-fold serial dilutions of macaque plasma, starting at 1:100. Cells were treated with a fluorogenic granzyme B substrate (OncoImmunin), and a flow cytometric assay was used to quantify the frequency of target cells (identified by a pre-loaded dye, TFL4) that contained active granzyme B. The cut-off for positive ADCC values was set at 8%, and endpoint titers were calculated as the highest reciprocal dilution of plasma producing a %granzyme B-positive value greater than or equal to the cut-off.

Statistical analysis

Statistical tests were performed using GraphPad Prism software unless otherwise noted. Log transformations were performed for data that were expressed as ratio; parametric or non-parametric tests were chosen for each analysis based on whether the data were normally distributed; and corrections for multiple comparisons were made as noted in each figure legend.

2.6. SUPPLEMENTARY DATA

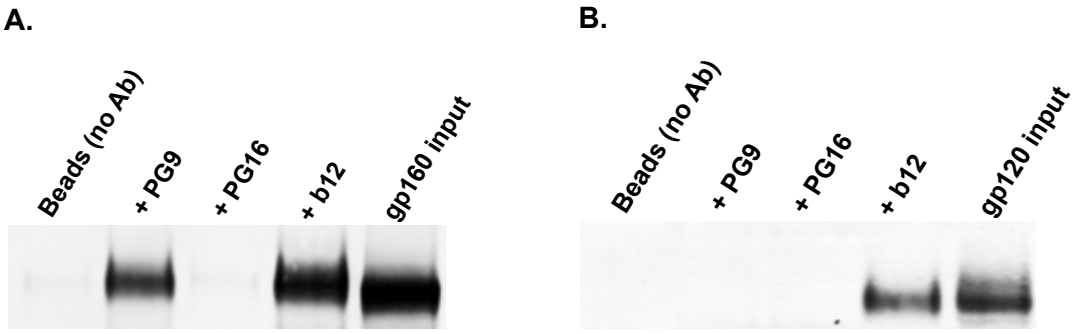

Supp. Fig. S2.1. Co-immunoprecipitation of D4T Env by bNAb PG9. BSC40 cells were infected with rVV expressing D4T Env (A) gp120 or (B) gp160 and were lysed and then incubated with antibody-coated magnetic beads. The beads were washed three times and prepared for SDS-PAGE and Western blot analysis, using a rabbit anti-gp120 polyclonal antibody.

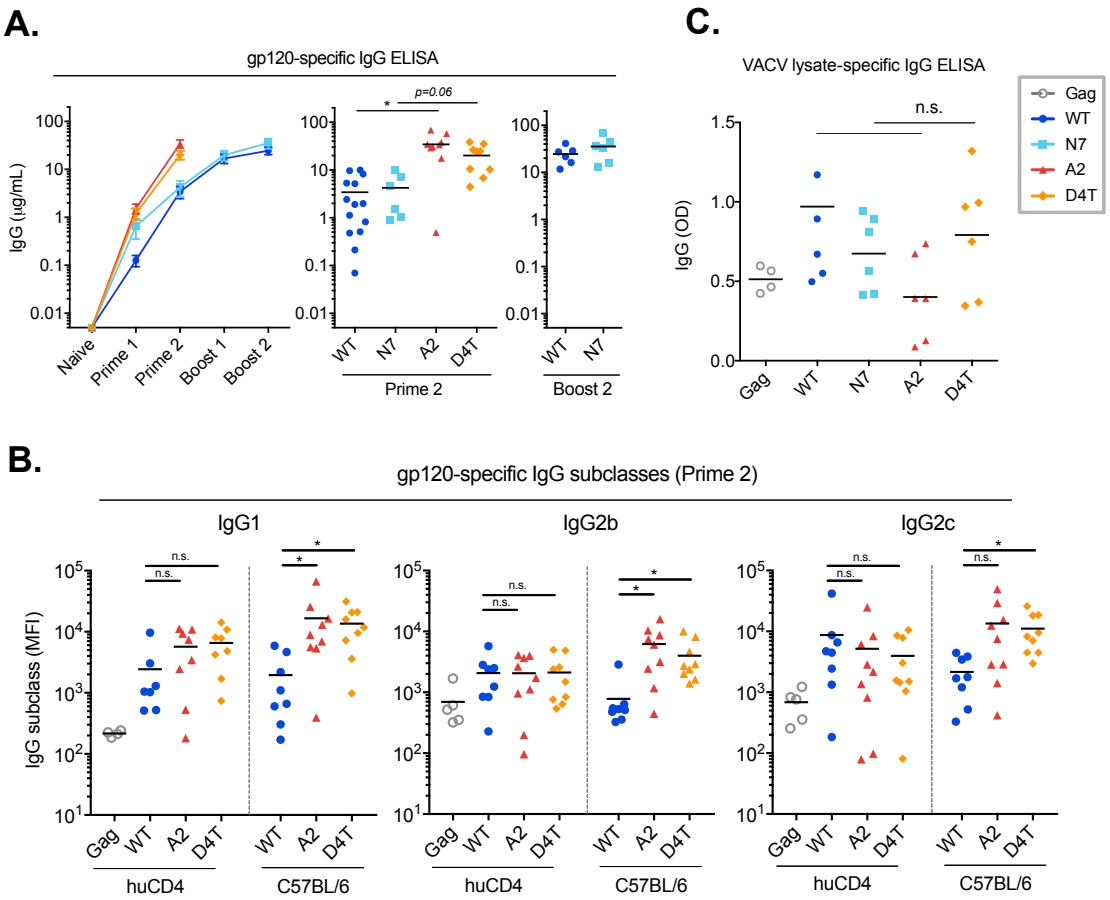

Supp. Fig. S2.2. CD4-independent Envs generate higher gp120-specific IgG in mice. (A) ELISA binding IgG to 89.6 WT gp120 was quantified by ELISA using mouse mAb 3B3 as a standard, and data is shown here for C57BL/6 mice (refer to Fig. 2.3 for similar responses in huCD4 mice). (B) IgG subclasses were measured using a multiplex immunoassay, and MFIs were determined using 1:100 sera. (C) The vector-specific antibody response was measured by ELISA using vaccinia (VACV) lysate as the coating antigen and 1:41,000 mouse sera. Data are shown for huCD4 mice. Horizontal bars indicate the mean. A2 and D4T were compared to WT and N7, respectively, by the Kruskal-Wallis test with Dunn's correction. Asterisks: $p<0.05$. ns: $P>0.05$.

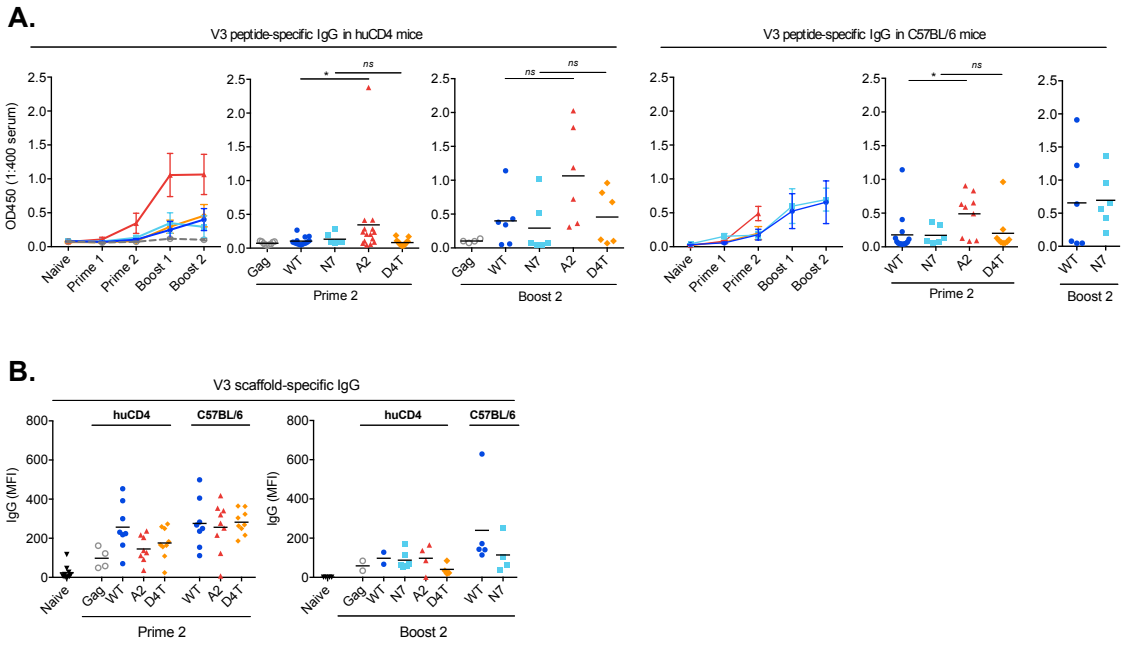

Supp. Fig. S2.3. CD4-independent Env A2 elicits a moderate increase in V3 peptide-specific IgG. (A) ELISA binding to a synthetic V3 peptide with HIV-1 89.6 WT sequence in huCD4 (left) and C57BL/6 (right) mice. (B) IgG binding to a clade B MN V3 scaffolded onto MLV gp70 was measured by a multiplex immunoassay using 1:200 sera from huCD4 and C57BL/6 mice after prime 2 (left) or boost 2 (right). A2 and D4T responses were compared to WT and N7, respectively, by Kruskal-Wallis with Dunn's correction. Horizontal bars: mean. Error bars: s.e.m. Asterisk: $p<0.05$. P-values were non-significant where indicated (ns) and in all comparisons in panel B.

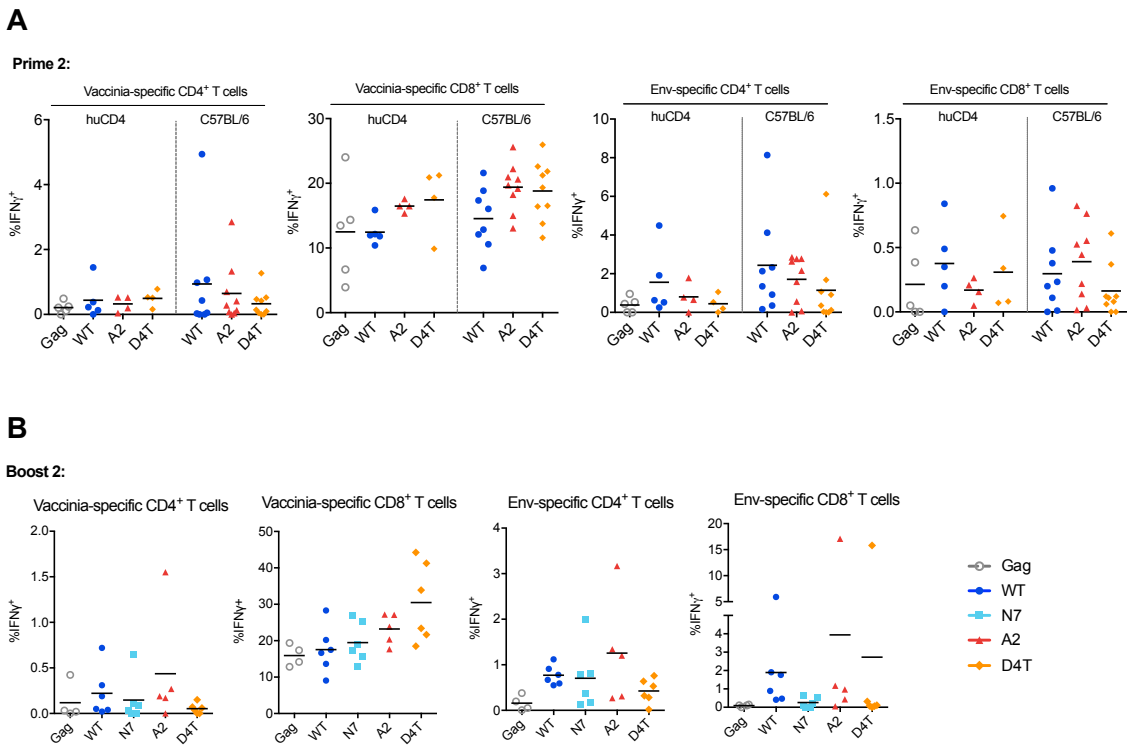

Supp. Fig. S2.4. CD4-independent and parental Envs elicit Env- and vaccinia-specific T cell responses of similar magnitude in mice. Mice were sacrificed after two rVV primes in C57BL/6 and huCD4 mice (A) or after two primes and two boosts in huCD4 mice (B) and splenocytes were stained for antigen-specific intracellular cytokine production in $CD4^+$ or $CD8^+$ T cells, as indicated. Splenocytes were stimulated with either immunodominant peptides from vaccinia virus or with four peptide pools from SHIV 89.6P Env (combined responses are shown). Frequencies have been background-subtracted. Horizontal bars indicate the mean and points represent individual mice.

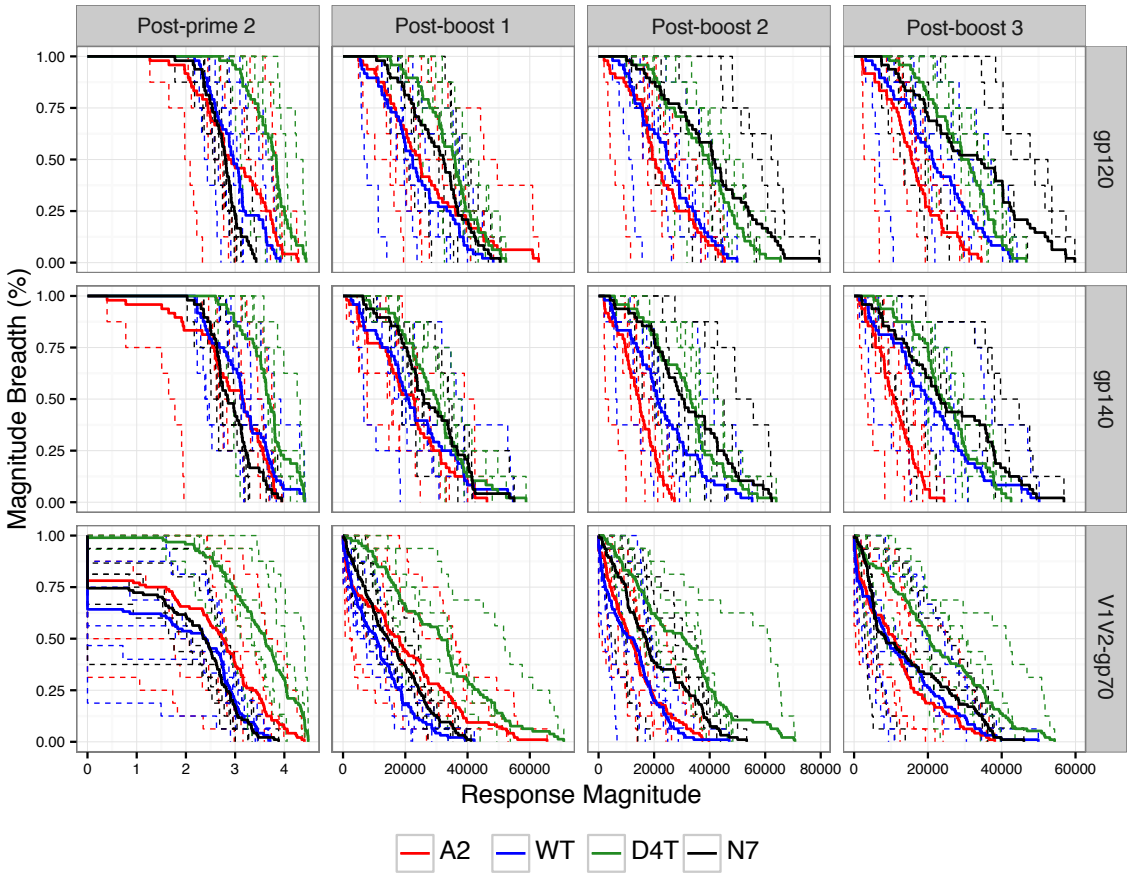

Supp. Fig. S2.5. CD4-independent Env D4T elicits a higher and broader response against V1V2-gp70 scaffold reagents compared to A2 or CD4-dependent Envs. Shown are magnitude-curves of binding to 17 gp120 proteins, 12 gp140 proteins, and 16 V1V2-gp70 scaffold proteins by pig-tailed macaque immune sera. Curves for individual animals are shown in dashed lines, and the combined response curves are shown as solid lines. The x-axis represents the magnitude of the response, derived from an MFI measurement from a single dilution for post-prime 2 and from an area under the curve for multiple dilutions for post-boost time points, and the y-axis represents the proportion of antigens bound at that magnitude.

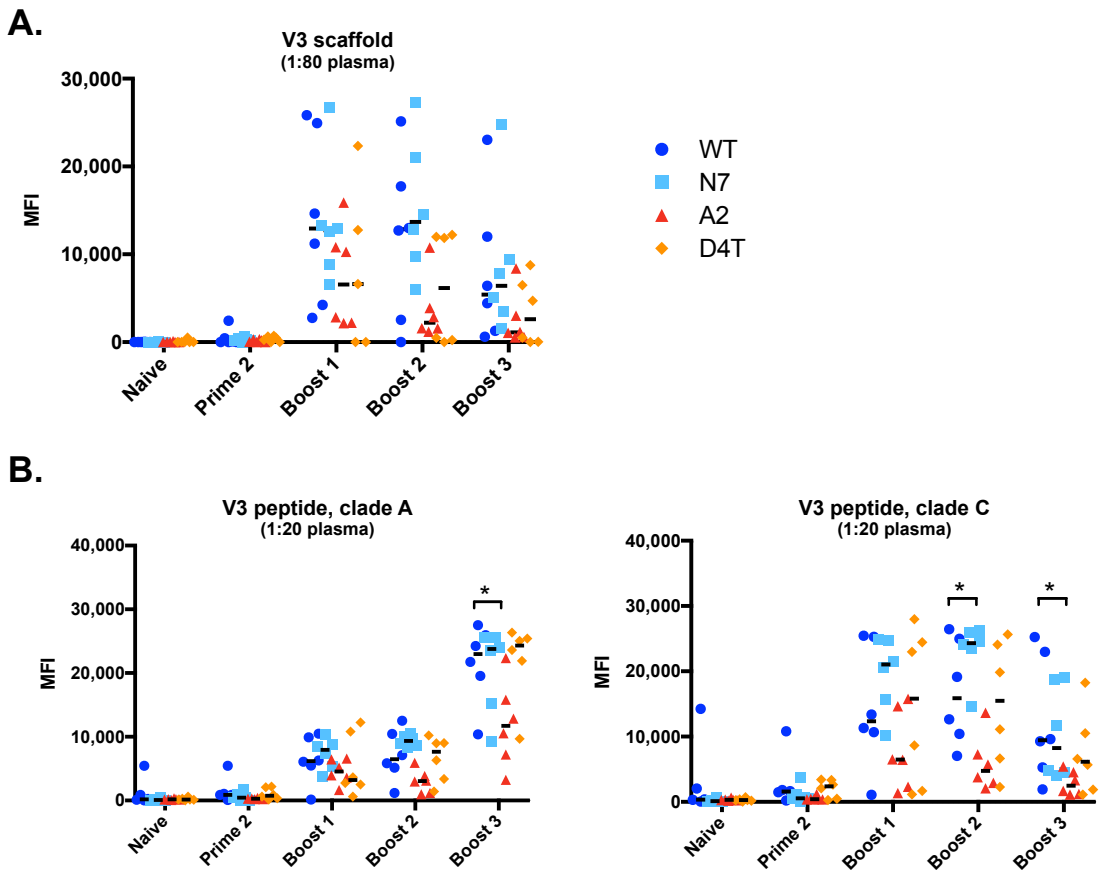

Supp. Fig. S2.6. V3-specific IgG response in pig-tailed macaques immunized with CD4-independent Envs. Shown are MFI values from a multiplex immunoassay for IgG binding to (A) gp70 scaffold containing V3 from clade B HIV-1 MN, (B) linear V3 peptide of a consensus clade A sequence, or (B) linear V3 peptide of a consensus clade C sequence. Plasma samples were tested at the indicated dilutions. A2 and D4T responses were compared to WT and N7, respectively by two-way ANOVA with Tukey's correction. Horizontal lines indicate the median and asterisks indicate $p<0.05$.

2.7. ACKNOWLEDGMENTS

Special thanks to Lifei Yang, the co-lead author of this work who performed extensive antigenic characterization of our Env variants, and to Angela Conde-Motter, who performed the mouse immunizations with me and analyzed T cell responses. Thanks also to the lab of Kelly Lee for HDX and affinity studies, the rest of the lab of Shiu-Lok Hu for production of vaccinia vectors, Bronwyn Gunn and Galit Alter for isotype assays and ADCC troubleshooting, and Shixia Wang, Dong Han, and Shan Lu for providing V1V2 scaffolds. We are grateful to Barton Haynes and David Easterhoff for providing valuable monoclonal antibodies, allowing us to assess the exposure of the V2 peptide in a highly clinically relevant manner. We thank Deb Diamond for providing much appreciated administrative support. We also acknowledge the technical support and contributions of Kelli Greene, Hongmei Gao, the Vaccine Immunology Statistical Center at Fred Hutchinson Cancer Research Center, Kathy Foulds and Rick Koup of the Comprehensive T Cell Vaccine Immune Monitoring Consortium (CTVIMC) at the NIH, Georgia Tomaras, Guido Ferrari, Celia LaBranche, and David Montefiori of the Comprehensive Antibody Vaccine Immune Monitoring Consortium (CAVIMC) at Duke University for providing critical data on epitope specificities, ADCC activity, and NAbs, and Farida Shaheen and Steven Bryan of the Viral and Molecular Core of the Penn Center for AIDS Research (P01 AI045008). This work was funded by NIH R01 AI090788, NIH T32 AI007632, and the Bill and Melinda Gates Foundation CAVD grant OPP1022102.

CHAPTER 3

INCREASED SURFACE EXPRESSION OF HIV-1 ENVELOPE IS ASSOCIATED WITH IMPROVED ANTIBODY RESPONSE IN VACCINIA PRIME–PROTEIN BOOST IMMUNIZATION

Adapted from the following manuscript:

Michael J. Hogan*, Angela Conde-Motter*, Andrea P.O. Jordan, Lifei Yang, Brad Cleveland, Wenjin Guo, Josephine Romano, Houping Ni, Norbert Pardi, Celia C. LaBranche, David C. Montefiori, Shiu-Lok Hu, James A. Hoxie, and Drew Weissman
(Manuscript submitted)

*These authors contributed equally to this work.

3.1. ABSTRACT

HIV-1 envelope (Env)-based vaccines have so far largely failed to achieve their goal of inducing antibodies that can prevent HIV-1 infection. Among these vaccine approaches are viral and genetic vectors that express native Env protein on the cell surface. Multiple factors have been hypothesized to limit the immunogenicity of cell-associated Env; one is its typically low level of expression on the cell surface, which could restrict its accessibility for immune responses. In this study, using a vaccinia prime-protein boost vaccine protocol, we explored the effects on immunogenicity of mutations in the Env cytoplasmic tail (CT) that increased Env surface expression, including a partial truncation and ablation of a known tyrosine-dependent endocytosis motif. Using two HIV-1 Env isolates, we show that these mutations markedly increased humoral immune responses relative to Envs with a wild-type CT. After two vaccinia vector primes, CT-modified Envs elicited up to a 7-fold increase in gp120-specific IgG. In addition, after two subsequent gp120 protein boosts, CT-modified Envs induced up to 16-fold greater Tier-1 HIV-1 neutralizing antibody titers, although results were variable between isolates. These data indicate that the immunogenicity of an HIV-1 Env in a prime-boost vaccine regimen can be enhanced by CT mutations that increase Env surface expression and highlight the key role of the priming step in this effect.

3.2. INTRODUCTION

The HIV-1 pandemic remains a major threat to global public health, with 2.6 million new infections annually, and a safe and effective vaccine is urgently needed [330,422]. Passive immunity experiments have demonstrated that anti-HIV-1 neutralizing antibodies (NAbs) can confer protection from infection in nonhuman primate models [140–142,423–425]; as a result, such antibodies are a major target of ongoing vaccine efforts [426]. The sole target of neutralizing or other protective antibodies on HIV-1 is the envelope glycoprotein (Env), which assembles as a trimer of heterodimers composed of surface gp120 and transmembrane gp41 subunits. The HIV-1 Env has evolved a variety of mechanisms to evade host antibody responses, including its ability to tolerate escape mutations in immunogenic epitopes [116,135], extensive glycosylation [17,114,244,332], conformational masking [119], mimicry of host proteins [118], and low expression of Env on virus-producing cells and on virions [125,126]. Together, these features create substantial barriers to the design of an effective Env-based vaccine.

Despite extensive pre-clinical studies and six efficacy trials of HIV-1 vaccines [154,155,161,162,178,187], only one, the RV144 trial, has shown any efficacy, with 31.2% protection in humans at 42 months post vaccination [187]. The RV144 vaccine regimen included four intramuscular inoculations of replication-incompetent canarypox vector expressing HIV-1 Gag, protease (Pro), and Env antigens and two injections of purified gp120 protein in alum. The primary correlates of protection were non-neutralizing IgG antibodies in plasma that bound to variable loops 1 and 2 (V1/V2) of gp120 and low levels of anti-Env IgA [192]. Secondary correlates from a post-hoc analysis included NAb activity and the ability of antibodies to mediate

antibody-dependent cellular cytotoxicity (ADCC) on HIV-1-infected target cells [192,347]. These results have generated renewed interest in the potential advantages of poxvirus prime-protein boost vaccine approaches, as well as possibly protective functions of non-neutralizing antibodies [350,427–429].

Studies have since attempted to improve the antibody responses elicited by poxvirus prime-protein boost vaccines by investigating different species of poxvirus vectors for the prime [430], adjuvants for the boost [211,214,218], and varied dose schedules [215]. In addition, there is considerable biological diversity among Envs that can be used in the prime or boost, including differences conformational dynamics [236], neutralization sensitivity [137], glycan organization [114], and their level of expression on cells or virions [343,431,432]. Overall, the contribution of these attributes to immunogenicity and vaccine efficacy are poorly understood. One study in nonhuman primates using a vaccinia prime-gp120 boost regimen, which evaluated the immunogenicity of Envs containing deletions of selected N-linked glycosylation sites, found that removal of a single glycan at position 197 [384] from the HIV-1 89.6 Env markedly increased the NAb responses [382]. However, the extent to which this enhancement is applicable to other viral isolates or other animal species is unclear, since a follow-up study in rabbits using an Env from a different HIV-1 isolate from which the same glycan had been deleted, did not show any improvement in NAb responses [433].

The low expression of HIV-1 Env on the cell surface has long been hypothesized to impede an effective antibody response to membrane-associated Env, including Env expressed using viral vector or nucleic acid vaccines [434]. This reduced expression has been attributed at least in part to the presence of multiple endocytosis motifs within the long cytoplasmic tail (CT) of Env [127,435–440]. The

CT regulates a variety of processes, including multiple intracellular trafficking pathways (reviewed in [128]), incorporation of Env into virions [62,441–445], and many more. It comprises over 150 amino acids and contains a variety of trafficking signals as well as three amphipathic helical regions that putatively interact with the inner leaflet of the plasma membrane: lytic lentiviral peptides (LLP) 1, 2, and 3, so named due to the ability of these peptides in synthetic form to disrupt the cell membrane [446,447] (see Fig. 3.0).

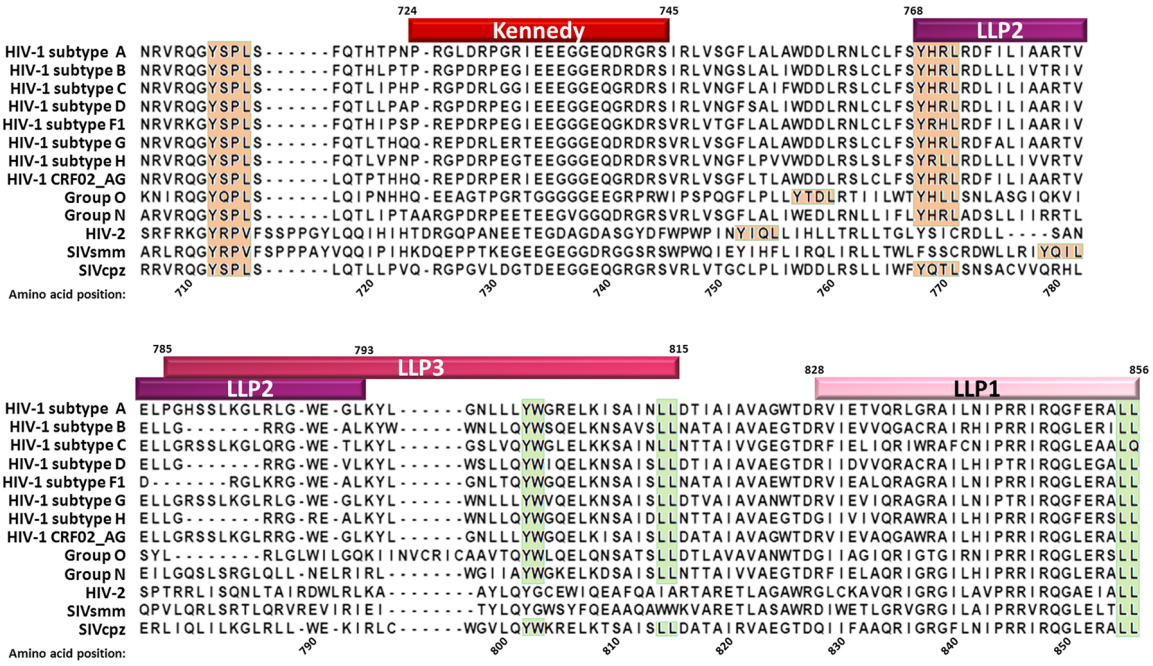

Figure 3.0. Schematic of the cytoplasmic tails of multiple primate lentiviruses. Shown are aligned sequences from HIV-1 group M subtypes A (92UG037), B (HXB2), C (ETH2220), D (SE365), F1 (93BR020), G (175), H (90CF056), CRF02_AG (93TH065); group O (ANT70), group N (YBF106); HIV-2 (UC2); SIVcpz (Ptt_04CAM155); and SIVsmm (H635). Numbering corresponds to the HXB2 sequence. Highlighted elements include the lentiviral lytic peptide (LLP) regions, Kennedy epitope, conserved YxxΦ motifs (orange), and conserved dileucine motifs (green). The figure was adapted with permission from Santos da Silva, *Retrovirology* 2013 [128], BioMed Central Ltd.

Another CT region of interest is the Kennedy epitope, which, controversially, has been proposed to be a target of neutralizing antibodies [448,449], though the implications of this for the topology of the CT remain unclear. Multiple sequences in the CT have been associated with endocytosis and/or other forms of intracellular trafficking. These include, among others, a diaromatic motif ($YW_{802-803}$) associated with endosome to trans-Golgi network (TGN) trafficking [450], palmitoylated cysteine(s) that have been variably associated with lipid raft targeting and Env incorporation [451,452], and a C-terminal dileucine motif implicated in both endocytosis and TGN-endosome shuttling [435,439].

One well-described signal in the CT is the membrane-proximal tyrosine (Tyr)-dependent endocytosis motif formed by the consensus amino acids GYxxΦ, where x is any amino acid and Φ is a bulky hydrophobic residue. This highly conserved motif binds to cellular adaptor protein complex 2 (AP-2) and recruits Env that is not incorporated into virions into clathrin-coated pits, thereby mediating internalization and clearance from the cell surface [436,438]. GYxxΦ has also been shown to bind adaptor protein complex 1 (AP-1), mediate directional budding of virus in polarized cell types [65,453] and to contribute importantly to pathogenesis in simian immunodeficiency virus (SIV) infection of pig-tailed macaques [454–456]. Additional but less well characterized internalization signals are present in the more distal CT [435,439], consistent with the view that a low steady-state expression of Env on infected cells is an important and conserved viral property.

Surface expression of HIV-1 and SIV Envs can be increased by mutations in the CT that ablate endocytosis signals. Our lab has previously described a variant of SIVmac251 termed CP-MAC that exhibited a marked increase (~25-fold) in surface expression on infected cells. This increase was shown to be the result of a

substitution of Tyr in the GYxxΦ motif and a premature stop codon immediately prior to the overlapping second exons of *tat* and *rev* [457–459]—a truncation that arises commonly when SIVs are propagated in human cells [460]. It is unknown whether comparable mutations in the HIV-1 Env CT would confer a similar increase in surface expression, thereby making a potentially useful immunogen. At least two studies have evaluated the immunogenicity of HIV-1 Env CT mutants with increased surface expression compared directly to WT Envs [328,329], and both noted improvements in gp120-binding IgG titers. However, the impact of increased surface expression on binding IgG and NAb responses in the context of a prime-boost vaccine regimen has not been well defined.

In the present study, we used a vaccinia prime-gp120 protein boost regimen to evaluate the impact of mutations in the HIV-1 Env CT that ablate its endocytosis signals and increase expression on the cell surface. We hypothesized that the magnitude and quality of the antibody response induced by an Env-expressing vaccinia vector would correlate with Env cell surface expression and thus the amount of native Env antigen available for interactions with B cells. Additionally, since the protein boost can be expected to expand pre-existing antibody lineages [461], we hypothesized that antibody activities elicited by the prime would be expanded by the protein boost.

3.3. RESULTS

Cytoplasmic tail (CT) mutations can increase HIV-1 Env surface expression in transfected HEK 293T cells.

We introduced several mutations into the cytoplasmic tail of the clade B HIV-1 R3A Env [462] that were designed to alter cell surface expression. Fig. 3.1A shows the organization of the HIV-1 CT and Fig. 3.1B shows mutations that were introduced, including combinations of: (1) a premature stop codon that removed the distal 147 of 151 predicted amino acids (a.a.) in the CT, removing all known trafficking motifs (denoted as ∆147) [463]; (2) a premature stop codon that removed 139 a.a., leaving intact the membrane-proximal endocytosis signal, ^{711}GYSPL^{715} (denoted as Δ139); and (3) a point mutation, Y_{712}I, that ablated this motif. In addition, we noted that some truncated SIV Env CT mutants with high surface expression, including CP-MAC, contain 6 a.a. (SSPPSY) prior to the start of the second exons of *tat* and *rev* that have no homolog in HIV-1 [128,458,460,464]. Considering the possibility that these could contribute to a trafficking motif regulating Env surface expression, we introduced a 13-a.a. segment from this region of the SIV Env CT into HIV-1 (denoted +SIV). On this background, we then introduced Y_{712}I, ∆139, or both changes together. For simplicity, the latter construct is referred to as TM1. A similar set of mutations was also made in the HIV-1 89.6 and JRFL Envs.

The effects of CT mutations on surface expression were first evaluated in the context of HIV-1 R3A Env. Plasmids encoding R3A Env variants were transfected into HEK 293T cells, and surface and total expression were measured by flow cytometry (Fig. 3.2A). Three Env mutants exhibited ≥2-fold increases in surface expression relative to wild-type (WT): Y_{712}I Δ139 (2-fold, p=0.09), Δ147 (3-fold,

p=0.02), and TM1 (4-fold, p=0.04). All Envs exhibited similar total cellular expression levels when assays were performed on permeabilized cells.

We next extended this evaluation to assess the effects of analogous mutations on clade B 89.6 and JRFL Envs (Fig. 3.2B-D). On 89.6, Env CT mutations with highest surface expression were similarly $Y_{712}I$ Δ139, Δ147, and TM1 (6-7 fold, p<0.01). The Δ147 and TM1 mutations also generated significant increases (3-4 fold, p<0.01) in surface expression of 89.6 N7 Env, which contains a deletion of a single glycan ($N_{197}Q$) and was previously shown to elicit a higher and broader NAb response in nonhuman primates [382]. A similar increase in surface Env was also observed for a JRFL Env containing the TM1 mutation (3 fold, p=0.04). Thus, across several HIV-1 Envs, CT mutations conferred an increase in surface expression, particularly constructs with the TM1 modifications (i.e. the +SIV segment, $Y_{712}I$, and Δ139), and this variant was selected for further study as an immunogen using a vaccinia expression protocol.

CT mutations increase Env surface expression in a vaccinia virus expression system

89.6, 89.6 N7, and JRFL Envs with unmutated or TM1-modified CTs were inserted into vaccinia virus (VACV) vectors derived from the replication-competent v-NY strain [465,466]. We infected HEK 293T cells with parental VACV and recombinant viruses expressing 89.6 or JRFL Envs with or without the TM1 mutations. Surface and total Env expression were assessed by flow cytometry using antibodies 2G12 and 2F5, which bind to gp120 and gp41, respectively (Fig. 3.3). TM1-modified 89.6, 89.6 N7, and JRFL Envs exhibited a roughly 2-fold increase in surface 2G12 stain and a 3-fold increase in surface 2F5 stain (all p<0.05), but no

differences in total Env. To control for transduction efficiency, VACV A33 protein expression was also assessed, and no significant differences were detected. Thus, similar to their expression from plasmid in HEK 293T cells, HIV-1 Envs containing the TM1 mutations also exhibited increased cell surface expression using a VACV expression system, making them amenable to evaluation of their immunogenicity in a VACV prime-protein boost vaccine regimen.

Envs containing CT mutations for high surface expression mediate fusion and maintain epitopes for broadly neutralizing antibodies

We also sought to determine whether the TM1 CT mutations altered Env function or the exposure of epitopes to which broadly neutralizing antibodies are directed. For HIV-1, CT truncations have previously been shown to affect HIV-1 Env fusion efficiency and antigenicity of the ectodomain [463,467–469]. In a cell-cell fusion assay, VACV-expressed TM1 Envs induced syncytium formation similarly to parental 89.6, 89.6 N7, and JRFL Envs, indicating that TM1-modified Envs maintain fusogenic function (Fig. 3.4A). Next, Envs with or without the TM1 mutations were expressed in HEK 293T cells and analyzed by flow cytometry for the relative expression of antibody epitopes including the CD4 binding site (VRC01, b12, CD4-IgG), co-receptor binding site (17b), V3 loop crown (447-52D), and the membrane-proximal external region (MPER) in gp41 (2F5, 4E10, 10E8) (Figs. 3.4B and C). No significant differences in antibody/ligand binding were observed between WT and TM1 Envs, suggesting that TM1 modification did not result in major antigenic changes within the epitopes for several groups of broadly neutralizing antibodies.

Immunization with CT-modified Envs in a vaccinia prime-protein boost protocol generated higher levels of gp120-specific IgG

The immunogenicity of Envs containing the TM1 mutations was evaluated using a poxvirus prime-protein boost strategy, similar to a regimen that showed partial protective efficacy in humans [187]. Our regimen used Env-expressing recombinant VACV vectors for the primes followed by purified gp120 protein for the boosts. We hypothesized that the level of Env surface expression driven by the priming vectors would correlate with the magnitude and quality of the Env-specific antibody responses after the primes and/or the boosts.

C57BL/6 mice (n=8-10/group) were injected intraperitoneally (i.p.) at weeks 0 and 4 with 10^8 pfu of VACV encoding 89.6 N7 and JRFL Envs with WT or TM1-modified CTs (Fig. 3.5A). A VACV vector encoding SIV Gag-Pol and lacking Env was used as a control. All groups of mice were boosted at weeks 8 and 12 with intramuscular (i.m.) injections of 5 μg of autologous gp120 protein in 1% alum (Fig. 3.5B).

To determine if mice received comparable effective doses of vector, VACV-specific antibody responses were measured by ELISA. In both immunization series, there were no significant differences between groups in VACV lysate-specific IgG measured 4 weeks after the second VACV prime (Figs. 3.5C and D). Consistent with this result, we also observed statistically equivalent VACV-specific $CD8^+$ T cell (Fig. S3.1A) and Env-specific $CD4^+$ T cell responses (Fig. S3.1B) elicited by vectors expressing 89.6 N7 Env with or without the TM1 mutations at the time of euthanasia, 2 weeks after the second boost. The VACV-specific $CD4^+$ T cell and Env-specific $CD8^+$ T cell responses were negligible with the peptide pools used (data not shown).

Gp120-specific IgG responses were measured by ELISA after each immunization as outlined in Fig. 3.5A. Mice that were primed with 89.6 N7 TM1 Env generated significantly higher gp120-binding IgG than those primed with 89.6 N7 (Fig. 3.5E), with a 3-fold increase after the first prime and a 7-fold increase after the second prime. A similar effect was noted in the JRFL immunization, although to a lesser extent: mice primed with JRFL TM1 Env developed 2-fold higher gp120-specific IgG after one or two primes compared to JRFL WT (Fig. 3.5F). In both immunization series, gp120-specific IgG levels increased after the protein boosts, but differences between Envs with WT and mutated CTs were lost after the second boost.

Prime-boost immunizations with CT-modified Envs generated higher HIV-1 NAb titers

We next determined whether increased surface expression of Env could impact the development of anti-HIV-1 neutralizing antibodies. Using a TZM-bl pseudovirus reporter assay, we found that mice primed with 89.6 N7 Env containing the TM1 mutations generated markedly higher NAb titers compared to mice primed with parental 89.6 N7 (Fig. 3.6A). Neutralization of the Tier-1 (neutralization-sensitive) strain MN.3 was increased 11-fold after the second prime, 10-fold after the first boost, and 16-fold after second boost ($p=0.0007$). These findings were striking, given that there was no significant difference in gp120-specific binding IgG between 89.6 N7 and 89.6 N7 TM1 vaccinations after protein boosts (Fig. 3.5E).

In contrast to findings observed for the 89.6 N7 Envs, mice vaccinated with JRFL Envs with or without the TM1 mutations generated low NAb titers to Tier-1 MN.3 and SF162.LS strains after two VACV primes. After two protein boosts, mice

immunized with JRFL TM1 Env exhibited a 2-fold higher NAb titer against these strains, although this difference was not statistically significant (Fig. 3.6B). In both JRFL and 89.6 N7 immunizations, no significant NAb activity was observed against more neutralization-resistant viruses, including autologous JRFL and 89.6 (data not shown).

Thus, we observed similar trends for 89.6 N7 and JRFL Env immunizations, with Envs modified for increased surface expression generating improved antibody responses. These effects were greatest with 89.6 N7 TM1 Env, where increases in anti-gp120 IgG and NAb were seen after VACV primes and even greater increases in NAbs were seen after gp120 boosts.

CT modification did not change the immunogenicity of variable loops 1/2 and 3

Neutralizing antibody responses to Tier-1 HIV-1 isolates have been attributed to antibodies binding to hypervariable loops on gp120, particularly the V3 loop [470,471]. We investigated this possibility by evaluating sera from mice immunized with 89.6 N7 and 89.6 N7 TM1 Envs for binding to a V3 peptide from the 89.6 sequence. As shown in Figure S3.2A, no differences were observed. In addition, epitopes within the V1/V2 loops have been shown to be highly immunogenic and a target for neutralizing and non-neutralizing antibodies in various vaccine regimens [192,202,206]. However, when sera from mice immunized with 89.6 Envs were assessed for IgG to V1/V2 presented on a murine leukemia virus gp70 scaffold [192,472], only ~50% of mice made detectable V1/V2-specific IgG responses, and there was no difference between mice receiving parental or TM1-modified 89.6 N7 Envs (Fig. S3.2B). Thus, although immunodominant in several vaccine protocols,

antibody responses to V3 and V1/V2 loops were unaffected by differences in cell surface expression between these Envs in a vaccinia prime-gp120 boost protocol.

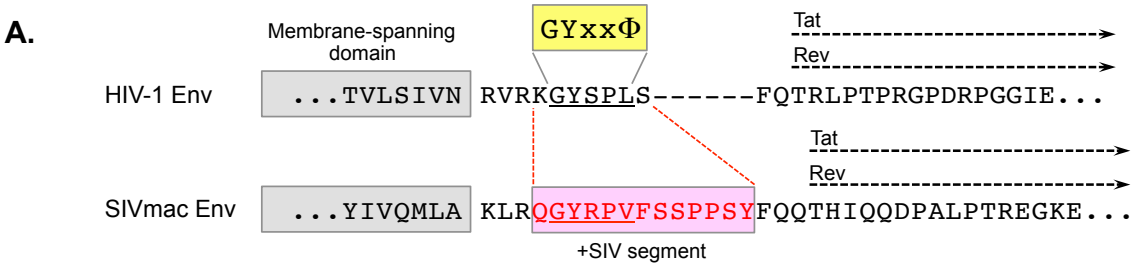

B.

HIV-1 cytoplasmic tail mutants

WT	RVRKGYSPLSF------QTRLPTPRGPDRPGGIE...
Δ147	RVR*
Δ139	RVRKGYSPLSF*
$Y_{712}I$	RVRKGISPLSF------QTRLPTPRGPDRPGGIE...
$Y_{712}I$,Δ139	RVRKGISPLSF*
+SIV	RVRQGYRPVFSSPPSYFQTRLPTPRGPDRPGGIE...
+SIV,$Y_{712}I$	RVRQGIRPVFSSPPSYFQTRLPTPRGPDRPGGIE...
+SIV,Δ139	RVRQGYRPVFSSPPSYF*
+SIV,$Y_{712}I$,Δ139 **("TM1")**	RVRQGIRPVFSSPPSYF*

SIV CP-MAC cytoplasmic tail KLRQGCRPVFSSPPSYF*

Figure 3.1. Schematic of HIV-1 Env cytoplasmic tail mutants. (A) Partial amino acid sequences of HIV-1 R3A and SIVmac239 Envs are shown, including part of the membrane-spanning domain and the highly conserved Tyr-dependent endocytosis motif (GYxxΦ). For both viruses, the positions overlapping the second exons of Tat and Rev in alternative reading frames are shown. The indicated segment from SIVmac (+SIV) was substituted into the HIV-1 CT to create Env constructs shown in Panel B. (B) HIV-1 Env CT mutants created to evaluate effects on Env surface expression. Substitutions (in blue) included a $Y_{712}I$ substitution (HXB2 numbering) and/or a premature termination codon (*). Mutations were made in the same positions in the Envs of HIV-1 89.6 and JRFL. Dashes (-) are used to facilitate alignment and highlight SIV residues with no homology in the HIV-1 CT (SSPPSY). The sequence of SIV CP-MAC, which exhibits high levels of Env surface expression [457–459], is shown for reference.

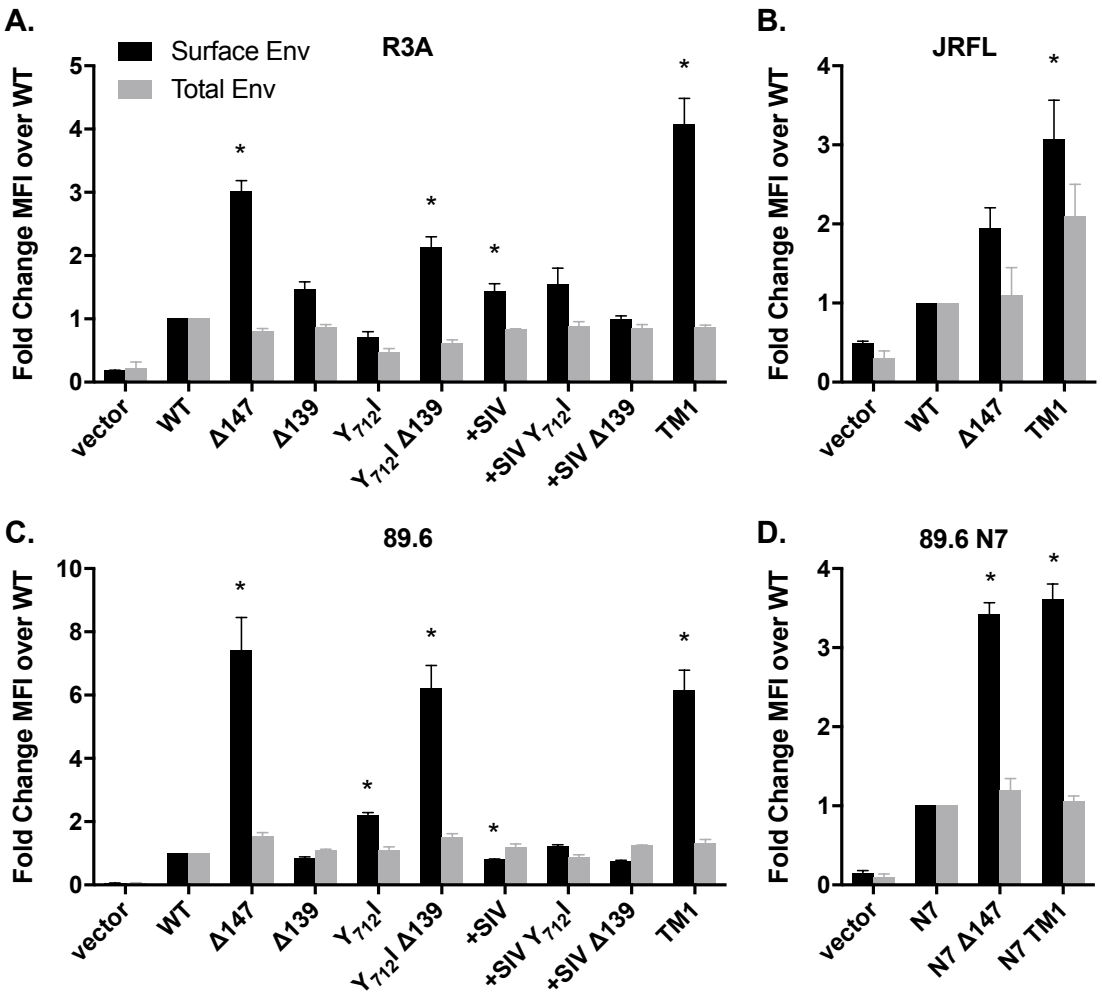

Figure 3.2. CT mutations increase surface expression of Envs in plasmid-transfected HEK 293T cells. The indicated CT mutations were made in four HIV-1 Envs: (A) R3A, (B) JRFL, (C) 89.6 WT, and (D) 89.6 N7 ($N_{197}Q$). HEK 293T cells were co-transfected with plasmids encoding GFP and Env and at 18 hrs were stained for Env using mAb 2G12 under non-permeabilizing (surface stain) and permeabilizing (total stain) conditions. Data represent the average fold change in Env-specific mean fluorescence intensity (MFI) of GFP^+ cells relative to parental Env in each experiment, with n=3 (A, B, D) or n=4 (C) replicates. Asterisks indicate Env variants that showed a significant fold difference ($p<0.05$) in surface expression from the parent Env (normalized to 1) by one-sample *t* test on log-transformed data with Bonferroni correction.

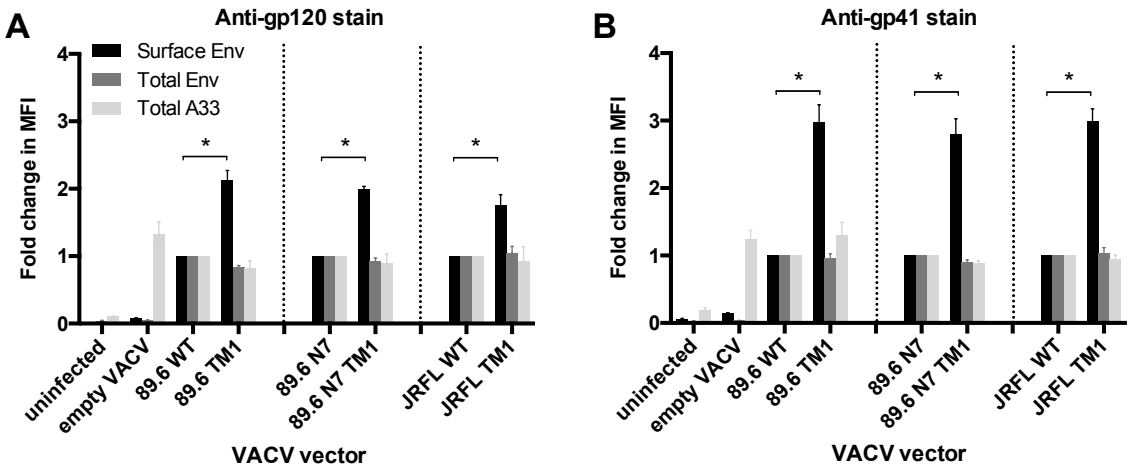

Figure 3.3. CT mutations increase surface expression of Envs in recombinant VACV-infected cells. HEK 293T cells were infected (MOI=3) with the indicated Env-expressing recombinant VACV or parental VACV (empty). After 16 hrs, cells were stained for Env using (A) 2G12, an anti-gp120 mAb, or (B) 2F5, an anti-gp41 mAb under permeabilizing (total) or non-permeabilizing (surface) conditions (n=3). In each experiment, VACV A33 protein staining was performed under permeabilizing conditions to control for transduction efficiency. The MFI of Env and A33 stains are shown relative to parental Envs, with comparison groups separated by dotted lines. Asterisks indicate a significant fold difference ($p<0.05$) in Env expression by one-sample *t* test on log-transformed data with Bonferroni correction.

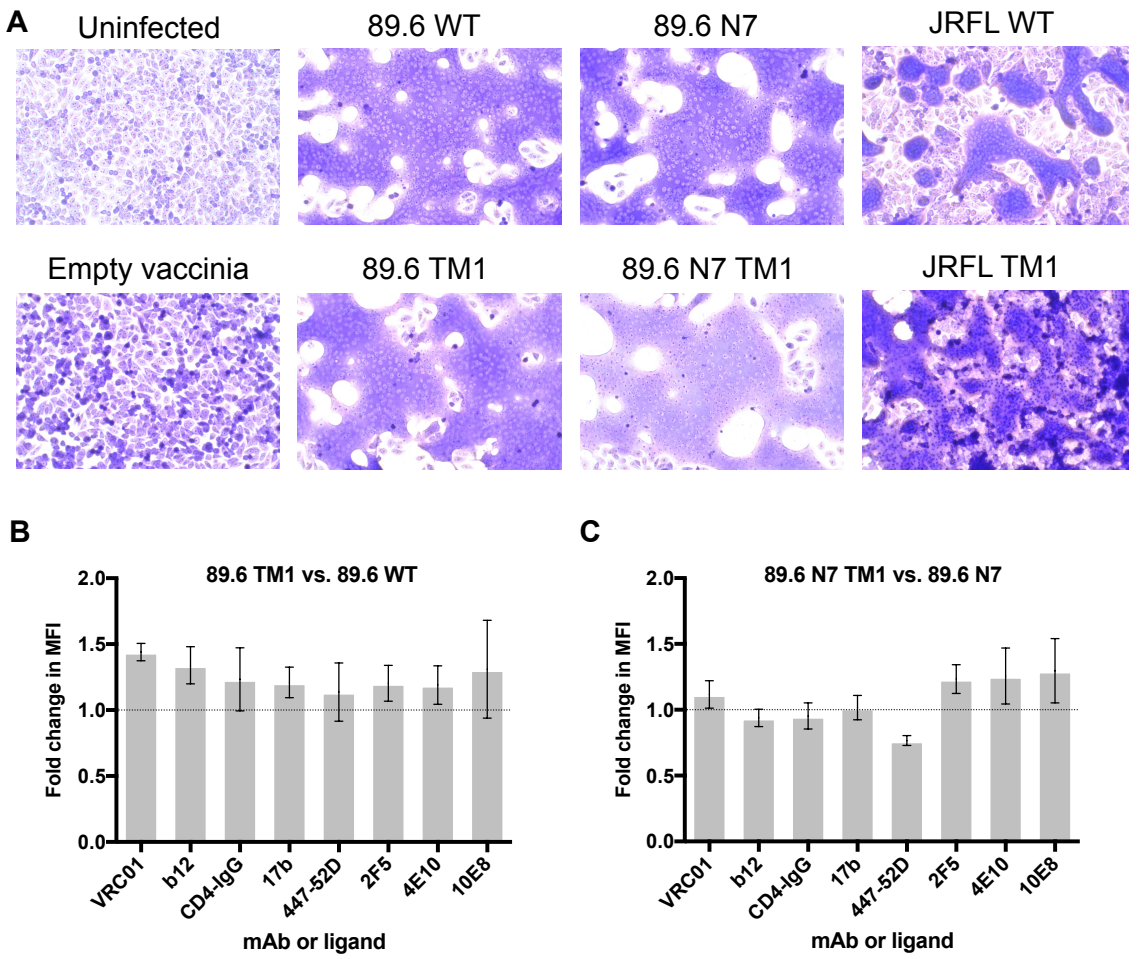

Figure 3.4. **TM1 modified Env is functional and does not exhibit major antigenic changes.** (A) A cell-cell fusion assay was performed by infecting (MOI=1) HIV-permissive TZM-bl cells with recombinant VACV vectors encoding HIV-1 Envs with WT or TM1 mutated CTs or a control VACV encoding no recombinant gene. Cells were fixed at 18 hrs and syncytia were visualized by Giemsa stain. (B) HEK 293T cells were transduced with recombinant VACV vectors encoding Envs with WT or TM1 mutated CTs, and cells were stained (n=3) under non-permeabilizing conditions with the indicated mAbs or a CD4-IgG fusion protein. Fold changes in MFI were normalized to 2G12 stain and are expressed relative to the parental Env with WT CT. No significant fold differences ($p>0.05$) relative to parental Env (dashed line) were noted using one-sample *t* test on log-transformed data with Bonferroni correction.

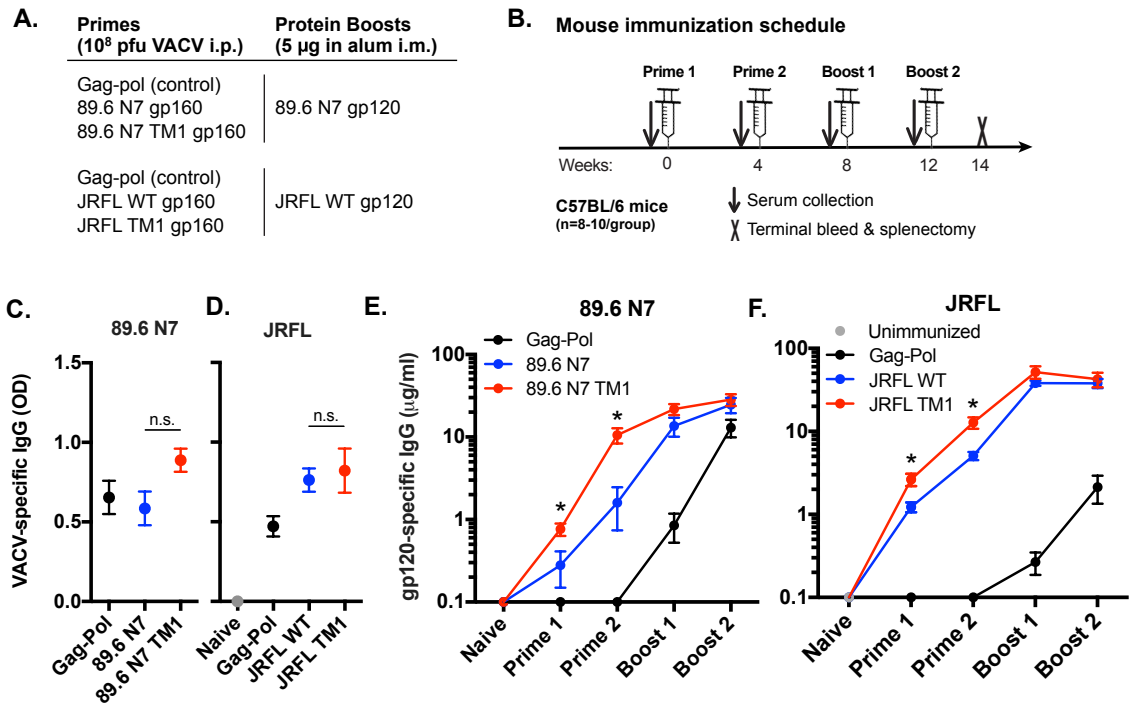

Figure 3.5. Increased gp120-specific IgG responses in mice primed with TM1 modified Envs. (A) Immunogens and doses used in two prime-boost immunization series. (B) Timeline of immunizations and sample collection. (C,D) VACV lysate-specific IgG was measured by ELISA using serum from mice primed twice with VACV vectors encoding the indicated (C) 89.6 N7 and (D) JRFL Envs or Gag-Pol. Data represent the mean OD using serum diluted (C) 1:20,000 and (D) 1:30,000. (E) 89.6 N7 gp120-specific IgG and (F) JRFL gp120-specific IgG were measured by ELISA in mice primed with the indicated VACV vectors and boosted with (E) 89.6 N7 gp120 or (F) JRFL gp120. Time points correspond to bleeds collected after the indicated immunizations. N=8-10 mice per immunized group. Separate unimmunized mice (n=4) were used as negative controls in (D) and (F). Error bars indicate the SEM, and asterisks denote a significant difference ($p<0.05$) between WT CT and TM1 groups by one-way ANOVA with Tukey's test.

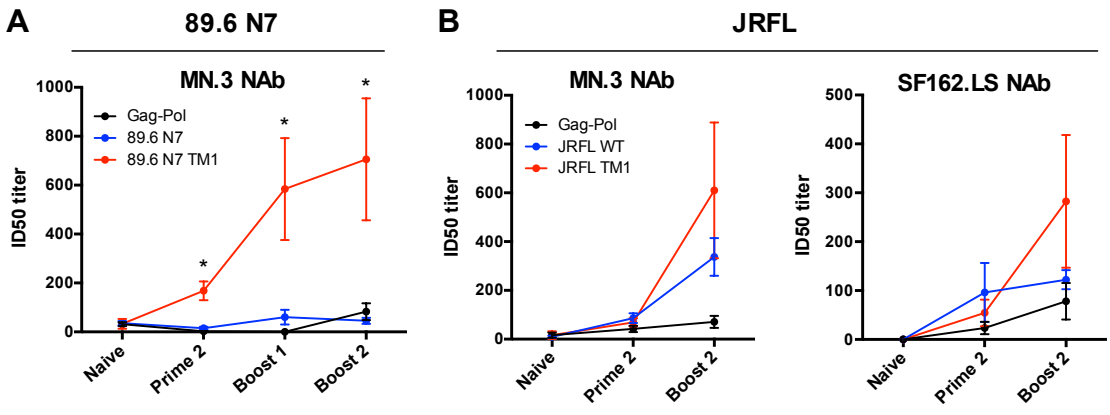

Figure 3.6. Increase in HIV-1 NAb responses in mice primed with TM1 modified Envs. NAb titers against HIV-1 MN.3 and SF162.LS pseudoviruses at the indicated time points were measured using TZM-bl reporter cells. The mean ID50 titers are shown for (A) 89.6 N7 and (B) JRFL Env immunization series. N=8-10 mice per immunized group. Background activity against MLV Env pseudovirus is subtracted from all data except the naive time point in (A), for which serum volume was limited. Error bars indicate the SEM, and asterisks denote a significant difference ($p<0.05$) in NAb titer between WT and TM1 CT groups by Kruskal-Wallis test with Dunn's correction.

3.4. DISCUSSION

HIV and SIV Env CTs contain a membrane-proximal Tyr-dependent endocytosis signal that serves to reduce the steady state expression of Env on infected cells [127,436–438]. The finding that this motif is absolutely conserved among the majority of primate and non-primate lentiviruses [128] and that there are additional but less well characterized endocytic motifs in more distal regions of these tails [437–439] has suggested that endocytic trafficking of Env could play an important role in pathogenesis, possibly by protecting virus-producing cells from humoral immune responses such as ADCC [473]. Indeed, for the pathogenic SIV molecular clone, SIVmac239, ablation of the membrane-proximal endocytosis signal (GYRPV) by deletion of $GY_{721-722}$ results in a virus that is highly replication-competent *in vivo* but is susceptible to host immune control in pig-tailed macaques [454–456]. The aim of the current study was to determine if mutations in the HIV-1 Env CT that ablated endocytosis motifs and, as a result, increased cell surface expression could impact Env immunogenicity in a vaccinia prime-protein boost vaccine regimen. Given recent findings in the RV144 vaccine trial that a poxvirus prime-protein boost protocol could confer partial protection from HIV infection and that this effect correlated with antibody responses to gp120 [192,347], we reasoned that modifications to Env that increased its expression on the cell surface could be a useful adjunct to improve the efficacy of this approach, particularly with regard to the poxvirus prime in which Env is expressed as a membrane-associated trimer on antigen-presenting cells.

We evaluated several HIV-1 Env CT modifications that were informed by our prior studies of CP-MAC, an *in vitro* derived variant of SIVmac251 that exhibited a

marked increase in Env surface expression on infected cells [457,458]. We showed previously that this phenotype resulted from the combined effects of a premature stop codon in the CT and the loss of the membrane-proximal, Tyr-dependent endocytosis motif, GYxxΦ. In the current study, we evaluated similar mutations in the HIV-1 Env CT and, based on differences in the organization of the SIV and HIV-1 CTs, created a set of novel HIV-1 Env chimeras containing a segment (+SIV) from the SIVmac CT spanning from the GYxxΦ motif (GYRPV) to the site of the stop codon in CP-MAC (Fig. 1). Analogous to CP-MAC, these chimeras were created with and without a $Y_{712}I$ mutation and the premature stop codon. The chimera containing both of these additional changes, termed TM1, exhibited marked increases in Env surface expression compared to WT Env, ranging from 3-8 fold. For R3A and JRFL Envs, this effect was greater compared to HIV-1 Envs that contained similar mutations but lacking the +SIV segment, or when the CT was completely deleted (i.e. Δ147). When HIV-1 89.6 Envs containing the TM1 set of mutations, with or without the $N_{197}Q$ glycan deletion [382], were expressed from a VACV vector commonly used in poxvirus prime-protein boost vaccination protocols [465,466], an increase was also seen to levels 2-3 fold greater than WT Env (Fig. 3). In addition, both 89.6 and 89.6 N7 Envs bearing the TM1 mutations exhibited no change in reactivity with anti-Env mAbs, including several broadly neutralizing antibodies, indicating that Envs altered to enhance surface expression maintained epitopes in the Env ectodomain that are of interest to the vaccine field.

When the immunogenicity of 89.6 N7 Envs with wild-type CT or the TM1 modification were compared in mice using a VACV prime-gp120 boost protocol, the TM1 Env elicited significantly higher gp120-specific binding IgG and NAb to a Tier-1 HIV-1 isolate. After two gp120 boosts, the difference in binding IgG was diminished,

but the difference in HIV-1 NAb titers was maintained and markedly enhanced, with a ~16 fold increase in ID50 after the second protein boost. Strikingly, although mice primed with 89.6 N7 Env with an unmutated CT generated high levels of binding IgG, these mice exhibited poor NAb titers even after the second boost, indicating that there were significant qualitative differences in antibody responses resulting from CT modification. Importantly, the improvement in NAb response after the second boost was attributable solely to differences in the VACV primes, suggesting the importance of the priming immunogens in determining the overall efficacy of this prime-boost regimen. This finding is consistent with clinical studies of poxvirus prime-boost vaccine regimens that have observed prime-dependent effects on the antibody specificity, subclass, and neutralizing and non-neutralizing functions measured after the protein boosts [209,347,474]. Although differences in immunogenicity were not as striking when JRFL Envs with or without the TM1 mutations were compared, these data suggest that, in some cases, high surface expression of Env could modulate the quality and the magnitude of antibody responses and possibly improve efficacy of prime-boost vaccine protocols.

We hypothesize that an increase in surface Env on antigen-presenting cells could enhance the ability of these cells to cross-link B cell receptors (BCR) and activate cognate B cells, resulting in increased Env-specific antibody responses. The multivalency of antigen/BCR cross-linking has a well documented effect on the efficiency of B cell activation, particularly for low affinity interactions [228,231,250,475]. This strategy has the potential to elicit antibodies directed towards epitopes expressed on functional Env trimers presented by the prime that could be further improved by appropriate protein boosts. Indeed, it has been suggested that high-affinity binding to the functional Env trimer is both necessary

and sufficient for an antibody to neutralize HIV-1 [391,392,476]. It is also possible that the CT mutations we introduced could have contributed to immunogenicity through alternative mechanisms. The SIV sequence that was inserted in the TM1 mutation contains part of a motif that has been shown to activate NF-κB [477], which can potently modulate host immune responses [478–480]. However, in preliminary results, we did not observe any difference in NF-κB signaling mediated by the TM1 modification in the context of a full-length Env or a fusion of the CD8 ectodomain and HIV-1 Env CT (data not shown), as previously described [477]. It is also well recognized that truncations in the HIV-1 CT can affect epitope exposure in the Env ectodomain, as well as neutralization sensitivity and fusion kinetics [467,468,481–484]. In particular, we note that quaternary epitopes in the V1/V2 domain could not be probed here using the available broad neutralizing antibodies (e.g. PG16, PGT145), as these do not bind to WT 89.6 or JRFL. Therefore, it is possible that antigenic differences not tested here could have affected the immunogenicity of TM1 mutants.

Our findings build on previous studies that demonstrated the ability of mutations in the Env CT to alter its immunogenicity [328,485] and demonstrate that CT mutations rationally designed to increase Env expression on the cell surface are associated with enhanced antibody responses in the context of a poxvirus prime-protein boost vaccine regimen in mice. Although these findings will require validation in larger animal models, this encouraging result supports the idea that low surface expression of Env functions as a immune evasion strategy for HIV-1 and that immunogenicity of Env-based vaccines can be improved when Envs are modified for high surface expression. An important aspect of this finding is that these modifications can be combined with other approaches that modify the Env

ectodomain to enhance the quality of antibody responses, including those that affect Env trimer stability and/or epitope exposure [208,249,382]. Env modifications that enhance efficacy of the prime can also be paired with improved boosting immunogens, such as stabilized SOSIP trimers [45,46,244,335], which have been shown to elicit NAb to neutralization-resistant, Tier-2 HIV-1 isolates [46,244]. Further studies will determine whether CT modifications that increase surface expression have the same effect on immunogenicity in nonhuman primates and for other viral vectors or nucleic acid-based vaccines.

3.5. METHODS

Ethics statement

The investigators faithfully adhered to the "Guide for the Care and Use of Laboratory Animals" by the Committee on Care of Laboratory Animal Resources Commission on Life Sciences, National Research Council. The animal facilities at the University of Pennsylvania are fully accredited by the American Association for Accreditation of Laboratory Animal Care (AAALAC). All studies were conducted under protocols approved by University of Pennsylvania IACUCs.

Generation of cytoplasmic tail (CT)-modified HIV-1 Env constructs

Mutant Env constructs were generated on HIV-1 R3A Env [462] in the pHSPG plasmid, HIV-1 89.6 Env [486] in the pCIneo plasmid (Promega), or JRFL Env [487] in the pSVIII plasmid. The 89.6 N7 ($N_{197}Q$) mutant was generated from 89.6 WT as previously described [382]. Env CT mutant TM1 was generated in each Env isolate using a three-step process with QuikChange II XL reagents (Agilent) and the following primers:

1.) 5'-CAGAGTGCGGCAGGGCATCCGGCCAGTGAGCTTCTAGACACTGCTG-3';

2.) 5'- GGCATCCGGCCAGTGTTCAGCTACTTCTAGACACTGCTG-3';

3.) 5'- CGGCCAGTGTTCAGCAGCCCCCCCAGCTACTTCTAGACACTGCTG-3'.

Amino acid sequences of all mutants are shown in Table 1.

Env expression analysis in plasmid-transfected HEK 293T cells

To measure the surface expression of CT-modified HIV-1 Envs, each Env mutant or wild-type/parental Env was co-transfected with 9 µL of Fugene 6

(Promega) into HEK 293T cells with GFP plasmid in a 12-well plate. For 89.6 Envs in pCIneo, 1.5 μg Env plasmid and 0.3 μg pmax-GFP (Lonza) was used. For JRFL Envs in the lower-expressing pSVIII vector, a higher Env:GFP plasmid ratio was used: 1.5 μg Env and 0.1 μg GFP. The pHSPG vector expressing R3A Envs expresses GFP, so no additional GFP plasmid was added in these experiments. After 18 hrs post-transfection, cells were harvested and stained for Env gp120 expression using 7.5 μg/mL 2G12 (NIH AIDS Reagent Program) and 1:300 secondary goat anti-human IgG Alexa Fluor 647 (Life Technologies). Cells were fixed with 4% paraformaldehyde and fluorescence was measured on a FACSCalibur (BD Biosciences). Analysis was performed using FlowJo software (Tree Star). Events were gated on GFP+ cells and median fluorescence intensity (MFI) was recorded and expressed relative to wild-type or parental Env.

Recombinant vaccinia viruses

HIV-1 Env-expressing recombinant vaccinia virus (VACV) vectors were made for this study by cloning each Env into a VACV virus shuttle vector, pGS20, under the control of the synthetic VACV virus early/late promoter, and then inserting it into the thymidine kinase gene of the v-NY strain of VACV virus (a replication-competent virus that was plaque purified from the New York City Board of Health strain) [465,466] by homologous recombination. The negative control VACV for immunization studies was made similarly and encodes an irrelevant antigen, SIVmac239 Gag-Pol, instead of Env. The empty VACV virus used *in vitro* is the parental v-NY virus with an intact TK gene.

Purified stocks, used for immunization studies, were prepared as follows: first, VACV-infected BSC40 cell pellets (~1 billion cells) were resuspended in 14 mL cold

10 mM Tris, pH=9.0, transferred to a 40 mL glass Dounce homogenizer, and homogenized with 40 strokes of a tight pestle on ice. The material was centrifuged for 5 min at 1360 RPM at 4°C, and supernatant was collected. 3 mL of cold 10 mM Tris was added and the material was centrifuged a second time. Supernatants from both spins were pooled and then sonicated in a 550 Sonic Dismembrator at an amplitude setting of 8. The material was sonicated at 1-min intervals three times in ice water with 1-3 min resting periods on ice. The material was gently layered onto 36% sucrose (10 mM Tris, pH=9.0) and spun at 15,800 rpm in a Beckman Coulter SW 28 rotor for 80 min at 4°C. The supernatant was aspirated and the virus pellet was resuspended in cold 1 mM Tris, pH=9.0, and sonicated as above before being stored at -80°C.

For *in vitro* Env expression studies, VACV crude lysates were prepared similarly as described above, but without sucrose gradient ultracentrifugation.

In vitro VACV infection and Env expression analysis

For analyses of Env expressed by VACV vectors, 1.6×10^6 HEK 293T cells were infected with VACV crude lysates at a multiplicity of infection (MOI) of 3. Virus was absorbed onto cells at 37°C for 1 hr in 0.5 mL DPBS with 10 mM $MgCl_2$ and 0.01% BSA, and then replaced with 2 mL of DMEM with 10% FBS. The infection was allowed to proceed for 16 hr post-absorption. Harvested cells were stained for HIV-1 Env with human mAbs 2G12 or 2F5 (NIH AIDS Reagent Program) at 7.5 µg/mL and 10 µg/mL, respectively, and 1:100 secondary goat anti-human IgG Alexa Fluor 647 conjugate (Invitrogen, A-21445). VACV A33 protein was stained using 1:300 rabbit anti-A33 serum (kindly provided by Dr. Stuart Isaacs) and 7.5 µg/mL goat anti-rabbit IgG FITC conjugate (BD Biosciences 552420). Each antibody was

incubated on cells for 30 min on ice, and each sample was stained with and without permeabilization with 0.1% saponin to allow total cellular stain. All samples were fixed with paraformaldehyde after staining and fluorescence was measured using a FACSCalibur flow cytometer. Ten thousand events were collected and live, A33+ cells were gated to determine the mean fluorescence intensity (MFI) of Env and A33 staining.

For antigenicity analysis, HEK 293T cells were infected as above and stained without permeabilization using 1:300 rabbit anti-A33 serum and the Env-specific mAbs 2G12, VRC01, b12, CD4-IgG, 17b, 447-52D, PG9, PG16, 2F5, 4E10, 10E8 (NIH AIDS Reagent Program), which bind to different antigenic determinants. Goat anti-rabbit IgG FITC and goat anti-human IgG Alexa Fluor 647 conjugates were used as secondary antibodies. Transduced cells were gated on using the A33 stain, and the MFI for each Env-specific mAb was normalized to the 2G12 signal to account for any differences in surface expression. These values were expressed as fold changes for CT-modified Envs relative to the parental Env.

Cell-cell fusion assay

The functionality of CT-modified Envs was qualitatively assessed using a cell-cell fusion assay as used previously [488]. TZM-bl cells (NIH AIDS Reagent Program) were infected with crude lysates of recombinant VACV vectors at an MOI of 1.0. After 18 hours of infection, cells were fixed in a solution of 95% ethanol and 5% acetic acid and stained with Giemsa to visualize syncytia.

gp120 expression and purification

89.6 N7 gp120 and JRFL WT gp120 were expressed in BSC40 cells by recombinant VACV infection and purified by a three-step procedure using lectin affinity, diethylaminoethanol (DEAE) anion exchange, and size exclusion chromatography, as previously described [410].

Mice

Female C57BL/6 (BL/6) mice were purchased from NCI and housed in a BSL2 containment facility. All mice were 6 weeks of age at the initiation of immunization studies.

Immunizations

Mice were immunized intraperitoneally with 1 x 10^8 PFU of recombinant VACV (v-NY strain) encoding HIV-1 Env variants or SIV Gag-Pol at weeks 0 and 4. At weeks 8 and 12, mice were immunized intramuscularly with 5 µg gp120 in PBS in 1% Alhydrogel alum adjuvant (Invivogen). Serum samples were collected immediately prior to the first immunization and each subsequent prime or boost. Splenectomies and final serum collection were performed two weeks after the second gp120 boost (week 14).

Enzyme-linked immunosorbent assays (ELISAs)

HIV-1 gp120-specific IgG in mouse serum was quantified by ELISA using a murine mAb against gp120 (3B3, NIH AIDS Reagent Program) as a standard. Immulon 4 HBX high-binding plates were coated with purified HIV-1 89.6 N7 gp120 or JRFL WT gp120 at a final concentration of 1 µg/mL in PBS overnight at 4°C. Incubation steps were performed at room temperature in 100 uL volumes. The plates

were washed once with wash buffer (0.05% Tween-20 in PBS) and blocked with blocking buffer (2% BSA in PBS) for 1 hr, followed by three more washes. Dilutions of sera and standard were made in blocking buffer and incubated on the plate for 1.5 hr. Sera and standard were removed and the plate was washed four times with wash buffer. Goat anti-mouse IgG HRP conjugate (Sigma-Aldrich A8924) at 1:10,000 in blocking buffer was incubated for 1 hr. After four washes, TMB substrate mixture (KPL) was added at 100 µL/well for 20 minutes. 2 N sulfuric acid (50 µL/well) was used to stop the reaction, and the optical density (OD) was read at 450 nm on a Dynex MRX Revelation microplate reader.

VACV-, V3-, and V1/V2-specific IgG ELISAs were performed similarly to gp120-specific IgG ELISA, with the following modifications. For VACV, the coating antigen was Western Reserve VACV lysed in RIPA buffer, diluted 1:200 in PBS (kindly provided by Dr. Stuart Isaacs). For V3, the coating antigen was synthetic 89.6 Env V3 peptide (GenScript) at 5 µg/mL in PBS. For V1/V2, the coating antigen was a scaffold protein containing HIV-1 92US715 V1/V2 fused to MLV gp70 (kindly provided by Dr. Shan Lu) at 1 µg/mL in PBS.

Splenocyte stimulation and intracellular cytokine staining

To perform Env-specific and VACV-specific T cell analyses, splenocytes (2 x 10^6) were incubated with four separate SHIV 89.6P Env peptide pools (NIH AIDS Reagent Program) and one immunodominant VACV peptide pool (NR-4058, BEI Resources) at 37°C and 5% CO_2. All peptides were used at 1 mg/mL, and DMSO was used as a control for background. After 1 hr, GolgiPlug (brefeldin A), GolgiStop (monensin), and anti-CD107a-FITC (BD Biosciences) were added and cells were incubated for an additional 5 hrs. Cells were washed in PBS and resuspended in

LIVE/DEAD Aqua Blue stain (Invitrogen) for 10 min at room temperature. A mixture of anti-CD44-PE/Cy5, anti-CD27-PE (BD Biosciences), anti-CD8-Pacific Blue, and anti-CXCR5-Brilliant Violet 605 (BioLegend) surface marker antibodies was added and incubated for 30 min at room temperature. Cells were washed in FACS buffer (PBS, 1% FBS), resuspended in FIX & PERM (BD Biosciences), and incubated for 20 min at room temperature. Cells were washed with Perm/Wash (BD Biosciences), then resuspended in a mixture of anti-TNFα-PE/Cy7, anti-IFNγ-Alexa Fluor 700, anti-IL2-APC, and anti-CD3-APC/Cy7 antibodies (BD Biosciences) and incubated at room temperature for 1 hr. Cells were washed, resuspended in 1% paraformaldehyde in PBS, and analyzed for fluorescence using an LSRII (BD Biosciences). Analysis was performed using FlowJo software (Tree Star). Events were gated on live (Aqua Blue-negative) cells. $CD4^+$ cells were identified as $CD3^+/CD8^-$ cells. Background-subtracted percentages of cytokine-positive cells in each of four Env peptide pools were added together to yield the Env-specific $CD4^+$ T cell response.

Neutralization assays

Pseudotype virus neutralization assays were performed in TZM-bl reporter cells as previously described [409] using pre-immune and post-immune mouse sera. Samples were assayed for neutralization of pseudoviruses expressing multiple HIV-1 Envs or murine leukemia virus (MLV) Env to measure nonspecific neutralization and cytotoxicity. Values were background-corrected and reported as the reciprocal of the serum dilution at which 50% reduction of luciferase activity is observed (ID50).

Statistical analysis

Statistical tests were performed using GraphPad Prism software. Env-specific IgG concentrations, distributed on a log scale, were log transformed before analysis. Parametric or non-parametric tests were chosen for each analysis based on whether the data were normally distributed.

3.6. SUPPLEMENTARY DATA

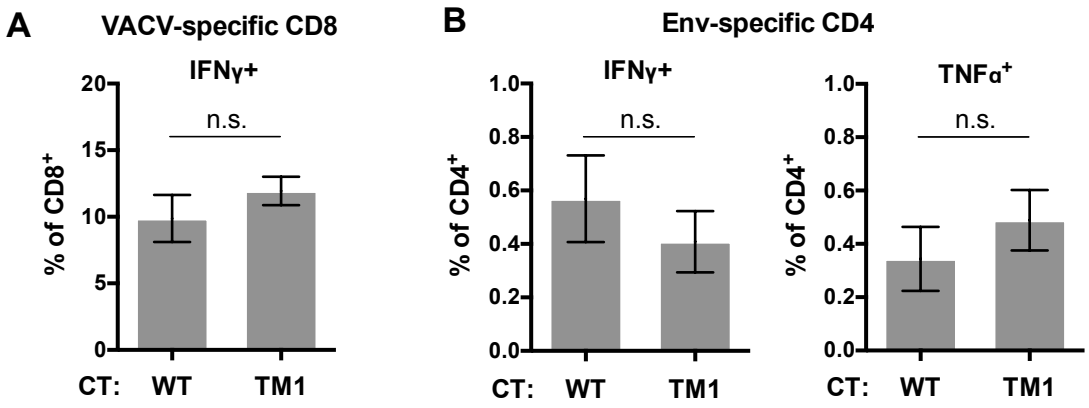

Supp. Fig. S3.1. No significant difference in vector-specific CD8$^+$ or Env-specific CD4$^+$ T cell responses resulting from TM1 CT modification. Splenocytes from mice immunized with 89.6 N7 Envs with WT or TM1 CT were stimulated with peptide pools from (A) VACV or (B) SHIV 89.6P Env and were stained for intracellular cytokine expression. Data represent mean frequencies of IFNγ$^+$ and TNFα$^+$ cells, as a percentage of total CD8$^+$ or CD4$^+$ T cells, and error bars are the SEM; n.s. = not significant ($p>0.05$) by Mann-Whitney test.

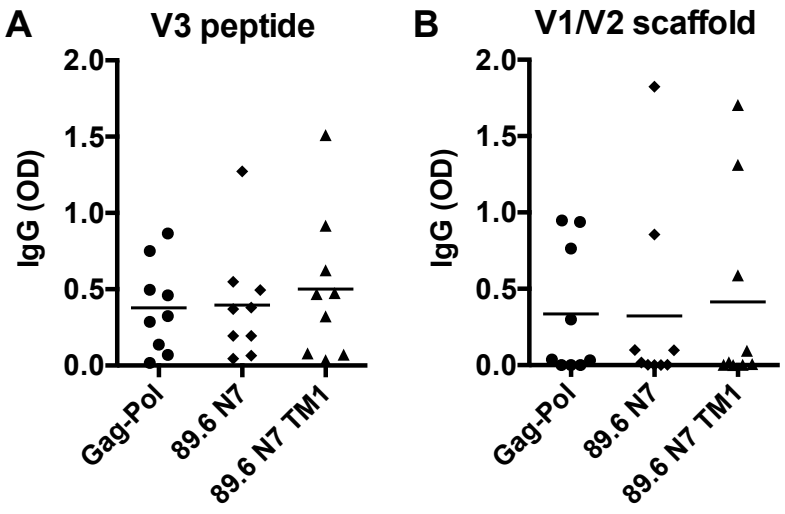

Supp. Fig. S3.2. No difference in V3 and V1/V2 epitope-specific IgG responses from TM1 modification. (A) V3-specific and (B) V1/V2-specific IgG responses were assayed by ELISA using synthetic V3 peptide and gp70-scaffolded V1/V2, respectively, as the coating antigens and post-boost two serum diluted (A) 1:2,000 or (B) 1:200. Points represent OD values for individual mice and horizontal lines indicate the mean. Groups were not statistically different ($p>0.05$) by Kruskal-Wallis test with Dunn's correction.

3.7. ACKNOWLEDGMENTS

Special thanks to Angela Conde-Motter, the co-lead author of this work, who performed mouse immunizations with me, analyzed T cells, and began the studies of Env surface expression. Thanks also to Brad Cleveland, Lifei Yang, and Wenjin Guo for the production and characterization of vaccinia vectors, including Env expression and antigenicity, and to Celia LaBranche and David Montefiori for analyzing NAbs. We gratefully acknowledge Shan Lu, Shixia Wang, Dong Han, Stuart Isaacs, Xiaoying Shen, Kelli Greene, Hongmei Gao, Georgia Tomaras, and Deb Diamond for their technical and administrative support, and assistance from the Viral/Molecular Core of the Penn Center for AIDS Research (P01 AI045008). This work was funded by NIH R01 AI090788, NIH T32 AI007632, and the Bill and Melinda Gates Foundation CAVD grant OPP1022102.

CHAPTER 4

ZIKA VIRUS PROTECTION BY A SINGLE LOW-DOSE NUCLEOSIDE MODIFIED MESSENGER RNA VACCINATION

Adapted from the following publication:

Norbert Pardi*, Michael J. Hogan*, Rebecca S. Pelc, Hiromi Muramatsu, Hanne Andersen, Christina R. DeMaso, Kimberly A. Dowd, Laura L. Sutherland, Richard M. Scearce, Robert Parks, Wendeline Wagner, Alex Granados, Jack Greenhouse, Michelle Walker, Elinor Willis, Jae-Sung Yu, Charles E. McGee, Gregory D. Sempowski, Barbara L. Mui, Ying K. Tam, Yan-Jang Huang, Dana Vanlandingham, Veronica M. Holmes, Harikrishnan Balachandran, Sujata Sahu, Michelle Lifton, Stephen Higgs, Scott E. Hensley, Thomas D. Madden, Michael J. Hope, Katalin Karikó, Sampa Santra, Barney S. Graham, Mark G. Lewis, Theodore C. Pierson, Barton F. Haynes, and Drew Weissman. *Nature* 2017; 543: 248-251

Additional contributions are from Martin S. Naradikian, Kaela Parkhouse, and Michael P. Cancro.

*These authors contributed equally to this work.

4.1. ABSTRACT

Zika virus (ZIKV) has recently emerged as an explosive pandemic associated with severe neuropathology in newborns and adults. There are no ZIKV-specific treatments or preventatives; thus, development of a safe and effective vaccine is a high priority. Messenger RNA (mRNA) has emerged as a versatile and highly effective platform to deliver vaccine antigens and therapeutic proteins. Here, we demonstrate that a single low-dose intradermal immunization with lipid nanoparticle-encapsulated nucleoside-modified mRNA (mRNA-LNP) encoding the pre-membrane and envelope (prM-E) glycoproteins of a 2013 ZIKV outbreak strain elicited potent and durable neutralizing antibody responses in mice and non-human primates. Immunization with 30 μg of nucleoside-modified ZIKV mRNA-LNPs protected mice from ZIKV challenges at 2 weeks or 5 months post-vaccination, and a single dose of 50 μg was sufficient to protect non-human primates from a challenge at 5 weeks post-vaccination. These data demonstrate that nucleoside-modified mRNA-LNPs elicit rapid and durable protective immunity and thus represent a new and promising vaccine candidate for the global fight against ZIKV.

4.2. INTRODUCTION

ZIKV, first identified in 1947 [274,275], is a mosquito-borne and sexually transmitted flavivirus that has recently been associated with microcephaly and other birth defects in newborns and Guillain-Barré syndrome in adults [280,288,489–491]. Effective vaccines have been approved for other closely related flaviviruses [492–494], but vaccine candidates for ZIKV have only recently been developed [295,297–301,306,495]. Multiple vaccine formats have been shown to protect mice or non-human primates (NHPs) from ZIKV infection, including plasmid DNA [295,297–299], purified inactivated virus [295,297], live attenuated virus [301], protein subunit [300], adenovirus vectors [297,300], and mRNA, as described in our recent publication [307] and two subsequent reports [306,495].

The ideal vaccine for ZIKV would be safe and induce protective immunity after a single immunization, regardless of prior serologic history. Of the candidate Zika vaccines described prior to publication of these data, only a rhesus adenovirus platform (RhAd52) has been shown to confer protection after a single immunization in NHPs; however, the efficacy of the RhAd52 vector in humans is currently undefined. Additionally, pre-existing immunity to adenovirus serotypes can limit the efficacy of such vectors [496,497], and low neutralizing titers to rhesus adenoviruses, including RhAd52, have been detected in humans [498].

mRNA has emerged as a promising new vaccine modality that can elicit potent immune responses (reviewed in [303,499]), while avoiding the safety risks and anti-vector immunity associated with some live virus vaccines (reviewed in [500]). Vaccination with mRNA offers several advantages over other vaccine platforms: (i) it is a non-integrating, non-infectious gene vector that can be readily

designed to express any protein with high efficiency, (ii) it has the potential for cost-effective and highly scalable manufacturing, and (iii) small doses are sufficient to induce protective immune responses. mRNA therefore represents a promising method to generate an effective and widely distributable vaccine for ZIKV.

4.3. RESULTS

To design a ZIKV vaccine that would generate protective immunity after a single vaccination, we used a recently developed vaccine platform consisting of purified [311], *in vitro* transcribed mRNA containing the modified nucleoside 1-methylpseudouridine (m1Ψ), which prevents innate immune sensing and increases mRNA translation *in vivo* [320]. The nucleoside-modified mRNA was formulated for vaccination in lipid nanoparticles (LNPs), which have been shown to mediate efficient and prolonged protein expression by mRNA *in vivo* [309]. We first showed that this is a highly effective vaccine platform using influenza hemagglutinin (HA) as a target antigen. Mice were immunized a single time intradermally (i.d.) with 30 μg of m1Ψ-modified HA mRNA-LNPs or luciferase-encoding mRNA-LNPs as a control. The hemagglutination inhibition (HAI) titers in HA mRNA-immunized mice rose rapidly to >4,000 and were maintained above ~2,000 for 13 months (Fig. 4.1A). After this time, immunized and control mice were challenged with a lethal dose of influenza PR8. All control mice died while HA mRNA-immunized mice survived (Fig. 4.1B) with no weight loss.

To determine the mechanism of the potent antibody response, we evaluated total T follicular helper (Tfh) and germinal center (GC) B cell responses in the spleen and found that the absolute counts of both of these cell types were highly elevated during vaccination with m1Ψ-containing HA mRNA-LNPs compared to control mice that received luciferase mRNA-LNPs or a conventional inactivated influenza virus vaccine (Figs. 4.1D and E). In contrast, we found that uridine-containing HA mRNA-LNPs did not stimulate Tfh and GC B cell responses above background levels, and accordingly the HAI titers were low and comparable to inactivated virus (Fig. 4.1C).

Similar results were obtained when antigen-specific Tfh cells in the spleen were quantified based on Bcl6 and IFN-γ expression in response to HA peptide stimulation (data not shown). Thus, nucleoside modification appears necessary for the ability of this vaccine platform to stimulate potent germinal center reactions and NAb responses following a single immunization.

We used the above method to design a novel, potent anti-ZIKV vaccine in which the prM-E glycoproteins of ZIKV H/PF/2013 [501] were encoded by purified, m1Ψ-containning mRNA (Supp. Fig. S4.1A). Studies of ZIKV and other flaviviruses have demonstrated that co-expression of prM and E proteins is sufficient to assemble and secrete subviral particles [298,502]. ZIKV prM-E-encoding mRNA was first characterized by transfecting HEK 293T cells and human and murine dendritic cells (DCs). ZIKV E protein was produced by all cell types and was secreted into the supernatant of 293T cells (Supp. Fig. S4.1B). We hypothesize that DCs also secrete E protein and that it is rapidly endocytosed, as has been proposed for HIV Gag [503]. E protein in supernatant was pelleted by ultracentrifugation when incubated with PBS, but not with 0.5% Triton X-100, consistent with subviral particle production from prM-E mRNA [502] (Supp. Fig. S4.1C).

The immune response induced by the nucleoside-modified ZIKV prM-E mRNA-LNP vaccine was first evaluated in C57BL/6 mice. Animals were immunized i.d. with 30 μg of ZIKV prM-E mRNA-LNPs or poly(C) RNA-LNPs (negative control). No inflammation or other adverse events were observed at the sites of injection. Polyfunctional E protein-specific $CD4^+$ T cell responses were detected based on intracellular IFN-γ, TNF-α, and IL-2 production by ZIKV E protein-stimulated splenocytes at week 2 post-vaccination (Fig. 4.2A and Supp. Fig. S4.2). ZIKV E-specific serum IgG developed quickly in vaccinated mice and stabilized at an

endpoint titer of 180,000 (~90 μg/ml) at weeks 8 to 12 (Fig. 4.2B and Supp. Fig. 4.3A). Anti-ZIKV neutralizing antibodies (NAb) were measured using two independent assays: a standard plaque reduction neutralization test (PRNT) and a ZIKV reporter viral particle (RVP) assay [298]. The mean $PRNT_{50}$ titer against ZIKV MR-766 peaked at ~1,300 at week 8 (Fig. 4.2C) and was relatively stable until week 12. The mean RVP NAb titer (EC_{50}) against ZIKV H/PF/2013 reached ~10^5 at weeks 8 and 12 (Fig. 4.2D). The detection of higher NAb titers in the RVP assay compared to other assay formats similar to PRNT has been previously reported [298]. In addition, we noted that the ratio of RVP to PRNT titers was not fixed and varies with the animal model and viral isolate.

Immunogenicity of the nucleoside-modified ZIKV prM-E mRNA-LNP vaccine was next evaluated in BALB/c mice. E-specific serum IgG peaked at week 8 and remained stable between weeks 8 and 20 (endpoint titers ~200,000; 90-130 μg/ml) (Fig. 4.2E and Supp. Fig. S4.3B). $PRNT_{50}$ NAb increased to a maximum of ~1,100 at week 16 and remained stable until week 20 (Fig. 4.2F). The RVP NAb titer rose to 50,000 at week 8 and remained above 20,000 until week 20 (Fig. 4.2G).

A challenge study was conducted in BALB/c mice immunized i.d. with 30 μg of nucleoside-modified ZIKV prM-E mRNA-LNPs or poly(C) RNA-LNPs. Mice were intravenously (i.v.) challenged at week 2 (short-term) or week 20 (long-term) post-immunization with 200 plaque-forming units (PFU) of ZIKV PRVABC59. In the short-term protection study, 8 of 9 control mice developed viremia by day 3, with a median peak of ~14,000 copies/ml. All ZIKV mRNA-immunized mice (n=9) were protected from detectable viremia (Fig. 4.3A). In the long-term study, all control mice (n=5) showed viremia on day 3, with a median peak of 1,200 copies/ml, while none of the ZIKV mRNA-immunized mice (n=10) had detectable viremia at days 3 or 7 (Fig.

4.3B). These data demonstrate that a single immunization with nucleoside-modified ZIKV prM-E mRNA-LNPs rapidly elicits durable protection from detectable viremia with a heterologous ZIKV strain in mice.

We next evaluated the efficacy of the nucleoside-modified ZIKV mRNA-LNP vaccine in rhesus macaques (*Macaca mulatta*), a non-human primate species that recapitulates several features of ZIKV infection in humans [504]. Macaques were immunized i.d. with doses of 600 μg, 200 μg or 50 μg of nucleoside-modified ZIKV prM-E mRNA-LNPs. As in mice, no inflammation or other adverse events were observed. E-specific binding IgG and NAb were efficiently induced by all three vaccine doses, with no statistically significant differences between groups. Endpoint IgG titers rose to >300,000 in all groups at week 4 and were maintained at ≥100,000 until week 12 (Fig. 4.4A). $PRNT_{50}$ NAb titers against MR-766 peaked at ~400 at week 2 (Supp. Fig. S4.4A). To facilitate comparison of NAb titers across laboratories, the neutralization curve is shown for a human ZIKV-neutralizing mAb, A3594, in the PRNT assay (Supp. Fig. S4.5). NAb titers obtained with a focus reduction neutralization test (FRNT), which has a format similar to PRNT, were stable around 400 against ZIKV MEX I-44 at weeks 2 through 12 (Fig. 4.4B). The RVP assay revealed NAb titers against H/PF/2013 of ~10,000 at week 2 and ~17,000 at week 4 (Fig. 4.4C), and a titer of ~3,000 against MR-766 at week 4 (Supp. Fig. S4.4B). The neutralization of both Asian- and African-lineage viruses is consistent with a prior report demonstrating the existence of only one serotype of ZIKV [291]. The absence of a significant dose-dependent effect on the antibody response in any assay (Kruskal-Wallis test, $p>0.05$) suggests that a low dose of 50 μg (approximately 0.02 mg/kg) was sufficient, or possibly more than sufficient, to induce robust anti-ZIKV immunity in macaques.

Rhesus macaques were challenged at week 5 by subcutaneously (s.c.) injecting 10^4 $TCID_{50}$ of ZIKV PRVABC59 into five vaccinated animals and six control animals (Supp. Table S4.1). All control animals became infected with median peak plasma viremia of 7,000 ZIKV RNA copies/ml (Fig. 4.5). In contrast, vaccinated macaques were highly protected from ZIKV infection. Four of five animals — including three that received the lowest dose of 50 µg and one that received the medium dose of 200 µg — had no detectable viremia (<50 copies/ml) at all time points. We detected a low and transient viral blip of 100 copies/ml at day 3 post-challenge in one animal that received the highest dose of 600 µg of ZIKV prM-E mRNA-LNPs, representing a ~99% reduction in peak viremia compared to the control animals. This animal exhibited among the lowest NAb titers in multiple assays at week 4 post-vaccination: $PRNT_{50}$ of 36 to MR-766, $FRNT_{50}$ of 226 to MEX I-44, and RVP titers of 986 to MR-766 and 5,812 to H/PF/2013 (Fig. 4.4 and Supp. Fig. S4.4). The significance of a low-level viral blip in one animal, including implications for a correlate of protection, are as yet uncertain and warrant further study with a greater number of animals.

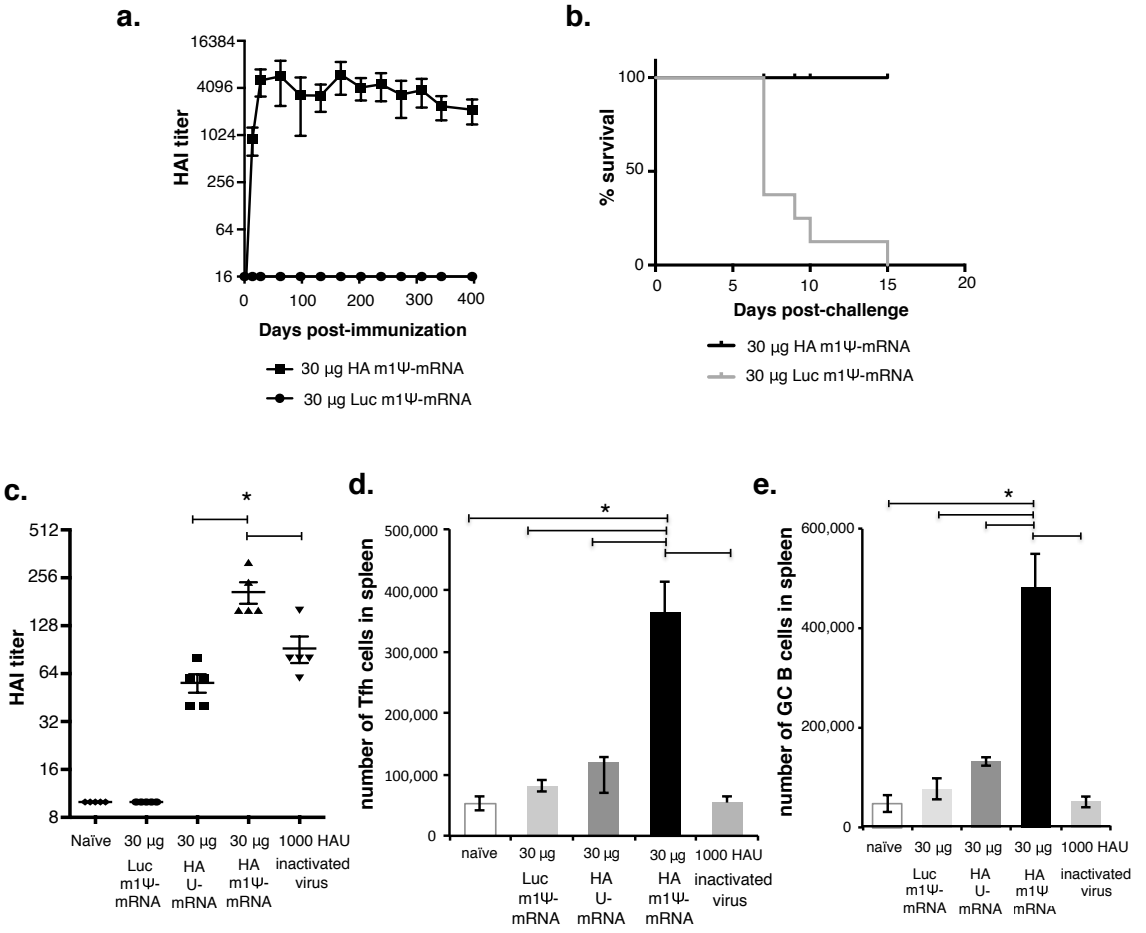

Figure 4.1. Nucleoside-modified mRNA-LNP vaccination generates robust T follicular helper (Tfh) cell and germinal center (GC) B cell responses. The potency of the nucleoside-modified mRNA-LNP platform was first investigated using influenza hemagglutinin (HA) as a target antigen. (A) BALB/c mice were immunized i.d. with 30 µg of FPLC-purified, 1-methylpseudouridine (m1Ψ)-containing mRNA encoding HA or luciferase (Luc) in LNPs, and serum HAI titers were measured for 13 months. (B) After 13 months, mice were challenged with a lethal dose of influenza PR8 and monitored for survival. (C-E) Mice were immunized i.d. with 30 µg of HA-encoding m1Ψ- or uridine (U)-containing mRNA-LNPs, Luc-encoding m1Ψ-mRNA-LNPs, or inactivated influenza vaccine, and then sacrificed after 10 days. (C) HAI titers were measured. Splenocytes were analyzed for the frequency of (D) Tfh cells ($TCR\beta^+$, $CD19^-$, $CD4^+$, $CD62L^-$, $CXCR5^+$, $PD\text{-}1^+$) and (E) GC B cells (IgM^-, IgD^-, $B220^+$, $CD19^+$, $CD138^-$, $CD38^{low}$, PNA^{high}. Tfh and GC B cell experiments were repeated at least twice to achieve sufficient numbers of values for mice in each group (n=5-8 mice/group). Error bars are s.e.m. Statistical analysis: one-way ANOVA with Bonferroni correction, *$p<0.05$.

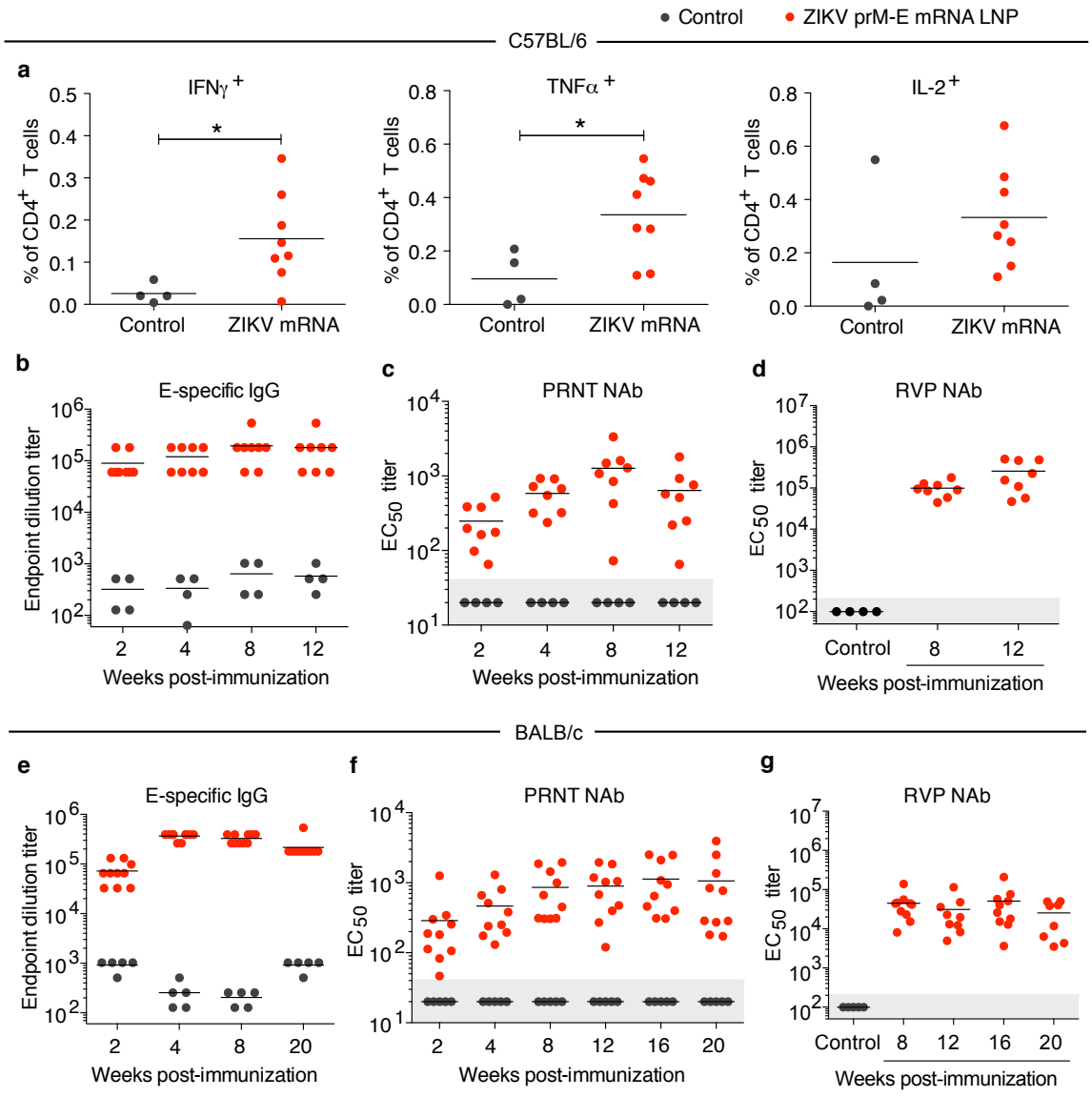

Figure 4.2. Nucleoside-modified ZIKV mRNA-LNP immunization elicits ZIKV-specific T helper and neutralizing antibody responses. a-d, C57BL/6 mice were immunized i.d. with 30 μg of nucleoside-modified ZIKV prM-E mRNA-LNPs (n=8) or control poly(C) RNA-LNPs (n=4). **(a)** At week 2, splenic antigen-specific $CD4^+$ T cells were detected by intracellular cytokine staining. The antibody response was monitored by **(b)** ELISA, **(c)** PRNT using ZIKV MR-766, and **(d)** RVP using ZIKV H/PF/2013. **e-g,** BALB/c mice were immunized similarly with ZIKV mRNA-LNPs (n=10) or poly(C) RNA-LNPs (n=5) and monitored by **(e)** ELISA, **(f)** PRNT using MR-766, and **(g)** RVP using H/PF/2013. Points represent individual mice; horizontal lines show the mean; shaded area indicates values below the limit of detection. The controls in **d** and **g** are from the week 8 time point. Asterisk indicates $p<0.05$ in unpaired t-test; antibody responses in vaccine and control groups were compared at each time point by Mann-Whitney test: $p<0.01$ for all comparisons.

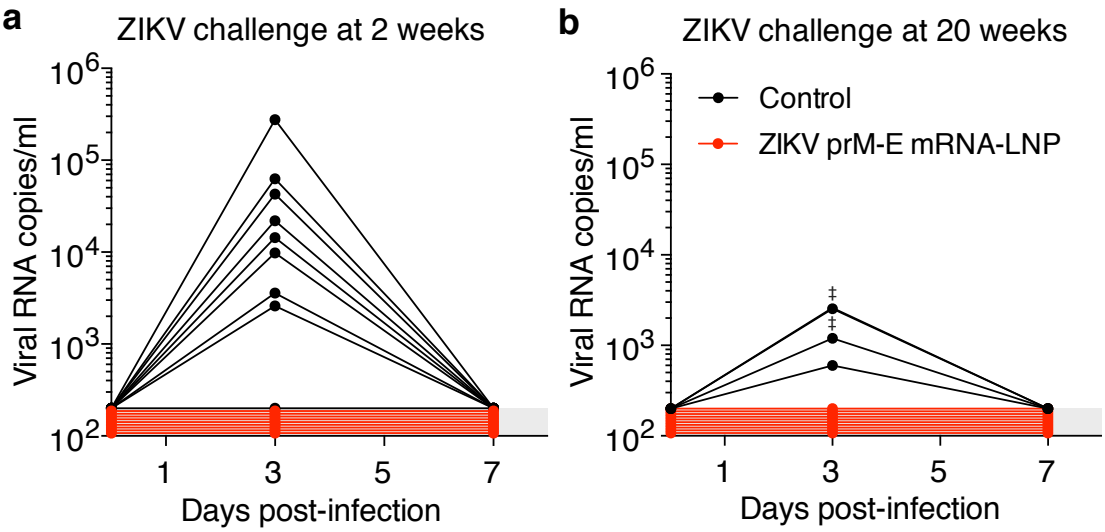

Figure 4.3. A single immunization of nucleoside-modified ZIKV prM-E mRNA-LNPs provides rapid and durable protection from ZIKV challenge in mice. BALB/c mice immunized i.d. with 30 μg of ZIKV prM-E mRNA-LNPs or control poly(C) RNA-LNPs were challenged i.v. with 200 PFU ZIKV PRVABC59 at **(a)** 2 weeks (n=9 per group) or **(b)** 20 weeks (n=5 control mice; n=10 ZIKV mRNA-LNP mice) post-vaccination, and plasma viral loads were measured by qRT-PCR for ZIKV capsid RNA. ‡ symbol indicates two overlapping curves. Shaded area indicates values below the limit of detection (200 copies/ml), with undetectable curves staggered to show individual mice. Day 3 viremia in vaccine and control groups was compared by Mann-Whitney test: $p<0.001$ for both challenges.

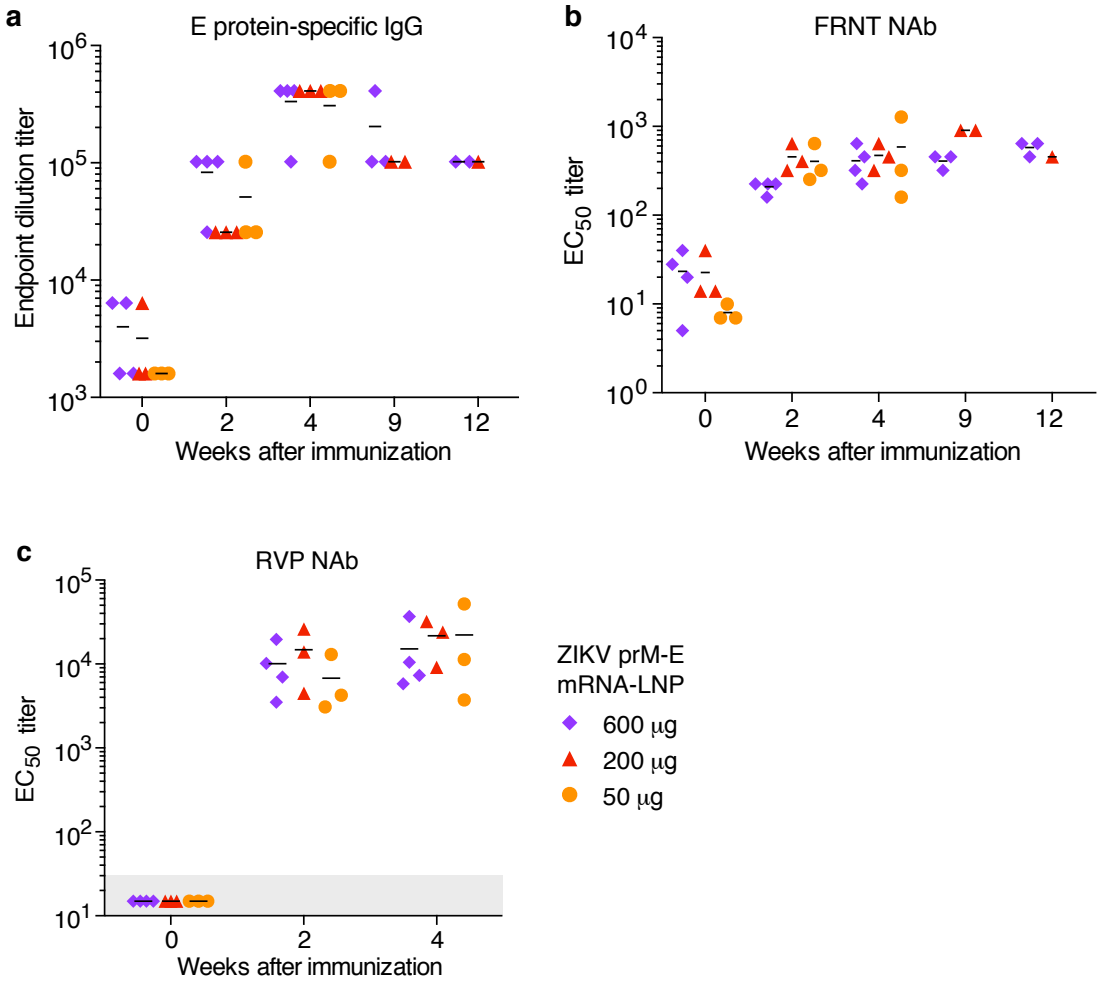

Figure 4.4 Nucleoside-modified ZIKV mRNA-LNP immunization elicits potent ZIKV-specific neutralizing antibody responses in non-human primates. Rhesus macaques were immunized with 600 μg (n=4), 200 μg (n=3), or 50 μg (n=3) of ZIKV prM-E mRNA-LNPs, and the antibody response was quantified by **(a)** ELISA, **(b)** FRNT using ZIKV MEX I-44, and **(c)** RVP using ZIKV H/PF/2013. Pre-challenge (weeks 0 to 4) and unchallenged animal data are shown. Points represent individual monkeys; shaded area indicates values below the limit of detection; horizontal lines indicate the mean. Immune responses in dose groups were compared by Kruskal-Wallis test: $p>0.05$ for all comparisons.

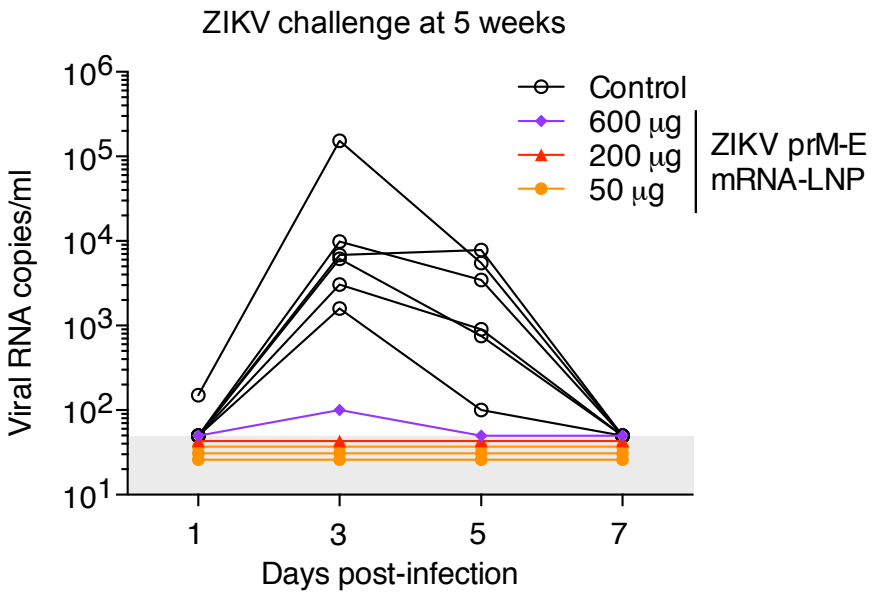

Figure 4.5. A single immunization of nucleoside-modified ZIKV prM-E mRNA-LNPs protects rhesus macaques from ZIKV challenge at 5 weeks post-immunization. Six unvaccinated control macaques and five vaccinated macaques that received 50 μg (n=3), 200 μg (n=1), or 600 μg (n=1) of ZIKV mRNA-LNPs at week 0 were challenged s.c. with 10^4 $TCID_{50}$ of ZIKV PRVABC59 at week 5. Viral loads were measured in plasma by qRT-PCR for ZIKV capsid RNA. Shaded area indicates values below the limit of detection (50 copies/ml), and undetectable values were staggered to show individual animals. Day 3 and 5 viremia in vaccine and control groups was compared by Mann-Whitney test: $p<0.001$.

4.4. DISCUSSION

In this report, we demonstrate that a single, low-dose i.d. immunization with nucleoside-modified ZIKV prM-E mRNA-LNPs is protective in both mice and rhesus macaques and elicits higher NAb responses than a single immunization of multiple recently reported ZIKV vaccine candidates, including purified inactivated virus (PIV) and plasmid DNA vaccines encoding prM-E or M-E [295,297,298]. In mice, $PRNT_{50}$ NAb increased steadily over several months, rising to levels 50-100 times higher than those induced by a single immunization with PIV or DNA vaccines [295,298]. The ZIKV mRNA-LNP vaccine conferred complete, rapid, and durable protection in mice that was maintained for at least 5 months, and likely much longer, since NAb titers were stable. The mouse challenge studies also revealed that ZIKV PRVABC59 replicated more efficiently ($p=0.02$, Mann-Whitney test) in 8 week-old BALB/c mice compared to 25 week-old mice, when two identical aliquots and doses of challenge virus stock were used. A prior report has shown that ZIKV-related mortality in immune-competent mice decreases between 1 and 4 weeks of age [505], but ZIKV replication in adult mice has not yet been well described.

In rhesus macaques, a single immunization with 50 μg ZIKV prM-E mRNA-LNPs induced RVP NAb titers that were 50 times higher than those induced by one immunization of 1 mg DNA vaccine and over 2 times higher than those induced by two immunizations of DNA [298], as measured by the same assay in the same laboratory. ZIKV mRNA-LNP NAb titers may overlap with those elicited by one injection of PIV or RhAd52 ZIKV vaccines in macaques, although differing assay formats prevent a precise comparison. The FRNT NAb titers elicited by ZIKV mRNA-

LNP in macaques were maintained at a stable level until 12 weeks post-immunization, suggesting that protection may be durable.

Although Tfh and GC B cells were not measured in ZIKV-immunized animals, the data obtained with influenza HA and the potency of the anti-ZIKV NAbs both imply that Tfh and GC B cells were robustly induced by the ZIKV prM-E vaccine in mice and macaques. The influenza data also suggest that nucleoside modification was likely an important contributor to the ability of this vaccine to generate potent and durable NAbs with only a single immunization. Future studies will quantify the Tfh and GC B cell responses in mice and macaques immunized with ZIKV mRNA-LNPs and determine whether nucleoside modification and/or purification of the mRNA were required for potent NAb responses.

In other future directions, the nucleoside-modified ZIKV mRNA-LNP will be investigated in multiple models of fetal infection to test the applicability of this vaccine in preventing birth defects, including microcephaly. In one line of investigation, immune competent female CD-1 mice will be immunized normally with the ZIKV mRNA-LNP vaccine, and 1-2 weeks later will be bred. When pregnant, the mice will be challenged with live ZIKV by an intrauterine inoculation at embryonic day 10, as described previously [287]. This is performed by making a small incision in the abdomen and directly injecting the virus into the myometrium. This infection method has been shown to generate a high level of viral replication in fetal tissues including the placenta and brain, leading to thinning of the cerebral cortex and in some cases fetal death. This is a useful model for vaccine protection from fetal protection, as the immune system of the mother is still intact to allow a full vaccine response. Concurrently, we will pursue another line of investigation in immunocompromised *Ifnar1-/-* mice [284]. Although the immune response in these

mice may be perturbed, they are highly susceptible to infection in both adult mice and in the fetus following physiologic, subcutaneous inoculation. This model may also be combined with a passive transfer of serum from immune competent, vaccinated mice. Together these studies will reveal whether the level of immunity provided by the ZIKV mRNA-LNP is sufficient to protect a fetus from pathogenic ZIKV infection. Additional future studies will investigate the impact of a vaccine boost on NAb titers and fetal protection, and the consequences of ZIKV mRNA-LNP immunization for infection with heterologous flaviviruses, a subject discussed further in Chapter 5.

4.5. METHODS

Ethics statement

Animals: The investigators faithfully adhered to the "Guide for the Care and Use of Laboratory Animals" by the Committee on Care of Laboratory Animal Resources Commission on Life Sciences, National Research Council. Mouse studies were conducted under protocols approved by the University of Pennsylvania (UPenn) IACUCs. Rhesus macaques (*Macaca mulatta*) were housed at BIOQUAL Inc. (Rockville, MD). Macaque experiments were reviewed and approved by BIOQUAL and UPenn Animal Care and Use Committees. All animals were housed and cared for according to local, state and federal policies in an Association for Assessment and Accreditation of Laboratory Animal Care International (AAALAC)-accredited facility.

Human cells: Research involving human cells complied with the Declaration of Helsinki. De-identified leukapheresis cells were obtained from the UPenn Immunology Core under their Institutional Review Board (IRB) approved protocol, and were deemed exempt by the UPenn IRB.

Antibody reagents

The pan-flavivirus murine monoclonal antibody 4G2, clone D1-4G2-4-15 (EMD Millipore MAB10216) was used to detect ZIKV E protein by Western blot. The following antibodies were used for flow cytometry: anti-CD4 PerCP/Cy5.5 (Clone GK1.5, Biolegend), anti-CD3 APC-Cy7 (Clone 145-2C11, BD Biosciences), anti-CD27 PE (Clone LG.3A10, BD Biosciences), anti-TNF-α PE-Cy7 (Clone MP6-XT22, BD Biosciences), anti-IFN-γ AF700 (Clone XMG1.2, BD Biosciences), anti-IL-2 APC (Clone JES6-5H4, BD Biosciences), anti-Bcl6 PE (Clone K112-91, BD Biosciences),

anti-CXCR5 BV605 (Clone L138D7, Biolegend), anti-CXCR5 PE-Cy7 (Streptavidin, BD Biosciences), anti-PD-1 BV785 (Clone 29F.1A12, Biolegend), anti-PD-1 BV421 (Clone EH12.2H7, Biolegend). LIVE/DEAD Fixable Aqua Dead Cell Stain Kit (Life Technologies) was used to discriminate dead cells and debris. The following antibodies were used for ELISA assays: goat anti-mouse IgG HRP (Sigma 4416), goat anti-monkey IgG HRP (Sigma 2054), and ZIKV E protein-binding mAb NR-4747 clone E19 (BEI Resources). ZIKV-neutralizing human monoclonal antibody Ab3594 was provided by the Duke University, Duke-NUS Graduate Medical School, National University of Singapore team of Charles McGee, Gregory D. Sempowski, Robert Parks, Eng Eong Ooi, Barton F. Haynes, M. Anthony Moody, Shee-Mei Lok, and Hua-Xin Liao.

Protein reagents

Purified recombinant ZIKV E protein (Aalto Bioreagents AZ 6312) was used in ELISAs to detect E protein-specific IgG, in Western blots as a positive control and in mouse splenocyte stimulation.

mRNA production

mRNA was produced as previously described [506] using T7 RNA polymerase on linearized plasmid (pTEV-ZIKVprM-E-A101) encoding codon-optimized [507] ZIKV strain H/PF/2013 (Asian lineage, French Polynesia, 2013, GenBank: KJ776791) prM-E glycoproteins. mRNA was transcribed to contain 101 nucleotide-long poly(A) tails. 1-methylpseudouridine-5'-triphosphate (TriLink) instead of UTP was used to generate modified nucleoside-containing mRNA. mRNA was capped using the m7G capping kit with 2'-*O*-methyltransferase to obtain cap1 and

was purified by a fast protein liquid chromatography (FPLC) method, as described [322]. mRNA was analyzed by agarose gel electrophoresis and stored frozen at -20°C.

Cell culture

Human embryonic kidney (HEK) 293T cells (ATCC) were cultured in Dulbecco's modified Eagle's medium (DMEM) supplemented with 2 mM L–glutamine (Life Technologies) and 10% fetal calf serum (FCS) (HyClone) (complete medium). The 293T cell line was tested for mycoplasma contamination after receipt from ATCC and before expansion and cryopreservation. Human dendritic cells (huDCs) were generated from monocytes, as described [318], and grown in RPMI 1640 medium containing 2 mM L–glutamine (Life Technologies) and 10% fetal calf serum (FCS) (HyClone) (complete medium) supplemented with 50 µg/ml recombinant human GM-CSF and 100 µg/ml recombinant human IL-4 (R&D systems). Cells were maintained by adding fresh medium containing IL-4 and GM-CSF every 3 days and used on day 7. Murine dendritic cells (muDCs) were generated from bone marrow cells obtained from the femurs of animals and grown in complete medium supplemented with 50 µg/ml murine GM-CSF (R&D systems). Cells were maintained by adding fresh medium containing murine GM-CSF every 3 days and used on day 7.

mRNA transfection

Transfection of human and murine DCs and HEK 293T cells was performed with TransIT-mRNA (Mirus Bio) according to the manufacturer instructions: mRNA (0.3 µg) was combined with TransIT-mRNA Reagent (0.34 µl) and Boost Reagent

(0.22 µl) in 17 µl of serum free medium, and the complex was added to 2×10^5 cells in 183 µl complete medium. Supernatant was collected and cells were lysed for 1 hr on ice in RIPA buffer (Sigma) at 18 hr post-transfection.

Western blot analysis of E protein expression

Whole cell lysates and supernatants from ZIKV prM-E transfected cells were assayed for ZIKV E protein by non-denaturing SDS-PAGE Western blot. Samples were combined with 4x Laemmli buffer (Bio-Rad) and separated on a 4-15% precast polyacrylamide Criterion TGX gel (Bio-Rad) for 45 min at 200 V. Transfer to PVDF membrane was performed using a semi-dry apparatus (Ellard Instrumentation, Ltd.) at 10 V for 1 hr. The membrane was blocked with 5% non-fat dry milk in TBS buffer containing 0.5% Tween-20. E protein was detected using 1:10,000 4G2 ascites for 1 hr, followed by secondary goat anti-mouse IgG HRP 1:10,000 for 1 hr. Antibody incubations were performed at room temperature in blocking buffer. Blots were developed using Luminata Forte substrate (Millipore) and a Kodak X-OMAT 1000A processor.

Characterization of E protein in supernatant

Supernatant from HEK 293T cells transfected with ZIKV prM-E mRNA was tested for whether E protein could be pelleted and disrupted with detergent, consistent with subviral particles. Supernatant was incubated in PBS alone or PBS with 0.5% Triton X-100 for 1 hr on ice. Samples were then spun at 42,000 rpm for 2.5 hr in a Beckman TLA-55 rotor. The supernatant was then removed from the pellet, which was resuspended in 50 µl of PBS. Equal volumes of the input, pellet,

and post-centrifugation supernatant fractions were then analyzed by Western blot, as described above.

Lipid nanoparticle (LNP) formulation of the mRNA

FPLC-purified mRNAs and polycytidylic acid (poly(C) RNA) (Sigma) were encapsulated in LNPs using a self-assembly process in which an aqueous solution of mRNA at pH 4.0 is rapidly mixed with a solution of lipids dissolved in ethanol [508]. LNPs used in this study were similar in composition to those described previously [508,509], which an contain ionizable cationic lipid (proprietary to Acuitas), phosphatidylcholine, cholesterol, and PEG-lipid (50:10:38.5:1.5 mol/mol) and were encapsulated at an RNA to total lipid ratio of ~0.05 (wt/wt). They had a diameter of ~80 nm as measured by dynamic light scattering using a Zetasizer Nano ZS instrument (Malvern Instruments Ltd, Malvern, UK). RNA-LNP formulations were stored at -80°C at a concentration of RNA of ~1 µg/µl.

Administration of LNPs to mice and rhesus monkeys

Mice: Female BALB/c and C57BL/6 mice aged 8 weeks were purchased from Charles River Laboratories. mRNA-LNPs were diluted in PBS and injected into animals intradermally with a 3/10cc 29½G insulin syringe (BD Biosciences). Four sites of injection (30 µl each) over the lower back were used.

Monkeys: Ketamine anesthetized animals were shaved on their back and injected with mRNA-LNPs diluted in PBS. Ten sites of injection (60 µl each) were used. Animals of similar age and weight were randomly designated to dose groups.

Blood collection from mice and rhesus macaques

Mice: Blood was collected from the orbital sinus under isoflurane anesthesia. Blood was centrifuged for 10 min at 13,000 rpm and the serum was stored at -20°C and used for ELISA and virus neutralization assays. EDTA-plasma was collected to isolate RNA for qRT-PCR analysis.

Monkeys: Blood was collected by femoral venipuncture under ketamine anesthesia, and serum and EDTA-plasma were collected and stored at -80°C for ELISA, neutralization analysis, and to isolate RNA for qRT-PCR.

Stimulation and staining of splenocytes

Single cell suspensions from spleens were made in complete medium. For T cell analysis, splenocytes were washed once in PBS and resuspended in complete medium at 2×10^7 cells/ml. 2×10^6 cells (100 µl) per sample were stimulated for 6 hr at 37°C using 2 µg/ml of purified recombinant ZIKV E protein or two pools of influenza A/Puerto Rico/8/34 HA peptides (BEI NR-18973). Golgi Plug (brefeldin A, BD Biosciences) and Golgi Stop (monensin, BD Biosciences) were diluted 1:100 and 1:143 in complete medium, respectively, and 20 µl from both diluted reagents were added to each sample to inhibit the secretion of intracellular cytokines after 1 h. An unstimulated sample for each animal was included. PMA (10 ng/ml)-ionomycin (250 ng/ml) (Sigma) stimulated samples were used as positive controls.

After stimulation, cells were washed in PBS and stained using the LIVE/DEAD Fixable Aqua Dead Cell Stain Kit (Life Technologies) and then surface stained for CD4 and CD27, or, in the Tfh analysis, CD4, CXCR5, and PD-1. Antibodies were incubated with cells for 30 min at RT. Following surface staining, cells were washed in FACS buffer and fixed using the Cytofix/Cytoperm kit (BD Biosciences) according to the manufacturer`s instructions. Following fixation, the

cells were washed in the appropriate perm buffer and incubated with antibodies against CD3, TNF-α, IFN-γ, IL-2, and Bcl6 (Tfh stain only) for 1 hr at RT. Following staining, the cells were washed with the appropriate perm buffer, fixed (PBS containing 1% paraformaldehyde) and stored at 4°C until analysis.

For B cell subsets, enumeration of splenocytes prior to RBC-lysis was performed using a Vi-Cell (BD). After RBC-lysis (Lonza) for 30 sec, cells were stained with Zombie L/D Aqua (BioLegend) according to manufacturer's instructions, and stained for IgD, CD4, CD8, Gr-1, F4/80, B220, CD138, CD19, IgM, CD38 and PNA for 30 min in PBS with 0.5% BSA. Cells were filtered and subjected to flow analysis immediately. GC B cells were determined by gating for IgD^-, $DUMP^-$ ($CD4^-$, $CD8^-$, $Gr\text{-}1^-$, $F4/80^-$), $B220^+$, $CD138^-$, $CD19^+$, IgM^-, $CD38^-$, PNA^+ cells. Memory B cells were determined by gating for IgD^-, $DUMP^-$, $B220^+$, $CD138^-$, $CD19^+$, IgM^-, $CD38^+$, PNA^- cells. Plasma cells were determined by gating for IgD^-, $DUMP^-$, $CD138^+$ cells. Specific population counts were determined by multiplying percentage of live cells according to FACS with total live cell counts.

Flow cytometry

Splenocytes were analyzed on a modified LSR II flow cytometer (BD Biosciences). One hundred thousand events were collected per specimen. After the gates for each function were created, the Boolean gate platform was used to create the full array of possible combinations, equating to seven response patterns when testing three functions. Data were expressed by subtracting the percentages from the unstimulated stained cells from the E protein stimulated stained cells.

Enzyme-linked immunosorbent assays (ELISA) for ZIKV E-specific IgG

Immulon 4HXB ELISA plates were coated with 6 µg/ml purified recombinant ZIKV E protein in 0.1 M sodium bicarbonate buffer overnight at 4°C. The plate was blocked with 2% BSA in PBS for 1 hr, and washed three times with wash buffer (PBS with 0.05% Tween-20). Mouse or rhesus macaque sera were diluted in blocking buffer and incubated on the plate for 1 hr at room temperature, followed by four washes. Secondary antibody HRP conjugate was diluted 1:10,000 in blocking buffer and incubated on the plate for 1 hr, followed by four washes. TMB substrate (KPL) was applied to the plate and the reaction was stopped with 2 N sulfuric acid. The absorbance was measured at 450 nm using an MRX Revelation microplate reader. ZIKV E-specific IgG was expressed in two ways: as an endpoint dilution titer, defined as the highest reciprocal dilution of serum to give an OD greater than the sum of the background OD plus 0.01 units; and as an estimate of the absolute IgG concentration, which was based on the murine mAb NR-4747 as a standard (applicable only to mouse samples). All samples were run at least in technical duplicates.

ZIKV MR-766 plaque reduction neutralization tests (PRNT)

ZIKV strain MR-766 (African lineage, Uganda, 1947, GenBank: AY632535) (UTMB Arbovirus Reference Collection) was produced in Vero cells (ATCC CCL-81) and 50 plaque forming units were incubated with increasing dilutions of heat-inactivated sera in serum-free DMEM (Corning) medium for 1 hr at 37°C. The virus/serum mixture (200 µl) was added to a confluent monolayer of Vero cells in 6-well format and incubated for 1.5 hr at 37°C with intermittent rocking. Then, 3 ml of overlay, containing a final concentration of 0.5% methylcellulose (4,000 centipoise) (Sigma), 1X DMEM (Gibco), 16 mM HEPES, 0.56% sodium bicarbonate, 1.6X

GlutaMAX (Gibco), 1X penicillin/streptomycin (Corning), and 4 µg/ml amphotericin B (Gibco), was added to each well, and plates were incubated for 5 days at 37°C in 5% CO_2. The overlay was aspirated and cells were fixed and stained with 0.5% crystal violet (Sigma) in 25% methanol, 75% deionized water. Wells were rinsed with deionized water to visualize plaques. Neutralization titers (EC_{50}) were determined by plotting a line through the linear portion of the curve that crossed 50% inhibition and calculating the reciprocal dilution of sera required for 50% neutralization of infection. EC_{50} titers below the limit of detection are reported as half of the limit of detection.

ZIKV MEX I-44 focus reduction neutralization tests (FRNT)

ZIKV MEX I-44 (Asian lineage, Mexico, 2016, GenBank: KX856011) stocks were generated via propagation in Vero 76 cells (ATCC CRL-1587) and harvested as clarified cell culture lysate/supernatant. Stock titers were quantified via standard focus forming assay. FRNT was performed by combining a standard dose of ZIKV with two-fold serial dilutions of heat-inactivated serum for one hour at 37˚C. Virus-serum mixtures (100 µl) were then inoculated onto Vero 76 monolayers, incubated at 37˚C for 1 hr and overlayed with an Avicel (FMC Biopolymer)-containing growth medium. After 3 days of incubation, plates were formalin-fixed, permeabilized, blocked, and stained via sequential incubation with biotin-conjugated 4G2 mAb (ATCC HB-112), streptavidin-HRP (BD Biosciences) and TrueBlue Peroxidase Substrate (KPL). Virus input was verified in parallel (acceptable range: 20-60 foci). $FRNT_{50}$ (EC_{50} titers) are reported as the highest reciprocal dilution giving a focus count ≤ the 50% neutralization cutoff, and the geometric mean was computed for technical duplicates.

Reporter virus particle (RVP) production

Pseudo-infectious RVPs were produced by complementation of a GFP-expressing WNV sub-genomic replicon [291,510] with a plasmid encoding the viral structural proteins (capsid-prM-E). Briefly, ZIKV MR-766 and ZIKV H/PF/2013 RVPs were produced via co-transfection of HEK-293T cells with the structural gene and replicon plasmids (3:1 ratio by mass) using Lipofectamine 3000 per the manufacturer's protocol (Invitrogen). Transfected cells were incubated at 30°C and RVP-containing supernatants harvested on days 3-6. Stocks were passed through a 0.2 μm filter and aliquots stored at -80°C until use. Stock titers were determined by infecting Raji-DCSIGNR cells with serial dilutions of filtered RVP supernatants. GFP-positive cells were assessed by flow cytometry at 48 hr post-infection and RVP titers calculated.

RVP neutralization assay

Previously titered RVPs were diluted to ensure antibody excess at informative points on the dose-response curves and incubated with serial dilutions of mouse or macaque sera for 1 hr at 37°C to allow for steady-state binding. Raji-DCSIGNR cells were then infected with antibody-RVP complexes in duplicate technical replicates. Infections were carried out at 37°C and GFP-positive infected cells detected by flow cytometry 24-48 hr later. Neutralization results were analyzed by non-linear regression to estimate the reciprocal dilution of sera required for half-maximal neutralization of infection (EC_{50} titer) (Prism 6, GraphPad). The initial dilution of sera (based on the final volume of RVPs, cells, and sera) was set as the limit of confidence of the assay. Titers for which non-linear regression was predicted to be

below this threshold were reported as a titer half the limit of confidence. Individual EC_{50} titers are reported as the geometric mean of technical replicates.

Preparation of challenge ZIKV virus

Mice: Challenge ZIKV strain PRVABC59 (Asian lineage, Puerto Rico, 2015, GenBank: KU501215) (BEI Resources NR-50240) was grown in Vero CCL81 cells. A T175 flask of cells at 75-90% confluency was inoculated with an MOI of 0.01 ZIKV in 10 ml of serum-free DMEM medium. The flask was incubated at 37°C, 5% CO_2 for 1.5 hr with intermittent gentle rocking, then warmed media was added to a final concentration of 1.5% FBS, 1X GlutaMAX (Gibco) and 1X penicillin/streptomycin (Corning) in a final volume of 25 ml. The flask was incubated for 4 days or until cytopathic effects were visible. Then supernatant was collected and ultra-centrifuged at 20,000 rpm for 1 hr at 4°C in a Sorvall SureSpin 630 rotor. The supernatant was removed and the pellet was resuspended in 1 ml of serum-free DMEM, aliquoted, and stored at -80°C. Before challenge, virus was thawed and diluted in PBS to 2,000 PFU/ml.

Monkeys: Challenge ZIKV strain PRVABC59 was grown in Vero 76 CRL-1587 cells. T150 flasks of cells at 80-85% confluency were used for propagation. Infection was performed with 100 µl stock virus diluted in 4 ml of fresh L-15 media (Gibco) supplemented with 10% fetal bovine serum (Gibco), 10% tryptose phosphate broth (Sigma Aldrich), 1X penicillin/streptomycin (Gibco) and L-glutamine (Gibco) and adsorbed for 1 hr at room temperature with gentle agitation every 15 min. Each flask received 7 ml of fresh L-15 media after adsorption and was incubated for 4 days at 37°C. Cellular debris was removed by centrifugation at 1,200 rpm for 5 min

at 4°C in an Eppendorf A-4-62 rotor. Virus stocks were aliquoted and stored at -80°C.

Zika virus challenge in mice and rhesus macaques

Mice: Two or 20 weeks after vaccination, mice were bled and then challenged intravenously with 200 PFU of ZIKV-PR (PRVABC59) in 100 µl of PBS. Blood was collected 3 and 7 days post-challenge to determine viral loads (ZIKV RNA copies/ml) in plasma.

Monkeys: Macaques were anesthetized with ketamine and injected subcutaneously in the hind thigh with 10^4 $TCID_{50}$ of ZIKV-PR in a volume of 1 ml in PBS. Blood was collected 1, 3, 5, and 7 days post-challenge to determine viral loads (ZIKV RNA copies/ml) in plasma.

Viral load quantification (qRT-PCR)

Using blinded samples, RNA was isolated from 200 µl (macaque) or 50 µl (mouse) plasma using the QIAamp MinElute Virus spin kit (Qiagen). Extracted RNA was used for amplification using the SensiFAST Probe Lo-ROX One-Step Kit (Bioline BIO-78005) on a 7500 Real-Time PCR system (Applied Biosystems). Primers and probe were designed to amplify a conserved region of the capsid gene from ZIKV BeH815744, as follows:

Fwd: 5'GGAAAAAAGAGGCTATGGAAATAATAAAG;

Rev: 5'CTCCTTCCTAGCATTGATTATTCTCA;

probe: 5'AGTTCAAGAAAGATCTGGCTG.

Primers and probe were used at a final concentration of 2 µM, and the following program was run: 48°C for 30 min, 95°C for 10 min, followed by 40 cycles of 95°C for

15 sec and 1 min at 60°C. Assay sensitivity was 50 copies/ml for macaque and 200 copies/ml for mouse samples.

Statistical analysis

GraphPad Prism 5.0f was used to perform Mann-Whitney and Kruskal-Wallis (with Dunn's correction) tests to compare immune responses in vaccinated and control mice and in different dose groups of macaques, respectively. SPICE 5.35 and Microsoft Excel software was used to perform Student's *t* tests to compare T cell responses in vaccinated and control mice.

4.6. SUPPLEMENTARY DATA

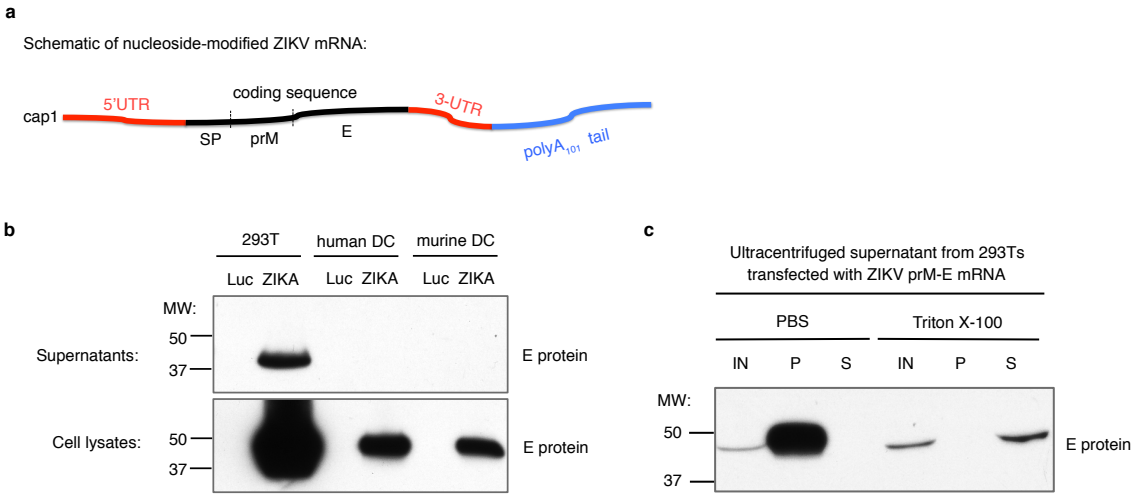

Supp. Fig. S4.1. Design and characterization of ZIKV prM-E mRNA. (a) The ZIKV mRNA encodes the signal peptide (SP) from MHC class II and prM and E glycoproteins from ZIKV H/PF/2013. (**b**) mRNA was transfected into 293T cells (n=3), human DC (n=3), or murine DC (n=2). E protein expression in cell lysate and supernatant was probed by Western blot, using firefly luciferase-encoding mRNA-transfected cells as a negative control. (**c**) ZIKV mRNA supernatant from transfected 293T cells was characterized by ultracentrifugation in the presence and absence of 0.5% Triton X-100, followed by Western blot of input (IN), pellet (P), and final supernatant (S) fractions (n=3).

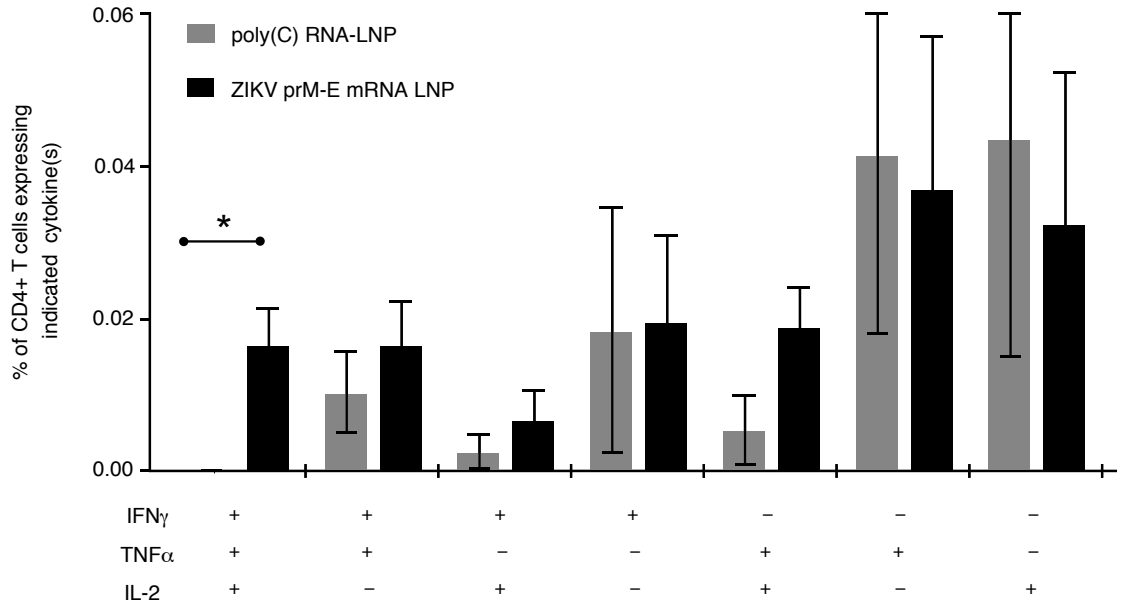

Supp. Fig. S4.2. Nucleoside-modified ZIKV mRNA-LNP immunization elicits polyfunctional ZIKV E-specific CD4$^+$ T cell responses. C57BL/6 mice were immunized with 30 µg of nucleoside-modified ZIKV prM-E mRNA-LNPs (n=8) or control poly(C) RNA-LNPs (n=4). At week 2, antigen-specific CD4$^+$ T cells were detected by intracellular cytokine staining. Bar graph shows mean frequencies of combinations of cytokines produced by CD4$^+$ T cells. Error bars indicate the SEM, and asterisk indicates a significant difference ($p<0.05$) by Student's *t*-test.

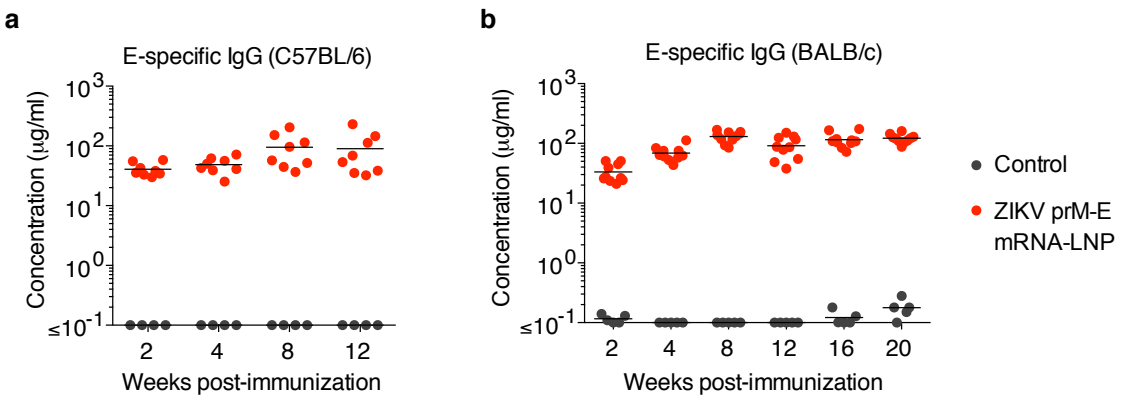

Supp. Fig. S4.3. ZIKV E-specific IgG concentration in mice. Sera from **(a)** C57BL/6 mice (n=4 control; n=8 ZIKV mRNA-LNP) or **(b)** BALB/c mice (n=5 control; n=10 ZIKV mRNA-LNP) were assayed by ELISA, and estimates of ZIKV E-specific IgG concentrations were calculated using murine mAb NR-4747 as a standard. Points represent individual mice; horizontal lines indicate the mean. Responses in vaccine and control groups were compared at each time point by Mann-Whitney test: $p<0.01$ for all comparisons.

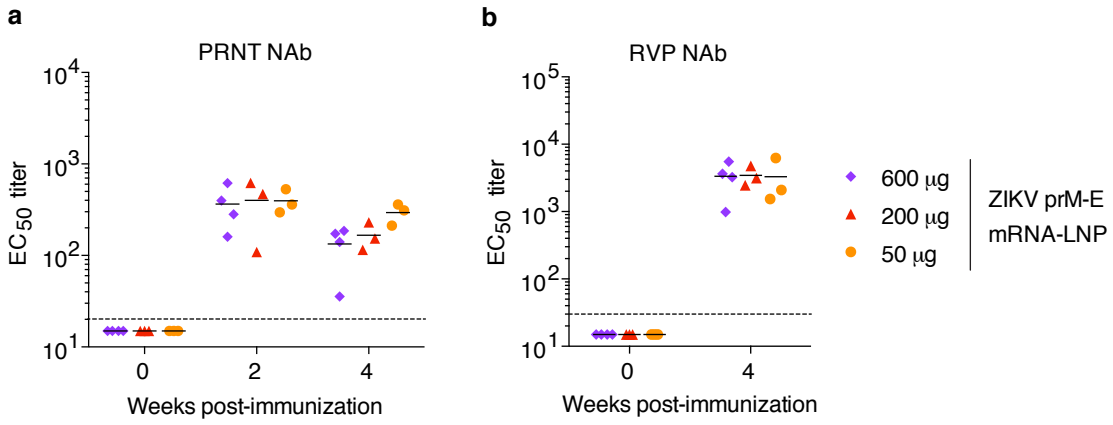

Supp. Fig. S4.4. Neutralizing antibody responses against ZIKV MR-766 in macaques immunized with ZIKV prM-E mRNA-LNPs. Sera from immunized macaques were evaluated for neutralization of ZIKV MR-766 using (a) the PRNT assay or (b) the RVP assay at the indicated time points. Horizontal bars indicate the mean, and values below the dotted line are below the limit of detection. Immune responses in dose groups were compared by Kruskal-Wallis test: $p>0.05$ for all comparisons.

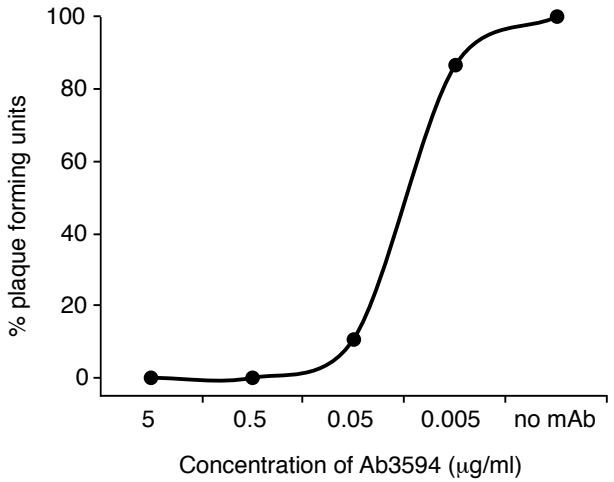

Supp. Fig. S4.5. Neutralization curve for a human anti-ZIKV neutralizing mAb. ZIKV MR-766 was neutralized by Ab3594, a human ZIKV-neutralizing monoclonal antibody, as a positive control in the PRNT assay. Shown is a representative curve (n=4). Mean EC_{50} = 0.026 μg/ml, SD=5.4.

Immunization	Group	ID	Weight (kg)	Sex	DOB
ZIKV prM-E mRNA-LNP, 600 μg	1	6858	3.3	M	5/19/14
		150250	3.05	F	3/22/15
		150793	2.55	M	4/1/15
		150796 *	2.75	F	4/13/15
ZIKV prM-E mRNA-LNP, 200 μg	2	150251	2.95	M	3/22/15
		150795	2.55	M	4/12/15
		150798 *	2.35	F	4/26/15
ZIKV prM-E mRNA-LNP, 50 μg	3	6857 *	3.15	F	6/6/14
		150252 *	2.15	F	3/25/15
		150794 *	2.75	M	4/5/15
Challenge control group (unimmunized)	4	6143 *	7.85	F	7/3/09
		6154 *	8.95	F	4/6/10
		6076 *	7.6	M	10/20/11
		6150 *	11.55	M	1/26/10
		6211 *	8.65	M	5/2/10
		6157 *	10.15	F	4/3/10

Supp. Table S4.1. Characteristics of rhesus macaques in vaccination and challenge experiments. Asterisk indicates the animals that were challenged with ZIKV.

4.7. ACKNOWLEDGMENTS

Special thanks to Norbert Pardi, the co-lead author of this work who generated the mRNA and performed mouse immunizations. We thank Elinor Willis, Scott Hensley, and Susan Weiss for providing valuable ZIKV-related reagents and technical expertise, and Barton Haynes and the team at Duke University for providing access to rhesus macaques, without which this work would not have been possible. We also thank Rebecca Pelc and the lab of Ted Pierson for performing RVP NAb assays, and Robert Tesh at the UTMB World Reference Center for Emerging Viruses and Arboviruses for providing ZIKV stocks. We gratefully acknowledge the technical or administrative support of M. Bertrand, L. Arwood, C. Sample, M. J. Barr, C. Vivian, T. Gurley and M. A. Moody, E. E. Ooi, S. Lok, H.-X. Liao, Sita Awasthi, Lauren Hook, Farida Shaheen, and the UPenn CFAR. The Virology Unit of the Duke Regional Biocontainment Laboratory (Duke Human Vaccine Institute) received support from the NIH, UC6-AI058607. The Duke Center for HIV/AIDS Vaccine Immunology received support from NIH AI100645. D.V. received funding from the Department of Diagnostic Medicine and Pathobiology, College of Veterinary Medicine, Kansas State University. R.S.P., C.R.D., K.A.D., T.C.P. and B.S.G. were funded by the NIAID Division of Intramural Research and the Vaccine Research Center. S.E.H. received funding through NIH U19-AI057229. M. Hogan received funding from NIH T32 AI007632-14. D.W. received funding from NIH R01-AI050484, R01-AI124429 and R01-AI084860, and Takeda Pharmaceuticals, New Frontier Science.

CHAPTER 5

CONCLUSIONS AND FUTURE DIRECTIONS

5.1. Overview

Modern vaccinology faces two principal challenges: (i) how to design effective vaccines against pathogens that have evolved to successfully evade the adaptive immune system, and (ii) how to produce safe and effective vaccines on a timescale appropriate to respond to emerging epidemics. In this dissertation, and with the help of many colleagues, I have addressed the first question in the context of HIV-1, a virus that is adept at avoiding humoral immune responses; and I have addressed the second question by using the newly developed nucleoside-modified mRNA-LNP platform to design a potent, single-dose vaccine against ZIKV.

Chapter 2 of this dissertation detailed structural perturbations resulting from CD4 independence and how these changes related to immunogenicity in mice and rhesus macaques. To our knowledge, this is the first description of enhanced antigenicity and immunogenicity of the V2 peptide epitope in CD4-independent Envs, or possibly any Env mutant specifically in the context of a functional, cell-associated trimer. The immunogens described here, particularly the D4T Env, have the potential to be useful in vaccines designed to elicit non-neutralizing antibodies against HIV-1 that mediate ADCC against infected cells.

Chapter 3 addressed the impact of cytoplasmic tail (CT) mutations that increased the expression of HIV-1 Env immunogens on the cell surface in a recombinant vaccinia vector immunization with gp120 boost. Although many groups have truncated most or all of the CT to increase surface expression, few have

directly compared these immunogens to the wild-type version or have sought to optimize surface expression through targeted manipulations of trafficking signals within the functionally complex CT. Our data suggest that increasing surface expression of Env leads to an incremental improvement in the antibody response, and, importantly, that the immune response generated by the priming immunogen has an outsize impact on the antibody response after subsequent protein boosts.

Chapter 4 presents the design and preclinical efficacy of a ZIKV vaccine using prM-E-encoding mRNA containing the modified nucleoside 1-methylpseudo-uridine (m1Ψ), purified by FPLC, and delivered in lipid nanoparticles (LNPs). We show that mice immunized with the ZIKV mRNA-LNP vaccine generated extremely high NAb titers after a single immunization—an exceptional level of immunogenicity for a non-replicating vector, which is likely driven by a strong Tfh response. Immune-competent mice were completely protected from short- and long-term challenges with a ZIKV strain from Puerto Rico. Rhesus macaques immunized with various doses of the vaccine also showed high and sustained levels of NAbs after a single vaccination and experienced a 99-100% reduction in viremia when challenged, compared to control animals. Importantly, as little as 50 μg of mRNA (0.02 mg/kg body weight) was sufficient for protection in this primate species, suggesting that mRNA-based vaccines may be well suited for urgent mass vaccination campaigns.

The following is a discussion of some of the broader implications and important future directions of the work presented above.

5.2. Towards Structure-Guided Vaccine Design with CD4-independent Envs

Many of the immediate future directions of the CD4-independent Env study are already ongoing, as outlined in Section 2.4. Most important will be the

characterization of V2 peptide exposure on trimeric forms of CD4-independent Envs and extension of this analysis to include additional human mAbs against the V2 peptide. Additionally, it will be interesting to map the exact specificities that are responsible for the enhanced ADCC activity in D4T-primed macaques at time points prior to the boosts. This could be achieved by blocking ADCC activity in macaque serum using available mAbs, or, more comprehensively, by isolating mAbs from immunized macaques. This would permit mutational studies that would reveal the specific residues important for recognition by ADCC-mediating antibodies, and may suggest ways to further boost this response.

While the data presented here raise the hypothesis that CD4-independent Envs elicit antibody specificities and functions that could provide protection in a vaccine, effective utilization of this approach will likely require further investigation into the relationship between biological phenotype, structure, and immunogenicity. Several important questions regarding this relationship remain unanswered, namely: (i) What is the nature of the V2 peptide exposure on CD4-independent Envs? (ii) Given the disparate V2-specific responses to A2 and D4T in macaques, do these Envs display the V2 loop with distinct secondary structures, spatial orientations, and/or levels of steric occlusion? (iii) Are the levels of trimer openness or the exposure of key epitopes in V2, V3, and C1 different on these versus other CD4-independent Envs [373–376] that are more globally sensitive to antibody-mediated neutralization? These questions and others will be best addressed in the future using techniques that allow atomic-level resolution of the epitopes of interest. X-ray crystallography and cryo-EM structures of CD4-independent Env trimers and/or gp120 monomers will provide the clearest information about the exposure, orientation, and secondary structure of critical epitopes. Crystal structures of

antibody-Env complexes have previously shown that the angle of antibody approach was associated with its ADCC potency [511]. Likewise, these structural methods may provide useful information about the specific modes of recognition of CD4-independent Envs by antiviral antibodies. Such high-resolution structural data would allow for the same kind of structure-guided rational vaccine design used to optimize the prefusion RSV [41] and HIV-1 Env SOSIP [512] immunogens. For example, if atomic-resolution structures of CD4-independent Envs reveal an exposed V2 peptide, it might be possible to predict mutations, such as hydrophobic cavity-filling amino acids, that could further stabilize its exposure or alter its angle of display. This approach could elevate HIV-1 vaccine efforts focusing on non-neutralizing antibodies from a predominantly empirical pursuit to a more rational and efficient process. Indeed, this method is relevant not only to CD4-independent Envs but to any Env immunogens designed to elicit a particular antibody specificity.

To complement these high-resolution studies, traditional structure/function analysis should be performed on A2 and D4T to determine which residues are required for CD4-independent replication and which are required for V2 antigenicity and immunogenicity. It has previously been shown that CD4 independence is dissociable from global neutralization sensitivity [373], and it is likely that it is also dissociable from V2 peptide antigenicity. CD4-independent variants have been derived from a number of other HIV-1 Envs in our lab (e.g. clade B JRFL and YU2, clade A QA255 and BG505, and clade C 1086.C and CH505), and in some cases only a few mutations were required for CD4-independent growth. Due to their simplicity relative to the heavily mutated A2 and D4T, these other Envs may serve as a useful system in which to probe the relationship between specific residue changes, CD4 independence, and antigenicity or immunogenicity. Compared to vaccinia, the

mRNA vaccine platform would be an expedient method to test the immunogenicity of multiple Env mutants in parallel, and would likely also enhance the affinity and quality of the V2-specific antibody response.

An alternative application for CD4-independent HIV-1 Envs is to use them to elucidate mechanisms of pathogenesis and correlates of immune protection or elite control. Data from our laboratory indicate that a CD4-independent, non-CD4-tropic variant of SIVmac239, called iMac239ΔD385, replicates well in rhesus macaques but is effectively controlled by the adaptive immune response [513], likely due in large part to its high neutralization sensitivity [373]. This virus shows a distinct pattern of infection in lymph nodes and favors cells in the medulla rather than the cortex or B cell follicles, suggesting that Tfh cells are not specifically targeted. Remarkably, the animals infected with this virus developed robust germinal center reactions compared to animals infected with pathogenic SIVmac239 (Constantinos Petrovas, personal communication). When iMac239ΔD385-infected animals were challenged with heterologous, pathogenic SIVsmE660, they showed delayed acquisition of infection and over the course of several months developed antibodies that neutralized a Tier-2 stain of SIV up to 100% inhibition of infection (V_{max})—an effect that had not been previously observed in the SIV model [513]. These data generated the hypothesis that the CD4-independent infection primed animals to mount a qualitatively different humoral immune response, and provided a proof of concept that Tier-2 NAb activity can be effectively generated in settings where the germinal center reaction is promoted. Our lab has an interest in continuing this work by deriving CD4-independent and non-CD4-tropic SHIVs. In fact, the CD4-independent Envs A2 and D4T were derived in the context of SHIV 89.6 and are already well positioned for analysis *in vivo*. Several of the other CD4-independent

Envs derived in our lab, including BG505 and CH505, were also derived in a SHIV background. These two SHIVs were designed to take advantage of a recently reported strategy that allows Envs from primary and transmitted-founder strains of HIV-1 to be incorporated into SHIVs that replicate well *in vivo* [405]. This is accomplished by substitution of the Ser375 residue in Env, which abuts the CD4bs and increases HIV-1 Env affinity for rhesus macaque CD4; and by replacement of 33 amino acids from the distal CT of HIV-1 Env with 58 amino acids from the corresponding region of SIV. Introducing CD4-independent and non-CD4-tropic Envs into nonhuman primates in the form of SHIVs may provide useful information regarding the types of humoral immune responses that can prevent infection when conserved epitopes are exposed on Env and germinal centers are unimpeded by viral infection of Tfh cells.

5.3. Elucidating the Functions of the HIV-1 Env Cytoplasmic Tail

The results presented in Chapter 3 indicate that CT modifications (i.e. the TM1 mutations) that alter Env surface expression can have a marked effect on immunogenicity in a vaccinia prime-gp120 boost vaccine protocol. While the NAb activity elicited by TM1 Envs was restricted to Tier-1 strains in this experiment, we believe that the data may demonstrate a generalizable principle: that Env surface expression in the prime is critical for the overall immunogenicity of prime-boost vaccination. As a corollary, we hypothesize that alternative, more potent vaccine strategies might be improved in much the same way. For example, we found that two immunizations of mice with nucleoside-modified mRNA encoding an HIV-1 Env resulted in a low level of NAbs against a Tier-2 strain, X2278 (N. Pardi, unpublished data) [514]. It is possible that such potent immune responses could be enhanced if

the surface expression level of Env were further increased. Additionally, since Env-encoding mRNA has demonstrated the potential to generate potent NAb responses, we propose that a stabilized Env trimer, such as the SOSIP, would be an appropriate boosting reagent for this vaccine platform and may specifically drive the affinity maturation of antibody precursors that target the closed state of the Env trimer.

Another important implication of the work in Chapter 3 is that the trafficking signals in HIV-1 Env remain poorly understood. Our strategy was designed to take advantage of previous observations about CT mutations that dramatically increased Env surface expression in the SIV clone CP-MAC. However, it became clear that HIV-1 Env did not respond similarly to SIV when the CT was truncated and the membrane-proximal endocytosis motif was ablated, with a much more modest effect on surface expression, at least in human cells. The basis of this difference and how Env maintains low surface expression even in the absence of known endocytosis motifs requires further investigation. Preliminary data from our laboratory illustrate that this problem is even more pronounced in dendritic cells (DCs) than in cell lines. In DCs, Env surface expression could not be increased by the TM1 modification or even complete truncation of the CT (Δ147) when expressed by plasmid nucleofection (M. Hogan and A. Conde-Motter, unpublished data). For all Env variants tested, the level of Env detectable on the surface of unpermeabilized DCs represented a small fraction of the Env detectable in permeabilized cells, indicating that the majority of Env was intracellular at steady-state. In contrast, other proteins such as CD2 and CD20 could be highly expressed on the surface of DCs by the same nucleofection method, suggesting that the restriction of surface expression was specific to Env. When Envs were expressed in DCs by vaccinia vector, the effect of the TM1 modification was variable, but at most this resulted in only a

modest increase in surface expression (M. Hogan, A. Conde-Motter, unpublished data). Overall, these data suggest that there could be mechanisms independent of the CT that restrict HIV-1 Env surface expression, especially in DCs. Future work in this area should begin by mapping this effect to specific regions of Env, which might be accomplished in part by constructing HIV-SIV chimeric Env proteins, beginning with the membrane-spanning domain. The cellular mechanisms of this restriction could be identified by inhibiting pathways of endocytosis and knocking out proteins known to interact with Env on the cell surface, such as entry and attachment factors, which might contribute to internalization. A more detailed understanding of Env internalization could potentially be exploited in future viral or gene-based vaccines to greatly increase surface expression on DCs and more potently activate Env-specific B cells.

A related research interest in our laboratory that may similarly inform immunogen design is the role of the CT in coordinating Env incorporation into viral particles. This aspect of HIV-1 biology also remains poorly understood after decades of research, and deciphering it may allow for the design of particulate immunogens containing dense arrays of Env protein—an optimal mode of displaying antigen in order to maximally activate B cells [515]. There are at least four proposed mechanisms of Env incorporation, which are not mutually exclusive and may vary depending on the cell type, CT length, and other factors [516]. Two related theories state that Env is actively recruited into sites of viral budding by either a (i) direct or (ii) indirect (protein intermediate) interaction between the Env CT and Gag, or specifically matrix [517–520]. The other models hold that (iii) Env is passively or randomly incorporated into particles [62], or that (iv) Env and Gag are co-targeted to sites of budding through membrane microdomain interactions or other mechanisms

of intracellular trafficking [445,521–523]. Some of the available data on direct or indirect interactions have been either refuted [518,519] or never reproduced [520]; nevertheless, this model has been repeatedly suggested by mutation complementation experiments. For example, Freed and Martin showed that certain point mutations in matrix (L12E and L30E) blocked incorporation of wild-type but not cytoplasmically truncated Env [442,444]. And investigators later showed that a 5-amino acid deletion in the amphipathic helix LLP-3 of the CT resulted in defects in Env incorporation and viral growth but was rescued by V34I or Q62R point mutations in matrix [441,443]. In addition, recent reports suggest that matrix oligomerization may be important for Env incorporation into virions, possibly by promoting multivalent interactions with the Env CT [524,525]. Overall, the data are suggestive that the long CT must be engaged by viral and/or cellular factors to recruit Env into assembling particles through an active process, though CT truncation may shift Env incorporation to a passive process in certain cell types.

In this complicated landscape of Env incorporation, our laboratory has made some relevant new observations. During serial passage of HIV-1, we noted the acquisition of a premature stop codon at position 810 in the Env CT, which was predicted to abrogate Env incorporation into virions, localization to detergent-resistant membranes, and replication fitness [442,523]. We discovered that this virus was able to incorporate Env and remain infectious as a result of a previously described point mutation in matrix, V35I, or V34I in the numbering used by Freed. Intriguingly, we found that matrix V35I can rescue Env incorporation to wild-type or greater levels when combined with otherwise deleterious premature stop codons in the distal CT (positions 810 or 831) but not in the middle CT (positions 773 and 793) (M. Hogan, unpublished data). Truncations in the membrane-proximal CT did not

result in Env incorporation defects in HEK 293T cells and were unaffected by matrix V35I. Surface expression was not affected by the truncation at position 810, suggesting that this phenotype is result of a specific block in Env incorporation. Taken together with the previous observations by Freed and colleagues and the view that the CT is largely composed of membrane-interactive amphipathic alpha helices, these data seem to support a model of Env and Gag co-targeting to specific membrane microdomains, such as detergent-resistant membranes or lipid rafts. If a large surface area of interaction between the CT and the lipid membrane is required for proper Env trafficking and incorporation, this could explain why multiple different deletions within the Env CT could impose similar defects in Env incorporation. Although the mechanism by which V35I rescues these CT mutants is unknown, an available crystal structure of matrix shows that the hydrophobic side chain of Val35 projects up into the lipid membrane, again suggesting that membrane interaction may be involved. Future directions for this project should determine whether V35I influences the targeting of wild-type and truncated Envs to detergent-resistant membranes or other membrane microdomains, whether it has an effect on matrix oligomerization, and whether it promotes a protein-protein interaction between matrix and the CT. This investigation is likely to shed light not only on the mechanism(s) of Env incorporation, but also on the complex functions of the CT in general, and will be informative for any vaccine design in which the CT might be manipulated to increase immunogenicity.

5.4. The Path Forward for Zika Virus mRNA Vaccines

The ZIKV vaccine described here conferred a high degree of protection in mice and nonhuman primates with a single low-dose immunization of a non-

infectious vector. These properties fulfill the specifications submitted by WHO for an ideal ZIKV vaccine [290], and therefore further tests are warranted to translate this vaccine to the clinic. To achieve this goal, several requirements must be fulfilled, including the development of Good Manufacturing Practice (GMP) production methods, toxicology studies, and resolution of intellectual property concerns.

Encouragingly for the prospects of an mRNA-based ZIKV vaccine, Moderna Therapeutics has initiated a Phase 1/2 clinical trial [526] to test the safety and immunogenicity of a similarly designed vaccine [306], reported by Richner, Diamond, and colleagues shortly after the publication described in Chapter 4 [307]. In this vaccine, the ZIKV prM-E proteins were similarly encoded by 1-methylpseudouridine-containing mRNA, which was delivered with comparable lipid nanoparticles (LNPs). The principal difference between our vaccine designs was that Richner et al. did not report any purification step to remove dsRNA contaminants from the preparation. One intramuscular injection of this vaccine generated NAb titers that were roughly 5-fold lower than the vaccine reported here using a dose that was 3-fold lower; consequently, it is difficult to ascertain whether the lower immunogenicity was due to the low dose, the presence of inhibitory dsRNA contaminants, or both. In any case, the authors administered a booster injection of the mRNA vaccine and subsequently obtained NAb titers comparable to ours. They performed a stringent challenge experiment in which mice lacking the receptors for IFN-α/β and IFN-γ were immunized and then injected subcutaneously with live ZIKV. All of the control mice died, while all mice immunized twice survived the infection. A similar result was obtained in immune-competent C57BL/6 and BALB/c mice that were infused with an IFN α/β receptor (IFNAR)-blocking antibody. In these cases, the vaccinated animals survived the challenge, and viremia was prevented in animals that were immunized

with a version of their vaccine that was optimized for high expression. No immunizations were performed in nonhuman primates.

While the data described above produced similar findings to our report, Richner and colleagues went on to describe a novel modification they made to their vaccine to address an important problem inherent to ZIKV and DENV vaccines. Epidemiological data show that infection with one of the four DENV serotypes generates type-specific (homotypic) protection from reinfection but later increases the risk of more severe of disease caused by secondary heterotypic DENV infection [527]. A related observation is that infants become predisposed to more severe DENV infections as maternal antibodies wane to sub-neutralizing levels [528]. The severe manifestations of dengue hemorrhagic fever and dengue shock syndrome are characterized by thrombocytopenia, hemorrhage, activated complement, and vascular leakage, which can lead to shock and death [529,530]. Enhanced disease is typically thought to be caused by cross-reactive, non-neutralizing antibodies that can bind to prM or E protein on the surface of DENV virions and facilitate their uptake into Fcγ receptor-expressing cells [531]. Low concentrations of such antibodies can increase infection efficiency by >100-fold in myeloid cell lines that are normally poorly permissive to infection [532]. This phenomenon has been dubbed antibody-dependent enhancement, or ADE. *In vitro* ADE activity of serum antibodies has correlated with enhanced viral replication and disease in animal models of DENV infection [533,534]. However, due to the lack of a well-validated animal model, the causes of enhanced disease in humans are not well established, and multiple alternative mechanisms have been proposed, including: (i) the ability of antibodies to engage activating versus inhibitory Fcγ-receptors (i.e. IgG1/IgG2 ratio, afucosylation of IgG1) [535], (ii) direct toxicity of the secreted viral nonstructural

protein 1 (NS1) [529], (iii) cross-reactivity of antibodies between NS1 and platelets, causing thrombocytopenia [535], and (iv) T cell-mediated effects [536,537].

It has now been shown that antibodies raised against ZIKV can mediate ADE of DENV infection, both *in vitro* [538] and in IFN-α/β/γ receptor-deficient mice [306,539]. Conversely, antibodies raised against DENV or even West Nile virus can enhance ZIKV infection *in vitro* [540] and in *Stat2-/-* mice, which are also deficient in type I IFN signaling [541]. This is not surprising given the high amount of sequence and structural homology between the E proteins of these viruses [540]. Because DENV and ZIKV are spread by the same *Aedes aegypti* mosquito and co-circulate in DENV-endemic areas, ADE is a major concern for any candidate ZIKV vaccine. It has even been speculated that ZIKV/DENV cross-reactivity has contributed to the severe outcomes of ZIKV infection observed in the Americas, particularly Brazil, although direct evidence for this is currently lacking.

It is essential that any ZIKV vaccine used in humans do not cause enhanced DENV disease, which is potentially fatal. Promisingly, there are strategies being developed to mitigate the potential for ADE in ZIKV vaccines. In their recent report [306], Richner and colleagues noted that a large portion of ADE activity could be attributed to a single epitope in the immunodominant fusion loop of the flaviviral E protein. This epitope is highly conserved across flaviviruses [542], likely due to its role in mediating fusion, and therefore it is a significant source of cross-reactive antibodies. However, because it is only exposed on the postfusion form [543], the fusion loop is a poor epitope for neutralization compared to other regions of the E protein and instead contributes significantly to ADE [544,545]. Richner and coworkers demonstrated that serum from mice immunized with wild-type ZIKV prM-E-encoding mRNA produced significant ADE of DENV-1 *in vitro* (>200-fold enhanced

infection). When the serum was passively transferred into IFN-α/β/γ receptor-deficient mice, it significantly increased the lethality of infection by DENV-2. To address this, Richner and coworkers created a version of their mRNA vaccine in which they introduced four amino acid substitutions into the ZIKV E protein fusion loop that had been shown to abrogate the binding of cross-reactive, poorly neutralizing antibodies [542,546]. Immunization with this construct decreased the potency (EC_{50}) of *in vitro* ADE by multiple logs and resulted in less morbidity and mortality in DENV-2 infection of mice. However, results were mixed, because the introduction of fusion loop mutations was also associated with ~1 log lower NAb titers to ZIKV and considerably reduced protection from ZIKV viremia during a challenge. Nonetheless, this study provides a proof of concept that mutations in cross-reactive epitopes can modulate the generation of ADE-mediating antibodies. Future work by their group and ours should identify mutations in the E protein that can reduce ADE while maintaining potent neutralization of ZIKV.

Another approach that may address the ADE issue is to vaccinate against all four DENV serotypes and ZIKV simultaneously. This is a favored approach in our laboratory, as it has the potential to solve two problems at once: mitigating ADE and providing a much needed vaccine to protect against DENV. DENV is estimated to cause tens to hundreds of millions of human infections per year and up to a half million cases of severe disease each year [547]. As a tropical disease, the people affected by DENV live disproportionately in resource-limited settings, exacerbating the health-related and economic burden. A safe and effective vaccine is therefore an urgent need for DENV, but its development has been plagued by issues of low efficacy and the fear of ADE [548]. In order to minimize the risk of ADE, a DENV vaccine is typically held to the standard of demonstrating a high level of protection

against all four serotypes of DENV, but in practice immunogenicity has been highly variable between serotypes and in different populations [549]. In 2016, the WHO announced its recommendation for the use of a three-dose, live-attenuated combination vaccine against all four DENV serotypes (CYD-TDV, or Dengvaxia) [550]. In two phase 3 clinical trials, the vaccine had partial efficacy, reducing confirmed symptomatic cases of DENV infection by roughly 60% (type-specific efficacy ranging from 43-77%) and severe DENV disease by almost 80% [551]. But based on estimated risks and benefits, it is currently only recommended for use in areas where there is a high burden of disease and in people aged 9 years or older [550,552]. Therefore, there is an unmet need for a DENV vaccine that provides potent immunity against all four serotypes, ideally with a single immunization, without adverse events. Due to its characteristic potency, the nucleoside-modified, purified mRNA-LNP platform may be well suited to fulfill such a need. Plans are underway to prepare mRNAs encoding the prM-E proteins of the four DENV serotypes and to immunize mice with a pentavalent, pan-DENV/ZIKV vaccine. The efficacy readouts will include NAbs against the five viruses and the potency of ADE compared to monovalent vaccines, measured *in vitro* and in available animal models [533,534]. Although we hypothesize that potent type-specific NAbs will be generated against all components of the vaccine, mitigating any ADE activity, it is also possible that a pentavalent vaccine would focus the antibody response on non-neutralizing, ADE-associated epitopes. Therefore, protection will have to be determined empirically.

5.5. The Promise of Nucleoside-Modified mRNA Vaccines

Just over a decade ago, there were few and modest prospects for the use of mRNA as a vaccine platform. This pessimism was due to the significant challenges

of stabilizing and expressing synthetic mRNA *in vivo*. But as of 2017, the work of Karikó and others has demonstrated that *in vivo* translation of mRNA can be dramatically increased through the suppression of innate immune sensing [311,318–320]. Incorporation of naturally occurring modified nucleosides, such as pseudouridine or 1-methylpseudouridine, in combination with dsRNA removal, has improved synthetic mRNA expression by several orders of magnitude, particularly in DCs, which are critical drivers of T and B cell responses [311]. Encapsulation of mRNA in ionizable LNPs has allowed efficient uptake of mRNA *in vivo*, with a much higher magnitude and longer half-life of expression compared to previous delivery methods [309]. In light of these advances, our laboratory has developed mRNA-based vaccines for a number of important viral pathogens. In the case of the ZIKV and influenza vaccines, the NAb responses are noteworthy in that they approximate or exceed the titers elicited during pathogenic infection. To our knowledge, this is the first non-replicating vaccine platform described that is capable of eliciting such robust NAb responses after only a single administration.

Since any protein antigen can be encoded by mRNA, the potential future applications for mRNA-based vaccines are almost without limit. Experimental plans to determine the extent of heterologous protection generated by the mRNA-based influenza vaccine are already ongoing. Projects are also planned to develop mRNA-based vaccines against a variety of other viral targets, including chikungunya virus, filoviruses, coronaviruses, and HCV. Like HIV-1, HCV is antigenically diverse and adept at evading humoral immune responses [12,553]. The preliminary data obtained with our HIV-1 mRNA vaccine reveal that, even in this uniquely potent vaccine platform, HIV-1 Env is still a poorly immunogenic target for NAb responses,

so it is possible that other strategies of antigen display will be required for protective humoral responses against pathogens like HIV-1 and HCV.

One strategy that has been proposed to generate potent antibodies against HIV-1 is to immunize with a sequence of Envs that represent the evolving virus in infected individuals who have naturally generated bNAbs [225]. The principle behind this approach is that early Envs in the lineage should be able to activate naïve or precursor B cells that can be matured into bNAbs by later Envs in the lineage. In collaboration with other investigators, we plan to deliver such sequential Env immunogens to rhesus macaques using the mRNA-LNP platform. This immunization series has the potential to potently stimulate germinal center reactions over a prolonged time period with a gradually evolving antigen, thereby reflecting the natural development of bNAbs. Thus, the mRNA platform is a well-suited vehicle to test the effectiveness of the sequential immunization approach.

In another future direction, our laboratory plans to immunize animals with mRNAs encoding stabilized SOSIP protein, in either secreted or membrane-associated form. Encouragingly, preliminary data suggest that the Env-encoding mRNA-LNP elicits significantly higher Tfh cell responses than SOSIP protein plus adjuvant (N. Pardi, Derek Cain, unpublished data). The main disadvantage of using mRNA to deliver SOSIPs is that it is impossible to purify the SOSIP trimers based on desired antigenic properties. For example, previous immunizations with SOSIPs have selected for closed-state trimers using various chromatographic methods. In mRNA delivery, there would likely be a mix of closed-state trimers and non-native forms of Env that may serve as more immunogenic decoys for the antibody response. To address this concern, we are planning to compare SOSIP immunizations using mRNA alone versus mRNA primes with protein boosts, as well

as the simultaneous injection of mRNA and protein. Such approaches may theoretically combine the benefits of potent Tfh cell and germinal center responses induced by the mRNA with the ability of purified SOSIP protein to focus the antibody response against poorly immunogenic, glycan-containing bNAb epitopes on the closed-state trimer.

The most fundamental future directions for mRNA vaccines regard basic biology (outlined in Fig. 5.1): First, what cells take up and express nucleoside-modified mRNA *in vivo* when delivered by LNPs? This question could be addressed by intradermally injecting reporter gene-encoding mRNAs into mice, and then identifying the cell types using immunoassays and histology. A related question is which cell types are most critical for the generation of potent NAbs. This could be addressed by vaccinating genetically modified mouse strains that lack specific immune cell types in the skin, such as Langerhans cells [554–556] and multiple populations of myeloid dermal DCs [557–561]. Another basic question is what molecule(s) provide the adjuvant activity driving DC maturation and migration to lymph nodes. Nucleoside-modified, purified mRNA contains no known pathogen-associated molecular patterns (PAMPs) and does not stimulate type I IFNs in DCs *in vitro*, nor does it result in measurable systemic IFN-α when injected into mice complexed with LNPs (N. Pardi, H. Ni, unpublished data). It is unclear, then, how such potent immune responses can be induced without a known adjuvant. One possibility is that the mRNA itself contains an additional, novel PAMP that induces DC maturation and migration. A perhaps likelier possibility was suggested by a report showing that various forms of virus-like particles and fusogenic liposomes were sensed by DCs in a STING-dependent manner and resulted in the upregulation of transcripts for IFN-β, CXCL10, and other chemokines and interferon-stimulated

genes [562]. These gene products have yet not been specifically tested in the context of our mRNA-LNP platform. A plausible scenario is that mRNA-LNP delivery results in local production of chemokines that recruit DCs, which take up and translate the mRNA. Then, DCs are matured by IFN-β and migrate to the draining lymph node to initiate $CD4^+$ and $CD8^+$ T cell responses. These possibilities will be relatively straightforward to test: first by assaying for the upregulation of these chemokines and cytokines during mRNA-LNP delivery *in vitro* and *in vivo*, and then by antagonizing or adding in each of them during vaccination. In addition, it may be possible to use LNPs as an adjuvant for protein subunit immunization, in the absence of or in combination with antigen-encoding mRNA.

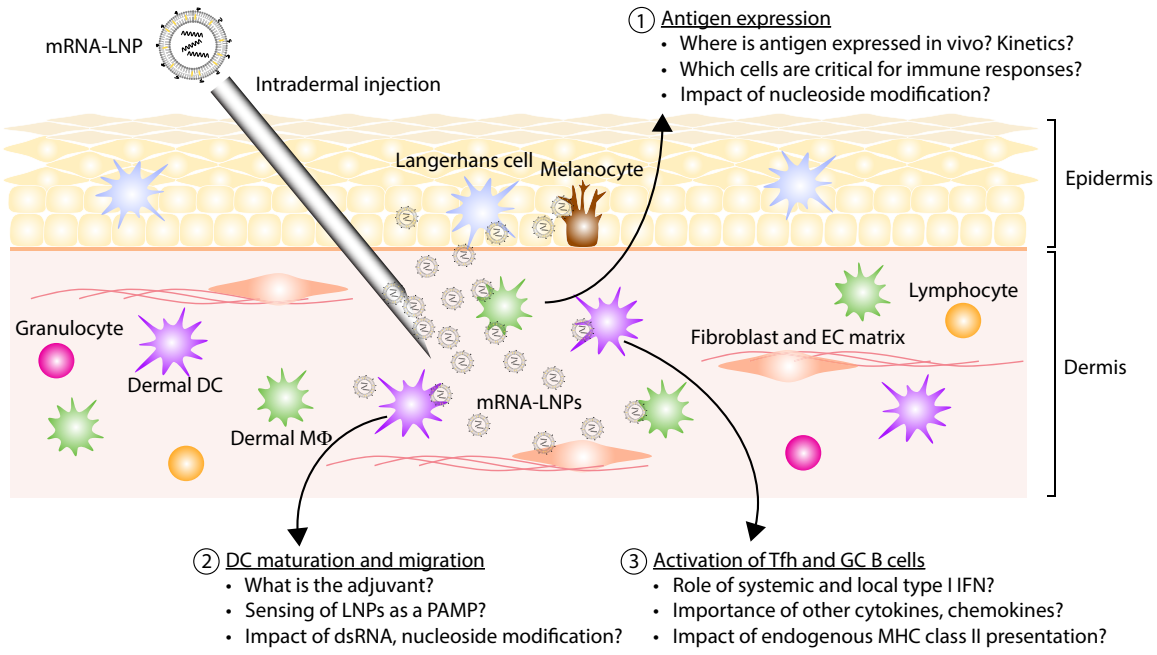

Figure 5.1. Future directions in mRNA vaccine biology. Represented is a schematic of intradermal mRNA-LNP vaccination with likely cellular milieu. Indicated are important questions on topics that likely impact the efficacy of mRNA vaccines, regarding 1) *in vivo* expression, 2) DC maturation and adjuvant activity, and 3) activation of potent Tfh and GC B cell responses. EC, extracellular; MΦ, macrophage; PAMP, pathogen-associated molecular pattern.

An exciting area of research that is just beginning in our laboratory is defining the mechanism of the potent Tfh and germinal center (GC) B cell responses induced by the mRNA-LNP platform. We were surprised by the finding in Fig. 4.1 that nucleoside modification was strictly necessary for the generation of Tfh and GC B cell responses and potent HAI antibody titers. To explain this result, we considered the fact unmodified HA-encoding mRNA-LNP, when injected intravenously into mice, provokes a massive systemic IFN-α response (>40 ng/mL), while nucleoside-modified mRNA produces no detectable IFN-α (N. Pardi, unpublished data). As type I IFNs have been identified as potent inhibitors of the differentiation of Tfh-like cells [265], we hypothesized that nucleoside modification prevented the inhibition of Tfh responses by type I IFNs. To test this idea, we conducted immunizations in mice that lacked type I IFN signaling due to a genetic deficiency or an infusion of an IFNAR1-antagonizing antibody. In fact, type I IFN signaling was required for a potent Tfh response (N. Pardi, Arpita Myles, M. Hogan, unpublished data). This supports a role for local IFN production in providing adjuvant activity to DCs, but it creates an apparent paradox for the role of type I IFNs in the Tfh response. Disentangling the contributions of IFN-α, IFN-β, and other cytokines and chemokines in the potent Tfh induction by nucleoside-modified mRNA is a critical future direction that will pave the way for more effective vaccine designs.

A final consideration for mRNA-based vaccines that could contribute to potent Tfh and GC B cell responses is the endogenous nature of the antigen production and presentation on MHC class II. The classical model of MHC class II presentation states that $CD4^+$ T cells are typically activated by peptides derived from “exogenous” or extracellular antigens that are phagocytosed, degraded in the endocytic pathway, loaded onto MHC class II in late endosomes, and then transported to the cell surface

[563]. However, there is increasing evidence that alternative pathways of MHC class II presentation may be prevalent, or even predominant, in the immune response to viral infections [564,565]. Recent work by Miller, Eisenlohr, and colleagues demonstrated that the $CD4^+$ T cell response to influenza infection in mice consisted mainly of endogenously presented epitopes, that is, peptides synthesized within infected antigen-presenting cells [323]. Notably, this $CD4^+$ T cell response was significantly broader and higher in magnitude than that induced by inactivated influenza virus, which necessarily uses the exogenous pathway, and it was also associated with a significantly more potent HAI antibody response. These data suggest that the quality and magnitude of the immune response can be influenced by the pathway of MHC class II presentation. A possible mechanism for this effect is enhanced signal strength and duration of T cell receptor activation, which have been associated with $CD4^+$ T cell activation efficiency [566–568]. It is plausible that endogenous epitopes are presented at a greater level or for a greater length of time by virtue of the fact that they derive from a continuously synthesized pool of antigen. One way to determine whether this pathway contributes to the efficacy of mRNA vaccines would be to design an extracellular or transmembrane antigen that contains no $CD4^+$ T cell epitopes restricted by the single MHC class II allele of C57BL/6 mice, and then encode this antigen on an mRNA together with a validated $CD4^+$ T cell epitope for which the pathway is known. In this scenario, the entire $CD4^+$ T cell response should be directed to one epitope, and thus the pathway can be varied to determine its effect on the antibody response. If the pathway of MHC class II presentation influences the generation of Tfh cells, $CD4^+$ in general, or GC B cells, these results would be significant for the design of future vaccines.

5.6. Epilogue

In the course of this dissertation, I have described the approaches taken by my laboratory and myself to address some of the major issues confronted by vaccinologists today. As illustrated in Fig. 5.2, these challenges can be largely categorized into the areas of 1) the quality of the immune response and 2) the speed of vaccine development and immune protection. Most viral vaccine targets can be segregated into one area or the other; but certain targets such as influenza virus present challenges in both areas, leaving much room for technological progress.

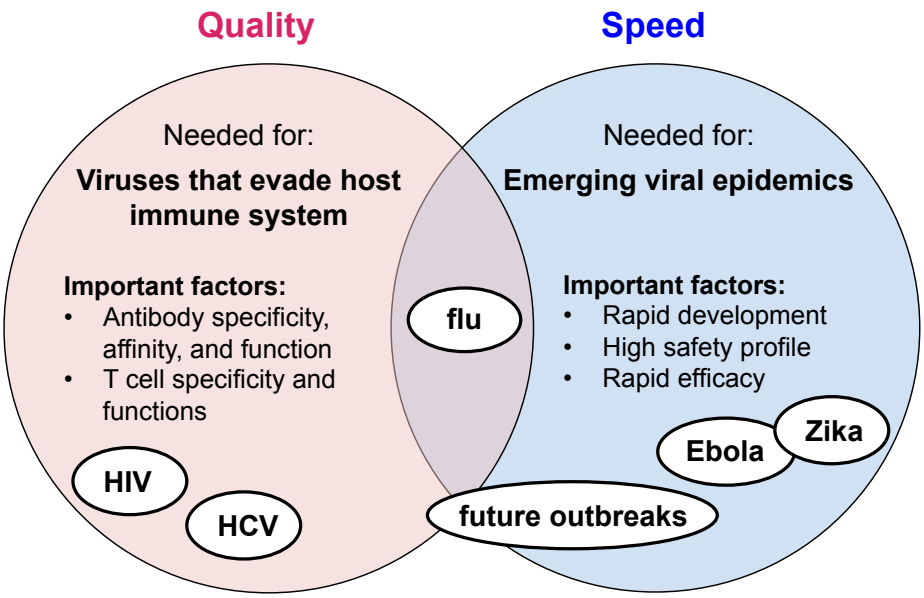

Figure 5.2. Challenges of modern vaccine design. Viruses that successfully evade the adaptive immune system, such as HIV and HCV, require vaccine designs that can generate the appropriate quality of immune response (left), while acute viruses that emerge in new epidemics, such as Ebola and Zika viruses, require vaccine development to occur on a more rapid timescale (right).

Regarding HIV-1 vaccine design, this dissertation explored multiple ways to improve or modify the quality of antibody response against Env, including altering epitope-specific responses (Chapter 2), enhancing the potency of a viral vector

prime (Chapter 3), and using mRNA vaccines to induce strong Tfh cell and germinal center reactions (Chapter 4). Although the path to an effective HIV-1 vaccine is as yet uncertain, immunogen design strategies such as these will be likely critical for the development of effective immune responses against HIV-1 and other pathogens that evade the adaptive immune system.

In the case of rapidly emerging viral epidemics such as Zika virus, modern vaccine design is also limited by the slow speed at which new vaccines are developed, manufactured, approved, and implemented in the clinic. As demonstrated in Chapter 4, the mRNA platform offers advantages in this area that distinguish it from other vaccine modalities. New mRNA-based vaccines can be designed and produced using standardized methods on an extremely rapid timescale (weeks) and can generate potent immune responses with only a single administration. Given these features, it is possible that mRNA-based vaccines may have a significant impact on the effectiveness of future epidemic control.

REFERENCES

1. Centers for Diseases Control and Prevention. Epidemiology and Prevention of Vaccine-Preventable Diseases. [Internet]. 13th ed. Hamborsky J, Kroger A, Wolfe S, editors. Washington D.C.: Public Health Foundation; 2015. Available: www.cdc.gov/vaccines/pubs/pinkbook/index.html

2. World Health Organization. Global Vaccine Action Plan 2011-2020 [Internet]. 2013. Available: http://www.who.int/immunization/global_vaccine_action_plan

3. Nabel GJ. Designing tomorrow's vaccines. N Engl J Med. 2013;368(6): 551–60.

4. Celentano LP, Carrillo-Santisteve P, O'Connor P, Danielsson N, Huseynov S, Derrough T, et al. Global polio eradication: Where are we in Europe and what next? Vaccine. 2017; Epub ahead of print.

5. Greenwood B. The contribution of vaccination to global health: past, present and future. Philos Trans R Soc Lond B Biol Sci. 2014;369(1645): 20130433.

6. Flannery B, Schrag S, Bennett NM, Lynfield R, Harrison LH, Reingold A, et al. Impact of childhood vaccination on racial disparities in invasive Streptococcus pneumoniae infections. JAMA. 2004;291(18): 2197–2203.

7. Doolan DL, Apte SH, Proietti C. Genome-based vaccine design: The promise for malaria and other infectious diseases. Int J Parasitol. 2014;44(12): 901–913.

8. Pantaleo G, Koup R a. Correlates of immune protection in HIV-1 infection: what we know, what we don't know, what we should know. Nat Med. 2004;10(8): 806–810.

9. Plotkin S. History of vaccination. Proc Natl Acad Sci. 2014;111(34): 12283–12287.

10. Virgin HW, Wherry EJ, Ahmed R. Redefining chronic viral infection. Cell. 2009;138(1): 30–50.

11. Lučin P, Mahmutefendić H, Blagojević Zagorac G, Ilić Tomaš M. Cytomegalovirus immune evasion by perturbation of endosomal trafficking. Cell Mol Immunol. 2015;12(2): 154–69.

12. Burke KP, Cox AL. Hepatitis C Virus Evasion of Adaptive Immune Responses - A Model for Viral Persistence. Immunol Res. 2010;47(1–3):

216–227.

13. Hoxie JA. Toward an antibody-based HIV-1 vaccine. Annu Rev Med. 2010;61: 135–52.

14. Peterlin BM, Trono D. Hide, shield and strike back: how HIV-infected cells avoid immune eradication. Nat Rev Immunol. 2003;3(2): 97–107.

15. Graham BS. Vaccines against respiratory syncytial virus: The time has finally come. Vaccine. 2016;34(30): 3535–3541.

16. Nabel GJ, Fauci AS. Induction of unnatural immunity: prospects for a broadly protective universal influenza vaccine. Nat Med. 2010;16(12): 1389–1391.

17. Zhou T, Doria-Rose NA, Cheng C, Stewart-Jones GBE, Chuang GY, Chambers M, et al. Quantification of the Impact of the HIV-1-Glycan Shield on Antibody Elicitation. Cell Rep. 2017;19(4): 719–732.

18. Carter JJ, Koutsky LA, Hughes JP, Lee SK, Jane Kuypers, Kiviat N, et al. Comparison of human papillomavirus types 16, 18, and 6 capsid antibody responses following incident Infection. J Infect Dis. 2000;181: 1911–9.

19. Day PM, Kines RC, Thompson CD, Jagu S, Roden RB, Lowy DR, et al. In vivo mechanisms of vaccine-induced protection against HPV infection. Cell Host Microbe. 2010;8(3): 260–270.

20. Bissett SL, Draper E, Myers RE, Godi A, Beddows S. Cross-neutralizing antibodies elicited by the Cervarix human papillomavirus vaccine display a range of Alpha-9 inter-type specificities. Vaccine. 2014;32(10): 1139–1146.

21. De Gregorio E, Rappuoli R. From empiricism to rational design: a personal perspective of the evolution of vaccine development. Nat Rev Immunol. 2014;14(7): 505–514.

22. Rappuoli R, Bottomley MJ, D'Oro U, Finco O, De Gregorio E. Reverse vaccinology 2.0: Human immunology instructs vaccine antigen design. J Exp Med. 2016;213(4): 469–81.

23. Rueckert C, Guzmán CA. Vaccines: From Empirical Development to Rational Design. Plos Pathog. 2012;8(11).

24. Walker LM, Burton DR. Rational antibody-based HIV-1 vaccine design: current approaches and future directions. Curr Opin Immunol. 2010;22(3): 358–66.

25. Mascola JR. The modern era of HIV-1 vaccine development. Science. 2015;349(6244): 139–140.

26. Pancera M, Changela A, Kwong PD. How HIV-1 entry mechanism and broadly neutralizing antibodies guide structure-based vaccine design. Curr Opin HIV AIDS. 2017; 1.

27. Ward AB, Wilson IA. The HIV-1 envelope glycoprotein structure: nailing down a moving target. Immunol Rev. 2017;275(1): 21–32.

28. Glezen W, Taber L, Frank A, Kasel J. Risk of primary infection and reinfection with respiratory syncytial virus. Am J Dis Child. 1986;140(6): 543–6.

29. Lozano R, Naghavi M, Foreman K, Lim S, Shibuya K, Aboyans V, et al. Global and regional mortality from 235 causes of death for 20 age groups in 1990 and 2010 : a systematic analysis for the Global Burden of Disease Study 2010. Lancet. 2012;380: 2095–2128.

30. Hall CB, Weinberg GA, Iwane MK, Blumkin AK, Edwards KM, Staat MA, et al. The Burden of Respiratory Syncytial Virus Infection in Young Children. N Engl J Med. 2009;360(6): 588–598.

31. Murphy BR, Hall SL, Kulkarni AB, Crowe JE, Collins PL, Connors M, et al. An update on approaches to the development of respiratory syncytial virus (RSV) and parainfluenza virus type 3 (PIV3) vaccines. Virus Res. 1994;32: 13–36.

32. Kapikian A, Mitchell R, Chanock R, Shvedoff R, Stewart C. An epidemiologic study of altered clinical reactivity to respiratory syncytial (RS) virus infection in children previously vaccinated with an inactivated RS virus vaccine. Am J Epidemiol. 1969;89(4): 405–421.

33. Knudson CJ, Hartwig SM, Meyerholz DK, Varga SM. RSV Vaccine-Enhanced Disease Is Orchestrated by the Combined Actions of Distinct CD4 T Cell Subsets. Plos Pathog. 2015;11(3): 1–23.

34. Murphy BR, Sotnikov A V, Lawrence LA, Banks SM, Prince GA. Enhanced pulmonary histopathology is observed in cotton rats immunized with formalin-inactivated respiratory syncytial virus (RSV) or purified F glycoprotein and challenged with RSV 3-6 months after immunization. Vaccine. 1990;8: 497–502.

35. Connors M, Collins P, Firestone C, Sotnikov A, Waitze A, Davis A, et al. Cotton rats previously immunized with a chimeric RSV FG glycoprotein develop enhanced pulmonary pathology when infected with RSV, a phenomenon not encountered following immunization with vaccinia--RSV recombinants or RSV. Vaccine. 1992;10(7): 1992.

36. Hildreth S, Baggs R, Brownstein D, Castleman W, Paradiso P. Lack of detectable enhanced pulmonary histopathology in cotton rats immunized

with purified F glycoprotein of respiratory syncytial virus (RSV) when challenged at 3-6 months after immunization. Vaccine. 1993;11(6): 615–8.

37. Mclellan JS, Yang Y, Graham BS, Kwong PD. Structure of Respiratory Syncytial Virus Fusion Glycoprotein in the Postfusion Conformation Reveals Preservation of Neutralizing Epitopes. J Virol. 2011;85(15): 7788–7796.

38. Calder LJ, González-Reyes L, García-Barreno B, Wharton SA, Skehel JJ, Wiley DC, et al. Electron Microscopy of the Human Respiratory Syncytial Virus Fusion Protein and Complexes That It Forms with Monoclonal Antibodies. Virology. 2000;271(1): 122–131.

39. Killikelly AM, Kanekiyo M, Graham BS. Pre-fusion F is absent on the surface of formalin-inactivated respiratory syncytial virus. Nat Publ Gr. 2016;(June): 1–7.

40. McLellan JS, Chen M, Leung S, Graepel KW, Du X, Yang Y, et al. Structure of RSV Fusion Glycoprotein Bound to a Prefusion-Specific Neutralizing Antibody. Science. 2013;340: 1113–1117.

41. McLellan JS, Chen M, Joyce MG, Sastry M, Stewart-Jones GBE, Yang Y, et al. Structure-Based Design of a Fusion Glycoprotein Vaccine for Respiratory Syncytial Virus. Science. 2013;342: 592–598.

42. Joyce MG, Zhang B, Ou L, Chen M, Chuang G-Y, Druz A, et al. Iterative structure-based improvement of a fusion-glycoprotein vaccine against RSV. Nat Struct Mol Biol. 2016;23(9): 811.

43. Schneider-Ohrum K, Cayatte C, Bennett AS, Rajani GM, McTamney P, Nacel K, et al. Immunization with Low Doses of Recombinant Postfusion or Prefusion Respiratory Syncytial Virus F Primes for Vaccine-Enhanced Disease in the Cotton Rat Model Independently of the Presence of a Th1-Biasing (GLA-SE) or Th2-Biasing (Alum) Adjuvant. J Virol. 2017;91(8): 1–19.

44. Dose, Safety, Tolerability and Immunogenicity of a Stabilized Prefusion RSV F Subunit Protein Vaccine, VRC-RSVRGP084-00-VP (DS-Cav1), Alone or With Alum Adjuvant, in Healthy Adults. In: ClinicalTrials.gov [Internet]. 2017 [cited 21 Jul 2017]. Available: https://clinicaltrials.gov/ct2/show/NCT03049488

45. Sanders RW, Derking R, Cupo A, Julien JP, Yasmeen A, de Val N, et al. A Next-Generation Cleaved, Soluble HIV-1 Env Trimer, BG505 SOSIP.664 gp140, Expresses Multiple Epitopes for Broadly Neutralizing but Not Non-Neutralizing Antibodies. Plos Pathog. 2013;9(9): e1003618.

46. Sanders RW, van Gils MJ, Derking R, Sok D, Ketas TJ, Burger J a., et al.

HIV-1 neutralizing antibodies induced by native-like envelope trimers. Science. 2015;349(6244): aac4223-1-10.

47. World Health Organization. Global Health Observatory data: HIV/AIDS [Internet]. 2017 [cited 20 May 2017]. Available: http://www.who.int/gho/hiv

48. AIDS.gov. U.S. Statistics [Internet]. 2016 [cited 20 May 2017]. Available: https://www.aids.gov/hiv-aids-basics/hiv-aids-101/statistics/

49. Sharp PM, Hahn BH. Origins of HIV and the AIDS epidemic. Cold Spring Harb Perspect Med. 2011;1: a006841.

50. Buonaguro L, Tornesello ML, Buonaguro FM. Human Immunodeficiency Virus Type 1 Subtype Distribution in the Worldwide Epidemic: Pathogenetic and Therapeutic Implications. J Virol. 2007;81(19): 10209–10219.

51. Wilen CB, Tilton JC, Doms RW. HIV: Cell Binding and Entry. Cold Spring Harb Perspect Med. 2012;2: a006866.

52. Keele BF, Giorgi EE, Salazar-Gonzalez JF, Decker JM, Pham KT, Salazar MG, et al. Identification and characterization of transmitted and early founder virus envelopes in primary HIV-1 infection. Proc Natl Acad Sci. 2008;105(21): 7552–7557.

53. Connor RI, Sheridan KE, Ceradini D, Choe S, Landau NR. Change in Coreceptor Use Correlates with Disease Progression in HIV-1-Infected Individuals. J Exp Med. 1997;185(4): 621–628.

54. Hayashida T, Tsuchiya K, Kikuchi Y, Oka S, Gatanaga H. Emergence of CXCR4-tropic HIV-1 variants followed by rapid disease progression in hemophiliac slow progressors. 2017; 1–13.

55. Raymond S, Delobel P, Mavigner M, Cazabat M, Encinas S, Souyris C, et al. CXCR4-using viruses in plasma and peripheral blood mononuclear cells during primary HIV-1 infection and impact on disease progression. AIDS. 2010;(June): 1.

56. Arhel N. Revisiting HIV-1 uncoating. Retrovirology. 2010;7(1): 96.

57. Hu W, Hughes SH. HIV-1 Reverse Transcription. Cold Spring Harb Perspect Med. 2012;2: a006882.

58. Craigie R, Bushman FD. HIV DNA integration. Cold Spring Harb Perspect Med. 2012;2(7): 1–18.

59. Das AT, Harwig A, Berkhout B. The HIV-1 Tat Protein Has a Versatile Role in Activating Viral Transcription. J Virol. 2011;85(18): 9506–9516.

60. Karn J, Stoltzfus CM. Transcriptional and posttranscriptional regulation of HIV-1 gene expression. Cold Spring Harb Perspect Med. 2012;4: a006916.

61. Sundquist WI, Krausslich H-G. HIV-1 Assembly, Budding, and Maturation. Cold Spring Harb Perspect Med. 2012; a006924.

62. Murakami T, Freed EO. The long cytoplasmic tail of gp41 is required in a cell type-dependent manner for HIV-1 envelope glycoprotein incorporation into virions. Proc Natl Acad Sci. 2000;97(1): 343–8.

63. Tedbury PR, Freed EO. The role of matrix in HIV-1 envelope glycoprotein incorporation. Trends Microbiol. 2014;22(7): 372–378.

64. Postler TS, Desrosiers RC. The Tale of the Long Tail: the Cytoplasmic Domain of HIV-1 gp41. J Virol. 2012;87(1): 2–15.

65. Deschambeault J, Lalonde JP, Cervantes-Acosta G, Lodge R, Cohen EA, Lemay G. Polarized human immunodeficiency virus budding in lymphocytes involves a tyrosine-based signal and favors cell-to-cell viral transmission. J Virol. 1999;73(6): 5010–7.

66. Koup RA, Safrit JT, Cao Y, Andrews CA, McLeod G, Borkowsky W, et al. Temporal association of cellular immune responses with the initial control of viremia in primary human immunodeficiency virus type 1 syndrome. J Virol. 1994;68(7): 4650–5.

67. Coffin J, Swanstrom R. HIV pathogenesis: dynamics and genetics of viral populations and infected cells. Cold Spring Harb Perspect Med. 2012;3: a012526.

68. Walker B, McMichael A. The T-cell response to HIV. Cold Spring Harb Perspect Med. 2012;2(11): 1–20.

69. Fraser C, Hollingsworth TD, Chapman R, de Wolf F, Hanage WP. Variation in HIV-1 set-point viral load: epidemiological analysis and an evolutionary hypothesis. Proc Natl Acad Sci. 2007;104(44): 17441–6.

70. Mohri H, Bonhoeffer S, Monard S, Perelson a S, Ho DD. Rapid turnover of T lymphocytes in SIV-infected rhesus macaques. Science. 1998;279(February): 1223–1227.

71. Vrisekoop N, Drylewicz J, Van Gent R, Mugwagwa T, Van Lelyveld SFL, Veel E, et al. Quantification of naive and memory T-cell turnover during HIV-1 infection. AIDS. 2015;29(16): 2071–2080.

72. Doitsh G, Galloway NLK, Geng X, Yang Z, Monroe KM, Zepeda O, et al. Cell death by pyroptosis drives CD4 T-cell depletion in HIV-1 infection. Nature. 2013;505: 509–514.

73. Karim R, Mack WJ, Stiller T, Operskalski E, Frederick T, Landay A, et al. Association of HIV clinical disease progression with profiles of early immune activation: results from a cluster analysis approach. AIDS June. 2013;1(279): 1473–1481.

74. Estes JD. Pathobiology Of HIV/SIV-Associated Changes In Secondary Lymphoid Tissues. Immunol Rev. 2013;254(1): 65–77.

75. Crowe SM, Carlin JB, Stewart KI, Lucas CR, Hoy JF. Predictive Value of CD4 Lymphocyte Numbers for the Development of Opportunistic Infections and Malignancies in HIV-Infected Persons. J Acquir Immune Defic Syndr. 1991;4: 770–776.

76. Holmes CB, Losina E, Walensky RP, Yazdanpanah Y, Freedberg KA. Review of human immunodeficiency virus type 1-related opportunistic infections in sub-saharan africa. Clin Infect Dis. 2003;36: 652–662.

77. Arts EJ, Hazuda DJ. HIV-1 antiretroviral drug therapy. Cold Spring Harb Perspect Med. 2012;2: a007161.

78. Baeten JM, Donnell D, Ndase P, Mugo NR, Campbell JD, Wangisi J, et al. Antiretroviral Prophylaxis for HIV Prevention in Heterosexual Men and Women. N Engl J Med. 2012;367(5): 399–410.

79. Donnell D, Baeten JM, Bumpus NN, Brantley J, Bangsberg DR, Haberer JE, et al. HIV Protective Efficacy and Correlates of Tenofovir Blood Concentrations in a Clinical Trial of PrEP for HIV Prevention. JAIDS J Acquir Immune Defic Syndr. 2014;66(3): 340–348.

80. World Health Organization. 17 million people with access to antiretroviral therapy [Internet]. 2016 [cited 12 Jun 2017]. Available: http://www.who.int/hiv/mediacentre/news/global-aids-update-2016-news/en/

81. Siliciano JD, Kajdas J, Finzi D, Quinn TC, Chadwick K, Margolick JB, et al. Long-term follow-up studies confirm the stability of the latent reservoir for HIV-1 in resting CD4+ T cells. Nat Med. 2003;9(6): 727–728.

82. Chun T-W, Moir S, Fauci AS. HIV reservoirs as obstacles and opportunities for an HIV cure. Nat Immunol. 2015;16(6): 584–589.

83. Barton K, Winckelmann A, Palmer S. HIV-1 Reservoirs During Suppressive Therapy. Trends Microbiol. 2016;24(5): 345–355.

84. Lederman MM, Funderburg NT, Sekaly RP, Klatt NR, Hunt PW. Residual immune dysregulation syndrome in treated HIV infection. Adv Immunol. 2013;119: 51–83.

85. Freiberg MS, Chang C-CH, Kuller LH, Skanderson M, Lowy E, Kraemer KL, et al. HIV Infection and the Risk of Acute Myocardial Infarction. JAMA Intern Med. 2013;173(8): 614.

86. Sandstrom TS, Ranganath N, Angel JB. Impairment of the type I interferon response by HIV-1: Potential targets for HIV eradication. Cytokine Growth Factor Rev. 2017;

87. Malim MH, Bieniasz PD, Swanstrom R, Coffin J, Walker B, Mcmichael A, et al. HIV Restriction Factors and Mechanisms. 2014;

88. Barouch DH, Ghneim K, Bosche WJ, Li Y, Berkemeier B, Hull M, et al. Rapid Inflammasome Activation following Mucosal SIV Infection of Rhesus Monkeys. Cell. 2016;165(3): 656–667.

89. Hirao LA, Grishina I, Bourry O, Hu WK, Somrit M, Sankaran- S, et al. Early Mucosal Sensing of SIV Infection by Paneth Cells Induces IL-1 b Production and Initiates Gut Epithelial Disruption. 2014;10(8).

90. Katsikis PD, Mueller YM, Villinger F. The cytokine network of acute hiv infection: A promising target for vaccines and therapy to reduce viral set-point? Plos Pathog. 2011;7(8).

91. Jin BX, Bauer DE, Tuttleton SE, Lewin S, Gettie A, Blanchard J, et al. Dramatic Rise in Plasma Viremia after CD8+ T Cell Depletion in Simian Immunodeficiency Virus–infected Macaques. J Exp Med. 1999;189(6): 991–998.

92. Fellay J, Shianna K V., Ge D, Colombo S, Ledergerber B, Weale M, et al. A Whole-Genome Association Study of Major Determinants for Host Control of HIV-1. Science. 2007;317(5840): 944–947.

93. The International HIV Controllers Study. The Major Genetic Determinants of HIV-1 Control Affect HLA Class I Peptide Presentation. Science. 2010;330(6010): 1551–1557.

94. Goulder PJR, Watkins DI. Impact of MHC class I diversity on immune control of immunodeficiency virus replication. Nat Rev Immunol. 2008;8(8): 1–7.

95. Olson AD, Meyer L, Prins M, Thiebaut R, Gurdasani D, Guiguet M, et al. An evaluation of HIV elite controller definitions within a large seroconverter cohort collaboration. PLoS One. 2014;9(1).

96. Migueles SA, Sabbaghian MS, Shupert WL, Bettinotti MP, Marincola FM, Martino L, et al. HLA B*5701 is highly associated with restriction of virus replication in a subgroup of HIV-infected long term nonprogressors. Proc Natl Acad Sci. 2000;97(6): 2709–2714.

97. Betts MR, Nason MC, West SM, Rosa SC De, Migueles SA, Abraham J, et al. HIV nonprogressors preferentially maintain highly functional. Blood. 2006;107(12): 4781–4790.

98. Hersperger AR, Pereyra F, Nason M, Demers K, Sheth P, Shin LY, et al. Perforin expression directly ex vivo by HIV-specific CD8 T-cells is a correlate of HIV elite control. Plos Pathog. 2010;6(5): e1000917.

99. Yang OO, Thi P, Sarkis N, Ali A, Harlow JD, Brander C, et al. Determinants of HIV-1 Mutational Escape From Cytotoxic T Lymphocytes. 2003;197(10).

100. Ganusov V V, Goonetilleke N, Liu MKP, Ferrari G, Shaw GM, Mcmichael AJ, et al. Fitness Costs and Diversity of the Cytotoxic T Lymphocyte (CTL) Response Determine the Rate of CTL Escape during Acute and Chronic Phases of HIV Infection. J Virol. 2011;85(20): 10518–10528.

101. Schwartz O, Maréchal V, Le Gall S, Lemonnier F, Heard JM. Endocytosis of major histocompatibility complex class I molecules is induced by the HIV-1 Nef protein. Nat Med. 1996;2(3): 338–342.

102. Cohen GB, Gandhi RT, Davis DM, Mandelboim O, Chen BK, Strominger JL, et al. The Selective Downregulation of Class I Major Histocompatibility Complex Proteins by HIV-1 Protects HIV-Infected Cells from NK Cells are encoded in the cytoplasmic tail of all HLA-A and. Immunity. 1999;10: 661–671.

103. Collins KL, Chen BK, Kalams SA, Walker BD, Baltimore D. HIV-1 Nef protein protects infected primary cells against killing by cytotoxic T lymphocytes. Nature. 1998;391(6665): 397–401.

104. Apps R, Del Prete GQ, Chatterjee P, Lara A, Brumme ZL, Brockman MA, et al. HIV-1 Vpu Mediates HLA-C Downregulation. Cell Host Microbe. 2016;19(5): 686–695.

105. Perreau M, Savoye A, Crignis E De, Corpataux J, Cubas R, Haddad EK, et al. Follicular helper T cells serve as the major CD4 T cell compartment for HIV-1 infection , replication , and production. 2013;210(1): 143–156.

106. Douek DC, Brenchley JM, Betts MR, Ambrozak DR, Hill BJ, Okamoto Y, et al. HIV preferentially infects HIV-specific CD4+ T cells. Nature. 2002;417(May): 95–98.

107. Yamamoto T, Lynch RM, Gautam R, Matus-nicodemos R, Schmidt SD, Boswell KL, et al. Quality and quantity of TFH cells are critical for broad antibody development in SHIV AD8 infection. Sci Trans Med. 2015;7(298).

108. Day CL, Kaufmann DE, Kiepiela P, Brown J a, Moodley ES, Reddy S, et al. PD-1 expression on HIV-specific T cells is associated with T-cell

exhaustion and disease progression. Nature. 2006;443(7109): 350–4.

109. Hu H, Fernando K, Ni H, Weissman D. HIV envelope suppresses CD4+ T cell activation independent of T regulatory cells. J Immunol. 2008;180(8): 5593–5600.

110. Fernando K, Hu H, Ni H, Hoxie J a., Weissman D. Vaccine-delivered HIV envelope inhibits CD4+ T-cell activation, a mechanism for poor HIV vaccine responses. Blood. 2007;109(6): 2538–2544.

111. Masci AM, Galgani M, Cassano S, Simone S De, Gallo A, Rosa V De, et al. HIV-1 gp120 induces anergy in naive T lymphocytes through CD4-independent protein kinase-A-mediated signaling. J Leukoc Biol. 2003;74(6): 1117–1124.

112. Tateyama M, Oyaizu N, Mccloskey TW, Than S, Pahwa S. CD4 T lymphocytes are primed to express Fas ligand by CD4 cross-linking and to contribute to CD8 T-cell apoptosis via Fas / FasL death signaling pathway. Blood. 2000;96(1): 195–202.

113. Moulard M, Decroly E. Maturation of HIV envelope glycoprotein precursors by cellular endoproteases. Biochim Biophys Acta. 2000;1469: 121–132.

114. Stewart-Jones GBE, Soto C, Lemmin T, Chuang GY, Druz A, Kong R, et al. Trimeric HIV-1-Env Structures Define Glycan Shields from Clades A, B, and G. Cell. 2016;165(4): 813–826.

115. Leonard K, Spellman W, Harris RJ, Thomas N. Assignment of Intrachain Disulfide Bonds and Characterization of Potential Glycosylation Sites of the Type 1 Recombinant Human Immunodeficiency Virus Envelope Glycoprotein (gp120) Expressed in Chinese Hamster Ovary Cells. J Biol Chem. 1990;265(18): 10373–10382.

116. Wei X, Decker JM, Wang S, Hui H, Kappes JC, Wu X, et al. Antibody neutralization and escape by HIV-1. Nature. 2003;422(6929): 307–312.

117. Scanlan CN, Offer J, Zitzmann N, Dwek RA. Exploiting the defensive sugars of HIV-1 for drug and vaccine design. Nature. 2007;446(April): 1038–1045.

118. Yang G, Holl TM, Liu Y, Li Y, Lu X, Nicely NI, et al. Identification of autoantigens recognized by the 2F5 and 4E10 broadly neutralizing HIV-1 antibodies. J Exp Med. 2013;210(2): 241–256.

119. Kwong PD, Doyle ML, Casper DJ, Cicala C, Leavitt S a, Majeed S, et al. HIV-1 evades antibody-mediated neutralization through conformational masking of receptor-binding sites. Nature. 2002;420(6916): 678–682.

120. Chen L, Kwon Y Do, Zhou T, Wu X, O'Dell S, Cavacini L, et al. Structural Basis of Immune Evasion at the Site of CD4 Attachment on HIV-1 gp120. Science. 2009;326(5956): 1123–7.

121. Xiang S, Sodroski J, Robinson JE. Characterization of CD4-Induced Epitopes on the HIV Type 1 gp120 Envelope Glycoprotein Recognized by Neutralizing Human Monoclonal Antibodies Characterization of CD4-Induced Epitopes on the HIV Type 1. 2002;

122. Hoffman TL, LaBranche CC, Zhang W, Canziani G, Robinson J, Chaiken I, et al. Stable exposure of the coreceptor-binding site in a CD4-independent HIV-1 envelope protein. PNAS. 1999;96(11): 6359–6364.

123. Veillette M, Désormeaux A, Medjahed H, Gharsallah N-E, Coutu M, Baalwa J, et al. Interaction with cellular CD4 exposes HIV-1 envelope epitopes targeted by antibody-dependent cell-mediated cytotoxicity. J Virol. 2014;88(5): 2633–44.

124. Ferrari G, Pollara J, Kozink D, Harms T, Drinker M, Freel S, et al. An HIV-1 gp120 envelope human monoclonal antibody that recognizes a C1 conformational epitope mediates potent antibody-dependent cellular cytotoxicity (ADCC) activity and defines a common ADCC epitope in human HIV-1 serum. J Virol. 2011;85(14): 7029–7036.

125. Zhu P, Chertova E, Bess J, Lifson JD, Arthur LO, Liu J, et al. Electron tomography analysis of envelope glycoprotein trimers on HIV and simian immunodeficiency virus virions. Proc Natl Acad Sci. 2003;100(26): 15812–7.

126. Chertova E, Bess JW, Crise BJ, Ii RCS, Schaden TM, Joanne M, et al. Envelope Glycoprotein Incorporation, Not Shedding of Surface Envelope Glycoprotein (gp120/SU), Is the Primary Determinant of SU Content of Purified Human Immunodeficiency Virus Type 1 and Simian Immunodeficiency Virus. J Virol. 2002;76(11): 5315.

127. Egan MA, Carruth LM, Rowell JF, Yu X, Siliciano RF. Human immunodeficiency virus type 1 envelope protein endocytosis mediated by a highly conserved intrinsic internalization signal in the cytoplasmic domain of gp41 is suppressed in the presence of the Pr55gag precursor protein. J Virol. 1996;70(10): 6547–56.

128. da Silva ES, Mulinge M, Bercoff DP. The frantic play of the concealed HIV envelope cytoplasmic tail. Retrovirology. 2013;10(1): 54.

129. Klein JS, Bjorkman PJ. Few and far between: how HIV may be evading antibody avidity. Plos Pathog. 2010;6(5): e1000908.

130. Forthal DN, Moog C. Fc receptor-mediated antiviral antibodies. Curr Opin

HIV AIDS. 2009;4(5): 388–393.

131. Topham NJ, Hewitt EW. Natural killer cell cytotoxicity: How do they pull the trigger? Immunology. 2009;128(1): 7–15.

132. Lowin B, Beermann F, Schmidt A, Tschopp J. A null mutation in the perforin gene impairs cytolytic T lymphocyte- and natural killer cell-mediated cytotoxicity. PNAS. 1994;91(Nov): 11571–11575.

133. Santoro MM, Perno CF. HIV-1 Genetic Variability and Clinical Implications. ISRN Microbiol. 2013;2013: 481314.

134. Richman DD, Wrin T, Little SJ, Petropoulos CJ. Rapid evolution of the neutralizing antibody response to HIV type 1 infection. Proc Natl Acad Sci. 2003;100(7): 4144–4149.

135. Moody MA, Gao F, Gurley TC, Amos JD, Kumar A, Hora B, et al. Strain-Specific V3 and CD4 Binding Site Autologous HIV-1 Neutralizing Antibodies Select Neutralization-Resistant Viruses. Cell Host Microbe. 2015;18(3): 354–362.

136. Hraber P, Seaman MS, Bailer RT, Mascola JR, Montefiori DC, Korber BT. Prevalence of broadly neutralizing antibody responses during chronic HIV-1 infection. AIDS. 2014;28(2): 163–169.

137. Seaman MS, Janes H, Hawkins N, Grandpre LE, Devoy C, Giri A, et al. Tiered categorization of a diverse panel of HIV-1 Env pseudoviruses for assessment of neutralizing antibodies. J Virol. 2010;84(3): 1439–52.

138. Landais E, Huang X, Havenar-Daughton C, Murrell B, Price MA, Wickramasinghe L, et al. Broadly Neutralizing Antibody Responses in a Large Longitudinal Sub-Saharan HIV Primary Infection Cohort. Plos Pathog. 2016;12(1): 1–22.

139. Burton DR, Hangartner L. Broadly Neutralizing Antibodies to HIV and Their Role in Vaccine Design. Annu Rev Immunol. 2016;34: 635–59.

140. Parren PWHI, Marx PA, Hessell AJ, Harouse J, Cheng-mayer C, John P, et al. Antibody Protects Macaques against Vaginal Challenge with a Pathogenic R5 Simian/Human Immunodeficiency Virus at Serum Levels Giving Complete Neutralization In Vitro. J Virol. 2001;75(17): 8340–8347.

141. Hessell AJ, Rakasz EG, Poignard P, Hangartner L, Landucci G, Forthal DN, et al. Broadly neutralizing human anti-HIV antibody 2G12 is effective in protection against mucosal SHIV challenge even at low serum neutralizing titers. Plos Pathog. 2009;5(5): e1000433.

142. Gautam R, Nishimura Y, Pegu A, Nason MC, Klein F, Gazumyan A, et al.

A single injection of anti-HIV-1 antibodies protects against repeated SHIV challenges. Nature. 2016;533(7601): 105–9.

143. Moldt B, Rakasz EG, Schultz N, Chan-Hui P-Y, Swiderek K, Weisgrau KL, et al. Highly potent HIV-specific antibody neutralization in vitro translates into effective protection against mucosal SHIV challenge in vivo. PNAS. 2012;109(46): 18921–5.

144. Saunders KO, Wang L, Joyce MG, Yang Z, Balazs AB, Cheng C, et al. Broadly Neutralizing Human Immunodeficiency Virus Type 1 Antibody Gene Transfer Protects Nonhuman Primates from Mucosal Simian-Human Immunodeficiency Virus Infection. J Virol. 2015;89(16): 8334–8345.

145. Hessell AJ, Hangartner L, Hunter M, Havenith CEG, Beurskens FJ, Bakker JM, et al. Fc receptor but not complement binding is important in antibody protection against HIV. Nature. 2007;449(7158): 101–4.

146. Santra S, Tomaras GD, Warrier R, Nicely NI, Liao HX, Pollara J, et al. Human Non-neutralizing HIV-1 Envelope Monoclonal Antibodies Limit the Number of Founder Viruses during SHIV Mucosal Infection in Rhesus Macaques. Plos Pathog. 2015;11(8): 1–38.

147. Frolich D, Giesecke C, Mei HE, Reiter K, Daridon C, Lipsky PE, et al. Secondary Immunization Generates Clonally Related Antigen-Specific Plasma Cells and Memory B Cells. J Immunol. 2010;185(5): 3103–3110.

148. Moody MA, Zhang R, Walter EB, Woods CW, Ginsburg GS, McClain MT, et al. H3N2 influenza infection elicits more cross-reactive and less clonally expanded anti-hemagglutinin antibodies than influenza vaccination. PLoS One. 2011;6(10).

149. Yu L, Guan Y. Immunologic basis for long HCDR3s in broadly neutralizing antibodies against HIV-1. Front Immunol. 2014;5(250): 1–8.

150. Pancera M, McLellan JS, Wu X, Zhu J, Changela A, Schmidt SD, et al. Crystal Structure of PG16 and Chimeric Dissection with Somatically Related PG9: Structure-Function Analysis of Two Quaternary-Specific Antibodies That Effectively Neutralize HIV-1. J Virol. 2010;84(16): 8098–8110.

151. McLellan JS, Pancera M, Carrico C, Gorman J, Julien J-P, Khayat R, et al. Structure of HIV-1 gp120 V1/V2 domain with broadly neutralizing antibody PG9. Nature. 2011;480(7377): 336–43.

152. Liu M, Yang G, Wiehe K, Nicely NI, Vandergrift NA, Rountree W, et al. Polyreactivity and Autoreactivity among HIV-1 Antibodies. J Virol. 2015;89(1): 784–798.

153. O'Connell RJ, Kim JH, Corey L, Michael NL. Human Immunodeficiency Virus Vaccine Trials. Cold Spring Harb Perspect Med. 2012;2: a007351.

154. The rgp120 HIV Vaccine Study Group. Placebo-Controlled Phase 3 Trial of a Recombinant Glycoprotein 120 Vaccine to Prevent HIV-1 Infection. J Infect Dis. 2005;191: 654–665.

155. Pitisuttithum P, Gilbert P, Gurwith M, Heyward W, Martin M, Griensven F Van, et al. Randomized, Double-Blind, Placebo-Controlled Efficacy Trial of a Bivalent Recombinant Glycoprotein 120 HIV-1 Vaccine among Injection Drug Users in Bangkok, Thailand. J Inf Dis. 2006;194: 1661–1671.

156. Shiver JW, Fu T, Chen L, Casimiro DR, Davies M, Evans RK, et al. Replication-incompetent adenoviral vaccine vector elicits effective anti-immunodeficiency-virus immunity. Nature. 2002;415: 331–335.

157. Zhang Z, Fu T, Casimiro DR, Davies M, Liang X, Schleif W a, et al. Mamu-A*01 Allele-Mediated Attenuation of Disease Progression in Simian-Human Immunodeficiency Virus Infection Mamu-A ٭ 01 Allele-Mediated Attenuation of Disease Progression in Simian-Human Immunodeficiency Virus Infection. J Virol. 2002;76(24): 12845–12854.

158. Pal R, Venzon D, Letvin NL, Santra S, Montefiori DC, Miller NR, et al. ALVAC-SIV-gag-pol-env-Based Vaccination and Macaque Major Histocompatibility Complex Class I (A*01) Delay Simian Immunodeficiency Virus SIV mac-Induced Immunodeficiency. J Virol. 2002;76(1): 292–302.

159. Mothé BR, Weinfurter J, Wang C, Rehrauer W, Wilson N, Allen TM, et al. Expression of the Major Histocompatibility Complex Class I Molecule Mamu-A * 01 is associated with control of Simian Immunodeficiency Virus SIV mac 239 replication. J Virol. 2003;77(4): 2736.

160. Casimiro DR, Wang F, Schleif WA, Liang X, Zhang Z, Tobery TW, et al. Attenuation of Simian Immunodeficiency Virus SIVmac239 Infection by Prophylactic Immunization with DNA and Recombinant Adenoviral Vaccine Vectors Expressing Gag. J Virol. 2005;79(24): 15547–15555.

161. Buchbinder SP, Mehrotra D V, Duerr A, Fitzgerald DW, Mogg R, Li D, et al. Efficacy assessment of a cell-mediated immunity HIV-1 vaccine (the Step Study): a double-blind, randomised, placebo-controlled, test-of-concept trial. Lancet. 2008;372: 1881–1893.

162. Gray GE, Allen M, Moodie Z, Churchyard G, Bekker L, Nchabeleng M, et al. Safety and efficacy of the HVTN 503/Phambili Study of a clade-B-based HIV-1 vaccine in South Africa : a double-blind, randomised, placebo-controlled test-of-concept phase 2b study. Lancet Infect Dis. 2011;11: 507–515.

163. McElrath MJ, De Rosa SC, Moodie Z, Dubey S, Kierstead L, Janes H, et al. HIV-1 vaccine-induced immunity in the test-of-concept Step Study : a case – cohort analysis. Lancet. 2008;372(9653): 1894–1905.

164. Huang Y, Follmann D, Nason M, Zhang L, Huang Y, Mehrotra D V., et al. Effect of rAd5-vector HIV-1 preventive vaccines on HIV-1 acquisition: A participant-level meta-analysis of randomized trials. PLoS One. 2015;10(9): 1–19.

165. Duerr A, Huang Y, Buchbinder S, Coombs RW, Sanchez J, Del Rio C, et al. Extended follow-up confirms early vaccine-enhanced risk of HIV acquisition and demonstrates waning effect over time among participants in a randomized trial of recombinant adenovirus HIV vaccine (Step Study). J Infect Dis. 2012;206(2): 258–266.

166. Gray GE, MBBCH, Moodie Z, Metch B, Gilbert PB, Bekker L-G, et al. The phase 2b HVTN 503/Phambili study test-of-concept HIV vaccine study, investigating a recombinant adenovirus type 5 HIV gag/pol/nef vaccine in South Africa: unblinded, long-term follow-up. Lancet Infect Dis. 2014;14(5): 388–396.

167. Qureshi H, Ma Z-M, Huang Y, Hodge G, Thomas MA, DiPasquale J, et al. Low-Dose Penile SIVmac251 Exposure of Rhesus Macaques Infected with Adenovirus Type 5 (Ad5) and Then Immunized with a Replication-Defective Ad5-Based SIV gag/pol/nef Vaccine Recapitulates the Results of the Phase IIb Step Trial of a Similar HIV-1 Vaccine. J Virol. 2012;86(4): 2239–2250.

168. Benlahrech A, Harris J, Meiser A, Papagatsias T, Hornig J, Hayes P, et al. Adenovirus vector vaccination induces expansion of memory CD4 T cells with a mucosal homing phenotype that are readily susceptible to HIV-1. Proc Natl Acad Sci. 2009;106(47): 19940–19945.

169. Perreau M, Pantaleo G, Kremer EJ. Activation of a dendritic cell–T cell axis by Ad5 immune complexes creates an improved environment for replication of HIV in T cells. J Exp Med. 2008;205(12): 2717–2725.

170. Hutnick NA, Carnathan DG, Dubey SA, Cox KS, Kierstead L, Ratcliffe SJ, et al. Baseline Ad5 serostatus does not predict Ad5 HIV vaccine–induced expansion of adenovirus-specific CD4+ T cells. Nat Med. 2009;15(8): 876–878.

171. O'Brien KL, Liu J, King SL, Sun Y-H, Schmitz JE, Lifton MA, et al. Adenovirus-specific immunity after immunization with an Ad5 HIV-1 vaccine candidate in humans. Nat Med. 2009;15(8): 873–875.

172. Masek-Hammerman K, Li H, Liu J, Abbink P, La Porte A, O'Brien KL, et al. Mucosal Trafficking of Vector-Specific CD4+ T Lymphocytes following

Vaccination of Rhesus Monkeys with Adenovirus Serotype 5. J Virol. 2010;84(19): 9810–9816.

173. Gray G, Buchbinder S, Duerr A. Overview of STEP and Phambili trial results: two phase IIb test of concept studies investigating the efficacy of MRK ad5 gag/pol/nef sub-type B HIV vaccine. Curr Opin HIV AIDS. 2010;5(5): 357–361.

174. Barouch DH, Korber B. HIV-1 vaccine development after STEP. Annu Rev Med. 2010;61(13): 153–67.

175. Zak DE, Andersen-Nissen E, Peterson ER, Sato A, Hamilton MK, Borgerding J, et al. Merck Ad5/HIV induces broad innate immune activation that predicts CD8+ T-cell responses but is attenuated by preexisting Ad5 immunity. PNAS. 2012;109(50): E3503–E3512.

176. Fauci AS, Marovich MA, Dieffenbach CW, Hunter E, Buchbinder SP. Immune Activation with HIV Vaccines. Science. 2014;344(6179): 49–51.

177. Graham BS, Enama ME, Nason MC, Gordon IJ, Peel SA, Ledgerwood JE, et al. DNA Vaccine Delivered by a Needle-Free Injection Device Improves Potency of Priming for Antibody and CD8+ T-Cell Responses after rAd5 Boost in a Randomized Clinical Trial. PLoS One. 2013;8(4).

178. Hammer SM, Sobieszczyk ME, Janes H, Karuna ST, Mulligan MJ, Grove D, et al. Efficacy Trial of a DNA/rAd5 HIV-1 Preventive Vaccine. N Engl J Med. 2013;369(22): 2083–2092.

179. Letvin NL, Rao SS, Montefiori DC, Seaman MS, Sun Y, Lim S-Y, et al. Immune and Genetic Correlates of Vaccine Protection Against Mucosal Infection by SIV in Monkeys. Sci Transl Med. 2011;3(81): 81ra36.

180. Fauci A, Johnston M, Dieffenbach C. HIV vaccine research: the way forward. Science. 2008;530.

181. Watkins DI, Burton DR, Kallas EG, Moore JP, Koff WC. Nonhuman primate models and the failure of the Merck HIV-1 vaccine in humans. Nat Med. 2008;14(6): 617–621.

182. Barouch DH, Alter G, Broge T, Linde C, Ackerman ME, Brown EP, et al. Protective efficacy of adenovirus/protein vaccines against SIV challenges in rhesus monkeys. Science. 2015;896(2014): 597–598.

183. Abbink P, Lemckert AAC, Ewald BA, Lynch DM, Denholtz M, Smits S, et al. Comparative Seroprevalence and Immunogenicity of Six Rare Serotype Recombinant Adenovirus Vaccine Vectors from Subgroups B and D. J Virol. 2007;81(9): 4654–4663.

184. Baden LR, Walsh SR, Seaman MS, Tucker RP, Krause KH, Patel A, et al. First-in-human evaluation of the safety and immunogenicity of a recombinant adenovirus serotype 26 HIV-1 Env vaccine (IPCAVD 001). J Infect Dis. 2013;207(2): 240–247.

185. Keefer MC, Gilmour J, Hayes P, Gill D, Kopycinski J, Cheeseman H, et al. A phase I double blind, placebo-controlled, randomized study of a multigenic HIV-1 adenovirus subtype 35 vector vaccine in healthy uninfected adults. PLoS One. 2012;7(8).

186. Capone S, D'Alise AM, Ammendola V, Colloca S, Cortese R, Nicosia A, et al. Development of chimpanzee adenoviruses as vaccine vectors: challenges and successes emerging from clinical trials. Expert Rev Vaccines. 2013;12(4): 379–393.

187. Rerks-Ngarm S, Pitisuttithum P, Nitayaphan S, Kaewkungwal J, Chiu J, Paris R, et al. Vaccination with ALVAC and AIDSVAX to prevent HIV-1 infection in Thailand. N Engl J Med. 2009;361(23): 2209–20.

188. Montefiori DC, Safrit JT, Lydy SL, Barry AP, Bilska M, Vo HTT, et al. Induction of Neutralizing Antibodies and Gag-Specific Cellular Immune Responses to an R5 Primary Isolate of Human Immunodeficiency Virus Type 1 in Rhesus Macaques. J Virol. 2001;75(13): 5879–5890.

189. Salmon-Ceron D, Excler J-L, Finkielsztejn L, Autran B, Gluckman J-C, Sicard D, et al. Safety and Immunogenicity of a Live Recombinant Canarypox Virus Expressing HIV Type 1 gp120 MN tm/gag/protease LAI (ALVAC-HIV, vCP205) Followed by a p24E-V3 MN Synthetic Peptide (CLTB-36) Administered in Healthy Volunteers at Low Risk for HIV Infection. AIDS Res Hum Retroviruses. 1999;15(7): 633–645.

190. Cao H, Kaleebu P, Hom D, Flores J, Agrawal D, Jones N, et al. Immunogenicity of a Recombinant Human Immunodeficiency Virus (HIV)–Canarypox Vaccine in HIV‐Seronegative Ugandan Volunteers: Results of the HIV Network for Prevention Trials 007 Vaccine Study. J Infect Dis. 2003;187(6): 887–895.

191. Burton DR, Desrosiers RC, Doms RW, Feinberg MB, Gallo RC, Hahn B, et al. A sound rationale needed for phase III HIV-1 vaccine trials. Science. 2004;303(5656): 316.

192. Haynes B, Tomaras GD, Ph D, Alam SM, Evans DT, Montefiori DC, et al. Immune-Correlates Analysis of an HIV-1 Vaccine Efficacy Trial. N Engl J Med. 2012;366(14): 1275–1286.

193. Gilbert P, Wang M, Wrin T, Petropoulos C, Gurwith M, Sinangil F, et al. Magnitude and breadth of a nonprotective neutralizing antibody response in an efficacy trial of a candidate HIV-1 gp120 vaccine. J Infect Dis.

2010;202(4): 595–605.

194. Dugast AS, Chan Y, Hoffner M, Licht A, Nkolola J, Li H, et al. Lack of protection following passive transfer of polyclonal highly functional low-dose non-neutralizing antibodies. PLoS One. 2014;9(5).

195. Burton DR, Hessell AJ, Keele BF, Klasse PJ, Ketas TA, Moldt B, et al. Limited or no protection by weakly or nonneutralizing antibodies against vaginal SHIV challenge of macaques compared with a strongly neutralizing antibody. Proc Natl Acad Sci. 2011;108(27): 11181–11186.

196. Bonsignori M, Pollara J, Moody MA, Alpert MD, Chen X, Hwang K-K, et al. Antibody-dependent cellular cytotoxicity-mediating antibodies from an HIV-1 vaccine efficacy trial target multiple epitopes and preferentially use the VH1 gene family. J Virol. 2012;86(21): 11521–32.

197. Tolbert WD, Gohain N, Veillette M, Chapleau JP, Orlandi C, Visciano ML, et al. Paring Down HIV Env: Design and Crystal Structure of a Stabilized Inner Domain of HIV-1 gp120 Displaying a Major ADCC Target of the A32 Region. Structure. 2016;24(5): 697–709.

198. Guan Y, Pazgier M, Sajadi MM, Kamin-lewis R, Al-darmarki S, Flinko R, et al. Diverse specificity and effector function among human antibodies to HIV-1 envelope glycoprotein epitopes exposed by CD4 binding. PNAS. 2012;110(1): 69–78.

199. Pollara J, Bonsignori M, Moody MA, Pazgier M, Haynes BF, Ferrari G. Epitope specificity of human immunodeficiency virus-1 antibody dependent cellular cytotoxicity [ADCC] responses. Curr HIV Res. 2013;11(5): 378–87.

200. Veillette M, Coutu M, Richard J, Batraville L-A, Dagher O, Bernard N, et al. The HIV-1 gp120 CD4-bound conformation is preferentially targeted by antibody-dependent cellular cytotoxicity-mediating antibodies in sera from HIV-1-infected individuals. J Virol. 2015;89(1): 545–51.

201. Tomaras GD, Ferrari G, Shen X, Alam SM, Liao H-X, Pollara J, et al. Vaccine-induced plasma IgA specific for the C1 region of the HIV-1 envelope blocks binding and effector function of IgG. PNAS. 2013;

202. Liao H-X, Bonsignori M, Alam SM, McLellan JS, Tomaras GD, Moody MA, et al. Vaccine Induction of Antibodies against a Structurally Heterogeneous Site of Immune Pressure within HIV-1 Envelope Protein Variable Regions 1 and 2. Immunity. 2013;38(1): 176–86.

203. Pollara J, Bonsignori M, Moody MA, Liu P, Alam SM, Hwang K-K, et al. HIV-1 Vaccine-Induced C1 and V2 Env-Specific Antibodies Synergize for Increased Antiviral Activities. J Virol. 2014;88(14): 7715–26.

204. Karasavvas N, Billings E, Rao M, Williams C, Zolla-Pazner S, Bailer RT, et al. The Thai Phase III HIV Type 1 Vaccine trial (RV144) regimen induces antibodies that target conserved regions within the V2 loop of gp120. AIDS Res Hum Retroviruses. 2012;28(11): 1444–57.

205. Zolla-Pazner S, Decamp AC, Cardozo T, Karasavvas N, Gottardo R, Williams C, et al. Analysis of V2 Antibody Responses Induced in Vaccinees in the ALVAC/AIDSVAX HIV-1 Vaccine Efficacy Trial. PLoS One. 2013;8(1): e53629.

206. Rolland M, Edlefsen PT, Larsen BB, Tovanabutra S, Sanders-Buell E, Hertz T, et al. Increased HIV-1 vaccine efficacy against viruses with genetic signatures in Env V2. Nature. 2012;490(7420): 417–20.

207. Edlefsen PT, Rolland M, Hertz T, Tovanabutra S, Gartland AJ, DeCamp AC, et al. Comprehensive sieve analysis of breakthrough HIV-1 sequences in the RV144 vaccine efficacy trial. PLoS Comput Biol. 2015;11(2): e1003973.

208. Alam SM, Liao H-X, Tomaras GD, Bonsignori M, Tsao C-Y, Hwang K-K, et al. Antigenicity and immunogenicity of RV144 vaccine AIDSVAX clade E envelope immunogen is enhanced by a gp120 N-terminal deletion. J Virol. 2013;87(3): 1554–68.

209. Yates NL, Liao H-X, Fong Y, DeCamp A, Vandergrift NA, Williams WT, et al. Vaccine-Induced Env V1–V2 IgG3 Correlates with Lower HIV-1 Infection Risk and Declines Soon After Vaccination. Sci Trans Med. 2014;6(228): 228ra39.

210. Safety of and Immune Response to Vaccination With 2 Experimental HIV Vaccines in Healthy Adults (HVTN 097). In: ClinicalTrials.gov [Internet]. 2014 [cited 21 Jul 2017]. Available: https://clinicaltrials.gov/ct2/show/NCT02109354

211. A Safety and Immune Response Study of 2 Experimental HIV Vaccines. In: ClinicalTrials.gov [Internet]. 2015 [cited 21 Jul 2017]. Available: https://clinicaltrials.gov/ct2/show/NCT02404311

212. Study of Late Boost Strategies for HIV-uninfected Participants From Protocol RV 144. In: ClinicalTrials.gov [Internet]. 2017 [cited 21 Jul 2017]. Available: https://clinicaltrials.gov/ct2/show/NCT01435135

213. Study of Boosting Strategies After Vaccination With ALVAC-HIV and AIDSVAX® B/E. In: ClinicalTrials.gov [Internet]. 2017 [cited 21 Jul 2017]. Available: https://clinicaltrials.gov/ct2/show/NCT01931358

214. Pivotal Phase 2b/3 ALVAC/Bivalent gp120/MF59 HIV Vaccine Prevention Safety and Efficacy Study in South Africa (HVTN702). In: ClinicalTrials.gov

[Internet]. 2016 [cited 21 Jul 2017]. Available: https://clinicaltrials.gov/ct2/show/NCT02968849

215. Easterhoff D, Moody MA, Fera D, Cheng H, Ackerman M, Wiehe K, et al. Boosting of HIV envelope CD4 binding site antibodies with long variable heavy third complementarity determining region in the randomized double blind RV305 HIV-1 vaccine trial. Plos Pathog. 2017;13(2): e1006182.

216. HIV Vaccine Trials Network. Ongoing HVTN Trials [Internet]. 2016 [cited 20 May 2017]. Available: https://www.hvtn.org/content/dam/hvtn/Science/studies/HVTN Trials%2C March 2017_ HVTN website.pdf

217. Bekker L-G. Meeting the “Go” criteria: immunogenicity from HVTN100, a phase 1-2 randomized, double-blind, placebo-controlled trial of clade C ALVAC-® (vCP2438) and bivalent subtype C gp120/MF59®in HIV-uninfected South African adults. 21st International AIDS Conference, Durban (Abstract). 2016. Available: http://programme.aids2016.org/Abstract/Abstract/10652

218. Vaccari M, Gordon SN, Fourati S, Schifanella L, Liyanage NPM, Cameron M, et al. Adjuvant-dependent innate and adaptive immune signatures of risk of SIVmac251 acquisition. Nat Med. 2016;22(7): 762–770.

219. Zolla-Pazner S, Powell R, Yahyaei S, Williams C, Jiang X, Li W, et al. Rationally Designed Vaccines Targeting the V2 Region of HIV-1 gp120 Induce a Focused, Cross-Clade-Reactive, Biologically Functional Antibody Response. J Virol. 2016;90(24): 10993–11006.

220. Kwong PD, Mascola JR, Nabel GJ. Rational Design of Vaccines to Elicit Broadly Neutralizing Antibodies to HIV-1. Cold Spring Harb Perspect Med. 2011;1: a007278.

221. Moore PL, Gray ES, Wibmer CK, Bhiman JN, Nonyane M, Sheward DJ, et al. Evolution of an HIV glycan – dependent broadly neutralizing antibody epitope through immune escape. Nat Med. 2012;18(11): 1688–1693.

222. Wibmer CK, Gorman J, Ozorowski G, Bhiman JN, Sheward DJ, Elliott DH, et al. Structure and Recognition of a Novel HIV-1 gp120-gp41 Interface Antibody that Caused MPER Exposure through Viral Escape. Plos Pathog. 2017;13(1): e1006074.

223. Bonsignori M, Zhou T, Sheng Z, Liao H, Peter D, Haynes BF. Maturation Pathway from Germline to Broad HIV-1 Neutralizer of a CD4-Mimic Antibody Article Maturation Pathway from Germline to Broad HIV-1 Neutralizer of a CD4-Mimic Antibody. 2016; 1–15.

224. Saunders KO, Nicely NI, Wiehe K, Bonsignori M, Meyerhoff RR, Parks R,

et al. Vaccine Elicitation of High Mannose-Dependent Neutralizing Antibodies against the V3-Glycan Broadly Neutralizing Epitope in Nonhuman Primates. Cell Rep. 2017;18(9): 2175–2188.

225. Bonsignori M, Liao HX, Gao F, Williams WB, Alam SM, Montefiori DC, et al. Antibody-virus co-evolution in HIV infection: paths for HIV vaccine development. Immunol Rev. 2017;275(1): 145–160.

226. Sok D, Briney B, Jardine JG, Kulp DW, Menis S, Pauthner M, et al. Priming HIV-1 broadly neutralizing antibody precursors in human Ig loci transgenic mice. Science. 2016;353(6307): 1557.

227. Jardine JG, Ota T, Sok D, Pauthner M, Kulp DW, Kalyuzhniy O, et al. Priming a broadly neutralizing antibody response to HIV-1 using a germline-targeting immunogen. Science. 2015;349(6244): 156–161.

228. Jardine J, Julien J-P, Menis S, Ota T, Kalyuzhniy O, McGuire A, et al. Rational HIV Immunogen Design to Target Specific Germline B Cell Receptors. Science. 2013;340(6133): 711–16.

229. Jardine JG, Kulp DW, Havenar-Daughton C, Sarkar A, Briney B, Sok D, et al. HIV-1 broadly neutralizing antibody precursor B cells revealed by germline-targeting immunogen. Science. 2016;351(6280): 1458.

230. Mcguire AT, Glenn JA, Lippy A, Stamatatos L. Diverse Recombinant HIV-1 Envs Fail To Activate B Cells Expressing the Germline B Cell Receptors of the Broadly Neutralizing Anti-HIV-1. 2014;88(5): 2645–2657.

231. Ota T, Doyle-Cooper C, Cooper AB, Huber M, Falkowska E, Doores KJ, et al. Anti-HIV B Cell lines as candidate vaccine biosensors. J Immunol. 2012;189(10): 4816–24.

232. Mcguire AT, Gray MD, Dosenovic P, Gitlin AD, Freund NT, Petersen J, et al. Specifically modified Env immunogens activate antibodies in transgenic mice. Nat Commun. 2016;7: 1–10.

233. Dosenovic P, Soldemo M, Scholz JL, O'Dell S, Grasset EK, Pelletier N, et al. BLyS-mediated modulation of naive B cell subsets impacts HIV Env-induced antibody responses. J Immunol. 2012;188(12): 6018–26.

234. Melchers M, Bontjer I, Tong T, Chung NPY, Klasse PJ, Eggink D, et al. Targeting HIV-1 envelope glycoprotein trimers to B cells by using APRIL improves antibody responses. J Virol. 2012;86(5): 2488–500.

235. Kelsoe G, Haynes BF. Host controls of HIV broadly neutralizing antibody development. Immunol Rev. 2017;275: 79–88.

236. Munro JB, Gorman J, Ma X, Zhou Z, Arthos J, Burton DR, et al.

Conformational dynamics of single HIV-1 envelope trimers on the surface of native virions. Science. 2014;346(6210): 759–763.

237. Medina-ramı M, Sanders RW, Sattentau QJ. Stabilized HIV-1 envelope glycoprotein trimers for vaccine use. Curr Opin HIV AIDS. 2017;(12): 1–9.

238. Sanders RW, Vesanen M, Schuelke N, Master A, Schiffner L, Kalyanaraman R, et al. Stabilization of the soluble, cleaved, trimeric form of the envelope glycoprotein complex of human immunodeficiency virus type 1. J Virol. 2002;76(17): 8875–89.

239. Yasmeen A, Ringe R, Derking R, Cupo A, Julien JP, Burton DR, et al. Differential binding of neutralizing and non-neutralizing antibodies to native-like soluble HIV-1 Env trimers, uncleaved Env proteins, and monomeric subunits. Retrovirology. 2014;11(1): 41.

240. Klasse PJ, Depetris RS, Pejchal R, Julien J-P, Khayat R, Lee JH, et al. Influences on Trimerization and Aggregation of Soluble, Cleaved HIV-1 SOSIP Envelope Glycoprotein. J Virol. 2013;87(17): 9873–9885.

241. Julien J-P, Cupo A, Sok D, Stanfield RL, Lyumkis D, Deller MC, et al. Crystal Structure of a Soluble Cleaved HIV-1 Envelope Trimer. Science. 2013;342(6165): 1477–1484.

242. Lyumkis D, Julien J-P, de Val N, Cupo A, Potter CS, Klasse P-J, et al. Cryo-EM Structure of a Fully Glycosylated Soluble Cleaved HIV-1 Envelope Trimer. Science. 2013;342(6165): 1484–1490.

243. Pancera M, Zhou T, Druz A, Georgiev IS, Soto C, Gorman J, et al. Structure and immune recognition of trimeric pre-fusion HIV-1 Env. Nature. 2014;514(7523): 455–461.

244. McCoy LE, van Gils MJ, Ozorowski G, Ward AB, Sanders RW, Burton DR, et al. Holes in the Glycan Shield of the Native HIV Envelope Are a Target of Trimer-Elicited Neutralizing Antibodies. Cell Rep. 2016;16(9): 1–12.

245. Kwon Y Do, Pancera M, Acharya P, Georgiev IS, Crooks ET, Gorman J, et al. Crystal structure, conformational fixation and entry-related interactions of mature ligand-free HIV-1 Env. Nat Struct Mol Biol. 2015;22(7): 522–531.

246. Klasse PJ, Labranche CC, Ketas TJ, Ozorowski G, Cupo A, Pugach P, et al. Sequential and Simultaneous Immunization of Rabbits with HIV-1 Envelope Glycoprotein SOSIP.664 Trimers from Clades A, B and C. Plos Pathog. 2016; 1–31.

247. Sharma SK, deVal N, Bale S, Guenaga J, Tran K, Feng Y, et al. Cleavage-Independent HIV-1 Env Trimers Engineered as Soluble Native Spike Mimetics for Vaccine Design. Cell Rep. 2015;11(4): 539–550.

248. Guenaga J, Dubrovskaya V, de Val N, Sharma SK, Carrette B, Ward AB, et al. Structure-Guided Redesign Increases the Propensity of HIV Env To Generate Highly Stable Soluble Trimers. J Virol. 2016;90(6): 2806–2817.

249. Liang Y, Guttman M, Williams JA, Verkerke H, Alvarado D, Hu S-L, et al. Changes in structure and antigenicity of HIV-1 Env trimers resulting from removal of a conserved CD4 binding site-proximal glycan. J Virol. 2016;90(20): 9224–36.

250. Ingale J, Stano A, Guenaga J, Sharma SK, Nemazee D, Zwick MB, et al. High-Density Array of Well-Ordered HIV-1 Spikes on Synthetic Liposomal Nanoparticles Efficiently Activate B Cells. Cell Rep. 2016;15(9): 1986–1999.

251. Hansen SG, Ford JC, Lewis MS, Ventura AB, Hughes CM, Coyne-Johnson L, et al. Profound early control of highly pathogenic SIV by an effector memory T-cell vaccine. Nature. 2011;473(7348): 523–7.

252. Hansen SG, Jr MP, Ventura AB, Hughes CM, Gilbride RM, Ford JC, et al. Immune clearance of highly pathogenic SIV infection. Nature. 2013;502(7469): 100–104.

253. Hansen SG, Vieville C, Whizin N, Coyne-Johnson L, Siess DC, Drummond DD, et al. Effector memory T cell responses are associated with protection of rhesus monkeys from mucosal simian immunodeficiency virus challenge. Nat Med. 2009;15(3): 293–9.

254. Hansen SG, Sacha JB, Hughes CM, Ford JC, Burwitz BJ, Scholz I, et al. Cytomegalovirus Vectors Violate CD8+ T Cell Epitope Recognition Paradigms. Science. 2013;340(6135): 1237874–1237874.

255. Hansen SG, Wu HL, Burwitz BJ, Hughes CM, Hammond KB, Ventura AB, et al. Broadly targeted CD8+ T cell responses restricted by major histocompatibility complex E. Science. 2016;351(6274): 714.

256. Collaboration for AIDS Vaccine Discovery. Picker: Development of Attenuated CMV Vectors for an HIV/AIDS Vaccine [Internet]. [cited 12 Jun 2017]. Available: https://www.cavd.org/grantees/Pages/Grantee-Picker1.aspx

257. Havenar-Daughton C, Lee JH, Crotty S. Tfh cells and HIV bnAbs, an immunodominance model of the HIV neutralizing antibody generation problem. Immunol Rev. 2017;275(1): 49–61.

258. De Silva NS, Klein U. Dynamics of B cells in germinal centres. Nat Rev Immunol. 2015;15(3): 137–148.

259. Vinuesa CG, Linterman MA, Yu D, MacLennan ICM. Follicular Helper T

Cells. Annu Rev Immunol. 2016;34(1): 335–368.

260. Qi H. T follicular helper cells in space-time. Nat Rev Immunol. 2016;16(10): 612–625.

261. Weisel FJ, Zuccarino-Catania G V., Chikina M, Shlomchik MJ. A Temporal Switch in the Germinal Center Determines Differential Output of Memory B and Plasma Cells. Immunity. 2016;44(1): 116–130.

262. Good-Jacobson KL, Szumilas CG, Chen L, Sharpe AH, Tomayko MM, Shlomchik MJ. PD-1 regulates germinal center B cell survival and the formation and affinity of long-lived plasma cells. Nat Immunol. 2010;11(6): 535–542.

263. Breitfeld D, Ohl L, Kremmer E, Ellwart J, Sallusto F, Lipp M, et al. Follicular B helper T cells express CXC chemokine receptor 5, localize to B cell follicles, and support immunoglobulin production. J Exp Med. 2000;192(11): 1545–52.

264. Schaerli P, Willimann K, Lang AB, Lipp M, Loetscher P, Moser B. CXC chemokine receptor 5 expression defines follicular homing T cells with B cell helper function. J Exp Med. 2000;192(11): 1553–62.

265. Locci M, Wu JE, Arumemi F, Mikulski Z, Dahlberg C, Miller AT, et al. Activin A programs the differentiation of human TFH cells. Nat Immunol. 2016;17(8): 976–984.

266. Schmitt N, Liu Y, Bentebibel S-E, Munagala I, Bourdery L, Venuprasad K, et al. The cytokine TGF-β co-opts signaling via STAT3-STAT4 to promote the differentiation of human TFH cells. Nat Immunol. 2014;15(9): 856–865.

267. Ray JP, Marshall HD, Laidlaw BJ, Staron MM, Kaech SM, Craft J. Transcription factor STAT3 and type I interferons are corepressive insulators for differentiation of follicular helper and T helper 1 cells. Immunity. 2014;40(3): 367–377.

268. Coltart CEM, Lindsey B, Ghinai I, Johnson AM, Heymann DL. The Ebola outbreak, 2013–2016: old lessons for new epidemics. Philos Trans R Soc B Biol Sci. 2017;372(1721): 20160297.

269. World Health Organization. Situation Report: Ebola Virus Disease [Internet]. 2016 [cited 20 May 2017]. Available: http://apps.who.int/iris/bitstream/10665/208883/1/ebolasitrep_10Jun2016_eng.pdf?ua=1

270. Jones SM, Feldmann H, Ströher U, Geisbert JB, Fernando L, Grolla A, et al. Live attenuated recombinant vaccine protects nonhuman primates against Ebola and Marburg viruses. Nat Med. 2005;11(7): 786–790.

271. Henao-Restrepo AM, Longini IM, Egger M, Dean NE, Edmunds WJ, Camacho A, et al. Efficacy and effectiveness of an rVSV-vectored vaccine expressing Ebola surface glycoprotein: interim results from the Guinea ring vaccination cluster-randomised trial. Lancet. 2015;386(9996): 857–866.

272. Pavot V. Ebola virus vaccines: Where do we stand? Clin Immunol. 2016;173: 44–49.

273. Ye Q, Liu Z-Y, Han J-F, Jiang T, Li X-F, Qin C-F. Genomic characterization and phylogenetic analysis of Zika virus circulating in the Americas. Infect Genet Evol. 2016;43: 43–49.

274. Dick GWA. Zika Virus (I). Isolations and serological specificity. Trans R Soc Trop Med Hyg. 1952;46(5): 509–520.

275. Dick GWA. Zika Virus (II) Pathogenicity and Physical Properties. Trans R Soc Trop Med Hyg. 1952;46(5): 521–534.

276. Musso D, Gubler D. Zika Virus. Clin Microbiol Rev. 2016;29(3): 487–503.

277. Musso D, Roche C, Robin E, Nhan T, Teissier A, Cao-Lormeau VM. Potential sexual transmission of zika virus. Emerg Infect Dis. 2015;21(2): 359–361.

278. D'Ortenzio E, Matheron S, Lamballerie X de, Hubert B, Piorkowski G, Maquart M, et al. Evidence of Sexual Transmission of Zika Virus. N Engl J Med. 2016;374(22): 2193–2195.

279. Cao-Lormeau VM, Blake A, Mons S, Lastere S, Roche C, Vanhomwegen J, et al. Guillain-Barré Syndrome outbreak caused by ZIKA virus infection in French Polynesia. Lancet. 2017;387(10027): 1531–1539.

280. Mlakar J, Korva M, Tul N, Popović M, Poljšak-Prijatelj M, Mraz J, et al. Zika Virus Associated with Microcephaly. N Engl J Med. 2016;374(10): 951–8.

281. Centers for Disease Control and Prevention. Facts about Microcephaly [Internet]. 2016 [cited 12 Jun 2017]. Available: https://www.cdc.gov/ncbddd/birthdefects/microcephaly.html

282. Calvet G, Aguiar RS, Melo ASO, Sampaio SA, de Filippis I, Fabri A, et al. Detection and sequencing of Zika virus from amniotic fluid of fetuses with microcephaly in Brazil: a case study. Lancet Infect Dis. 2016;16(6): 653–660.

283. Cauchemez S, Besnard M, Bompard P, Dub T, Guillemette-artur P, Eyrolle-guignot D, et al. Association between Zika virus and microcephaly in French Polynesia , 2013 – 15 : a retrospective study. Lancet. 2016;387: 2125–2132.

284. Miner JJ, Cao B, Govero J, Smith AM, Fernandez E, Cabrera OH, et al. Zika Virus Infection during Pregnancy in Mice Causes Placental Damage and Fetal Demise. Cell. 2016;165: 1–11.

285. Li C, Xu D, Ye Q, Hong S, Jiang Y, Liu X, et al. Zika Virus Disrupts Neural Progenitor Development and Leads to Microcephaly in Mice. Cell Stem Cell. 2016;19: 1–7.

286. Tang H, Hammack C, Ogden SC, Wen Z, Qian X, Li Y, et al. Zika Virus Infects Human Cortical Neural Progenitors and Attenuates Their Growth. Cell Stem Cell. 2016;44(4): 193–194.

287. Vermillion MS, Lei J, Shabi Y, Baxter VK, Crilly NP, Mclane M, et al. Intrauterine Zika virus infection of pregnant immunocompetent mice models transplacental transmission and adverse perinatal outcomes. Nat Commun. 2017;8: 14575.

288. Brasil P, Pereira JP, Moreira ME, Ribeiro Nogueira RM, Damasceno L, Wakimoto M, et al. Zika Virus Infection in Pregnant Women in Rio de Janeiro. N Engl J Med. 2016;375(24): 2321–2334.

289. Pan American Health Organization/World Health Organization. Zika Cumulative Cases [Internet]. 2017 [cited 12 Jun 2017]. Available: http://www.paho.org/hq/index.php?option=com_content&view=article&id=12390&Itemid=42090&lang=en

290. WHO, UNICEF. Zika Virus Vaccine Target Product Profile [Internet]. 2016. Available: http://www.who.int/immunization/research/meetings_workshops/WHO_Zika_vaccine_TPP.pdf

291. Dowd KA, DeMaso CR, Pelc RS, Speer SD, Smith ARY, Goo L, et al. Broadly Neutralizing Activity of Zika Virus-Immune Sera Identifies a Single Viral Serotype. Cell Rep. 2016;16(6): 1485–91.

292. Sirohi D, Chen Z, Sun L, Klose T, Pierson TC, Rossmann MG, et al. The 3.8 Å resolution cryo-EM structure of Zika virus. Science. 2016;5316: 1–7.

293. Kostyuchenko VA, Lim EXY, Zhang S, Fibriansah G, Ng T-S, Ooi JSG, et al. Structure of the thermally stable Zika virus. Nature. 2016;

294. Fernandez E, Diamond MS. Vaccination strategies against Zika virus. Curr Opin Virol. 2017;23: 59–67.

295. Larocca RA, Abbink P, Peron JPS, Zanotto PM de A, Iampietro MJ, Badamchi-Zadeh A, et al. Vaccine protection against Zika virus from Brazil. Nature. 2016;536(7617): 474–478.

296. Haddow AD, Schuh AJ, Yasuda CY, Kasper MR, Heang V, Huy R, et al. Genetic characterization of zika virus strains: Geographic expansion of the asian lineage. PLoS Negl Trop Dis. 2012;6(2): e1477.

297. Abbink P, Larocca RA, De La Barrera RA, Bricault CA, Moseley ET, Boyd M, et al. Protective efficacy of multiple vaccine platforms against Zika virus challenge in rhesus monkeys. Science. 2016;353(6304): 1129–1132.

298. Dowd KA, Ko S, Morabito KM, Yang ES, Pelc RS, Christina R, et al. Rapid development of a DNA vaccine for Zika virus. Science. 2016;354(6309): 237–240.

299. Muthumani K, Griffin BD, Agarwal S, Kudchodkar SB, Reuschel EL, Choi H, et al. In vivo protection against ZIKV infection and pathogenesis through passive antibody transfer and active immunisation with a prMEnv DNA vaccine. npj Vaccines. 2016;1(August): 16021.

300. Kim E, Erdos G, Huang S, Kenniston T, Falo LD, Gambotto A. Preventative Vaccines for Zika Virus Outbreak: Preliminary Evaluation. EBioMedicine. 2016;13: 315–320.

301. Shan C, Muruato AE, Nunes BTD, Luo H, Xie X, Medeiros DBA, et al. A live-attenuated Zika virus vaccine candidate induces sterilizing immunity in mouse models. Nat Med. 2017;(December 2016): 1–7.

302. Petsch B, Schnee M, Vogel AB, Lange E, Hoffmann B, Voss D, et al. Protective efficacy of in vitro synthesized, specific mRNA vaccines against influenza A virus infection. Nat Biotechnol. 2012;30(12): 1210–1216.

303. Sahin U, Kariko K, Tureci O. mRNA-based therapeutics - developing a new class of drugs. Nat Rev Drug Discov. 2014;13(10): 759–780.

304. Chahal JS, Khan OF, Cooper CL, Mcpartlan JS, Tsosie JK. Dendrimer-RNA nanoparticles generate protective immunity against lethal Ebola, H1N1 influenza, and Toxoplasma gondii challenges with a single dose. Proc Natl Acad Sci. 2016;113(35): E5250–E5250.

305. Bahl K, Senn JJ, Yuzhakov O, Bulychev A, Brito LA, Hassett KJ, et al. Preclinical and Clinical Demonstration of Immunogenicity by mRNA Vaccines against H10N8 and H7N9 Influenza Viruses. Mol Ther. 2017;25(6): 1–12.

306. Richner JM, Himansu S, Dowd KA, Butler SL, Salazar V, Fox JM, et al. Modified mRNA Vaccines Protect against Zika Virus Infection. Cell. 2017;168: 1–12.

307. Pardi N, Hogan MJ, Pelc RS, Muramatsu H, Andersen H, DeMaso CR, et al. Zika virus protection by a single low-dose nucleoside-modified mRNA

vaccination. Nature. 2017;543: 248–251.

308. Islam MA, Reesor EKG, Xu Y, Zope HR, Bruce R, Shi J, et al. Biomaterials for RNA Delivery. Biomater Sci. 2015;3(12): 1519–1533.

309. Pardi N, Tuyishime S, Muramatsu H, Kariko K, Mui BL, Tam YK, et al. Expression kinetics of nucleoside-modified mRNA delivered in lipid nanoparticles to mice by various routes. J Control Release. 2015;217: 345–351.

310. Karikó K, Kuo A, Barnathan E. Overexpression of urokinase receptor in mammalian cells following administration of the in vitro transcribed encoding mRNA. Gene Ther. 1999;6: 1092–1100.

311. Karikó K, Muramatsu H, Ludwig J, Weissman D. Generating the optimal mRNA for therapy: HPLC purification eliminates immune activation and improves translation of nucleoside-modified, protein-encoding mRNA. Nucleic Acids Res. 2011;39(21): 1–10.

312. Anderson BR, Muramatsu H, Nallagatla SR, Bevilacqua PC, Sansing LH, Weissman D, et al. Incorporation of pseudouridine into mRNA enhances translation by diminishing PKR activation. Nucleic Acids Res. 2010;38(17): 5884–5892.

313. Donovan J, Whitney G, Rath S, Korennykh A. Structural mechanism of sensing long dsRNA via a noncatalytic domain in human oligoadenylate synthetase 3. Proc Natl Acad Sci. 2015;112(13): 3949–3954.

314. Nanduri S, Carpick BW, Yang Y, Williams BRG, Qin J. Structure of the double-stranded RNA binding domain of the protein kinase PKR reveals the molecular basis of its dsRNA-mediated activation. Embo J. 1998;17(18): 5458–65.

315. Li Y, Banerjee S, Wang Y, Goldstein SA, Dong B, Gaughan C, et al. Activation of RNase L is dependent on OAS3 expression during infection with diverse human viruses. Proc Natl Acad Sci. 2016;113(8): 2241–2246.

316. Tanji H, Ohto U, Shibata T, Taoka M, Yamauchi Y, Isobe T, et al. Toll-like receptor 8 senses degradation products of single-stranded RNA. Nat Struct Mol Biol. 2015;22(2): 109–115.

317. Zhang Z, Ohto U, Shibata T, Krayukhina E, Taoka M, Yamauchi Y, et al. Structural Analysis Reveals that Toll-like Receptor 7 Is a Dual Receptor for Guanosine and Single-Stranded RNA. Immunity. 2016;45: 1–12.

318. Karikó K, Muramatsu H, Welsh FA, Ludwig J, Kato H, Weissman D. Incorporation of Pseudouridine Into mRNA Yields Superior Nonimmunogenic Vector With Increased Translational Capacity and

Biological Stability. Mol Ther. 2008;16(11): 1833–1840.

319. Karikó K, Buckstein M, Ni H, Weissman D. Suppression of RNA Recognition by Toll-like Receptors: The Impact of Nucleoside Modification and the Evolutionary Origin of RNA. Immunity. 2005;23: 165–175.

320. Andries O, Mc Cafferty S, De Smedt SC, Weiss R, Sanders NN, Kitada T. N1-methylpseudouridine-incorporated mRNA outperforms pseudouridine-incorporated mRNA by providing enhanced protein expression and reduced immunogenicity in mammalian cell lines and mice. J Control Release. 2015;217: 337–344.

321. Jensen S, Thomsen a. R. Sensing of RNA Viruses: a Review of Innate Immune Receptors Involved in Recognizing RNA Virus Invasion. J Virol. 2012;86(January): 2900–2910.

322. Weissman D, Pardi N, Muramatsu H, Karikó K. HPLC Purification of In Vitro Transcribed Long RNA. Methods Mol Biol. 2013;969: 43–54.

323. Miller MA, Ganesan AP V, Luckashenak N, Mendonca M, Eisenlohr LC. Endogenous antigen processing drives the primary CD4+ T cell response to influenza. Nat Med. 2015;21(10): 1216–1222.

324. Wolf AI, Mozdzanowska K, Quinn WJ, Metzgar M, Williams KL, Caton AJ, et al. Protective antiviral antibody responses in a mouse model of influenza virus infection. J Clin Invest. 2011;121(10): 3954–64.

325. Wyatt LS, Earl PL, Liu JY, Smith JM, Montefiori DC, Robinson HL, et al. Multiprotein HIV Type 1 Clade B DNA and MVA Vaccines: Construction, Expression, and Immunogenicity in Rodents of the MVA Component. AIDS Res Hum Retroviruses. 2004;20(6): 645–653.

326. Evans TG, Keefer MC, Weinhold KJ, Wolff M, Montefiori D, Gorse GJ, et al. A canarypox vaccine expressing multiple human immunodeficiency virus type 1 genes given alone or with rgp120 elicits broad and durable CD8+ cytotoxic T lymphocyte responses in seronegative volunteers. J Infect Dis. 1999;180(2): 290–8.

327. Kibuuka H, Kimutai R, Maboko L, Sawe F, Schunk MS, Kroidl A, et al. A phase 1/2 study of a multiclade HIV-1 DNA plasmid prime and recombinant adenovirus serotype 5 boost vaccine in HIV-Uninfected East Africans (RV 172). J Infect Dis. 2010;201(4): 600–7.

328. Wyatt LS, Belyakov IM, Earl PL, Berzofsky J a, Moss B. Enhanced cell surface expression, immunogenicity and genetic stability resulting from a spontaneous truncation of HIV Env expressed by a recombinant MVA. Virology. 2008;372(2): 260–72.

329. Ye L, Bu Z, Vzorov A, Taylor D, Compans RW, Yang C. Surface stability and immunogenicity of the human immunodeficiency virus envelope glycoprotein: role of the cytoplasmic domain. J Virol. 2004;78(24): 13409–19.

330. GBD 2015 HIV Collaborators. Estimates of global, regional, and national incidence, prevalence, and mortality of HIV, 1980–2015: the Global Burden of Disease Study 2015. Lancet HIV. 2016;3: e361-87.

331. Guttman M, Cupo A, Julien J, Sanders RW, Wilson IA, Moore JP, et al. Antibody potency relates to the ability to recognize the closed, pre-fusion form of HIV Env. Nat Commun. 2015;6(6144): 1–11.

332. Behrens AJ, Vasiljevic S, Pritchard LK, Harvey DJ, Andev RS, Krumm SA, et al. Composition and Antigenic Effects of Individual Glycan Sites of a Trimeric HIV-1 Envelope Glycoprotein. Cell Rep. 2016;14(11): 2695–2706.

333. Crooks ET, Tong T, Osawa K, Binley JM. Enzyme digests eliminate nonfunctional Env from HIV-1 particle surfaces, leaving native Env trimers intact and viral infectivity unaffected. J Virol. 2011;85(12): 5825–39.

334. Lee JH, Ozorowski G, Ward AB. Cryo-EM structure of a native, fully glycosylated, cleaved HIV-1 envelope trimer. Science. 2016;351(6277): 1043–1048.

335. Pugach P, Ozorowski G, Cupo A, Ringe R, Yasmeen A, de Val N, et al. A native-like SOSIP.664 trimer based on a HIV-1 subtype B env gene. J Virol. 2015;89(29007): JVI.03473-14.

336. De Taeye SW, Ozorowski G, Torrents De La Peña A, Guttman M, Julien JP, Van Den Kerkhof TLGM, et al. Immunogenicity of Stabilized HIV-1 Envelope Trimers with Reduced Exposure of Non-neutralizing Epitopes. Cell. 2015;163(7): 1702–1715.

337. Feng Y, Tran K, Bale S, Kumar S, Guenaga J, Wilson R, et al. Thermostability of Well-Ordered HIV Spikes Correlates with the Elicitation of Autologous Tier 2 Neutralizing Antibodies. Plos Pathog. 2016;12(8): 1–26.

338. Hu JK, Crampton JC, Cupo A, Ketas T, van Gils MJ, Sliepen K, et al. Murine Antibody Responses to Cleaved Soluble HIV-1 Envelope Trimers Are Highly Restricted in Specificity. J Virol. 2015;89(20): 10383–10398.

339. Havenar-Daughton C, Carnathan DG, Torrents de la Peña A, Pauthner M, Briney B, Reiss SM, et al. Direct Probing of Germinal Center Responses Reveals Immunological Features and Bottlenecks for Neutralizing Antibody Responses to HIV Env Trimer. Cell Rep. 2016;17(9): 2195–2209.

340. Liu J, Bartesaghi A, Borgnia MJ, Sapiro G, Subramaniam S. Molecular architecture of native HIV-1 gp120 trimers. Nature. 2008;455(7209): 109–113.

341. Wang H, Cohen AA, Galimidi RP, Gristick HB, Jensen GJ, Bjorkman PJ. Cryo-EM structure of a CD4-bound open HIV-1 envelope trimer reveals structural rearrangements of the gp120 V1V2 loop. PNAS. 2016;113(46): E7151–E7158.

342. Tran EEH, Borgnia MJ, Kuybeda O, Schauder DM, Bartesaghi A, Frank GA, et al. Structural mechanism of trimeric HIV-1 envelope glycoprotein activation. Plos Pathog. 2012;8(7): 37.

343. White TA, Bartesaghi A, Borgnia MJ, Meyerson JR, Cruz MJV De, Bess JW, et al. Molecular Architectures of Trimeric SIV and HIV-1 Envelope Glycoproteins on Intact Viruses : Strain-Dependent Variation in Quaternary Structure. Plos Pathog. 2010;6(12): 1–14.

344. Nolan KM, Jordan APO, Hoxie J a. Effects of partial deletions within the human immunodeficiency virus type 1 V3 loop on coreceptor tropism and sensitivity to entry inhibitors. J Virol. 2008;82(2): 664–73.

345. Cormier E, Dragic T. The Crown and Stem of the V3 Loop Play Distinct Roles in Human Immunodeficiency Virus Type 1 Envelope Glycoprotein Interactions with the CCR5 Coreceptor. J Virol. 2002;76(17): 8953–8957.

346. Wyatt R, Moore J, Accola M, Desjardin E, Robinson J, Sodroski J. Involvement of the V1/V2 variable loop structure in the exposure of human immunodeficiency virus type 1 gp120 epitopes induced by receptor binding. J Virol. 1995;69(9): 5723–33.

347. Chung AW, Ghebremichael M, Robinson H, Brown E, Choi I, Lane S, et al. Polyfunctional Fc-Effector Profiles Mediated by IgG Subclass Selection Distinguish RV144 and VAX003 Vaccines. Sci Transl Med. 2014;6(228): 228ra38.

348. Tomaras GD, Ferrari G, Shen X, Alam SM, Liao H-X, Pollara J, et al. Vaccine-induced plasma IgA specific for the C1 region of the HIV-1 envelope blocks binding and effector function of IgG. PNAS. 2013;110(22): 9019–24.

349. Excler JL, Ake J, Robb ML, Kim JH, Plotkin SA. Nonneutralizing functional antibodies: A new “old” paradigm for HIV vaccines. Clin Vaccine Immunol. 2014;21(8): 1023–1036.

350. Forthal D, Hope TJ, Alter G. New paradigms for functional HIV-specific nonneutralizing antibodies. Curr Opin HIV AIDS. 2013;8(5): 393–401.

351. Bhattacharya J, Peters PJ, Clapham PR. CD4-independent infection of HIV and SIV: implications for envelope conformation and cell tropism in vivo. AIDS. 2003;17(Suppl 4): S35–S43.

352. Desrosiers RC. Simian Immunodeficiency Viruses. Ann Rev Microb. 1988;42: 607–25.

353. Olshevsky U, Helseth E, Furman C, Li J, Haseltine W, Sodroski J. Identification of individual human immunodeficiency virus type 1 gp120 amino acids important for CD4 receptor binding. J Virol. 1990;64(12): 5701–5707.

354. Ortiz AM. Depletion of CD4+ T cells abrogates post-peak decline of viremia in SIV-infected rhesus macaques. J Clin Invest. 2011;121(11): 4433–4445.

355. Francella N, Gwyn SE, Yi Y, Li B, Xiao P, Elliott STC, et al. CD4+ T Cells Support Production of Simian Immunodeficiency Virus Env Antibodies That Enforce CD4-Dependent Entry and Shape Tropism In Vivo. J Virol. 2013;87(17): 9719–9732.

356. Mori K, Ringler DJ, Kodama T, Desrosiers RC. Complex determinants of macrophage tropism in env of simian immunodeficiency virus. J Virol. 1992;66(4): 2067–2075.

357. Banapour B, Marthas ML, Ramos R a, Lohman BL, Unger RE, Gardner MB, et al. Identification of viral determinants of macrophage tropism for simian immunodeficiency virus SIVmac. J Virol. 1991;65(11): 5798–5805.

358. Sharma DP, Zink MC, Anderson M, Adams R, Clements JE, Joag S V, et al. Derivation of neurotropic simian immunodeficiency virus from exclusively lymphocytetropic parental virus: pathogenesis of infection in macaques. J Virol. 1992;66(6): 3550–3556.

359. Puffer BA, Pöhlmann S, Edinger AL, Carlin D, Sanchez MD, Reitter J, et al. CD4 independence of simian immunodeficiency virus Envs is associated with macrophage tropism, neutralization sensitivity, and attenuated pathogenicity. J Virol. 2002;76(6): 2595–2605.

360. Vödrös D, Thorstensson R, Doms RW, Fenyö EM, Reeves JD. Evolution of coreceptor use and CD4-independence in envelope clones derived from SIVsm-infected macaques. Virology. 2003;316(1): 17–28.

361. Edinger AL, Mankowski JL, Doranz BJ, Margulies BJ, Lee B, Rucker J, et al. CD4-independent, CCR5-dependent infection of brain capillary endothelial cells by a neurovirulent simian immunodeficiency virus strain. PNAS. 1997;94(26): 14742–7.

362. Reeves JD, Hibbitts S, Simmons G, Mcknight I, Azevedo-Pereira JM,

Moniz-Pereira J, et al. Primary Human Immunodeficiency Virus Type 2 (HIV-2) Isolates Infect CD4-Negative Cells via CCR5 and CXCR4: Comparison with HIV-1 and Simian Immunodeficiency Virus and Relevance to Cell Tropism In Vivo. J Virol. 1999;73(9): 7795–7804.

363. Martín-García J, Cao W, Varela-Rohena A, Plassmeyer ML, González-Scarano F. HIV-1 tropism for the central nervous system: Brain-derived envelope glycoproteins with lower CD4 dependence and reduced sensitivity to a fusion inhibitor. Virology. 2006;346(1): 169–179.

364. Zerhouni B, Nelson JAE, Saha K. Isolation of CD4-independent primary human immunodeficiency virus type 1 isolates that are syncytium inducing and acutely cytopathic for CD8+ lymphocytes. J Virol. 2004;78(3): 1243–55.

365. Ryzhova E, Whitbeck JC, Canziani G, Westmoreland S V, Cohen GH, Eisenberg RJ, et al. Rapid progression to simian AIDS can be accompanied by selection of CD4-independent gp120 variants with impaired ability to bind CD4. J Virol. 2002;76(15): 7903–7909.

366. Xiao P, Usami O, Suzuki Y, Ling H, Shimizu N, Hoshino H, et al. Characterization of a CD4-independent clinical HIV-1 that can efficiently infect human hepatocytes through chemokine (C-X-C motif) receptor 4. AIDS. 2008;22(14): 1749–57.

367. Zhang PF, Bouma P, Park EJ, Margolick JB, Robinson JE, Zolla-Pazner S, et al. A variable region 3 (V3) mutation determines a global neutralization phenotype and CD4-independent infectivity of a human immunodeficiency virus type 1 envelope associated with a broadly cross-reactive, primary virus-neutralizing antibody response. J Virol. 2002;76(2): 644–55.

368. Endres MJ, Clapham PR, Marsh M, Ahuja M, Turner JD, McKnight A, et al. CD4-independent infection by HIV-2 is mediated by Fusin/CXCR4. Cell. 1996;87(4): 745–756.

369. Hoxie JA, Labranche CC, Endres MJ, Turner JD, Berson JF, Doms RW, et al. CD4-independent utilization of the CXCR4 chemokine receptor by HIV-1 and HIV-2. J Reprod Immunol. 1998;41(1–2): 197–211.

370. Clapham PR, McKnight a, Weiss R a. Human immunodeficiency virus type 2 infection and fusion of CD4-negative human cell lines: induction and enhancement by soluble CD4. J Virol. 1992;66(6): 3531–3537.

371. LaBranche CC, Hoffman TL, Romano J, Haggarty BS, Edwards TG, Matthews TJ, et al. Determinants of CD4 independence for a human immunodeficiency virus type 1 variant map outside regions required for coreceptor specificity. J Virol. 1999;73(12): 10310–9. Available: http://jvi.asm.org/content/73/12/10310.abstract

372. Kolchinsky P, Mirzabekov T, Farzan M, Kiprilov E, Cayabyab M, Mooney LJ, et al. Adaptation of a CCR5-using, primary human immunodeficiency virus type 1 isolate for CD4-independent replication. J Virol. 1999;73(10): 8120–8126.

373. Swanstrom AE, Haggarty B, Jordan APO, Romano J, Leslie GJ, Aye PP, et al. Derivation and characterization of a CD4-independent, non-CD4 tropic simian immunodeficiency virus. J Virol. 2016;90(10).

374. Kolchinsky P, Kiprilov E, Sodroski J. Increased neutralization sensitivity of CD4-independent human immunodeficiency virus variants. J Virol. 2001;75(5): 2041–2050.

375. Boyd DF, Peterson D, Haggarty BS, Jordan APO, Hogan MJ, Goo L, et al. Mutations in HIV-1 Envelope That Enhance Entry with the Macaque CD4 Receptor Alter Antibody Recognition by Disrupting Quaternary Interactions within the Trimer. J Virol. 2015;89(2): 894–907.

376. Edwards TG, Hoffman TL, Baribaud F, Wyss S, Labranche CC, Romano J, et al. Relationships between CD4 Independence, Neutralization Sensitivity, and Exposure of a CD4-Induced Epitope in a Human Immunodeficiency Virus Type 1 Envelope Protein. J Virol. 2001;75(11): 5230–5239.

377. Thomas ER, Shotton C, Weiss R a, Clapham PR, McKnight A. CD4-dependent and CD4-independent HIV-2: consequences for neutralization. AIDS. 2003;17(3): 291–300.

378. White TA, Bartesaghi A, Borgnia MJ, de la Cruz MJ V., Nandwani R, Hoxie J a., et al. Three-Dimensional Structures of Soluble CD4-Bound States of Trimeric Simian Immunodeficiency Virus Envelope Glycoproteins Determined by Using Cryo-Electron Tomography. J Virol. 2011;85(23): 12114–12123.

379. Kolchinsky P, Kiprilov E, Bartley P, Rubinstein R, Sodroski J. Loss of a Single N-Linked Glycan Allows CD4-Independent Human Immunodeficiency Virus Type 1 Infection by Altering the Position of the gp120 V1 / V2 Variable Loops. J Virol. 2001;75(7): 3435–3443.

380. Kwong PD, Wyatt R, Robinson J, Sweet RW, Sodroski J, Hendrickson WA. Structure of an HIV gp120 envelope glycoprotein in complex with the CD4 receptor and a neutralizing human antibody. Nature. 1998;393: 648–659.

381. Zhang PF, Cham F, Dong M, Choudhary A, Bouma P, Zhang Z, et al. Extensively cross-reactive anti-HIV-1 neutralizing antibodies induced by gp140 immunization. Proc Natl Acad Sci. 2007;104(24): 10193–8.

382. Li Y, Cleveland B, Klots I, Travis B, Richardson BA, Anderson D, et al. Removal of a single N-linked glycan in human immunodeficiency virus type

1 gp120 results in an enhanced ability to induce neutralizing antibody responses. J Virol. 2008;82(2): 638–51.

383. Murray MK, Teran V a., Chapleau J-P, Wang B, Kim SH, LaBranche CC, et al. Soluble Envelope Glycoprotein Trimers from a CD4-Independent HIV-1 Elicit Antibody-Dependent Cellular Cytotoxicity-Mediating Antibodies in Guinea Pigs. J Virol. 2015;89(20): 10707–10711.

384. Townsley S, Li Y, Kozyrev Y, Cleveland B, Hu S-L. The conserved role of an N-linked glycan on the surface antigen of HIV-1 modulating virus sensitivity to broadly neutralizing antibodies against the receptor and coreceptor binding sites. J Virol. 2015;90(October): JVI.02321-15.

385. Wang W, Nie J, Prochnow C, Truong C, Jia Z, Wang S, et al. A systematic study of the N-glycosylation sites of HIV-1 envelope protein on infectivity and antibody-mediated neutralization. Retrovirology. 2013;10(1): 14.

386. Huang X, Jin W, Hu K, Luo S, Du T, Grif GE, et al. Highly conserved HIV-1 gp120 glycans proximal to CD4-binding region affect viral infectivity and neutralizing antibody induction. Virology. 2012;423(1): 97–106.

387. Gorny MK, Pan R, Williams C, Wang XH, Volsky B, O'Neal T, et al. Functional and immunochemical cross-reactivity of V2-specific monoclonal antibodies from HIV-1-infected individuals. Virology. 2012;427(2): 198–207.

388. Mayr LM, Cohen S, Spurrier B, Kong XP, Zolla-Pazner S. Epitope Mapping of Conformational V2-specific Anti-HIV Human Monoclonal Antibodies Reveals an Immunodominant Site in V2. PLoS One. 2013;8(7).

389. Spurrier B, Sampson J, Gorny MK, Zolla-Pazner S, Kong X-P. Functional implications of the binding mode of a human conformation-dependent V2 monoclonal antibody against HIV. J Virol. 2014;88(8): 4100–12.

390. Walker LM, Phogat SK, Chan-Hui P-Y, Wagner D, Phung P, Goss JL, et al. Broad and potent neutralizing antibodies from an African donor reveal a new HIV-1 vaccine target. Science. 2009;326(5950): 285–9.

391. Fouts TR, Binley JM, Trkola A, Robinson JE, Moore JP. Neutralization of the human immunodeficiency virus type 1 primary isolate JR-FL by human monoclonal antibodies correlates with antibody binding to the oligomeric form of the envelope glycoprotein complex. J Virol. 1997;71(4): 2779–85.

392. Tong T, Crooks ET, Osawa K, Binley JM. HIV-1 virus-like particles bearing pure env trimers expose neutralizing epitopes but occlude nonneutralizing epitopes. J Virol. 2012;86(7): 3574–87.

393. Killeen N, Sawada S, Littman DR. Regulated expression of human CD4 rescues helper T cell development in mice lacking expression of

endogenous CD4. EMBO J. 1993;12(4): 1547–53.

394. Marschner S, Hünig T, Cambier JC, Finkel TH. Ligation of human CD4 interferes with antigen-induced activation of primary T cells. Immunol Lett. 2002;82(1–2): 131–139.

395. Kawamura T, Gatanaga H, Borris DL, Connors M, Mitsuya H, Blauvelt A. Decreased Stimulation of CD4 + T Cell Proliferation and IL-2 Production by Highly Enriched Populations of HIV-Infected Dendritic Cells. J Immunol. 2003;170: 4260–4266.

396. Herzyk DJ, Gore ER, Polsky R, Nadwodny L, Maier CC, Liu S, et al. Immunomodulatory Effects of Anti-CD4 Antibody in Host Resistance against Infections and Tumors in Human CD4 Transgenic Mice Immunomodulatory Effects of Anti-CD4 Antibody in Host Resistance against Infections and Tumors in Human CD4 Transgenic Mice. Infect Immun. 2001;69(2): 1032–1043.

397. Moutaftsi M, Peters B, Pasquetto V, Tscharke DC, Sidney J, Bui H, et al. A consensus epitope prediction of murine T CD8+ cell responses to vaccinia virus. Nat Biotechnol. 2006;24(7): 817–819.

398. Xu R, Johnson AJ, Liggitt D, Bevan MJ, Michael J. Cellular and humoral immunity against vaccinia virus infection of mice. J Immunol. 2004;172(10): 6265–6271.

399. Gorman J, Soto C, Yang MM, Davenport TM, Guttman M, Bailer RT, et al. Structures of HIV-1 Env V1V2 with broadly neutralizing antibodies reveal commonalities that enable vaccine design. Nat Struct Mol Biol. 2015;23(1): 81–90.

400. Lee JH, Andrabi R, Su C-Y, Yasmeen A, Julien J-P, Kong L, et al. A Broadly Neutralizing Antibody Targets the Dynamic HIV Envelope Trimer Apex via a Long, Rigidified, and Anionic β-Hairpin Structure. Immunity. 2017;46(4): 690–702.

401. Sok D, van Gils MJ, Pauthner M, Julien J-P, Saye-Francisco KL, Hsueh J, et al. Recombinant HIV envelope trimer selects for quaternary-dependent antibodies targeting the trimer apex. Proc Natl Acad Sci. 2014;111(49): 17624–17629.

402. Doria-Rose NA, Schramm CA, Gorman J, Moore PL, Bhiman JN, Dekosky BJ, et al. Developmental pathway for potent V1V2-directed HIV-neutralizing antibodies. Nature. 2014;508(7498): 55–62.

403. Humes D, Emery S, Laws E, Overbaugh J. A Species-Specific Amino Acid Difference in the Macaque CD4 Receptor Restricts Replication by Global Circulating HIV-1 Variants Representing Viruses from Recent Infection. J

Virol. 2012;86(23): 12472–12483.

404. Humes D, Overbaugh J. Adaptation of subtype a human immunodeficiency virus type 1 envelope to pig-tailed macaque cells. J Virol. 2011;85(9): 4409–4420.

405. Li H, Wang S, Kong R, Ding W, Lee F-H, Parker Z, et al. Envelope residue 375 substitutions in simian-human immunodeficiency viruses enhance CD4 binding and replication in rhesus macaques. Proc Natl Acad Sci. 2016;113(24): E3413-22.

406. Del Prete GQ, Haggarty B, Leslie GJ, Jordan APO, Romano J, Wang N, et al. Derivation and characterization of a simian immunodeficiency virus SIVmac239 variant with tropism for CXCR4. J Virol. 2009;83(19): 9911–22.

407. O'Doherty U, Swiggard WJ, Malim MH. Human immunodeficiency virus type 1 spinoculation enhances infection through virus binding. J Virol. 2000;74(21): 10074–80.

408. Yang L, Song Y, Li X, Huang X, Liu J, Ding H, et al. HIV-1 virus-like particles produced by stably transfected Drosophila S2 cells: a desirable vaccine component. J Virol. 2012;86(14): 7662–76.

409. Montefiori DC. Evaluating neutralizing antibodies against HIV, SIV, and SHIV in luciferase reporter gene assays. Curr Protoc Immunol. 2005;Chapter 12: Unit 12.11.

410. Guo W, Cleveland B, Davenport TM, Lee KK, Hu SL. Purification of recombinant vaccinia virus-expressed monomeric HIV-1 gp120 to apparent homogeneity. Protein Expr Purif. 2013;90(1): 34–39.

411. Gao F, Morrison SG, Robertson DL, Thornton CL, Craig S, Karlsson G, et al. Molecular cloning and analysis of functional envelope genes from human immunodeficiency virus type 1 sequence subtypes A through G. WHO NIAID Networks for HIV Isolation. 1996;70(3): 1651–1667.

412. Kayman SC, Wu Z, Revesz K, Chen H, Kopelman R, Pinter A. Presentation of native epitopes in the V1/V2 and V3 regions of human immunodeficiency virus type 1 gp120 by fusion glycoproteins containing isolated gp120 domains. J Virol. 1994;68(1): 400–10.

413. Guttman M, Lee KK. A Functional Interaction between gp41 and gp120 Is Observed for Monomeric but Not Oligomeric, Uncleaved HIV-1 Env gp140. J Virol. 2013;87(21): 11462–11475.

414. Zhang Z, Zhang A, Xiao G. Improved protein hydrogen/deuterium exchange mass spectrometry platform with fully automated data processing. Anal Chem. 2012;84(11): 4942–4949.

415. Guttman M, Weis DD, Engen JR, Lee KK. Analysis of Overlapped and Noisy Hydrogen/Deuterium Exchange Mass Spectra. J Am Soc Mass Spectrom. 2013;24(12).

416. Weis DD, Engen JR, Kass IJ. Semi-Automated Data Processing of Hydrogen Exchange Mass Spectra Using HX-Express. J Am Soc Mass Spectrom. 2006;17(12): 1700–1703.

417. Santra S, Barouch DH, Korioth-Schmitz B, Lord CI, Krivulka GR, Yu F, et al. Recombinant poxvirus boosting of DNA-primed rhesus monkeys augments peak but not memory T lymphocyte responses. Proc Natl Acad Sci. 2004;101(30): 11088–11093.

418. Brown EP, Licht AF, Dugast AS, Choi I, Bailey-Kellogg C, Alter G, et al. High-throughput, multiplexed IgG subclassing of antigen-specific antibodies from clinical samples. J Immunol Methods. 2012;386(1–2): 117–123.

419. Tomaras GD, Yates NL, Liu P, Qin L, Fouda GG, Chavez LL, et al. Initial B-Cell Responses to Transmitted Human Immunodeficiency Virus Type 1: Virion-Binding Immunoglobulin M (IgM) and IgG Antibodies Followed by Plasma Anti-gp41 Antibodies with Ineffective Control of Initial Viremia. J Virol. 2008;82(24): 12449–12463.

420. Zurawski G, Shen X, Zurawski S, Tomaras GD, Montefiori DC, Roederer M, et al. Superiority in Rhesus Macaques of of Targeting HIV-1 Env gp140 to CD40 versus LOX-1 in Combination with Replication-Competent NYVAC-KC for Induction of Env-Specific Antibody and T Cell Responses. J Virol. 2017;91(9): e01596-16.

421. Pollara J, Hart L, Brewer F, Pickeral J, Packard BZ, Hoxie JA, et al. High-throughput quantitative analysis of HIV-1 and SIV-specific ADCC-mediating antibody responses. Cytom Part A. 2011;79 A(8): 603–612.

422. Harmon TM, Fisher KA, Mcglynn MG, Stover J, Warren J, Teng Y, et al. Exploring the Potential Health Impact and Cost-Effectiveness of AIDS Vaccine within a Comprehensive HIV/AIDS Response in Low- and Middle-Income Countries. PLoS One. 2016; 1–18.

423. Emini EA, Schleif WA, Nunberg JH, Conley AJ, Eda Y, Tokiyoshi S, et al. Prevention of HIV-1 infection in chimpanzees by gp120 V3 domain-specific monoclonal antibody. Nature. 1992;355(6362): 728–730.

424. Baba TW, Liska V, Hofmann-Lehmann R, Vlasak J, Xu W, Ayehunie S, et al. Human neutralizing monoclonal antibodies of the IgG1 subtype protect against mucosal simian-human immunodeficiency virus infection. Nat Med. 2000;6(2): 200–206.

425. Mascola JR, Lewis MG, Stiegler G, Harris D, VanCott TC, Hayes D, et al. Protection of macaques against pathogenic simian/human immunodeficiency virus 89.6PD by passive transfer of neutralizing antibodies. J Virol. 1999;73(5): 4009–18.

426. Haynes BF, Burton DR. Developing an HIV vaccine. Science. 2017;355(6330): 1129–1130.

427. Corey L, Gilbert PB, Tomaras G, Haynes BF, Pantaleo G, Fauci AS. Immune Correlates of Vaccine Protection Against HIV-1 Acquisition. Sci Transl Med. 2015;7(310): 310rv.7.

428. Ackerman ME, Mikhailova A, Brown EP, Dowell KG, Walker BD, Bailey-Kellogg C, et al. Polyfunctional HIV-Specific Antibody Responses Are Associated with Spontaneous HIV Control. Plos Pathog. 2016;12(1): 1–14.

429. Huang Y, Ferrari G, Alter G, Forthal DN, Kappes JC, Lewis GK, et al. Diversity of Antiviral IgG Effector Activities Observed in HIV-Infected and Vaccinated Subjects. J Immunol. 2016;197(12): 4603–4612.

430. Teigler JE, Phogat S, Franchini G, Hirsch VM, Michael NL, Barouch DH. The Canarypox Virus Vector ALVAC Induces Distinct Cytokine Responses Compared to the Vaccinia Virus-Based Vectors MVA and NYVAC in Rhesus Monkeys. J Virol. 2014;88(3): 1809–14.

431. Zhu P, Liu J, Bess J, Chertova E, Lifson JD, Grisé H, et al. Distribution and three-dimensional structure of AIDS virus envelope spikes. Nature. 2006;441(7095): 847–52.

432. Wang B-Z, Liu W, Kang S-M, Alam M, Huang C, Ye L, et al. Incorporation of high levels of chimeric human immunodeficiency virus envelope glycoproteins into virus-like particles. J Virol. 2007;81(20): 10869–78.

433. Townsley S, Mohamed Z, Guo W, Mckenna J, Cleveland B, Labranche C, et al. Induction of Heterologous Tier 2 HIV-1-Neutralizing and Cross-Reactive V1/V2-Specific Antibodies in Rabbits by Prime-Boost Immunization. J Virol. 2016;90(19): 8644–8660.

434. Marsh M, Pelchen-Matthews A, Hoxie JA. Roles for endocytosis in lentiviral replication. Trends Cell Biol. 1997;7(1): 1–4.

435. Wyss S, Berlioz-Torrent C, Boge M, Blot G, Höning S, Benarous R, et al. The highly conserved C-terminal dileucine motif in the cytosolic domain of the human immunodeficiency virus type 1 envelope glycoprotein is critical for its association with the AP-1 clathrin adapter. J Virol. 2001;75(6): 2982–92.

436. Boge M, Wyss S, Bonifacino JS, Thali M. A membrane-proximal tyrosine-

based signal mediates internalization of the HIV-1 envelope glycoprotein via interaction with the AP-2 clathrin adaptor. J Biol Chem. 1998;273(25): 15773–15778.

437. Rowell JF, Stanhope PE, Siliciano RF. Endocytosis of Endogenously Synthesized HIV-1 Envelope Protein. J Immunol. 1995; 474–488.

438. Bowers K, Pelchen-Matthews A, Höning S, Vance PJ, Creary L, Haggarty BS, et al. The simian immunodeficiency virus envelope glycoprotein contains multiple signals that regulate its cell surface expression and endocytosis. Traffic. 2000;1(8): 661–74.

439. Byland R, Vance PJ, Hoxie JA, Marsh M. A conserved dileucine motif mediates clathrin and AP-2-dependent endocytosis of the HIV-1 envelope protein. Mol Biol Cell. 2007;18(2): 414–25.

440. Berlioz-torrent C, Shacklett BL, Delamarre L, Bouchaert I, Dokhelar MC, Benarous R, et al. Interactions of the cytoplasmic domains of human and simian retroviral transmembrane proteins with components of the clathrin adaptor complexes modulate intracellular and cell surface expression of envelope glycoproteins. J Virol. 1999;73(2): 1350–61.

441. Tedbury PR, Ablan SD, Freed EO. Global rescue of defects in HIV-1 envelope glycoprotein incorporation: implications for matrix structure. Plos Pathog. 2013;9(11): e1003739.

442. Freed EO, Martin MA. Domains of the human immunodeficiency virus type 1 matrix and gp41 cytoplasmic tail required for envelope incorporation into virions. J Virol. 1996;70(1): 341–51.

443. Murakami T, Freed EO. Genetic evidence for an interaction between human immunodeficiency virus type 1 matrix and alpha-helix 2 of the gp41 cytoplasmic tail. J Virol. 2000;74(8): 3548–54.

444. Freed EO, Martin MA. Virion incorporation of envelope glycoproteins with long but not short cytoplasmic tails is blocked by specific, single amino acid substitutions in the human immunodeficiency virus type 1 matrix. J Virol. 1995;69(3): 1984–9.

445. Groppelli E, Len AC, Granger L a, Jolly C. Retromer Regulates HIV-1 Envelope Glycoprotein Trafficking and Incorporation into Virions. Plos Pathog. 2014;10(10): e1004518.

446. Chernomordik L, Chanturiya AN, Suss-Toby E, Nora E, Zimmerberg J. An amphipathic peptide from the C-terminal region of the human immunodeficiency virus envelope glycoprotein causes pore formation in membranes. J Virol. 1994;68(11): 7115–7123.

447. Kliger Y, Shai Y. A leucine zipper-like sequence from the cytoplasmic tail of the HIV-1 envelope glycoprotein binds and perturbs lipid bilayers. Biochemistry. 1997;36(17): 5157–5169.

448. Heap CJ, Reading SA, Dimmock NJ. An antibody specific for the C-terminal tail of the gp41 transmembrane protein of human immunodeficiency virus type 1 mediates post-attachment neutralization, probably through inhibition of virus-cell fusion. J Gen Virol. 2005;86(5): 1499–1507.

449. Buratti E, McLain L, Tisminetzky S, Cleveland SM, Dimmock NJ, Baralle FE. The neutralizing antibody response against a conserved region of human immunodeficiency virus type 1 gp41 (amino acid residues 731-752) is uniquely directed against a conformational epitope. J Gen Virol. 1998;79(11): 2709–2716.

450. Blot G, Janvier K, Le Panse S, Benarous R, Berlioz-Torrent C. Targeting of the human immunodeficiency virus type 1 envelope to the trans-Golgi network through binding to TIP47 is required for env incorporation into virions and infectivity. J Virol. 2003;77(12): 6931–45.

451. Bhattacharya J, Peters PJ, Clapham PR, Bhattacharya J, Peters PJ, Clapham PR. Human Immunodeficiency Virus Type 1 Envelope Glycoproteins That Lack Cytoplasmic Domain Cysteines: Impact on Association with Membrane Lipid Rafts and Incorporation onto Budding Virus Particles. J Virol. 2004;78(10): 5500–6.

452. Chan W-E, Lin H-H, Chen SS-L. Wild-type-like viral replication potential of human immunodeficiency virus type 1 envelope mutants lacking palmitoylation signals. J Virol. 2005;79(13): 8374–87.

453. Lodge R, Lalonde JP, Lemay G, Cohen EA. The membrane-proximal intracytoplasmic tyrosine residue of HIV-1 envelope glycoprotein is critical for basolateral targeting of viral budding in MDCK cells. EMBO J. 1997;16(4): 695–705.

454. Fultz PN, Vance PJ, Endres MJ, Tao B, Dvorin JD, Davis IANC, et al. In Vivo Attenuation of Simian Immunodeficiency Virus by Disruption of a Tyrosine-Dependent Sorting Signal in the Envelope Glycoprotein Cytoplasmic Tail. J Virol. 2001;75(1): 278–291.

455. Breed MW, Jordan APO, Aye PP, Lichtveld CF, Midkiff CC, Schiro FR, et al. Loss of a Tyrosine-Dependent Trafficking Motif in the Simian Immunodeficiency Virus Envelope Cytoplasmic Tail Spares Mucosal CD4 Cells but Does Not Prevent Disease Progression. J Virol. 2013;87(3): 1528–1543.

456. Breed MW, Elser SE, Torben W, Jordan APO, Aye PP, Midkiff C, et al.

Elite Control, Gut CD4 T Cell Sparing, and Enhanced Mucosal T Cell Responses in Macaca nemestrina Infected by a Simian Immunodeficiency Virus Lacking a gp41 Trafficking Motif. J Virol. 2015;89(20): 10156–10175.

457. LaBranche CC, Sauter MM, Haggarty BS, Vance PJ, Romano J, Hart TK, et al. Biological, molecular, and structural analysis of a cytopathic variant from a molecularly cloned simian immunodeficiency virus. J Virol. 1994;68(9): 5509–22.

458. LaBranche CC, Sauter MM, Haggarty BS, Vance PJ, Romano J, Hart TK, et al. A single amino acid change in the cytoplasmic domain of the simian immunodeficiency virus transmembrane molecule increases envelope glycoprotein expression on infected cells. J Virol. 1995;69(9): 5217–27.

459. Sauter MM, Pelchen-Matthews A, Bron R, Marsh M, LaBranche CC, Vance PJ, et al. An internalization signal in the simian immunodeficiency virus transmembrane protein cytoplasmic domain modulates expression of envelope glycoproteins on the cell surface. J Cell Biol. 1996;132(5): 795–811.

460. Kodama T, Wooley DP, Naidu YM, Daniel MD, Li Y, Desrosiers RC. Significance of Premature Stop Codons in env of Simian Immunodeficiency Virus. J Virol. 1989;63(11): 4709.

461. Kim JH, Skountzou I, Compans R, Jacob J. Original Antigenic Sin Responses to Influenza Viruses. J Immunol. 2009;183(5): 3294–3301.

462. Meissner EG, Duus KM, Gao F, Yu XF, Su L. Characterization of a thymus-tropic HIV-1 isolate from a rapid progressor: Role of the envelope. Virology. 2004;328(1): 74–88.

463. Yue L, Shang L, Hunter E. Truncation of the membrane-spanning domain of human immunodeficiency virus type 1 envelope glycoprotein defines elements required for fusion, incorporation, and infectivity. J Virol. 2009;83(22): 11588–98.

464. Hirsch V, Edmondson P, Murphey-Corb M, Arbeille B, Johnson P, Mullins J. SIV adaptation to human cells. Nature. 1989;341: 573–574.

465. Zarling JM, Morton W, Moran PA, McClure J, Kosowski SG, Hu S-L. T-cell responses to human AIDS virus in macaques immunized with recombinant vaccinia viruses. Nature. 1986;323: 344–346.

466. Cooney EL, McElrath MJ, Corey L, Hu SL, Collier a C, Arditti D, et al. Enhanced immunity to human immunodeficiency virus (HIV) envelope elicited by a combined vaccine regimen consisting of priming with a vaccinia recombinant expressing HIV envelope and boosting with gp160 protein. Proc Natl Acad Sci. 1993;90: 1882–1886.

467. Edwards TG, Wyss S, Reeves JD, Zolla-pazner S, Hoxie JA, Doms RW, et al. Truncation of the Cytoplasmic Domain Induces Exposure of Conserved Regions in the Ectodomain of Human Immunodeficiency Virus Type 1 Envelope Protein. J Virol. 2002;76(6): 2683–2691.

468. Chen J, Kovacs JM, Peng H, Rits-volloch S, Lu J, Park D, et al. Effect of the cytoplasmic domain on antigenic characteristics of HIV-1 envelope glycoprotein. Science. 2015;349(6244): 191–195.

469. Wyss S, Dimitrov AS, Baribaud F, Edwards TG, Blumenthal R, Hoxie JA. Regulation of Human Immunodeficiency Virus Type 1 Envelope Glycoprotein Fusion by a Membrane-Interactive Domain in the gp41 Cytoplasmic Tail. J Virol. 2005;79(19): 12231–12241.

470. Zolla-pazner S, Cohen SS, Boyd D, Kong X, Seaman M, Nussenzweig M, et al. Structure/Function Studies Involving the V3 Region of the HIV-1 Envelope Delineate Multiple Factors That Affect Neutralization Sensitivity. J Virol. 2016;90(2): 636–649.

471. Hioe CE, Wrin T, Seaman MS, Yu X, Wood B, Self S, et al. Anti-V3 monoclonal antibodies display broad neutralizing activities against multiple HIV-1 subtypes. PLoS One. 2010;5(4): e10254.

472. Zolla-Pazner S, DeCamp A, Gilbert PB, Williams C, Yates NL, Williams WT, et al. Vaccine-induced IgG antibodies to V1V2 regions of multiple HIV-1 subtypes correlate with decreased risk of HIV-1 infection. PLoS One. 2014;9(2): e87572.

473. von Bredow B, Arias JF, Heyer LN, Gardner MR, Farzan M, Rakasz EG, et al. Envelope Glycoprotein Internalization Protects Human and Simian Immunodeficiency Virus-Infected Cells from Antibody-Dependent Cell-Mediated Cytotoxicity. J Virol. 2015;89(20): 10648–10655.

474. Graham BS, Gorse GJ, Schwartz DH, Keefer MC, McElrath MJ, Matthews TJ, et al. Determinants of antibody response after recombinant gp160 boosting in vaccinia-naive volunteers primed with gp160-recombinant vaccinia virus. J Infect Dis. 1994;170(4): 782–786.

475. Bachmann MF, Rohrer UH, Thomas MK, Kurt B. The Influence of Antigen Organization on B Cell Responsiveness. Science. 1993;262(5138): 1448–1451.

476. Parren PWHI, Mondor I, Naniche D, Henrik J, Klasse PJ, Burton DR, et al. Neutralization of Human Immunodeficiency Virus Type 1 by Antibody to gp120 Is Determined Primarily by Occupancy of Sites on the Virion Irrespective of Epitope Specificity. J Virol. 1998;72(5): 3512–3519.

477. Postler TS, Desrosiers RC. The cytoplasmic domain of the HIV-1

glycoprotein gp41 induces NF-κB activation through TGF-β-activated kinase 1. Cell Host Microbe. 2012;11: 181–193.

478. Oeckinghaus A, Ghosh S. The NF-kappaB family of transcription factors and its regulation. Cold Spring Harb Perspect Biol. 2009;1: a000034.

479. Yoshimura S, Bondeson J, Foxwell BMJ, Brennan FM, Feldmann M. Effective antigen presentation by dendritic cells is NF-κB dependent: coordinate regulation of MHC, co-stimulatory molecules and cytokines. Int Immunol. 2001;13(5): 675–683.

480. Cancro MP. Signalling crosstalk in B cells: managing worth and need. Nat Rev Immunol. 2009;9(9): 657–61.

481. Wyma DJ, Jiang J, Shi J, Zhou J, Lineberger E, Miller MD, et al. Coupling of Human Immunodeficiency Virus Type 1 Fusion to Virion Maturation: a Novel Role of the gp41 Cytoplasmic Tail. J Virol. 2004;78(7): 3429–3435.

482. Jiang J, Aiken C. Maturation-Dependent Human Immunodeficiency Virus Type 1 Particle Fusion Requires a Carboxyl-Terminal Region of the gp41 Cytoplasmic Tail. J Virol. 2007;81(18): 9999–10008.

483. Murakami T, Ablan S, Freed E, Tanaka Y. Regulation of human immunodeficiency virus type 1 Env-mediated membrane fusion by viral protease activity. J Virol. 2004;78(2): 1026–31.

484. Joyner AS, Willis JR, Crowe JE, Aiken C. Maturation-induced cloaking of neutralization epitopes on hiv-1 particles. Plos Pathog. 2011;7(9): 1–9.

485. Ye L, Bu Z, Vzorov A, Taylor D, Compans RW, Yang C. Surface Stability and Immunogenicity of the HIV Envelope Glycoprotein: Role of the Cytoplasmic Domain. J Virol. 2004;78(24): 13409–13419.

486. Collman R, Balliet JW, Gregory S a, Friedman H, Kolson DL, Nathanson N, et al. An infectious molecular clone of an unusual macrophage-tropic and highly cytopathic strain of human immunodeficiency virus type 1. J Virol. 1992;66(12): 7517–7521.

487. Koyanagi Y, Miles S, Mitsuyasu RT, Merrill JE, Vinters H V, Chen IS. Dual infection of the central nervous system by AIDS viruses with distinct cellular tropisms. Science. 1987;236(4803): 819–822.

488. Bolmstedt A, Hemming A, Flodby P, Berntsson P, Travis B, Lin JPC, et al. Effects of mutations in glycosylation sites and disulphide bonds on processind, CD4-binding and fusion activity of human immunodeficiency virus envelope glycoproteins. J Gen Virol. 1991;72: 1269–1277.

489. Parra B, Lizarazo J, Jiménez-Arango JA, Zea-Vera AF, González-

Manrique G, Vargas J, et al. Guillain–Barré Syndrome Associated with Zika Virus Infection in Colombia. N Engl J Med. 2016;375(16): 1513–1523.

490. Pierson TC, Graham BS. Zika Virus: Immunity and Vaccine Development. Cell. 2016; 1–7.

491. Lessler J, Chaisson LH, Kucirka LM, Bi Q, Grantz K, Salje H, et al. Assessing the global threat from Zika virus. Science. 2016;46(24): 601–604.

492. Beck AS, Barrett AD. Current status and future prospects of yellow fever vaccines. Expert Rev Vaccines. 2015;14(11): 1479–1492.

493. Jarmer J, Zlatkovic J, Tsouchnikas G, Vratskikh O, Strauss J, Aberle JH, et al. Variation of the Specificity of the Human Antibody Responses after Tick-Borne Encephalitis Virus Infection and Vaccination. J Virol. 2014;88(23): 13845–13857.

494. Guy B, Jackson N. Dengue vaccine: hypotheses to understand CYD-TDV-induced protection. Nat Rev Microbiol. 2016;14(1): 45–54.

495. Chahal JS, Fang T, Woodham AW, Khan OF, Ling J, Anderson DG, et al. An RNA nanoparticle vaccine against Zika virus elicits antibody and CD8+ T cell responses in a mouse model. Sci Rep. 2017;7(1): 252.

496. Ledgerwood JE, Costner P, Desai N, Holman L, Enama ME, Yamshchikov G, et al. A replication defective recombinant Ad5 vaccine expressing Ebola virus GP is safe and immunogenic in healthy adults. Vaccine. 2010;29(2): 304–313.

497. Sumida SM, Truitt DM, Kishko MG, Arthur JC, Jackson SS, Gorgone DA, et al. Neutralizing Antibodies and CD8+ T Lymphocytes both Contribute to Immunity to Adenovirus Serotype 5 Vaccine Vectors. J Virol. 2004;78(6): 2666–2673.

498. Abbink P, Maxfield LF, Ng'ang'a D, Borducchi EN, Iampietro MJ, Bricault CA, et al. Construction and evaluation of novel rhesus monkey adenovirus vaccine vectors. J Virol. 2015;89(3): 1512–22.

499. Weissman D. mRNA transcript therapy. Expert Rev Vaccines. 2014;14(2): 1–17.

500. Minor PD. Live attenuated vaccines: Historical successes and current challenges. Virology. 2015;479–480: 379–392.

501. Baronti C, Piorkowski G, Charrel RN, Boubis L, Leparc-goffart I, Lamballerie D. Complete Coding Sequence of Zika Virus from a French Polynesia. Genome Announc. 2014;2(3): 2013–2014.

502. Wang PG, Kudelko M, Lo J, Yu Lam Siu L, Tsz Hin Kwok K, Sachse M, et al. Efficient assembly and secretion of recombinant subviral particles of the four dengue serotypes using native prM and E proteins. PLoS One. 2009;4(12).

503. Weissman D, Ni H, Scales D, Dude a, Capodici J, McGibney K, et al. HIV gag mRNA transfection of dendritic cells (DC) delivers encoded antigen to MHC class I and II molecules, causes DC maturation, and induces a potent human in vitro primary immune response. J Immunol. 2000;165(8): 4710–4717.

504. Dudley DM, Aliota MT, Mohr EL, Weiler AM, Lehrer-Brey G, Weisgrau KL, et al. A rhesus macaque model of Asian-lineage Zika virus infection. Nat Commun. 2016;7(May): 12204.

505. Lazear HM, Govero J, Smith AM, Platt DJ, Fernandez E, Miner JJ, et al. A Mouse Model of Zika Virus Pathogenesis. Cell Host Microbe. 2016;19: 1–11.

506. Pardi N, Muramatsu H, Weissman D, Karikó K. In Vitro Transcription of Long RNA Containing Modified Nucleosides. Methods Mol Biol. 2013;969: 29–42.

507. Thess A, Grund S, Mui BL, Hope MJ, Baumhof P, Fotin-Mleczek M, et al. Sequence-engineered mRNA Without Chemical Nucleoside Modifications Enables an Effective Protein Therapy in Large Animals. Mol Ther. 2015;23(9): 1456–1464.

508. Maier MA, Jayaraman M, Matsuda S, Liu J, Barros S, Querbes W, et al. Biodegradable Lipids Enabling Rapidly Eliminated Lipid Nanoparticles for Systemic Delivery of RNAi Therapeutics. Mol Ther. 2013;21(8): 1570–1578.

509. Jayaraman M, Ansell SM, Mui BL, Tam YK, Chen J, Du X, et al. Maximizing the potency of siRNA lipid nanoparticles for hepatic gene silencing in vivo. Angew Chemie - Int Ed. 2012;51(34): 8529–8533.

510. Pierson TC, Sánchez MD, Puffer BA, Ahmed AA, Geiss BJ, Valentine LE, et al. A rapid and quantitative assay for measuring antibody-mediated neutralization of West Nile virus infection. Virology. 2006;346(1): 53–65.

511. Acharya P, Tolbert WD, Gohain N, Wu X, Yu L, Liu T, et al. Structural definition of an antibody-dependent cellular cytotoxicity response implicated in reduced risk for HIV-1 infection. J Virol. 2014;88(21): 12895–906.

512. Chuang G-Y, Geng H, Pancera M, Xu K, Cheng C, Acharya P, et al. Structure-Based Design of a Soluble Prefusion-Closed HIV-1 Env Trimer

with Reduced CD4 Affinity and Improved Immunogenicity. J Virol. 2017;91(10): e02268-16.

513. Swanstrom A. Dissociating SIV Env and CD4: Consequences for Virus and Host (Dissertation). University of Pennsylvania; 2015.

514. deCamp A, Hraber P, Bailer RT, Seaman MS, Ochsenbauer C, Kappes J, et al. Global Panel of HIV-1 Env Reference Strains for Standardized Assessments of Vaccine-Elicited Neutralizing Antibodies. J Virol. 2014;88(5): 2489–2507.

515. Bachmann MF, Hengartner H, Zinkernagel RM. T helper cell-independent neutralizing B cell response against vesicular stomatitis virus: role of antigen patterns in B cell induction? Eur J Immunol. 1995;25(12): 3445–51.

516. Checkley MA, Luttge BG, Freed EO. HIV-1 envelope glycoprotein biosynthesis, trafficking, and incorporation. J Mol Biol. 2011;410(4): 582–608.

517. Wyma DJ, Kotov a, Aiken C. Evidence for a stable interaction of gp41 with Pr55(Gag) in immature human immunodeficiency virus type 1 particles. J Virol. 2000;74(20): 9381–9387.

518. Lopez-Vergès S, Camus G, Blot G, Beauvoir R, Benarous R, Berlioz-Torrent C. Tail-interacting protein TIP47 is a connector between Gag and Env and is required for Env incorporation into HIV-1 virions. Proc Natl Acad Sci. 2006;103(40): 14947–52.

519. Checkley MA, Luttge BG, Mercredi PY, Kyere SK, Donlan J, Murakami T, et al. Reevaluation of the requirement for TIP47 in human immunodeficiency virus type 1 envelope glycoprotein incorporation. J Virol. 2013;87(6): 3561–70.

520. Cosson P. Direct interaction between the envelope and matrix proteins of HIV-1. EMBO J. 1996;15(21): 5783–8.

521. Bhattacharya J, Repik A, Clapham PR. Gag regulates association of human immunodeficiency virus type 1 envelope with detergent-resistant membranes. J Virol. 2006;80(11): 5292–300.

522. Patil A, Gautam A, Bhattacharya J. Evidence that Gag facilitates HIV-1 envelope association both in GPI-enriched plasma membrane and detergent resistant membranes and facilitates envelope incorporation onto virions in primary CD4+ T cells. Virol J. 2010;7: 3.

523. Yang P, Ai L, Huang S-C, Li H-F, Chan W, Chang C, et al. The cytoplasmic domain of human immunodeficiency virus type 1 transmembrane protein gp41 harbors lipid raft association determinants. J Virol. 2010;84(1): 59–

75.

524. Tedbury PR, Novikova M, Ablan SD, Freed EO. Biochemical evidence of a role for matrix trimerization in HIV-1 envelope glycoprotein incorporation. Proc Natl Acad Sci. 2016;113(2): E182-90.

525. Alfadhli A, Mack A, Ritchie C, Cylinder I, Harper L, Tedbury PR, et al. Trimer Enhancement Mutation Effects on Hiv-1 Matrix Protein Binding Activities. J Virol. 2016;90(March): JVI.00509-16.

526. Safety, Tolerability, and Immunogenicity of mRNA-1325 in Healthy Adult Subjects. In: ClinicalTrials.gov [Internet]. 2017 [cited 21 Jul 2017]. Available: https://clinicaltrials.gov/ct2/show/NCT03014089

527. Guzman MG, Alvarez M, Halstead SB. Secondary infection as a risk factor for dengue hemorrhagic fever/dengue shock syndrome: An historical perspective and role of antibody-dependent enhancement of infection. Arch Virol. 2013;158(7): 1445–1459.

528. Chau TNB, Quyen NTH, Thuy TT, Tuan NM, Hoang DM, Dung NTP, et al. Dengue in Vietnamese Infants—Results of Infection‐Enhancement Assays Correlate with Age‐Related Disease Epidemiology, and Cellular Immune Responses Correlate with Disease Severity. J Infect Dis. 2008;198(4): 516–524.

529. Halstead SB. Dengue Antibody-Dependent Enhancement: Knowns and Unknowns. Microbiol Spectr. 2014; 1–18.

530. Khetarpal N, Khanna I. Dengue Fever: Causes, Complications, and Vaccine Strategies. J Immunol Res. 2016;2016(3).

531. Balsitis SJ, Williams KL, Lachica R, Flores D, Kyle JL, Johnson S, et al. Lethal Antibody Enhancement of Dengue Disease in Mice Is Prevented by Fc Modification. Plos Pathog. 2010;6(2): e1000790.

532. Beltramello M, Williams KL, Simmons CP, MacAgno A, Simonelli L, Quyen NTH, et al. The human immune response to dengue virus is dominated by highly cross-reactive antibodies endowed with neutralizing and enhancing activity. Cell Host Microbe. 2010;8(3): 271–283.

533. Goncalvez AP, Engle RE, St Claire M, Purcell RH, Lai C-J. Monoclonal antibody-mediated enhancement of dengue virus infection in vitro and in vivo and strategies for prevention. Proc Natl Acad Sci. 2007;104(22): 9422–9427.

534. Ng JKW, Zhang SL, Tan HC, Yan B, Maria Martinez Gomez J, Tan WY, et al. First Experimental In Vivo Model of Enhanced Dengue Disease Severity through Maternally Acquired Heterotypic Dengue Antibodies. Plos Pathog.

2014;10(4): e1004031.

535. Wang TT, Sewatanon J, Memoli MJ, Wrammert J, Bournazos S, Bhaumik SK, et al. IgG antibodies to dengue enhanced for FcgRIIIA binding determine disease severity. Science. 2017;355(6323): 395–398.

536. Duangchinda T, Dejnirattisai W, Vasanawathana S, Limpitikul W, Tangthawornchaikul N, Malasit P, et al. Immunodominant T-cell responses to dengue virus NS3 are associated with DHF. Proc Natl Acad Sci. 2010;107(39): 16922–16927.

537. Stephens HAF, Klaythong R, Sirikong M, Vaughn DW, Green S, Kalayanarooj S, et al. HLA-A and -B allele associations with secondary dengue virus infections correlate with disease severity and the infecting viral serotype in ethnic Thais. Tissue Antigens. 2002;60(4): 309–318.

538. Dejnirattisai W, Supasa P, Wongwiwat W, Rouvinski A, Barba-Spaeth G, Duangchinda T, et al. Dengue virus sero-cross-reactivity drives antibody-dependent enhancement of infection with zika virus. Nat Immunol. 2016;17(9): 1102–8.

539. Stettler K, Beltramello M, Espinosa DA, Graham V, Cassotta A, Bianchi S, et al. Specificity, cross-reactivity, and function of antibodies elicited by Zika virus infection. Science. 2016;353(6301): 823–826.

540. Priyamvada L, Quicke KM, Hudson WH, Onlamoon N, Sewatanon J. Human antibody responses after dengue virus infection are highly cross-reactive to Zika virus. PNAS. 2016; 2–7.

541. Bardina S V, Bunduc P, Tripathi S, Duehr J, Frere JJ, Brown JA, et al. Enhancement of Zika virus pathogenesis by preexisting antiflavivirus immunity. Science. 2017;356: 174–180.

542. Chabierski S, Barzon L, Papa A, Niedrig M, Bramson JL, Richner JM, et al. Distinguishing West Nile virus infection using a recombinant envelope protein with mutations in the conserved fusion-loop. BMC Infect Dis. 2014;14: 246.

543. Modis Y, Ogata S, Clements D, Harrison SC. Structure of the dengue virus envelope protein after membrane fusion. Nature. 2004;427(6972): 313–319.

544. Barba-Spaeth G, Dejnirattisai W, Rouvinski A, Vaney M-C, Medits I, Sharma A, et al. Structural basis of potent Zika–dengue virus antibody cross-neutralization. Nature. 2016;539(7628): 314–314.

545. Crill WD, Hughes HR, Trainor NB, Davis BS, Whitney MT, Chang GJJ. Sculpting humoral immunity through dengue vaccination to enhance

protective immunity. Front Immunol. 2012;3: 334.

546. Crill WD, Trainor NB, Chang GJJ. A detailed mutagenesis study of flavivirus cross-reactive epitopes using west Nile virus-like particles. J Gen Virol. 2007;88(4): 1169–1174.

547. World Health Organization. Dengue and severe dengue: Fact sheet [Internet]. 2017 [cited 10 Jun 2017]. Available: http://www.who.int/mediacentre/factsheets/fs117

548. Flipse J, Smit JM. The Complexity of a dengue vaccine: A review of the human antibody response. PLoS Negl Trop Dis. 2015;9(6): 1–18.

549. Guy B, Briand O, Lang J, Saville M, Jackson N. Development of the Sanofi Pasteur tetravalent dengue vaccine: One more step forward. Vaccine. 2015;33(50): 7100–7111.

550. World Health Organization. Dengue vaccine research [Internet]. 2017 [cited 10 Jun 2017]. Available: http://www.who.int/immunization/research/development/dengue_vaccines/en/

551. Hadinegoro SR, Arredondo-García JL, Capeding MR, Deseda C, Chotpitayasunondh T, Dietze R, et al. Efficacy and Long-Term Safety of a Dengue Vaccine in Regions of Endemic Disease. N Engl J Med. 2015;373(13): 1195–1206.

552. Ferguson NM, Rodríguez-Barraquer I, Dorigatti I, Mier-y-Teran-Romero L, Laydon DJ, Cummings DAT. Benefits and risks of the Sanofi-Pasteur dengue vaccine: Modeling optimal deployment. Science. 2016;353(6303): 1033–1036.

553. Pavio N, Lai MMC. The hepatitis C virus persistence: how to evade the immune system? J Biosci. 2003;28(3): 287–304.

554. Kaplan DH, Jenison MC, Saeland S, Shlomchik WD, Shlomchik MJ. Epidermal Langerhans Cell-Deficient Mice Develop Enhanced Contact Hypersensitivity. 2005;23: 611–620.

555. Bobr A, Olvera-gomez I, Igyarto BZ, Haley KM, Hogquist KA, Kaplan DH. Acute Ablation of Langerhans Cells Enhances Skin Immune Responses. 2017;

556. Kaplan DH, Li MO, Jenison MC, Shlomchik WD, Flavell RA, Shlomchik MJ. Autocrine / paracrine TGFb1 is required for the development of epidermal Langerhans cells. J Exp Med. 2007;204(11): 2545–2552.

557. Hildner K, Edelson BT, Purtha WE, Diamond M, Kohyama M, Calderon B,

et al. Batf3 Deficiency Reveals a Critical Role for CD8 α + Dendritic Cells in Cytotoxic T Cell Immunity. 2008;322(5904): 1097–1100.

558. Jung S, Unutmaz D, Wong P, Sano G, Santos KDL, Sparwasser T, et al. In Vivo Depletion of CD11c+ Dendritic Cells Abrogates Priming of CD8+ T Cells by Exogenous Cell-Associated Antigens. Immunity. 2002;17: 211–220.

559. Kissenpfennig A, Henri S, Dubois B, Laplace-builhé C, Perrin P, Romani N, et al. Dynamics and Function of Langerhans Cells In Vivo : Dermal Dendritic Cells Colonize Lymph Node Areas Distinct from Slower Migrating Langerhans Cells. 2005;22: 643–654.

560. Bennett CL, Rijn E Van, Jung S, Inaba K, Steinman RM, Kapsenberg ML. Inducible ablation of mouse Langerhans cells diminishes but fails to abrogate contact hypersensitivity. J Cell Biol. 2005;169(4): 569–576.

561. Nagao K, Ginhoux F, Leitner WW, Motegi S, Bennett CL, Merad M, et al. Murine epidermal Langerhans cells and langerin-expressing dermal dendritic cells. 2009;

562. Holm CK, Jensen SB, Jakobsen MR, Cheshenko N, Horan KA, Moeller HB, et al. Virus-cell fusion as a trigger of innate immunity dependent on the adaptor STING. Nat Immunol. 2012;13(8): 737–43.

563. Neefjes J, Jongsma MLM, Paul P, Bakke O. Towards a systems understanding of MHC class I and MHC class II antigen presentation. Nat Rev Immunol. 2011;11(12): 823–836.

564. Veerappan Ganesan AP, Eisenlohr LC. The elucidation of non-classical MHC class II antigen processing through the study of viral antigens. Curr Opin Virol. 2017;22: 71–76.

565. Tewari MK, Sinnathamby G, Rajagopal D, Eisenlohr LC. A cytosolic pathway for MHC class II – restricted antigen processing that is proteasome and TAP dependent. Nat Immunol. 2005;6(3): 287–294.

566. Gett A V., Sallusto F, Lanzavecchia A, Geginat J. T cell fitness determined by signal strength. Nat Immunol. 2003;4(4): 355–360.

567. Grakoui A, Bromley SK, Sumen C, Davis MM, Shaw AS, Allen PM, et al. The immunological synapse: a molecular machine controlling T cell activation. Science. 1999;285(5425): 221–227.

568. Wülfing C, Rabinowitz JD, Beeson C, Sjaastad MD, Mcconnell HM, Davis MM. Kinetics and Extent of T Cell Activation as Measured with the Calcium Signal. J Exp Med. 1997;185(10): 1815–1825.